2.5 Geology, Seismology, and Geotechnical Engineering

EF3 COL 2.0-26-A

2.5.1 Basic Geology and Seismic Information

Subsection 2.5.1 presents a geological and seismological characterization of the Fermi 3 site divided into two parts. Subsection 2.5.1.1 describes the geology including the physiographic, geologic, and tectonic setting of the (320 km [200 mi] radius) site region and Subsection 2.5.1.2 describes the geology including stratigraphy, structural geology, and engineering geology of the (40 km [25 mi] radius) site vicinity to (1 km [0.6 mi] radius) site location. The geological and seismological characterization was developed in accordance with the guidance provided in RG 1.206, Section C.I.2.5.1 "Basic Geologic and Seismic Information," and is intended to fulfill the requirements of 10 CFR 52 "Licenses, Certifications, and Approvals for Nuclear Power Plants" Section 52.79. The geological and seismological characterization presented in this section provides the basis for evaluating the geologic, seismic, and man-made hazards at the site.

The geological and seismological characterization presented in this section is developed from previously published reports for the Fermi 2 power plant, recent and historic geologic literature, field and aerial reconnaissance, and subsurface hydrogeologic and geotechnical investigations conducted in 2007 for the preparation of this FSAR. The review of recent literature was facilitated by using GeoRef electronic database (American Geological Institute). Additionally, the Michigan and Ohio Geological Survey offices were contacted for relevant unpublished geologic literature, studies, and projects.

2.5.1.1 Regional Geology

This subsection discusses the regional physiography, geologic history, stratigraphy, and tectonic setting within a 320 km (200 mi) radius of the Fermi 3 site which is shown on Figure 2.5.1-201 (Reference 2.5.1-201; Reference 2.5.1-202). Physiographic, regional structure, bedrock geologic, Quaternary geologic, basement crustal provinces and seismicity maps for the Fermi 3 site region (320 km [200 mi] radius) are shown on Figure 2.5.1-202 (Reference 2.5.1-203; Reference 2.5.1-204), Figure 2.5.1-203, Figure 2.5.1-204 (Reference 2.5.1-205; Reference 2.5.1-206), Figure 2.5.1-205 (Reference 2.5.1-207; Reference 2.5.1-208; Reference 2.5.1-209), Figure 2.5.1-206 (Reference 2.5.1-210; Reference 2.5.1-211), and Figure 2.5.1-207,

respectively. The site is located within the Central Stable Region tectonic province of the North American continent (Reference 2.5.1-212). Some regional faulting and seismic activity is known, but the region is characteristically one of relative stability. The site is located on the southeast side of the Michigan basin on the northwest flank of the Findlay arch (Figure 2.5.1-208, Reference 2.5.1-213). There are no known surface faults within 40 km (25 mi) of the site and there are no capable tectonic sources as defined by Regulatory Guide 1.206 within 320 km (200 mi) of the site. Pleistocene deposits of glacial and glaciolacustrine origin underlay the site area and are underlain by Paleozoic sedimentary rocks. Approximately 945 m (3100 ft) of Paleozoic sedimentary rocks are present in the site area and overlie the Precambrian basement. The underlying basement rocks within the region reflect a history of continental collisions, accretion, and periods of rifting. The Fermi 3 site is located near the boundaries between several different basement crustal provinces (Reference 2.5.1-210; Reference 2.5.1-214; Reference 2.5.1-211; Reference 2.5.1-215; Reference 2.5.1-216; Reference 2.5.1-217). The key aspects of the regional geology of the site are presented to provide the framework for an evaluation of the geologic and seismologic hazards as outlined in subsequent subsections.

2.5.1.1.1 Regional Physiography and Geomorphology

The Fermi 3 site is located in the northern portion of the Midwestern United States in the Eastern Lake section of the Central Lowlands physiographic province (Figure 2.5.1-202) (Reference 2.5.1-203; Reference 2.5.1-204). The (320 km [200 mi] radius) site region of Fermi 3 encompasses portions of two other physiographic provinces: Appalachian Plateaus and St. Lawrence Lowlands. The St. Lawrence physiographic province is located in adjacent southern Ontario, Canada. The physiographic provinces within the site region are described as follows.

2.5.1.1.1.1 Central Lowlands Physiographic Province

The Central Lowland physiographic province is generally located in the northern Midwest but also extends through Oklahoma into north-central Texas (Figure 2.5.1-202) (Reference 2.5.1-203). The Central Lowlands physiographic province is subdivided into eight sections. The Eastern Lake and Till Plains sections are located in the (320 km [200 mi] radius) site region and Fermi 3 is located within the Eastern Lake section.

The Eastern Lake section is characterized by glacial landforms, including end moraines, ground moraines, outwash plains, kames, eskers, and drumlins, and by beach and lacustrine deposits formed during the lake level fluctuations of the Great Lakes (Reference 2.5.1-218; Subsection 2.5.1.1.2.3.4.4). The ground surface is relatively flat with relief up to 7.6 m (25 ft) (Reference 2.5.1-219). The glacial sediments were deposited on a dissected bedrock topography with cuestas and valleys (Reference 2.5.1-218; Reference 2.5.1-220). The bedrock is exposed locally and consists of relatively flat-lying bedrock of Silurian to Jurassic rocks (Figure 2.5.1-204).

Fermi 3 is located on a lake plain formed during the high-water stages of Lake Erie (see Subsection 2.5.1.1.2.3.4.4). There is little topographic relief on the lake plain, which results in poor surface drainage. The lake plain has been dissected by eastward-flowing creeks and rivers. The relief on the lake plain within the vicinity of the project area is approximately 7.6 m (25 ft) (Reference 2.5.1-221).

The Till Plains section is characterized by flat to gently rolling glacial landforms including end moraines, ground moraines, recessional moraines, and outwash plains, along with some isolated lacustrine deposits adjacent to the boundary with the Eastern Lake section (Reference 2.5.1-219). The local relief is up to 76 m (250 ft). Bedrock is exposed locally and is relatively flat-lying. (Reference 2.5.1-219) The glacial deposits were deposited on a dissected bedrock surface with buried stream valleys. The bedrock surface tends to be gently rolling with well-developed valley systems. (Reference 2.5.1-220) The Till Plains section is differentiated by having greater relief and fewer lacustrine deposits than the Eastern Lake section (Reference 2.5.1-219).

Lake Erie occupies three basins that increase in depth from west to east. Away from the shore zone the three basins are broadly bowl-shaped, with the lake-bottom surface depths extending smoothly from nearshore down to greater depths. The bowl shape is inferred to be the result of postglacial deposition and sediment-smoothing in response to a gyre of water circulation in each basin, or progressive shoreline modifications in the zone of Holocene rising lake levels. The sediment-smoothing has diminished or eliminated surface relief formed during the last glaciation. (Reference 2.5.1-495)

The western Erie basin extends to depths of 10 to 11 m (33 to 36 ft), the central Erie basin extends to depths of 24 to 25 m (79 to 82 ft), and the

eastern Erie basin extends to depths exceeding 40 m (131 ft). Maps of western and eastern Lake Erie showing major geomorphic features are shown on Figure 2.5.1-263 and Figure 2.5.1-264, respectively.

2.5.1.1.1.2 Appalachian Plateaus Physiographic Province

The Appalachian Plateaus physiographic province is located to the southeast of Fermi 3 and the Central Lowlands physiographic province (Figure 2.5.1-202). The Appalachian Plateau physiographic province is subdivided into seven sections, two sections, Kanawha and Southern New York sections, are within the (320 km [200 mi] radius) site region.

The Kanawha section is characterized as a dissected plateau with broad valleys containing outwash and lacustrine deposits of Pleistocene Age. The local relief ranges up to 244 m (800 ft) (Reference 2.5.1-219). The section is underlain by flat-lying to broadly folded Paleozoic sediments of Mississippian age and younger. Layers of limestone and sandstone that are more resistant to erosion create the topographic highs. The Central Lowlands physiographic province has less local relief, thicker glacial deposits, and fewer exposures than the Kanawha section (Reference 2.5.1-219).

The Southern New York section is the glaciated portion of the Appalachian Plateaus physiographic province. The section is characterized by gently rolling to hilly topography with local relief up to 61 m (200 ft) and glacial landforms including end moraines, ground moraines, kames, eskers, kettles, outwash plains, and lacustrine deposits. Local ridges and hills expose bedrock and residual soils. The local relief is the greatest and elevation is the highest in the southeast bordering the Kanawha section and decreases to the north and west (Reference 2.5.1-219). The section is underlain by flat-lying to broadly folded Paleozoic sediments of Mississippian to Pennsylvanian age (Reference 2.5.1-220). Layers of limestone and sandstone that are more resistant to erosion create the topographic highs. Compared to the Kanawha section, the Southern New York section has a lower local relief and more glacial landforms and thicker glacial deposits. The Central Lowland physiographic province has a lower local relief and fewer bedrock exposures than the Southern New York section. (Reference 2.5.1-219)

2.5.1.1.1.3 St. Lawrence Lowlands Physiographic Province

The St. Lawrence Lowlands physiographic province in Canada extends to the east and northeast from Fermi 3 (Figure 2.5.1-202). This physiographic province is characterized by a low plain with distributed glacial landforms including moraines, outwash deposits, eskers, and drumlins along with beach and lacustrine landforms (Reference 2.5.1-222; Reference 2.5.1-223). The glacial deposits overlie relatively flat-lying Paleozoic sedimentary rocks of Silurian and Devonian age. Bedrock is locally exposed at the surface (Figure 2.5.1-204). The Niagara Escarpment, which extends from Niagara Falls to the southern part of Georgian Bay in the eastern portion of the site region, is a bedrock escarpment about 77 m (250 ft) high that was formed by differential erosion of Paleozoic sedimentary rocks (Reference 2.5.1-224).

2.5.1.1.2 Regional Geologic History

This subsection summarizes the geologic and tectonic history of the Fermi 3 site region. Figure 2.5.1-209 (Reference 2.5.1-225) presents the subdivisions of geologic time referred to in this subsection and in Subsection 2.5.1.1.3. The last major tectonic events in the site region were rifting associated with the Midcontinent Rift and Grenville Orogeny, 1.2 to 1.0 Ga (Subsection 2.5.1.1.2.2). Ga is defined to be billion years. Subsequent to these events, the history of the site region includes several transgressions and regressions of epeiric seas (shallow continental seas), episodes of widespread subsidence in the continental basins and widespread uplift in the arches, and minor activity on preexisting basement faults (Subsection 2.5.1.1.3.2). Prior to a billion years ago, the region was more tectonically active with continental and island arch collisions and rift events that were responsible for the formation of the North American craton.

2.5.1.1.2.1 Archean Geologic History

The earliest geologic history of the Fermi 3 site region consists of the assembly of the Superior province of the Canadian Shield during the Archean Eon to form the relatively stable continental lithosphere nuclei of proto–North America (Laurentia) (Reference 2.5.1-217). The Superior province consists of greenstone belts with granitic plutonic rocks, granitic gneisses, and gneissic and migmatitic rocks dating from 2.6 to 3.6 Ga (Reference 2.5.1-210) (Figure 2.5.1-206, Reference 2.5.1-210; Reference 2.5.1-211).

2.5.1.1.2.2 Proterozoic Geologic History

The Proterozoic Eon follows the Archean and is subdivided into the Paleoproterozoic (2.5 – 1.6 Ga), Mesoproterozoic (1.6 – 0.9 Ga), and Neoproterozoic (ca. 600 Ma) eras. Ma is defined to be million years.

In the early part of the Paleoproterozoic, at the end of the Archean (2.45 – 2.5 Ga), crustal extension and rifting led to the formation of a south-facing, passive continental margin along the southern margin of the Superior province (Reference 2.5.1-216). Major orogenies in the Paleoproterozoic that subsequently resulted in the continued growth of the Laurentian continent through the accretion of various basement terranes along the southern margin of the Superior province included the Trans-Hudson orogeny 1.91 – 1.81 Ga, the Penokean orogeny (1.88 – 1.83 Ga), and the Central Plains orogeny (1.80 – 1.62 Ga) (Reference 2.5.1-210). The latter two of these, which resulted in the accretion of basement terranes present in the study region, are described below in Subsection 2.5.1.1.2.2.1 and Subsection 2.5.1.1.2.2.2.

During the Mesoproterozoic the eastern and southern Granite-Rhyolite provinces matured along the southern and eastern margins of Laurentia, and several rifts developed within the crust, including the Mid-continent Rift System and the Fort Wayne rift (part of the east continent rift). This era culminated with the major Grenville orogeny along the eastern and southern margins of Laurentia. The structures are well defined by regional gravity and magnetic data, discussed in Subsection 2.5.1.1.4.2.

During the Neoproterozoic, rifting along the southeast margin of Laurentia to form the proto-Atlantic formed a number of failed rifts extending into the craton, including the Reelfoot rift, Rough Creek graben, and Rome trough (Reference 2.5.1-226).

The major tectonic events that led to the development of the various basement crustal provinces within the study region are summarized below.

2.5.1.1.2.2.1 Penokean Orogeny (1.88 – 1.83 Ga)

The Penokean orogeny occurred along the southern margin of the Superior province and is interpreted as the collision of an island arc located between the Archean Superior province and a north-moving Archean Marshfield terrane not associated with the Superior province (Reference 2.5.1-214) (Figure 2.5.1-206 and Figure 2.5.1-210).

As illustrated in the schematic diagram on Figure 2.5.1-210 (Reference 2.5.1-214), the initial southward subduction of oceanic crust off the southern margin of the Superior province (northern domain) resulted in the creation of an island arc (the Pembine-Wausau terrane) and in the movement of Huronian Supergroup rocks (Early Proterozoic passive margin and foreland sedimentary rocks) toward the trench. The collision of the arc with the northern domain deformed the arc and northern domain, folding Huronian Supergroup and younger Marquette Range Supergroup rocks about east-west axes and thrusting them northward over a crustal ramp along the northern domain (Reference 2.5.1-216; Reference 2.5.1-217). Subduction shifted to the south of the original arc and reversed polarity, forming a younger arc complex and trench. The Marshfield terrane collided with the arc, further deforming the arc complex and margin of the northern domain, and subducted the margin of the Marshfield terrane beneath the arc complex. The end of the Penokean orogeny marks the end of the assembly of Archean and earliest Proterozoic rocks to form the Hudsonian craton (Reference 2.5.1-215).

2.5.1.1.2.2.2 Central Plains Orogeny (1.80 – 1.62 Ga)

Rocks of the Central Plains orogeny and the Southern and Eastern Granite-Rhyolite provinces form the Transcontinental Proterozoic province (Reference 2.5.1-213). The Central Plains orogeny (CPO) occurred along the southern margin of the Hudsonian craton and truncates the Trans-Hudson orogeny and Penokean orogeny terranes (Figure 2.5.1-206). The southern and eastern extension of the CPO beneath the younger Granite-Rhyolite provinces, discussed in Subsection 2.5.1.1.2.2.3 below, is uncertain (Reference 2.5.1-211).

2.5.1.1.2.2.3 Eastern (ca. 1.47 Ga) and Southern (1.37 Ga) Granite-Rhyolite Provinces

As discussed above, rocks of the Southern and Eastern Granite-Rhyolite provinces, together with the rocks of the CPO, form the Transcontinental Proterozoic province (Reference 2.5.1-215). Approximately 1.47 Ga granitic and felsic volcanic rocks of the Eastern Granite-Rhyolite province occur buried in the subsurface of the central and eastern midcontinent region, and truncate the Penokean orogeny on the south and southeast and the CPO on the east (Reference 2.5.1-211) (Figure 2.5.1-206). Approximately 1.37 Ga granitic and felsic volcanic rocks of the Southern

Granite-Rhyolite province truncate the CPO on the south (Reference 2.5.1-211). These rocks are interpreted to represent a veneer of supercrustal and shallow plutonic rocks that lie on Early Proterozoic CPO crust, from which they were derived by partial melting (Reference 2.5.1-210).

The southern and eastern extension of the CPO beneath the younger Granite-Rhyolite provinces is uncertain. Van Schmus et al. (Reference 2.5.1-211) argue that older crust associated with the CPO is absent beneath the Southern and Eastern Granite-Rhyolite provinces southeast of a northeast-southwest-trending Nd isotope boundary extending from southwestern Ontario to southeastern Oklahoma (Figure 2.5.1-206). Van Schmus, et al. (Reference 2.5.1-211) interpret the crust northwest of this boundary to be Paleoproterozoic, and the crust southeast of this boundary to be Mesoproterozoic (ca. 1.5 Ga) juvenile crust of unknown nature and origin but possibly consisting of one or more juvenile terranes accreted to the southeastern margin in early Mesoproterozoic.

2.5.1.1.2.2.4 Mesoproterozoic Rifting (1.32 – 1.1 Ga)

Major continental rifts developed along the eastern margin of Laurentia after emplacement of the Eastern Granite-Rhyolite province rocks. These included the development of the northwest-trending Fort Wayne rift in western Ohio and eastern Indiana, and the arcuate Midcontinent Rift System (MRS) that extends from mid-Kansas to the Lake Superior region and then southeast across Michigan. (Reference 2.5.1-226; Reference 2.5.1-227; Reference 2.5.1-228; Reference 2.5.1-229) The Fort Wayne rift, which is coincident with a portion of the East Continent Gravity High (ECGH), is similar to, and possibly related to, the rifting event that developed the MRS (Reference 2.5.1-228). Alternatively, a whole-rock Rb/Sr date of 1.325 Ga is older than dates reported for the MRS, suggesting that Fort Wayne rifting formed during an earlier rifting event (Reference 2.5.1-228). Stark (Reference 2.5.1-229) concludes that the Fort Wayne Rift and the associated East Continent Rift Basin (ECRB) contains a northern mafic basalt fill sequence associated with the ECGH, and a southern depocenter filled with Proterozoic clastic rocks and minor volcanic flows. However, Stark (Reference 2.5.1-229) acknowledges that demonstrating an association between the MRS and ECRB requires additional research to resolve the inconsistent observations of basement lithology in northwestern Ohio.

The arcuate MRS is coincident with the Midcontinent Gravity High (MCGH) that extends from mid-Kansas to the Lake Superior region, the Mid-Michigan Gravity High (MMGH), and possibly portions of the ECGH from Ohio to Tennessee, a distance of over 2300 km (1429 mi) (Reference 2.5.1-226) (Figure 2.5.1-206). The rift is interpreted as a relatively short-lived breakup of Laurentia that was aborted by the Grenville collision and resulting foreland compression, discussed in Subsection 2.5.1.1.2.2.5 below (Reference 2.5.1-210). Volcanic, mafic intrusive rocks and sedimentary rocks associated with the rift were deposited in fault-bounded basins (grabens) (Reference 2.5.1-230). U-Pb (Uranium-Lead isotope dating) ages for syn-rift volcanic and mafic intrusive rocks range between about 1.109 and 1.087 Ga, and geochronologic and paleomagnetic data suggest that younger port-rift sedimentary rocks were also deposited about 1.1 – 1.0 Ga (Reference 2.5.1-210).

Gordon and Hempton (Reference 2.5.1-231) postulate that the MRS developed as a result of the Grenville collision (orogen), which caused the outward propagation of strike-slip faults into Laurentia and the development of extensional zones (pull-apart basins) that received lacustrine and fluvial and subsequently volcanic rocks as the crust was attenuated.

Gordon and Hempton (Reference 2.5.1-231) cite the Red Sea rift as an analog. Hauser (Reference 2.5.1-232) demonstrates that Gordon and Hempton's model does not recognize the nature of transform faults within a rift system and is not supported by identified strike-slip faults or the recognized sequence of rift deposition, which is volcanic and igneous rock first, followed by sedimentary rocks. Hauser (Reference 2.5.1-232) proposes that the MRS was initiated in relation to a rising mantle plume (Michipioten hot spot) located in the Lake Superior region, and that a block of lithosphere was translated and rotated clockwise away from Laurentia and probably into the embrace of the Grenville orogen, analogous to the Arabian plate moving away from the Red Sea rift and into the Tethyan-Alpine orogen of Turkey and Iran (Figure 2.5.1-211) (Reference 2.5.1-232). Compression associated with the Ottawan phase of the Grenville orogen (1.09 – 1.025 Ga) aborted rifting and partially inverted the rift, particularly in the Lake Superior region. Cannon (Reference 2.5.1-233) concludes that during compression, the southwest arm of the rift was closed about 30 km (18 mi), the central graben area in

the Lake Superior region was inverted, and the southeast arm was dominated by strike-slip faulting.

2.5.1.1.2.2.5 Grenville Orogen [1.25 Ga – 980 Million years ago (Ma)]

The Grenville orogen represents regionally extensive allochthonous terranes that collided with, and were accreted to, the southern margin of Laurentia (Reference 2.5.1-234). The Grenville orogen truncates the Granite-Rhyolite provinces and all other northern orogens (Figure 2.5.1-203 and Figure 2.5.1-206). At least three phases of the Grenville orogen are recognized: the Elzeverian (1.25 Ga), the Ottawan (1.09 – 1.025 Ga), and the Grenville Front tectonic zone (GFTZ) (Reference 2.5.1-232).

The history of the Grenville orogeny as interpreted by Culotta and Pratt (Reference 2.5.1-234) from the Consortium for Continental Reflection Profiling COCORP lines OH-1 and OH-2 that cross the central part of Ohio (see discussion in Subsection 2.5.1.1.4.2.2) is illustrated on Figure 2.5.1-212 (Reference 2.5.1-234). The location of COCORP lines OH-1 and OH-2 are shown on Figure 2.5.1-213 (Reference 2.5.1-235; Reference 2.5.1-214; Reference 2.5.1-236; Reference 2.5.1-216; Reference 2.5.1-237; Reference 2.5.1-238). As shown on these figures, the Central Gneiss Belt (CGB) island arc initially collides with Laurentia along an east-dipping subduction zone (proto-GFTZ), forming a foreland thrust belt. Subduction reversed polarity toward the west and an Andean-type arc and back-arc-basin developed within the Central Metasedimentary Belt (CMB). The Central Granulite Terrane (CGT) collides with the CMB along the west-dipping Coshocton Zone – Carthage-Colton mylonite zone, closing the back-arc-basin (Figure 2.5.1-212). During this latter collision, the GFTZ was reactivated. (Reference 2.5.1-234)

2.5.1.1.2.2.6 Neoproterozoic Rifting (ca. 600 Ma)

Neoproterozoic rifting along the southeast margin of Laurentia formed the proto-Atlantic and a number of failed rifts extending into the craton, including the Reelfoot rift, Rough Creek graben, and Rome trough (Reference 2.5.1-226).

2.5.1.1.2.3 Phanerozoic Geologic History

The Phanerozoic eon includes the Paleozoic, Mesozoic, and Cenozoic eras (Reference 2.5.1-223). During the Paleozoic, which was a period of extensive epeiric (inland) seas, a number of intracratonic basins and bounding arches developed in the site region, including the Michigan, Illinois, and Appalachian basins and the Cincinnati, Kankakee, Findlay, and Algonquin arches (Figure 2.5.1-208), which controlled the Paleozoic sedimentary depositional history of the region. The most significant with respect to the site are the Michigan basin and the Findlay and Algonquin arches.

2.5.1.1.2.3.1 Paleozoic Geologic History

Several orogenies occurred along the eastern margin of Laurentia during the Paleozoic and had little effect in the study region. These included the Late Cambrian[6] to Ordovician Penobscot event (ca. 510 – 490 Ma), the Middle to Late Ordovician Taconic event (ca. 470 – 440 Ma), the Late Silurian Acadian or Caledonian event, the Devonian[6] Arcadian event, and the Carboniferous – Permian Alleghenian collision between Laurentia and Gondwana (Reference 2.5.1-239, Reference 2.5.1-240).

2.5.1.1.2.3.2 Mesozoic Geologic History

Other than minor sedimentary deposition in the center of the Michigan basin (Middle Jurassic Ionia Formation) no geologic history during the Mesozoic exists in the region of the site (Reference 2.5.1-241). Along the southwest margin of Laurentia, Early Mesozoic extension resulted in the breakup of Pangaea into Laurasia, including Laurentia and Gondwana, and the formation of a rifted margin (Reference 2.5.1-226). Major Mesozoic rifts include the Mississippi embayment and the St. Lawrence Valley system. In addition, pre-Mesozoic rifts were reactivated during the Mesozoic, including the Reelfoot rift.

2.5.1.1.2.3.3 Cenozoic Geologic History

The Cenozoic Era consists of the Tertiary and Quaternary Periods. No early (Tertiary Period) Cenozoic history is preserved in the site region. The missing rock record spans Pennsylvanian to Pliocene time with the exception of some Jurassic sedimentary rocks. If rocks of these intervening ages did once exist, they were most likely eroded. The site region is considered to have been tectonically stable throughout the

6. Uncertain age

Cenozoic, and except for vertical crustal movement related to glacial isostatic adjustments there is no evidence for significant tectonic deformation during the Cenozoic (see discussion in Subsection 2.5.1.1.4).

2.5.1.1.2.3.4 Quaternary Geologic History

Quaternary geologic history is dominated by the growth and expansion of the continental Laurentide ice sheet that periodically extended into the Great Lakes region, with the ultimate limit of glaciation near the Ohio and Missouri rivers. Traditionally, the major glaciations in central North America were related to a simple fourfold stratigraphic framework (Wisconsinan, Illinonian, Kansan, and Nebraskan) (Reference 2.5.1-242). More recently, this nomenclature has been supplemented and replaced by correlations to stages of the marine oxygen isotope record (referred to as marine isotope stages, or MIS) (Reference 2.5.1-243). Oxygen isotope excursions in marine sediment are directly correlated with the volume of ice on land and thus are used as a proxy record for the timing and magnitude of glaciations (e.g., Reference 2.5.1-244; Reference 2.5.1-245, as cited in Reference 2.5.1-243). The current interglacial period, the Holocene, is referred to as MIS 1; the most recent glaciation, the Late Wisconsinan, is MIS 2; the Middle and Early Wisconsinan were the low-ice-volume periods that span MIS 3 – 5; and the Illinoian is MIS 6. Beyond the Illinoinan, only the MIS number is used with even numbers referring to time of higher ice volume.

The surficial sediments across the (320 km [200 mi] radius) site region are composed mainly of Illinoian- (MIS 6) and Wisconsinan-age (MIS 2) glacial sediments (Figure 2.5.1-205). As summarized in this subsection, the Great Lakes basins were deepened during glacial periods as they served as the primary pathways for the major ice lobes that projected south from the main body of the Laurentide ice sheet. The earlier Illinoian-age (MIS 6) glacial sediments were subject to a long period of soil formation and periglacial (adjacent to the glacial front) erosion during the time leading up to the most recent glaciation, the Late Wisconsin, when the ice lobes were dynamic with frequent fluctuations in extent. The north-flowing drainage was sometimes blocked, resulting in impoundment of streams and rivers forming proglacial lakes and temporary reversal of stream flow direction. Lake levels varied depending on the position of ice within the lake and on the outlet elevation (partly

controlled by isostatic rebound of the crust as glacial ice melted and retreated).

Fullerton (Reference 2.5.1-246) provides a comprehensive summary of the glacial history of the site region. The timing and advance of the major ice lobes in the study region during the Wisconsin glaciation is illustrated on Figure 2.5.1-214 (Reference 2.5.1-246). The commonly used names for the major lobes within the (320 km [200 mi] radius) study region are from west to east: Michigan, Huron (sometimes Huron-Erie), Saginaw (sometimes referred to as a sublobe of the Huron lobe), Erie (sometimes Erie-Ontario), Ontario, Little East White, Miami, Scioto, Killbuck, and Grand River. Historically, the advance and retreat histories of ice lobes have been correlated based on the assumption that they responded to the same climatic forcing and therefore operated in concert (Reference 2.5.1-247; Reference 2.5.1-248). Absolute synchrony is not possible to document, nor does it appear to be the rule (Reference 2.5.1-249), despite attempts to prove otherwise (Reference 2.5.1-250). Even for a single advance, a range of radiocarbon ages is possible (Reference 2.5.1-251) because a certain amount of imprecision is inherent in the radiocarbon[7] dating methods (Reference 2.5.1-249).

Ice lobes advance in response to ice sheet and ice stream dynamics and these dynamics overprint the response of an ice lobe to climate change. The boundaries of the ice sheet that influence a particular ice lobe (its ice shed) can also shift or evolve over time (Reference 2.5.1-254). Shifts in the ice shed areas that contributed to a given ice lobe are reflected in changes in flow lines, till provenance, and texture. Historically, some ice lobes have been given combined names (e.g., Huron-Erie and Erie-Ontario), partly in recognition of complexities in their flow direction or composition that were not completely understood at the time (e.g., Reference 2.5.1-246; Reference 2.5.1-248). For example, the boundary between the Ontario-Erie lobe and the more westerly Huron-Erie lobe was considered to be in the central part of the Lake Erie basin during the

7. Radiocarbon years do not equate to calendar years (Reference 2.5.1-251). Based on U-Th dated corals, marine and terrestrial sediments linked to calendar chronologies through high-resolution paleoclimate records, and U-Th dated speleothems, a radiocarbon calibration curve has been compiled (IntCal04) (Reference 2.5.1-252) and updated (Hughen and the IntCal Working Group (Reference 2.5.1-253). In this document, calendar years (cited as years before present [BP]) are used unless otherwise indicated. If the ages are based on radiocarbon dates that are not corrected to calendar years, the ages are given as radiocarbon years BP.

early part of the Late Wisconsinan glaciation (Reference 2.5.1-246) but was relocated to the west of the Bass Islands, just east of the Michigan shore for the later advances (Reference 2.5.1-246; Reference 2.5.1-248) (Figure 2.5.1-214).

2.5.1.1.2.3.4.1 Early and Middle Pleistocene Events

Ice sheets covered the proposed Fermi 3 (320 km [200 mi] radius) study region during the early and middle Pleistocene (pre-780 thousand years [ka] to 130 ka). The southern limit of early and middle Pleistocene glaciation extends from northeastern Kansas through Missouri, southern Illinois, the southern tip of Indiana, and the northern part of Kentucky, including all of Ohio, crossing the middle of West Virginia, and including all of New York and the northern part of New Jersey (Reference 2.5.1-255, as cited in Reference 2.5.1-243).

Early Pleistocene glaciations in the site region are suggested not only by the presence of buried glacial sediment and erosion surfaces but also by the indirect evidence of blocked drainages in older buried valley sediments (Reference 2.5.1-256). The deeply buried, northward-draining Teays-Mahomet bedrock valley, whose location does not coincide with that of modern streams, is filled in places with thick deposits of sand and gravel (Reference 2.5.1-209) (Figure 2.5.1-205). Two magnetically reversed clay layers separated by a soil horizon within the valley fill sequence suggest that at least two periods existed when its flow was blocked, most likely by ice, prior to the last magnetic reversal (Reference 2.5.1-256), now reported as 780 ka (Reference 2.5.1-257; Reference 2.5.1-258; Reference 2.5.1-259, as cited in Reference 2.5.1-243).

The middle Pleistocene (780 to 130 ka), which spans MIS 16 to 6 and lies completely within the Brunhes normal chron. The middle Pleistocene culminated in the Illinoian glaciation (MIS 6, approximately 160 ka), which is exposed beyond the late Wisconsinan glacial border in southern Indiana and Ohio and western Illinois, at the limits of the Fermi 3 site region (320 km [200 mi] radius). (Reference 2.5.1-243) It is recognized in the subsurface in Ontario and Ohio and discussed in the section on regional stratigraphy (see Subsection 2.5.1.1.3).

2.5.1.1.2.3.4.2 Late Pleistocene Events (MIS 5-3)

The interpretations of the extent of glaciation during early and middle Wisconsinan time were revised based on new dating methods, and this is

now considered to have been an ice-free time in the site region. The ice sheet, which was thin and highly dynamic during this period, was present to the north in eastern Ontario but did not extend into the site region. Thermoluminescence dates for an ice-proximal glaciolacustrine unit near Toronto suggest an ice margin was present there between 60,000 and 75,000 years ago (MIS 4) (Reference 2.5.1-260).

Soil and stratigraphic information from studies in Illinois (Reference 2.5.1-261), Indiana (Reference 2.5.1-262), Michigan (Reference 2.5.1-263), Ohio (Reference 2.5.1-264; Reference 2.5.1-248), and southern Ontario (Reference 2.5.1-260; Reference 2.5.1-265; Reference 2.5.1-266) confirm that ice free conditions existed in the Great Lakes region for the period after the Illinoian and prior to the late Wisconsinan (MIS 5-3), a period of approximately 130,000 years.

In Illinois the Farmdale and Sangamon geosols developed during this time and are dated by the accumulation of cosmogenic Be-10 in the soil horizon (Reference 2.5.1-261).

2.5.1.1.2.3.4.3 Late Pleistocene Events (MIS 2)

The ice sheet had a major expansion between 25,000 and 15,000 years ago (BP), as indicated by the low sea-level stand and magnitude of the oxygen isotopic excursion of MIS 2 (Reference 2.5.1-267). The many glacial advances of the late Wisconsinan, also known as the Woodfordian Substage, are referred to as stades or stadials (assumed to be cold periods). Periods of ice retreat are referred to as interstadials and are assumed to be warmer (Reference 2.5.1-256) (Figure 2.5.1-215, Reference 2.5.1-256). However, ice lobes advance in response to dynamics of the ice sheet, which have large time lags, and do not respond concurrently to local climate (Reference 2.5.1-254).

The first late Wisconsinan advance of the Michigan lobe is dated at approximately 24,000 radiocarbon years BP (Reference 2.5.1-256). In Ontario (Reference 2.5.1-268) and in Ohio, the Ontario and Huron-Erie lobes reached their maximum extent between 23,000 and 21,000 years BP, respectively, during the Late Wisconsinan. The first advance into Ohio occurred shortly after 24,600 radiocarbon years BP (Reference 2.5.1-269, as cited in Reference 2.5.1-270). The outer moraines of the Scioto lobe are overlapping and suggest some oscillation in the ice front when it was in Ohio, approximately 21,400 years BP

(Reference 2.5.1-270). This was followed in Ohio by a withdrawal of ice referred to as the Erie Interstade, which occurred approximately 16,000 radiocarbon years BP. This period is documented by a lake that formed in the Erie basin as the ice retreated into Ontario. No forests developed on the deglaciated landscape during this time and there is no good radiocarbon control to document this interval. (Reference 2.5.1-268)

Post-Erie Interstade tills are silty and clayey (Reference 2.5.1-271). The fine-grained till matrix (Reference 2.5.1-268) as well as areas of preserved lake sediment in the subsurface are used to infer the former presence of a lake that was completely overridden by the subsequent ice advances. In Michigan all but the Saginaw lobe readvanced to near their former positions. This allowed the Huron/Erie and Michigan lobes to expand into the area vacated by the Saginaw lobe during Post-Erie Interstade events.

Following the retreat of Late Woodfordian ice from the Lake Erie basin about 14,500 years ago, a series of lakes formed at high levels. These lakes, commonly referred to as glacial or deglacial lakes, were direct ancestors of present Lake Erie. The lakes, which can be grouped into proglacial (ice-dammed) and nonglacial low lake phases, resulted from repeated ice-marginal readvances, crustal warping due to glacial unloading and reloading, and downcutting of lake outlets during the overall ice-sheet dissipation. (Reference 2.5.1-297) Strandline features and deposits associated with these deglacial lake levels in the Fermi 3 site vicinity are discussed in Subsection 2.5.1.2.3.2.1. The early lakes first resided in Lake Erie and later expanded into the Lake Huron basin when ice retreated north of Port Huron. The retreat of ice was oscillatory with major recessions during the Lake Erie Interstade (about 15.5 ka), the Mackinaw Interstade (about 13.2 ka), and the Two Creeks Interstade (about 11.9 ka). (Reference 2.5.1-272) Lewis et al. (Reference 2.5.1-272) provide a summary time-distance diagram of lake levels for the Late Wisconsinan through the Holocene (Figure 2.5.1-216, Reference 2.5.1-272).

2.5.1.1.2.3.4.4 Latest Pleistocene to Holocene Lake History and the Final Glacial Advances

During the next withdrawal of ice, referred to as the Mackinaw Interstade, most of the lower peninsula of Michigan was ice free (Reference 2.5.1-263). This was followed by another advance during the Port Huron Stade at about 13,000 years BP. Lakes that had formed

during the Mackinaw Interstade in the regional basins were forced to higher levels. Collectively referred to as Lake Whittlesey, these lakes occupied part of the Huron, Erie, and Saginaw basins. The tills of the Port Huron Stade are fine grained, and the lobes appeared to have fluctuated to create two closely spaced moraines. (Reference 2.5.1-263)

As ice retreated, a series of lower lakes formed in the Great Lakes basins with continuous and discernable shorelines and outlets. Retreat was far enough north to allow waters of Lake Superior, containing red clays, to spill into the waters of the more southerly Great Lakes. All subsequent advances through the Huron and Michigan basins were therefore tinted red with the clays of Lake Superior. (Reference 2.5.1-263)

The next to last advance occurred approximately 11,700 years BP and is called the Greatlakean Substage (Reference 2.5.1-273). This advance is well dated in eastern Wisconsin where the Two Creeks Forest Bed was sheared off by the advancing ice. The ice lobe responsible for this shearing occupied the northern half of the Lake Michigan basin, raised lake levels once more, deposited red clayey till in western Michigan, and shaped the drumlin fields of northwestern Michigan. (Reference 2.5.1-256)

An unnamed interstade followed and the lakes within the site region reached the Algonquin high stand (lake water level). Water was confluent across the Lower Peninsula of Michigan and through the Straits of Mackinac (Reference 2.5.1-274). This was followed by declining lake levels as waters found new, lower outlets to the north with continued ice retreat. Most drainage eventually found its way to the Ottawa River Valley, a marine estuary. When the area now occupied by North Bay, Ontario, became free of ice, the Great Lakes were lowered to levels below those of the present time because this outlet was isostatically depressed. It had an elevation of 35 m(115 ft) above sea level. (Reference 2.5.1-256)

The final advance of the ice from the Laurentide ice sheet occurred between 10,230 and 9,545 years BP and is known from its position on the Upper Peninsula of Michigan as the Marquette advance. However, this ice advance barely reached the northwest perimeter of the site region and was not the cause of a return to the high lake levels that followed. (Reference 2.5.1-263) Subsequent changes in level can be attributed to the effects of rebound, climate change, and elevation change of the outlets (Reference 2.5.1-274). This level, when Lakes Superior,

Michigan, and Huron were confluent, is referred to as the Nipissing Great Lakes (4,000 to 3,800 years BP). This was when the dramatic barrier dune complex was formed that rises to great elevation immediately east of the modern shore in western Michigan (Reference 2.5.1-256). Lake levels continued to stay high or rise in the Nipissing Great Lakes, partly because the Port Huron outlet (southern end of Lake Huron) continued to be uplifted during the Holocene relative to the southern shore of Lake Michigan. See Subsection 2.5.1.2.2.2 for additional description of the extent of lake levels in the site region and site vicinity.

2.5.1.1.3 Regional Stratigraphy

This subsection covers the succession of geologic units in the 320 km (200 mi) radius site region. No rocks older than Ordovician age are exposed in the site region (Figure 2.5.1-204). All the physiographic provinces in the 320 km (200 mi) site region contain similar sequences of Paleozoic sedimentary rocks with only local variations in rock types. In general, thicker rock sequences exist in the center of the cratonic basins and thin onto the intervening arches and domes (Reference 2.5.1-275). As all the physiographic provinces in the site region have roughly similar sedimentary rock sequences, and the site location is on the Michigan basin side of the Findlay arch, the Michigan basin stratigraphy will be highlighted in this section. A stratigraphic column of the Michigan basin is shown in Figure 2.5.1-217 (Reference 2.5.1-241).

2.5.1.1.3.1 Precambrian Stratigraphy

Precambrian units are not exposed at the surface in the site region. The ages and description of major basement terranes are discussed in Subsection 2.5.1.1.2.2.

Limited drilling data exists for the Precambrian. Drill holes around the periphery of the Michigan basin indicate that the Grenville metamorphic front forms a separation in the stratigraphy of the basement rocks. The basement east of the front along Lake Erie consists of granite, gneiss, and schists. West of the front, the basement rocks are comprised of granites, with areas of metamorphosed sediments in southwestern Michigan. Areas of quartzite are found in northeast Michigan. Granite along with granite detritus was encountered in wells in northwestern Michigan at the Beaver Islands. In the center of the Lower Peninsula, the Sparks well encountered late Precambrian Keweenawan sedimentary red beds. (Reference 2.5.1-276)

2.5.1.1.3.2 Paleozoic and Mesozoic Stratigraphy of the Michigan Basin

Fermi 3 is located on the west side of the Findlay arch and the southeastern margin of the Michigan basin (Figure 2.5.1-208 and Figure 2.5.1-218). The discussion of the regional stratigraphy presented in this section will focus on the Michigan basin; however, the stratigraphy of the neighboring Appalachian and Illinois basins are similar. Some of the units thin over the arches and thicken in the basin (Reference 2.5.1-277). To the east and outside of the site region in the Appalachian Basin, the stratigraphy is more complex resulting from being near the continental margin and the effects of the orogenic events mentioned in Subsection 2.5.1.1.2.3.1 (Reference 2.5.1-278). This subsection is subdivided based on the cratonic sequences established by Sloss (Reference 2.5.1-275).

Deposition during Paleozoic and Mesozoic was controlled by repeated transgressions and regressions of epeiric seas (seas on the continental shelf or interior) over the North American Craton (Reference 2.5.1-275). A craton is the more or less tectonically stable interior region of a continent (Reference 2.5.1-279). A transgression is when the seas expand over the continents and is related to either sea level rise or a lowering of the land surface elevation. A regression is the opposite of a transgression. During a regression, sea level drops, more of the craton is exposed, and a period of non-deposition and/or erosion occurs, forming a stratigraphic boundary known as an unconformity. Major regressions expose all but the margins of the craton and produce interregional unconformities that can be mapped throughout the craton. A cratonic sequence is defined as a package of sediments between two interregional unconformities. Six cratonic sequences are identified for the North American Craton beginning in the Proterozoic after the Grenville Orogeny (approximately 1 Ga) to the present. While each cratonic sequence represents a major transgression and regression, many smaller transgression-regression cycles can occur within a cratonic sequence. These smaller cycles produced smaller areas of non-deposition and/or erosion resulting in local unconformities. Each of the cratonic sequences has been subdivided into two or three subsequences defined by larger regional unconformities. The subsequences are identified with Roman numerals after the cratonic sequence name, with Roman numeral I representing the oldest subsequence. (Reference 2.5.1-275)

The boundaries of the cratonic sequences and the classical geologic time scale (Cambrian, etc) are not well correlated; for example, the end of the first cratonic sequence (Sauk) is in the Early Ordovician and not at the Cambrian-Ordovician boundary. The classical geologic time scale is a biostratigraphic correlation based on the occurrence of fossils and relates only marginally to tectonic changes. The exact time the sequence starts depends upon the location of the point of interest. (Reference 2.5.1-275)

Cratonic sequences first develop along the cratonic margins and progressively extend (transgress) toward the center of the craton, because it takes longer for the sea level to reach higher elevations (Reference 2.5.1-275). Initial sequence deposits usually begin with beach and shoreline deposits including conglomerates, sandstones, paleosols (buried soils), and coal. These deposits grade into shallow marine shales and marine carbonates (limestone and dolomite) and finally into deep marine black shales at the peak of the transgression. The regression reverses the order of the sediments from deep marine to shoreline facies. Erosion episode during the regression can remove some or most of the sediments deposited during the transgression. (Reference 2.5.1-280)

Five of the six cratonic sequences are recognized in the (320 km [200 mi] radius) site region: Sauk (Cambrian to Early Ordovician), Tippecanoe (Middle Ordovician to Late Silurian), Kaskaskia (Early Devonian to Mississippian), Absaroka (Mississippian to Permian), and Zuni (Jurassic) (Reference 2.5.1-262). The youngest rocks (Middle Jurassic Ionia Formation of the Zuni sequence) in these cratonic sequences are found in the center of the Michigan basin (Figure 2.5.1-217) (Reference 2.5.1-241).

2.5.1.1.3.2.1 Sauk Cratonic Sequences

The Sauk cratonic sequence includes the Lower Cambrian to Lower Ordovician rocks and is subdivided into three subsequences (Reference 2.5.1-275). No rocks associated with the oldest Sauk I cratonic sequence have been recognized in the Michigan basin (Reference 2.5.1-276).

The Sauk II cratonic sequence includes Middle to Upper Cambrian rocks (Reference 2.5.1-275). The base of this sequence is the Mount Simon Sandstone composed of pink arkosic sandstone at the base and white subrounded sandstone near the top. This formation is over 458 m (1500

ft) thick (Reference 2.5.1-277). Above the Mount Simon is the Eau Claire Formation, which consists of sandstone, shale, and dolomite up to 61 m (200 ft) thick (Reference 2.5.1-281). The upper unit in the Sauk II sequence is the Galesville Sandstone, which is white sandstone that grades eastward into dolomitic sandstone and is up to 61 m (200 ft) thick (Reference 2.5.1-276). The Michigan basin during the Sauk II sequence differs from the following sequences by having two separate depocenters. A depocenter is the locus of deposition marked by the thickest sedimentary deposits during a sequence. The northern depocenter was in about the center of the lower peninsula of Michigan and the southern depocenter was shared with the Illinois basin. (Reference 2.5.1-276)

The Sauk III cratonic sequence includes the Upper Cambrian and Lower Ordovician (Reference 2.5.1-275). The basal unit is the Franconia Formation, which is shaly sandstones and dolomites that are up to 61 m (200 ft) thick (Reference 2.5.1-281). This is overlain by the Trempealeau Formation which is a dolomite with minor amounts of sandy or shaly dolomite (Reference 2.5.1-277). The Trempealeau Formation is over 92 m (300 ft) thick. Above the Trempealeau is the Prairie du Chien Group consisting of tan to white dolomite and zones of oolitic chert and sandstone (Reference 2.5.1-281). The upper unit in the Prairie du Chien Group is the Foster Formation, a dark shaly dolomitic siltstone (Reference 2.5.1-281). The Prairie du Chien Group including the Foster Formation is up to 762 m (2,500 ft) thick in the center of the Michigan basin (Reference 2.5.1-281). The top of the Sauk III sequence is unclear. In the western portion of the Michigan basin, an unconformity exists above the Prairie du Chien Group; while in the center of the basin the units appear continuous across the boundary. (Reference 2.5.1-276) The top of the Foster Formation is used as the upper boundary for the Sauk III sequence in this report. The center of the Michigan basin may have continued as a locus of deposition between the Sauk III and Tippecanoe I sequences. (Reference 2.5.1-276)

2.5.1.1.3.2.2 Tippecanoe Cratonic Sequences

The Tippecanoe cratonic sequence begins in the Lower Ordovician and extends into the Lower Devonian and is subdivided into two subsequences (Reference 2.5.1-275). The Tippecanoe I sequence extends from the Lower Ordovician to the top of the Upper Ordovician (Reference 2.5.1-275). The basal unit of the Tippecanoe I sequence is

the Ordovician St. Peter Sandstone, a sandstone with clear to white rounded quartz grains (Reference 2.5.1-277). The St. Peter Sandstone is overlain by the Glenwood Formation which is comprised of sandy shale with interbeds of sandstone and limestone that is up to 30 m (100 ft) thick (Reference 2.5.1-262; Reference 2.5.1-281). Above the Glenwood is a sequence of limestone units which includes the Black River and Trenton limestones (Reference 2.5.1-281). The Black River Limestone is older than the Trenton Limestone, is composed of brown to gray micritic limestone with brown chert nodules, and is up to 153 m (500 ft) thick (Reference 2.5.1-277). The Trenton Limestone is a light brown to brown and gray fossiliferous limestone that is up to 168 m (550 ft) thick (Reference 2.5.1-277). The Trenton-Black River Interval is a petroleum producer in southern Michigan (Reference 2.5.1-282). Overlying the Trenton Limestone is a shale sequence including the Collingwood, Utica, and Queenstown shales (Reference 2.5.1-276). The Collingwood Shale is up to 18 m (60 ft) of limestone and shale (Reference 2.5.1-281). The Utica Shale is composed of gray to black shale that is up to 122 m (400 ft) thick (Reference 2.5.1-277). The upper shale unit, the Queenston Shale is up to 284 m (930 ft) of shale with some dolomite (Reference 2.5.1-281). The Utica and Queenston shales make up the Richmond Group (Figure 2.5.1-217) mark the top of the Tippecanoe I sequence (Reference 2.5.1-276).

The Tippecanoe II sequence begins at the base of the Silurian and extends into the Lower Devonian (Reference 2.5.1-275). The rocks encountered during Fermi 3 subsurface investigation are part of the Tippecanoe II sequence. The basal unit of this sequence is the Manitoulin Dolomite which is comprised of gray to buff-weathering dolomite at the surface and limestone in the subsurface and is up to 15 m (50 ft) thick (Reference 2.5.1-281). The Manitoulin Dolomite is overlain by about 24 m (80 ft) of red, greenish-gray, and gray shales of the Cabot Head Shale (Reference 2.5.1-277). Above the Cabot Head Shale is a series of dolomites and argillaceous dolomites of the Niagara Group (Reference 2.5.1-281). At this time barrier reefs surrounded the Michigan Basin and pinnacle reefs developed toward the center of the basin from the barrier reefs (Reference 2.5.1-276). The development of the pinnacle reefs may have extended into the lower part of the Salina Group (Reference 2.5.1-283). The Salina Group overlays the Niagara Group and has been subdivided into a series of units given letter designations A through G. From the base, Units A-1 and A-2 are carbonates overlying

evaporate units. Units B, D and F are predominantly salts with shale and anhydrite interbeds in the center of the Michigan basin. At the margin of the basin the salt layers are thin or absent. Units C and G are gray to greenish gray to gray shales, and Unit E is a sequence of green, gray, and red shale and carbonate with anhydrite beds. (Reference 2.5.1-277) The upper unit in the Tippecanoe II sequence is the Bass Islands Group which is dominantly light gray dolomite with minor shale bands and anhydrite (Reference 2.5.1-267). This Bass Islands Group is up to 183 m (600 ft) thick in the center of the Michigan basin (Reference 2.5.1-284).

The Tippecanoe cratonic sequence represents a time of well established epeiric seas over the craton and the development of reefs that restricted water flow between cratonic basins. The formation of salt beds in the upper Tippecanoe II sequence is controversial with some researchers favoring deep basins with restricted water movement and others favoring tidal flats and possibly sabkhas (Reference 2.5.1-276). During minor regressions, the topographically higher areas on the Findlay arch would have been exposed and the evaporate deposits would be dissolved by fresh water (Reference 2.5.1-284).

2.5.1.1.3.2.3 Kaskaskia Cratonic Sequence

The Kaskaskia cratonic sequence includes the Devonian and most of the Mississippian and is subdivided into two subsequences (Reference 2.5.1-275). The Kaskaskia I sequence includes all but the uppermost Devonian units exposed in Michigan (Reference 2.5.1-276). The basal unit of this sequence is the Bois Blanc Formation which is comprised of cherty dolomite that is about 110 m (360 ft) thick (Reference 2.5.1-281). The Bois Blanc Formation is overlain by the Detroit River Group, which contains from oldest to youngest the Sylvania Sandstone, the Amherstburg Formation, and the Lucas Formation. The thickness of the Detroit River Group varies from 6 to 305 m (20 to 1,000 ft). The Sylvania Sandstone is comprised of well rounded and sorted fine- to medium-grained sandstone with silt, chert, and carbonate and is up to 6 m (20 ft) thick (Reference 2.5.1-277). The Amherstburg Formation is comprised of black to dark brown fossiliferous dolomite and is up to 99 m (325 ft) thick (Reference 2.5.1-277). The Lucas Formation is comprised of salt, dolomite, anhydrite, and sandstone and the thickness varies from 6 to 305 m (20 to 1,000 ft) (Reference 2.5.1-277). The Detroit River Group is overlain by the Dundee Limestone which is a buff to brown limestone to bioclastic limestone that is from 30 to 122 m (100 to 400 ft)

thick (Reference 2.5.1-276; Reference 2.5.1-281). Above the Dundee Limestone is the Traverse Group, which is subdivided into the older Bell Shale, the Traverse Limestone, and the Traverse Formation. The Bell Shale is up to 24 m (80 ft) of gray fossiliferous shale (Reference 2.5.1-281), and the Traverse Limestone is gray limestone and dolomite that grades eastward into shale (Reference 2.5.1-277). The Traverse Formation is interbedded gray to black shales and limestone (Reference 2.5.1-277). The Traverse Group is overlain by the Antrim Shale, which is composed of black to brown, hard, fissile, pyritic, organic-rich shale that is up to 305 m (1,000 ft) thick in northern Michigan (Reference 2.5.1-277; Reference 2.5.1-276). The Antrim Shale grades upwards into the Ellsworth Shale, which is composed of gray-green shale that is up to 244 m (800 ft) thick (Reference 2.5.1-281). The Ellsworth Shale is found on the west side of the Michigan basin and grades into the Bedford Shale to the east. The Bedford Shale is composed of gray shale that is up to 61 m (200 ft) thick. (Reference 2.5.1-277) The top of the Kaskaskia I sequence is placed at the top of the Bedford and Ellsworth shales (Reference 2.5.1-276).

The Kaskaskia II cratonic sequence includes the Upper Devonian and most of the Mississippian in the Michigan basin (Reference 2.5.1-275). The basal unit is the Berea Sandstone, which is up to 30.5 m (100 ft) of light gray sandstone interbedded with gray shales (Reference 2.5.1-281). According to the stratigraphic lexicon of Catacosinos et al. (Reference 2.5.1-281) the Berea Sandstone is Late Devonian placing the beginning of the Kaskaskia II sequence in the Devonian. The Berea Sandstone is overlain by up to 30.5 m (100 ft) of organic-rich black shale. This shale is called the Sunbury Shale, which is overlain by gray, bluish gray, and reddish fossiliferous shale with interbeds of red limestone and dolomite of the Coldwater Shale. (Reference 2.5.1-281) The Coldwater Shale is up to 335 m (1,100 ft) thick in the center of the basin and thins toward the margins to 152.5 m (500 ft) thick at the eastern margin of the basin (Reference 2.5.1-277). The Coldwater Shale is overlain by the Marshall Sandstone, which is comprised of red, tan, and green sandstone, siltstone, and micaceous sandstone and is up to 76 m (250 ft) thick (Reference 2.5.1-281). Above the Marshall Sandstone is the Michigan Formation which is comprised of gray and greenish gray shale, limestone, dolomite, anhydrite, gypsum, and sandstone that is up to 106 m (350 ft) thick (Reference 2.5.1-277; Reference 2.5.1-281). The upper unit of the Kaskaskia II sequence is the Bayport Limestone, which is

comprised of light to dark gray fossiliferous limestone and gray to tan cherty limestone (Reference 2.5.1-277). The Bayport Limestone is up to 30 m (100 ft) thick (Reference 2.5.1-277). Due to erosion, this unit is absent in parts of the Michigan basin (Reference 2.5.1-276).

2.5.1.1.3.2.4 Absaroka Cratonic Sequence

The Absaroka cratonic sequence begins in the Upper Mississippian, extends into the Lower Jurassic and is subdivided into three subsequences (Reference 2.5.1-275). In the Michigan basin, only the Absaroka I sequence is exposed and contains Upper Mississippian and Pennsylvanian rocks (Reference 2.5.1-276). The Pennsylvanian System in the Michigan basin is comprised of two units, the Saginaw and Grand River Formations, and has a maximum thickness of 233 m (765 ft) (Reference 2.5.1-277). The basal unit is the Parma Sandstone, which is coarse-grained quartzose sandstone of Late Mississippian age (Reference 2.5.1-281). Overlying the Parma Sandstone is the Saginaw Formation, which is comprised of interbedded sandstone, shale, limestone, and coal (Reference 2.5.1-277). The Saginaw Formation consists of both marine and non-marine units. The Saginaw Formation is overlain by the Grand River Formation, which is predominantly sandstone and difficult to distinguish from the Saginaw Formation (Reference 2.5.1-277; Reference 2.5.1-276).

2.5.1.1.3.2.5 Zuni Cratonic Sequence

The Zuni cratonic sequence begins in the Lower Jurassic and extends into the Paleocene and is subdivided into three subsequences (Reference 2.5.1-275). In the Michigan basin, only the Zuni I sequence is observed; the sequence is Jurassic in age (Reference 2.5.1-276), and is solely the Ionia Formation (Reference 2.5.1-281). The Ionia Formation is comprised of up to 120 m (400 ft) of poorly consolidated, red sandstones and shales along with some gypsum of terrestrial origin (Reference 2.5.1-277). These units were deposited in valleys cut into the Pennsylvanian age rocks (Reference 2.5.1-276).

2.5.1.1.3.3 Quaternary Stratigraphy

The oldest Quaternary features preserved in the 320 km (200 mi) site region are deeply incised bedrock valleys and their associated valley fills. Originally assigned to the Tertiary, these bedrock valleys are now considered to be early to middle Pleistocene in age. They occur at two

main elevations and are referred to as the Teays (Subsection 2.5.1.1.2.3.4.1) and the Deep Stage valleys (Reference 2.5.1-270). In Ohio these valleys are buried by Illinoinan and younger glacigenic sediment, and the trend of the valleys affected glacial advances (Reference 2.5.1-270).

Regionally, the oldest glacial sediment is interpreted to be Illinoian in age and generally lies directly on bedrock, although scattered occurrences of older glacial sediment are mentioned (e.g., Reference 2.5.1-270). Illinoian tills in Ohio are the Gahanna, Millbrook, and Chesterville tills. The tills are patchy and are associated with a bedrock surface having significant relief (Reference 2.5.1-270). In Ontario the Illinoian-age tills include the Bradtville, the browntill at Gowanda, the lowermost till at Guelph (Reference 2.5.1-265), the Sunny Point member of the Sunnybrook Formation (Reference 2.5.1-266), and the Don York Till (Reference 2.5.1-285). These tills lie on bedrock and were deposited by ice that had advanced into the eastern Lake Erie basin (Reference 2.5.1-270).

The subsequent early to middle Wisconsinan sediments are glaciolacustrine silts and clays of the Tyrconnell Formation deposited in a proglacial lake in the Erie basin (Reference 2.5.1-266). These glaciolacustrine deposits are overlain by the late Wisconsinan Catfish Creek till at the type section for the Tyrconnell Formation (Reference 2.5.1-265). In other places in Ontario the uppermost till overlying glaciolacustrine deposits is the Halton (Reference 2.5.1-268).

Significant soil development is a good criterion for identifying the ice-free period following Illinoian glaciation. As discussed in Subsection 2.5.1.1.2.3.4.2, evidence of a long ice-free period during the early to middle Wisconsinan is well documented. Generally, older tills with soil development that previously were interpreted as being early to middle Wisconsinan are increasingly relegated to the Illinoian. Tills above the Sangamon soil are designated as late Wisconsinan in age. Problem sections in Ohio involve glacigenic deposits that show soil development observed above what has been called the Sangamon soil (MIS 5). It is not certain if these represent early or middle Wisconsinan tills. (Reference 2.5.1-262; Reference 2.5.1-264)

In Illinois, northwestern Indiana, and Ohio, the texture of the surface tills varies systematically, with older tills having a coarser matrix texture (loamy to sandy) and younger tills having a more clayey matrix. The

clayey texture evolved with the second regional advance of the late Wisconsinan as ice incorporated lacustrine clay as it readvanced through proglacial lake basins (Reference 2.5.1-247; Reference 2.5.1-248).

2.5.1.1.4 Regional Tectonic Setting

The seismotectonic framework of a region, which includes the basic understanding of existing tectonic features and their relationship to the contemporary stress regime and seismicity, forms the foundation for assessments of seismic sources. In January 2012, the Electric Power Research Institute/U.S. Department of Energy/U.S. Nuclear Regulatory Commission (EPRI/USDOE/USNRC) published as NUREG-2115 the Central and Eastern United States Seismic Source Characterization (CEUS SSC) model (Reference 2.5.1-286) for use in assessing seismic hazard at nuclear facilities. As discussed in Subsection 2.5.2, the CEUS SSC model is used as the basis for characterizing the seismic hazard at the Fermi 3 site. The CEUS SSC model incorporates the latest knowledge of the geosciences community on seismic hazards in the CEUS. This section presents a summary of the current state of knowledge on the tectonic setting of the Fermi 3 site. The information presented in this section is relevant to characterization of seismic sources that was used in the development of the CEUS SSC model.

The following sections describe the region in terms of (1) the contemporary tectonic stress environment (Subsection 2.5.1.1.4.1); (2) regional geophysical data sets that have been used to evaluate basement geology and structures (Subsection 2.5.1.1.4.2); (3) primary structural provinces and tectonic features within the 320 km (200 mi) radius of the site (Subsection 2.5.1.1.4.3); and (4) significant seismic sources at distances greater than 320 km (200 mi) (Subsection 2.5.1.1.4.4). Prehistoric, historical, and instrumental seismicity is shown on Figure 2.5.1-207 and is described in Subsection 2.5.1.1.4.3 and Subsection 2.5.1.1.4.4. The historical and instrumental earthquake catalog for the Fermi 3 site is updated from the CEUS SSC earthquake catalog presented in NUREG-2115 (Reference 2.5.1-286), and is described in Subsection 2.5.2.1.

2.5.1.1.4.1 Contemporary Tectonic Stress Environment

Fermi 3 lies within a compressive midplate stress province, characterized by a relatively uniform east-northeast compressive stress field that extends from the midcontinent east toward the Atlantic continental

margin and possibly into the western Atlantic basin (Reference 2.5.1-287). Zoback and Zoback (Reference 2.5.1-287) note that although localized stresses may be important in places, the overall uniformity in the midplate stress pattern suggests a far-field source, and the range in orientations coincides with both absolute plate motion and ridge push directions for North America. Modeling of various tectonic processes using an elastic finite-element analysis has indicated that distributed ridge forces are capable of accounting for the dominant east-northeast trend of maximum compression throughout much of the North American Plate east of the Rocky Mountains (Reference 2.5.1-288).

Based on analysis of well-constrained focal mechanisms of North American midplate earthquakes, Zoback (Reference 2.5.1-289) concludes that earthquakes in the CEUS occur primarily on strike-slip faults that dip between 43 and 80 degrees, primarily in the range of 60 to 75 degrees and primarily in response to a strike-slip stress regime. This is indicated by a more recent compilation of worldwide stress information that shows east-northeast-oriented maximum horizontal compression and strike-slip events within the study region (Reference 2.5.1-290) (Figure 2.5.1-219). The World Stress Map displays the orientations of the maximum horizontal compressive stress S_H. The length of the stress symbols represents the data quality, with A being the best quality. Quality A data are assumed to record the orientation of S_H to within 10 to 15 degrees, quality B data to within 15 to 20 degrees, and quality C data to within 25 degrees. Quality D data are considered to give questionable tectonic stress orientations (Reference 2.5.1-290).

2.5.1.1.4.1.1 Glacial Isostatic Adjustments

Post-glacial rebound or glacial isostatic adjustment (GIA) is the response of the solid earth to changing surface loads brought on by the waxing and waning of large-scale ice sheets and glaciers. Tilting of relic lake shorelines, changes to modern lake levels, and secular (persisting for a long time) changes to surface gravity observations are manifestations of land uplift and subsidence brought about by GIA (Reference 2.5.1-291). GIA is suspected to be a cause of deformation within continental plates and may be a trigger of seismicity in eastern North America and other formerly glaciated regions (Reference 2.5.1-292). The spatial distribution of Holocene high seismicity areas in eastern North America is commonly explained by the isostatic stress perturbation in the lithosphere

associated with the melting of the Laurentide ice sheet about 19,000 – 8,000 years ago (Reference 2.5.1-484; Reference 2.5.1-485; Reference 2.5.1-292; Reference 2.5.1-460; Reference 2.5.1-480). Mazzotti and Adams (Reference 2.5.1-293), however, provide a discussion of this hypothesis and conclude that it is likely that only a very small percentage of the elastic postglacial rebound deformation translates into plastic deformation to produce earthquakes. Modeling of the strain and resulting changes in seismic stress caused by GIA in other areas (e.g., New Madrid seismic zone [Reference 2.5.1-460] and eastern Canada [Reference 2.5.1-293]) indicates that the effects on seismicity rates are expected to remain essentially unchanged over a few hundred to thousands of years. Therefore, it is not expected that seismicity rates in the site region will vary significantly in the future due to GIA.

Glacial and postglacial GIA in the study region is evidenced by deformation (tilting or warping) of glacial lake strandlines. Long-term average rebound information is most easily conveyed in plots of the elevation of a given shoreline across a distance (Reference 2.5.1-296). Figure 2.5.1-251 shows a summary plot of elevation versus distance of raised and uplifted shorelines of Lake Whittlesey and subsequent lake phases, as well as elevations of submerged features in the Lake Erie basin as compiled by Coakley and Lewis (Reference 2.5.1-296). Data for Lake Whittlesey in the Lake Erie basin yields a direction of maximum differential uplift of N24°E (Figure 2.5.1-251) and suggests that the post-Whittlesey change in elevation has been 52 m (171 ft) from Cleveland, Ohio to Buffalo, New York. Similarily, change in elevation since the lowest Lake Warren time has been about 43 m (141 ft) from Conneaut, Ohio to Buffalo and 66 m (217 ft) at its most northern point, 13 km (8.1 mi) north of Batavia, New York. (Reference 2.5.1-297)

Detailed mapping of strandlines and shoreline features related to glacial lakes provides information on the location of the ‘zero isobase’ (also referred to as the ‘hinge line’) for several individual relict lake strandlines (Reference 2.5.1-274; Reference 2.5.1-294; Reference 2.5.1-296). The zero isobase or hinge line as defined in early studies represents the general location of the boundary between a ‘zone of horizontality’ and zones of warping or relative uplift. Early rebound concepts of immediate rebound north of a “hinge-line” were eventually replaced, and it is now recognized that there was continued uplift and rebound over much of the region in the Holocene (Reference 2.5.1-295 and Reference 2.5.1-297).

Geodynamical models that predict how the viscous mantle of the earth moves under surface loads show that the glacioisostatic recovery with a northward migration of a collapsing forebulge for the Great Lakes is a more appropriate model (Reference 2.5.1-486).

In Michigan, the Lake Whittlesey, Lake Maumee, and Lake Arkona beaches were observed to rise northward from within an area located north of Detroit. The hinge line of the younger Lake Warren and Lake Wayne strands and of Lakes Grassmere and Lunday were recognized in the Lake Huron basin about 20 km (12.4 mi) and 117 km (72.7 mi) north of the Lake Whittlesey hinge line. (Reference 2.5.1-297).

Holcombe et al. (Reference 2.5.1-487) provide a revised Lake Erie postglacial lake level history based on new detailed bathymetry. Previous reconstructions (e.g., Reference 2.5.1-296; Reference 2.5.1-297) varied in detail and water levels, but shared the following salient features: (1) high lake level stages of proglacial lakes and Lake Algonquin followed by very low lake levels in early Holocene time; (2) isostatic rebound and concomitant gradual rise in lake levels in the early Holocene; (3) stable or slowly rising lake levels in Middle Lake Erie time; (4) rise in lake levels accompanying the Nipissing rise to slightly higher than at present; and (5) lowering of lake levels to just below present level following the Nipissing rise event. The reconstructions recognize that lake level has been controlled since deglaciation by isostatically rebounding outlet sills of the Niagara River, and that the Nipissing rise accompanied a shift in upper Great Lakes drainage from the North Bay outlet to the Port Huron outlet. In the new model, Holcombe et al. (Reference 2.5.1-487) note that in an isostatically rebounding lake, lake level histories vary with location, especially as a function of distance from the outlet sill. A new feature of the model is a proposed extended period of low lake level in the middle Holocene (9 – 6 ka), when lake level was controlled not by the level of the outlet sill, but by climate and water budget. Also contributing to a low water level during this time was flooding of the central basin of Lake Erie as isostatic rebound continued, greatly increasing lake surface area and concomitantly increasing surface evaporation. At the time of the Nipissing rise (5,400 – 3,600 years ago), water level in eastern Lake Erie was 4 – 5 m (13 – 16.4 ft) higher than present. The western subbasin was flooded, but water level was about 3 m (10 ft) below present lake level.

Larsen (Reference 2.5.1-274) reviewed various historical measurements and concluded that uplift continues to the present. In Lake Erie the

directional trend in uplift does not strictly correlate with those of proposed isostatic rebound, but is very small (less than 64 mm/century) (Reference 2.5.1-297). The main control on the level of Lake Erie now is the elevation of the Onondaga Limestone at Buffalo, New York (Reference 2.5.1-297), which is located 25 km (15.5 mi) upriver from Niagara Falls and has experienced some uplift . The outflow through the Niagara appears to have been variable; retreat of the falls is estimated to have been 1.6 m (5.25 ft) per year since its inception 12,400 years ago and 1.1 m/yr (3.6 ft/yr) between 1670 and 1969 (Reference 2.5.1-297). Lake level was lowered several meters during the interval 3,600 – 3,000 years ago by headward erosion of the Niagara gorge. In the western basin, water level did not fall significantly because lower water level at the sill was partially compensated by differential isostatic rebound in the west. (Reference 2.5.1-487)

Motions from 360 Global Positioning System (GPS) sites in Canada and the United States yield a detailed image of present-day vertical and horizontal velocity fields within the nominally stable interior of the North American Plate (Reference 2.5.1-291) (Figure 2.5.1-253 and Figure 2.5.1-254). Sella et al. (Reference 2.5.1-291) note that by far the strongest signal is the effect of GIA due to ice mass unloading during deglaciation. Vertical velocities show present-day uplift (approximately 10 mm/yr) near Hudson Bay, the site of thickest ice at the last glacial maximum. The uplift rates generally decrease with distance from Hudson Bay and change to subsidence (1 to 2 mm/yr) south of the Great Lakes. The hinge line marking the approximate boundary between regions of vertical rebound to the north and subsidence to the south lies close to the northern margin of the site region. The site lies at the southern margin of the region affected by GIA. The residual velocity field indicates subsidence (1 to 2 mm/yr) throughout most of the site region with possible minor uplift near the western end of Lake Erie (Reference 2.5.1-291).

Monitoring of present-day tilting of the Great Lakes region based on water level gauges illustrates uplift in the northeast and subsidence in the south, indicating a pattern of land tilting upward to the northeast consistent with expected GIA (Reference 2.5.1-298). The data are consistent with the geodetic data that show the Fermi 3 site and surrounding region is not characterized by strong vertical gradients or anomalies.

2.5.1.1.4.2 Regional Geophysical Data

Regional gravity and magnetic survey maps are important data sets that in conjunction with borehole data and regional seismic profile surveys have been used to decipher major structural and rheological boundaries within the basement underlying the site region.

2.5.1.1.4.2.1 Gravity and Magnetic Survey Data and Maps

Regional gravity and magnetic survey data and derivative maps are used to study the basement geology of the midcontinent region, including the lithology and depth of basement rocks and the location and origin of basement structures. Patterns and lineaments on gravity maps are used to infer faults, structure boundaries, and the boundaries between basement provinces. Strong magnetic anomalies are used to infer basalt and related mafic igneous rock which are often associated with basement rifts.

Portions of the Gravity Anomaly Map of North America (Reference 2.5.1-299) and the Magnetic Anomaly Map of North America (Reference 2.5.1-300) covering the site region are reproduced as Figure 2.5.1-220 and Figure 2.5.1-221, respectively. Several prominent gravity anomalies are shown on Figure 2.5.1-220, including the Mid-Michigan Gravity Anomaly (MGA), the East Continent Gravity High (ECGH), the Anorthosite Complex Anomaly (ACA), the Seneca anomaly, and the Butler anomaly (Reference 2.5.1-301; Reference 2.5.1-302; Reference 2.5.1-227; Reference 2.5.1-303).

The MGA, located in the southern peninsula of Michigan, is associated with the midcontinent gravity anomaly, which extends southwestward from Lake Superior. Both anomalies are associated with the Midcontinent Rift System (MRS) and are characterized by a strong, curvilinear gravity high flanked by gravity lows, and both are associated with magnetic highs (Reference 2.5.1-301).

The ECGH is a chain of positive gravity anomalies from southwestern Michigan to north-central Tennessee (Reference 2.5.1-227). It is associated with the East Continent Rift System (ECRS), which may be related to the MRS, as discussed in Subsection 2.5.1.1.2.2.4.

The Anorthosite Complex anomaly of southern Ohio was described by Lucius and von Frese (Reference 2.5.1-302) as an oblong gravity and magnetic maximum that, based on modeling, was interpreted as an anorthosite body at intermediate crustal depths. Subsequent modeling by

Harbi supports this hypothesis and suggests that the anorthosite body dips 8 degrees to the east at midcrustal depths (Reference 2.5.1-303).

The Seneca anomaly, located in northeastern Ohio, is visible on Figure 2.5.1-220 and Figure 2.5.1-221 as a circular magnetic and gravity high. Based on gravity and magnetic modeling, Lucius and von Frese (Reference 2.5.1-302) interpreted the Seneca anomaly as a shallow gabbroic intrusion surrounded by a large, homogeneous granitic body. This model was later confirmed by the presence of gabbro in a core drilled by the Ohio Department of Natural Resources (Reference 2.5.1-303).

The Butler anomaly of southwestern Ohio is visible on Figure 2.5.1-220 as a large, positive circular gravity and magnetic maximum. It was first modeled by Lucius and von Frese (Reference 2.5.1-302) as a crystallized magma chamber that extends to intermediate crustal depths. Harbi (Reference 2.5.1-303) interpreted it as a cylindrical mafic batholith.

Regional gravity and magnetic data sets are used to identify crustal boundaries and lineaments (Reference 2.5.1-301; Reference 2.5.1-228; Reference 2.5.1-304; Reference 2.5.1-305). Hinze et al. (Reference 2.5.1-301) interpreted the boundary between the Penokean and Granite-Rhyolite provinces to lie between 43 and 44 degrees latitude based on the east-southeast-trending anomalies in the Penokean province and the broad positive gravity anomaly with local positive magnetic anomalies in the Granite-Rhyolite province. Atekwana (Reference 2.5.1-228) noted that the Penokean province is characterized by high-frequency, high-amplitude gravity and magnetic anomalies, whereas the Eastern Granite-Rhyolite province is characterized by northwest-southeast-trending lower-frequency and lower-amplitude anomalies. Atekwana (Reference 2.5.1-228) identified a lineament separating these two provinces based on regional data sets and their derivative maps. The boundary between the Penokean and Granite-Rhyolite provinces is a transition zone and is not well constrained (Reference 2.5.1-301). Figure 2.5.1-220 illustrates the boundary interpreted by Van Schmus (Reference 2.5.1-210).

The location of the Grenville Front Tectonic Zone (GFTZ) has been placed in several locations. In Michigan, Hinze et al. (Reference 2.5.1-301) interpreted areas of positive, northeast-southwest-trending gravity and magnetic anomalies as characteristic of the Grenville province consistent with the trend of

anomalies of exposed Grenville province rocks in Ontario. Lucius and von Frese (Reference 2.5.1-302) placed the GFTZ west of the anorthosite anomaly based on their model that the Anorthosite Complex anomaly was uplifted during the Grenville orogeny after forming in the deep crust. Atekwana (Reference 2.5.1-228) characterized the Grenville province as having higher-amplitude and higher-frequency magnetic anomalies that trend northwest to north in Kentucky, Ohio, and southeastern Michigan, and north-northeast in southwestern Ontario. Easton and Carter (Reference 2.5.1-306) interpreted the location of the GFTZ by incorporating these results with deep seismic profiles and borehole data, as described in the following section (Subsection 2.5.1.1.4.2.2).

In the western third of Ohio, the gravity and magnetic models of Lucius and von Frese (Reference 2.5.1-302) indicate high-density, low-magnetization intrusions into lower and middle crustal depths associated with the MRS. Drahovzal et al. (Reference 2.5.1-227) later postulated that these anomalies are associated with the East Continent Rift Basin (ECRB) and were overprinted by the GFTZ.

Within the Grenville province, Carter et al. (Reference 2.5.1-304) correlated regional west-northwest- to northeast-trending magnetic anomalies with deformed, magnetite-bearing plutons in southwestern Ontario, Canada, and concluded that the trends are associated with the strikes of gneissic layering and fold axes. Boyce and Morris (Reference 2.5.1-305) identified northeast-trending lineaments that parallel the Central Metasedimentary Belt Boundary Zone (CMBBZ), northwest-trending lineaments that parallel Georgian Bay and Lake Huron, and east-west geophysical anomalies that parallel Lakes Erie and Ontario.

2.5.1.1.4.2.2 Seismic Profiles

The Consortium for Continental Reflection Profiling (COCORP) and the Great Lakes International Multidisciplinary Program on Crustal Evolution (GLIMPCE) collected a series of seismic lines in the midcontinent region (Figure 2.5.1-213).

Several deep seismic lines transect the MRS COCORP lines MI-1, MI-2, and MI-3 were located in the center of the Michigan basin, near the deep McClure-Sparks oil well to aid in the correlation of stratigraphy. Brown et al. (Reference 2.5.1-235) interpreted this data with limited success as

poor data quality obscured structural relationships. Zhu and Brown later reprocessed and reinterpreted these lines, concluding that the MRS is poorly imaged as a south-dipping rotated block (Reference 2.5.1-307). The MRS is exposed at the surface surrounding Lake Superior and is therefore well imaged by GLIMPCE lines (Reference 2.5.1-308; Reference 2.5.1-236). Interpretation of the GLIMPCE lines A, C, and F in Lake Superior show a segmented rift structure composed of inverted, normal faulted asymmetric half grabens separated by zones of accommodation (faults transverse to rift axis) (Reference 2.5.1-236).

The Granite-Rhyolite province was imaged in COCORP line IL-1 in Illinois, IN-1 in Indiana and in the western portion of COCORP line OH-1, in Ohio (Reference 2.5.1-238). The seismic data in lines IL-1, IN-1, and OH-1 reveal discontinuous, subhorizontal reflectors that can be traced laterally for up to 80 km (49 mi) and that are as thick as 11 km (6.7 mi). Pratt et al. (Reference 2.5.1-238) interpreted these reflectors as felsic igneous rocks underlain or intermixed with mafic igneous or sedimentary rocks. This discontinuous layering is absent in COCORP lines MO-1 and IL-2, which transect the Proterozoic caldera complexes of the St. Francois Mountains.

The GFTZ and the Grenville province are imaged by COCORP lines OH-1 and OH-2 in central Ohio (Reference 2.5.1-238; Reference 2.5.1-234; Reference 2.5.1-309) and GLIMPCE lines I and J in Lake Huron (Reference 2.5.1-216; Reference 2.5.1-310). Green et al. (Reference 2.5.1-216) interpreted the GFTZ as a 32 km (19.5 mi) wide, steeply dipping zone of east-dipping reflections. After reprocessing these data, Mereu et al. (Reference 2.5.1-310) interpreted these reflectors as mylonite zones associated with ductile faulting. Pratt et al. (Reference 2.5.1-238) interpreted east-dipping parallel reflectors as the GFTZ in Ohio. Farther east in line OH-2, the Grenville province is characterized by west-dipping, mid- to deep-crustal reflectors (Reference 2.5.1-238) (Figure 2.5.1-221). Culotta and Pratt (Reference 2.5.1-234) later synthesized these results (Figure 2.5.1-222) and interpreted the GFTZ as a 50 km (30 mi) wide, 25- to 30-degree east-dipping zone penetrating to 25 km (15 mi) deep, attributing the west-dipping reflectors to the CMB. Easton and Carter (Reference 2.5.1-306) combined this data with results of drill data in southwestern Ontario and interpreted the location of the GFTZ (Figure 2.5.1-203, Figure 2.5.1-220, and Figure 2.5.1-221).

GLIMPCE line H, which transects Lake Michigan, images structures and basement terrane boundaries associated with the Penokean orogeny as illustrated on Figure 2.5.1-210 and Figure 2.5.1-213 (Reference 2.5.1-213; Reference 2.5.1-300) (see Subsection 2.5.1.1.2.2.1).

2.5.1.1.4.3 Regional Tectonic Structures (within 320 km [200 Mi] Radius)

The Fermi 3 site is located in the stable continental region of the North American Craton, which is characterized by low earthquake activity and low stress (Reference 2.5.1-311; Reference 2.5.1-312; Reference 2.5.1-313; Reference 2.5.1-314) (Figure 2.5.1-207). The site lies within the Central Stable Region tectonic province of the North American continent (Reference 2.5.1-212). This tectonic province is characterized by a thick sequence of sedimentary strata overlying the Precambrian basement. The Precambrian basement is exposed in Wisconsin, Minnesota, the upper peninsula of Michigan, and Ontario, Canada. As described in Subsection 2.5.1.1.4.1, regional geophysical data have been used to infer the major structural and rheological boundaries within subsurface basement in the site region.

The (320 km [200 mi] radius) site region lies within a transition zone between the central Appalachian foreland and the Illinois and Michigan interior cratonic basins; this transition zone contains a variety of structural features that were intermittently active throughout the entire Paleozoic. Basement faults in this zone were initiated, in part, by Precambrian plate convergent episodes at the margin of Laurentia and were reactivated throughout the Paleozoic, principally as growth faults of modest displacement. Deformational loads that accumulated at the Laurentian plate margin during the Taconic and Alleghenian orogenies in the central Appalachians created arches in the site region. (Reference 2.5.1-213) There is no evidence to indicate that reactivation of structures in the Mesozoic, such as occurred in the New Madrid seismic zone to the southwest, occurred within the site region.

The Fermi 2 UFSAR (Reference 2.5.1-221) concluded that there were no capable tectonic faults within the Fermi 2 site region. Recent reviews of suspected Quaternary tectonic features in the CEUS by Crone and Wheeler (Reference 2.5.1-316) and Wheeler (Reference 2.5.1-317) did not identify any Class A Quaternary tectonic faults or Class B tectonic features in the site region. Crone and Wheeler (Reference 2.5.1-316)

define Class A features as those where geologic evidence demonstrates the existence of a Quaternary fault of tectonic origin. Class B features are those where the fault may not extend deeply enough to be a potential source of significant earthquakes, or where the currently available geologic evidence is not definitive enough to assign the feature to Class C or to Class A. Class C features are those for which geologic evidence is insufficient to demonstrate the existence of a tectonic fault, Quaternary slip, or deformation associated with the feature. Crone and Wheeler (Reference 2.5.1-316) identify two Class C seismic zones in the site region that are described below in Subsection 2.5.1.1.4.3.3. The CEUS SSC study (Reference 2.5.1-286) does not identify any Repeated Large Magnitude Earthquake (RLME) seismic sources within 320 km (200 mi) of the Fermi 3 site.

A description of major basins and arches in the site region is provided in Subsection 2.5.1.1.4.3.1; specific tectonic features and structures are described in Subsection 2.5.1.1.4.3.2; and seismic zones in the site region are described in Subsection 2.5.1.1.4.3.3.

2.5.1.1.4.3.1 Basins and Arches

Intracratonic basins and bounding arches developed in the (200 mi-radius) site region during the Paleozoic (570 – 250 Ma) and include the Michigan, Illinois, and Appalachian basins, and the Cincinnati, Kankakee, Findlay, and Algonquin arches (Figure 2.5.1-208 and Figure 2.5.1-218). The most significant with respect to the site are the Michigan basin and the Findlay and Algonquin arches. In addition to these structures, the now outdated name “Washtenaw Anticlinorium” was proposed by Ells (Reference 2.5.1-318) to describe a broad northwest plunging structure in southeast Michigan and was discussed in the Fermi 2 UFSAR (Reference 2.5.1-221). As defined, local structures included within this broad structural feature are the Bowling Green (Lucas-Monroe) fault/anticline (northern segment) and the Howell (Howell-Northville) anticline/fault described in Subsection 2.5.1.1.4.3.2.

2.5.1.1.4.3.1.1 Michigan Basin

The intracratonic Michigan basin is nearly circular, about 400 km (240 mi) in diameter, and 5 km (3 mi) deep. The basin exhibits only minor syndepositional (contemporaneous with sedimentation) faulting that has an insignificant effect on basin-scale geometry of stratigraphic units (Reference 2.5.1-240). The proto-Michigan basin developed in the Late

Cambrian with the deposition of the Mount Simon Sandstone in an elongate trough, possibly representing a northern continuation of the Reelfoot rift – Illinois basin (Reference 2.5.1-240). Basin-centered subsidence began in the Early to Middle Ordovician, separating the basin from the Illinois basin along the Kankakee arch and from the Appalachian basin along the Findlay arch as shown in Figure 2.5.1-218 (Reference 2.5.1-240). The subsequent depositional history through the early Carboniferous records episodic basin subsidence with basin geometry alternating between broad-basin centered, narrow-basin centered, and eastward tilting. These changes in basin geometry may correlate with periods of the Appalachian orogen occurring contemporaneously along the southwest margins of the craton. (Reference 2.5.1-239) These orogenic events included the Late Cambrian[6] to Ordovician Penobscot event (ca. 510 – 490 Ma), the Middle to Late Ordovician Taconic event (ca. 470 – 440 Ma), the Late Silurian Acadian or Caledonian event, the Devonian[6]Arcadian event, and the Carboniferous – Permian Alleghenian collision between Laurentia and Gondwana (Reference 2.5.1-240).

As a result of this long history, a variety of structural styles are present in the Michigan basin including deep-seated (i.e., basement-involved) and shallow structures. Structural interpretations of these features range from broad, gently dipping, closed anticlines to a complex of horsts and grabens (and associated listric faults) trending northwest-southeast. Many of the large Devonian structures in the central basin are thought to have formed over faulted basement horsts or rotated blocks (Reference 2.5.1-319). The dominant structures in the basin are considered by Fisher (Reference 2.5.1-320) to be the result of vertical tectonics. Structures in the southeast and south-central parts of the basin appear to have been modified by zones of locally developed left-lateral shear that was related to compression directed from the southeast (i.e., the Appalachian mobile belt) (Reference 2.5.1-321, Reference 2.5.1-322). These conclusions contrast with other work indicating a northeast-southwest compressional component (Reference 2.5.1-323). North-south flexures are also known in the southern parts of the basin, indicating a due east-west compressional stage.

Based on seismic evidence, Fisher and Barratt (Reference 2.5.1-324) report that only a few of the largest faults that offset Precambrian

basement rocks extend stratigraphically up into Middle Devonian rocks. No evidence of faulting of the Carboniferous unconformity is reported in the literature. Other structures within the basin include solution-collapse features and differential compaction anticlines located over buried topographic highs and reefs (Reference 2.5.1-318).

2.5.1.1.4.3.1.2 Findlay and Algonquin Arches

The northeast-trending, northeast-plunging Findlay arch in western Ohio and southeast Michigan, and the northeast-trending, southwest-plunging Algonquin arch in Canada separate the Michigan and Appalachian basins. The Findlay and Algonquin arches are part of the same feature that was present in the Precambrian, and remained a passive, positive feature as flanking basins settled. The Findlay and Algonquin arches influenced Paleozoic sedimentary deposition into the Middle Devonian (Reference 2.5.1-325) (Figure 2.5.1-208 and Figure 2.5.1-218). The east-west-trending Chatham sag, one of several major inlets into the Michigan basin, formed by the mutual plunges of the arches (Figure 2.5.1-208) but did not have a significant influence on sedimentation until the Late Silurian.

2.5.1.1.4.3.1.3 Kankakee Arch

The northwest-southeast-trending Kankakee arch, located mainly in northern Indiana, separates the Michigan and Illinois basins. The orientation of the Kankakee arch is different than the generally northeast-southwest orientation of the Findlay, Algonquin, and Cincinnati arches (Figure 2.5.1-208). Unlike the Cincinnati arch, which developed in direct response to plate convergent processes associated with the Alleghenian orogeny in the Appalachians, the Kankakee arch developed from subsidence in the adjacent Michigan and Illinois basins (Reference 2.5.1-213). The Kankakee arch was a generally positive feature that developed in the Early to Middle Ordovician[6] due to basin-centered subsidence in the Michigan and Illinois basins. The Kankakee arch influenced Paleozoic sedimentary deposition into the Early Devonian. (Reference 2.5.1-239)

2.5.1.1.4.3.1.4 Appalachian Basin

The intercratonic Appalachian basin (Figure 2.5.1-208) is located southeast of the Findlay and Algonquin arches and the Cincinnati arch, which separate it from the Michigan and Illinois basins. The basin

probably developed in the Late Cambrian at the same time the Illinois and Michigan basins developed. The Appalachian basin was filled with carbonate sediments (as were the Illinoian and Michigan basins), and received clastic sediments eroded from the proto-Appalachian Mountains resulting from several orogenies along the eastern margin of Laurentia during the Paleozoic (Reference 2.5.1-240). These included the Late Cambrian[6] to Ordovician Penobscot event (ca. 510 – 490 Ma), the Middle to Late Ordovician Taconic event (ca. 470 – 440 Ma), the Late Silurian Acadian or Caledonian event, the Devonian[6] Arcadian event, and the Carboniferous – Permian Alleghenian collision between Laurentia and Gondwana, which terminated basin deposition (Reference 2.5.1-239).

2.5.1.1.4.3.1.5 Cincinnati Arch

The northeast-trending Cincinnati arch in Tennessee, Kentucky, and southern Ohio separate the Illinois and Appalachian basins (Figure 2.5.1-208). Root and Onasch (Reference 2.5.1-213) interpret the Cincinnati arch as a forebulge (anticline or dome that forms on the craton away from the orogenic belt) structure associated with the Alleghenian orogeny. The Cincinnati arch, as expressed in the Precambrian basement surface, is coincident with the underlying GFTZ on a regional scale, and the GFTZ is interpreted to have been a major crustal suture that served to localize and control the history of the Cincinnati arch. Local deviations in the location of the arch and front are explained by the presence of Proterozoic rift basins filled with low-density sedimentary rocks, as well as by the interactions between the developing Appalachian, Michigan, and Illinois basins and by the northward decrease in Alleghenian orogeny tectonic loading. The Cincinnati arch began its history with a period of regional uplift as early as the Middle to Late Ordovician followed by maximum arch development in the Pennsylvanian in response to the Alleghenian orogeny. (Reference 2.5.1-213) The intersection of the Findlay, Kankakee, and Cincinnati arches is termed the Indiana-Ohio platform.

2.5.1.1.4.3.1.6 Illinois Basin

The interior cratonic Illinois basin underlies Illinois, southwest Indiana, and western Kentucky (Figure 2.5.1-208). As discussed above in Subsection 2.5.1.1.4.3.1.3, the proto-Illinois basin developed in the Late Cambrian (Reference 2.5.1-240). Basin-centered subsidence in the Early to Middle Ordovician separated the Illinois basin from the Michigan basin

along the Kankakee arch (Reference 2.5.1-240) and from the Appalachian basin along the Cincinnati arch (Figure 2.5.1-208).

2.5.1.1.4.3.2 Principal Faults in the Site Region

Principal faults and tectonic features in the (320 km [200 mi] radius) site region and surrounding portions of the CEUS (Figure 2.5.1-203) reflect the cumulative deformation associated with tectonic events throughout the Precambrian, Paleozoic, Mesozoic, and Cenozoic eras. Table 2.5.1-201 provides a summary of information on faults within the (320-km [200-mi] radius) site region. Descriptions of the major faults and tectonic structures in the study region are provided in the following sections and are organized alphabetically; summaries for these structures and additional minor structures in the site region that are shown on Figure 2.5.1-203 are provided in Table 2.5.1-201, also organized alphabetically.

2.5.1.1.4.3.2.1 Akron Magnetic Boundary

The Akron magnetic boundary is a northeast-southwest-trending magnetic anomaly (low) in the subsurface of Wayne, Portage, Geauga, Lake, and Ashtabula Counties, Ohio (Reference 2.5.1-237), which may extend northeast into Canada (Reference 2.5.1-326). Muskett (Reference 2.5.1-327) speculates that historical earthquakes along the south shore of Lake Erie may be the result of adjustment or movement of pre-existing basement fault zones, such as the Akron magnetic boundary, due to a lake-loading piezomagnetic effect. Wallach et al. (Reference 2.5.1-326) associate the Akron magnetic boundary with the Niagara-Pickering linear zone, which trends along the New York – Canadian border (see also Reference 2.5.1-328). The Akron Magnetic Boundary is associated with the Northeastern Ohio Seismic Zone, discussed in Subsection 2.5.1.1.4.4.1.

2.5.1.1.4.3.2.2 Albion-Scipio Anticline/Fault

The Albion-Scipio structure is a northwest-southeast-trending faulted anticline in the subsurface of Hillsdale and Calhoun Counties, Michigan (Figure 2.5.1-203). Fisher (Reference 2.5.1-329) postulates that the Albion-Scipio anticline and associated en-echelon wrench faults control the Albion-Pulaski-Scipio-trend oil and gas field. The mapped length of the fault is approximately 48 km (30 mi) and the structure is subparallel to the Howell anticline and portions of the northern segment of the Bowling Green fault (Reference 2.5.1-329). The sense of displacement is

uncertain; Fisher (Reference 2.5.1-329) shows a southwest-side-down fault, whereas Fisher (Reference 2.5.1-330) postulates mainly strike-slip displacement due to the lack of vertical displacement. The youngest unit affected by the structure is the Middle Ordovician Trenton Formation (Reference 2.5.1-331).

2.5.1.1.4.3.2.3 Bowling Green (Lucas-Monroe) Fault/Monocline

The Bowling Green fault, known locally as the Lucas-Monroe monocline or fault, in the subsurface of Ohio and Michigan, consists of three segments: (1) a central north-south-trending, generally linear segment; (2) a southern, southeast-trending splay of faults; and (3) a northern, northwest-trending segment of stepped faults (Table 2.5.1-201 and Figure 2.5.1-203, Figure 2.5.1-223, and Figure 2.5.1-224). The total length of the three segments is approximately 190 km (118 mi) (Figure 2.5.1-203). At its closest distance, the Bowling Green fault is approximately 40 km (24 mi) west of the site.

The central segment, known as the Bowling Green fault, extends from approximately the southeastern corner of Hancock County, Ohio, north to the middle of the boundary between Lenawee and Monroe Counties, Michigan, and is well studied because of quarry exposures. The fault displaces the Precambrian unconformity surface west-side-down (Reference 2.5.1-237), and has had at least six episodes of displacement through the Middle Silurian (Reference 2.5.1-332) (Figure 2.5.1-223).

As exposed in the Waterville quarry in southern Lucas County, the fault is a 10 m (33 ft) wide near-vertical zone of highly sheared rock striking N10° to 20°W, with secondary faulting extending out 10 to 90 m (33 to 300 ft) on either side (Reference 2.5.1-332). The fault juxtaposes the uppermost Silurian Bass Islands Group on the west against the Tymochtee Dolomite, which stratigraphically underlies the Bass Islands Group on the east. The contact between the two units is offset approximately 70 m (230 ft), west-side-down (Reference 2.5.1-332) (Figure 2.5.1-224). Maximum displacement appears to be approximately 122 m (400 ft), west-side-down, on the top of the Middle Silurian Lockport Dolomite (Reference 2.5.1-332). The latest Silurian Bass Islands Group is the youngest unit displaced by the Bowling Green fault; no younger units except for unfaulted Pleistocene glacial deposits occur along the fault (Reference 2.5.1-332). Onasch and Kahle (Reference 2.5.1-332) speculate fault-parallel, east-dipping thrust faults with maximum

displacements of less than 5 m (16 ft), (Episode VI on Figure 2.5.1-223), generally on the east side of the fault, are consistent with the contemporary stress field and, if related to contemporary stresses, the Bowling Green fault is Late Cretaceous or younger. The central segment of the fault is essentially coincident with the GFTZ and the Findlay arch (Figure 2.5.1-203). Onasch and Kahle (Reference 2.5.1-332) suggest that the location of the fault and recurrent displacement through latest Silurian on the fault are controlled by the Grenville Front and Paleozoic orogenic activity to the east, including the Middle to Late Ordovician Taconic event (ca. 470 – 440 Ma), the Late Silurian Acadian or Caledonian event, the Devonian[6] Arcadian event, and possibly the Carboniferous – Permian Alleghenian event. Onasch and Kahle (Reference 2.5.1-332) speculate that the recurrent displacement may have been due to stresses related to migration of the Findlay arch (as a forebulge) during the Acadian and/or Alleghenian events.

The southern segment consists of several steeply dipping to vertical, southeast-trending fault splays in Ohio that extend from approximately the southern boundary of Wood County to the southern portion of Marion County. These faults roughly define a northwest-southeast-trending high and low on the map of the Precambrian unconformity surface in Ohio, and include the Outlet (northeast-side-down) and Marion (also northeast-side-down) faults and several unnamed faults (Reference 2.5.1-237). The Outlet fault zone trends northwest and extends from Wyandot County to Wood County. Based on the sense of folding and nature of displacement between the Outlet and Bowling Green faults, the Outlet fault is interpreted as a large synthetic shear zone to the Bowling Green fault (Reference 2.5.1-453). Based on boreholes along the fault zone, the Ordovician Trenton limestone has been extensively fractured and brecciated in a zone that is a few hundred to a few thousand feet wide. Vertical displacement on the Outlet fault zone ranges from approximately 6 to 30 m (20 to 100 ft). The amount of lateral displacement cannot be determined (Reference 2.5.1-453). Deposition of the Late Ordovician Cincinnati Group and possibly the Point Pleasant Formation also were affected by the Outlet fault zone (Reference 2.5.1-454). The Marion fault is one of several small faults that have been recognized based on well data. The structural trends of the Marion and other faults are supported by subsurface data on the top of the Trenton limestone, unpublished lineament analyses by the Ohio

Geological Survey, analysis of proprietary seismic data, and anomalies in gravity and magnetic maps (Reference 2.5.1-454).

The northern segment, also known as the Lucas-Monroe monocline/fault, consists of short, steeply dipping to vertical, southwest-side-down, northwest-southeast- to north-trending, right- and left-stepping faults that extend from the middle of the boundary between Lenawee and Monroe Counties to the northwestern corner of Livingston County, where the segment appears to merge with the Howell anticline (Figure 2.5.1-203). The youngest unit affected by the structure is the early Carboniferous Sunbury Shale (Reference 2.5.1-333). A magnitude 3.4 earthquake occurred September 2, 1994, on a N70°W, left-lateral, strike-slip fault at a depth of 10 – 15 km (6 – 9 mi) in Precambrian basement rocks near Potterville, approximately 21 km (12.6 m) southwest of Lansing, Michigan, and approximately 130 km (90 mi) northwest of Fermi 3 (Reference 2.5.1-334). Faust et al. (Reference 2.5.1-334) suggest that this earthquake was on a hypothetical fault associated with a northwest extension of the Lucas-Monroe fault, or possibly on a shallow dipping feature associated with the MRS/MMGH. Structure contour maps of Paleozoic units (e.g., see Figure 2.5.1-225) do not support the Lucas-Monroe fault extension hypothesis. Because the epicenter and zone of intense shaking of this earthquake are approximately 25 km (15.5 mi) southwest of, and not coincident with, the southwest margin of the MRS /MMGH (Reference 2.5.1-334), it is unlikely that the earthquake is associated with this structure.

2.5.1.1.4.3.2.4 Burning Springs Anticline/Fault – Cambridge Arch/Fault

The Burning Springs anticline/fault and Cambridge arch/fault comprise a narrow zone of recurrent Paleozoic faults in the cores of anticlinal structures embedded in the Precambrian Grenville province about 100 km (60 mi) east of the Grenville Front (Reference 2.5.1-336) (Figure 2.5.1-203). The zone trends north to south in northern West Virginia and extends N20°W across Ohio to Lake Erie, a total distance of approximately 350 km (213 mi).

The southern segment of the zone in northern West Virginia is termed the Burning Springs anticline and has a length of approximately 50 km (30 mi) up to about 150 km (91 mi) if the Mann Mountain anticline south of the Burning Springs anticline is included. Near the Ohio River the structure loses definition and appears to step en-echelon to the west

toward splays of the southeast end of the Cambridge arch (Reference 2.5.1-336). Between the structures at the Ohio River is an approximately 16 km (10 mi) break. The structure is present in the Precambrian unconformity surface as an east-side-down normal fault. (Reference 2.5.1-237) Paleozoic displacement on the structure included: (1) reactivation of older basement faults during the Silurian which created an evaporite basin east of the structure, (2) displacement during deposition of Devonian through Permian units, and (3) northwest-directed Alleghanian orogeny thrusting on decollements in the Salina salt units, which created ramp faults and a system of imbricate thrusts in the cores of anticlines (Reference 2.5.1-336). Seismic data across the Burning Springs anticline shows a steep, east-dipping normal, east-side-down fault extending from the basement into the lower Middle Devonian Onondaga Limestone (Reference 2.5.1-336). At least 300 m (1,000 ft) of displacement is present on the base of the Cambrian, decreasing to approximately 250 m (820 ft) at the base of the Onondaga Limestone (Reference 2.5.1-336). Anticline folding is dominant in Upper Silurian Salina Group through Pennsylvanian-Permian units (Reference 2.5.1-336).

The northern segment of the zone in Ohio is termed the Cambridge arch and has a length of approximately 100 km (60 mi). The N20° W trending structure is a fault-bounded arch (horst) about 1.5 km (0.9 mi) wide with a half graben (Parkersburg-Lorain syncline) on the west that splays into three arches at the Ohio River. The bounding normal faults dip 80° southwest and northeast, respectively. Some right-lateral slip may have occurred at the north end of the arch. Maximum structural relief is approximately 80 m (262 ft) on the Devonian Onondaga Limestone. The latest Early Carboniferous Berea Sandstone has 52 m (170 ft) of offset at the south end of the segment and 45 m (148 ft) of offset at the north end in an outcrop near Lake Erie. Offsets at the intersection of the COCORP OH-2 line are 37 m (121 ft) on the Precambrian unconformity surface, 18 m (59 ft) on the Silurian Packer Shell horizon, and 27 m (88 ft) on the latest Early Mississippian Berea Sandstone (Reference 2.5.1-336; Reference 2.5.1-237).

Although the Burning Springs anticline/fault and Cambridge arch/fault are aligned and have similarities, they probably should not be considered the same structure. There is a 16 km (10 mi) break between the structures at the Ohio River, and the structure contour map on the Precambrian

unconformity surface (Reference 2.5.1-237) shows cross faults in this area between the structures. In addition, the characteristics of the structures are different and the magnitude of displacement on the Burnings Springs anticline/fault is significantly greater than on the Cambridge arch/fault. At their closest, Burning Springs anticline/fault is approximately 327 km (203 mi) east and the Cambridge arch/fault is approximately 118 km (73 mi) southeast of Fermi 3 (Figure 2.5.1-203)

2.5.1.1.4.3.2.5 Chatham Sag and Electric Fault

The Chatham sag and associated Electric fault are subsurface structures in southwestern Ontario, Canada. The east-west-trending Chatham sag, one of several major inlets into the Michigan basin, formed by the mutual plunges of the Findlay and Algonquin arches (Figure 2.5.1-203). Although present in the Precambrian, the sag did not have a significant influence on sedimentation until the Late Silurian (Reference 2.5.1-325).

The northern margin of the Chatham sag is defined by the east-west-trending Electric fault, which deflects the nose of the Algonquin arch to the west, and extends from the mouth of the Saint Clair River to the northwest corner of Kent County, Ontario, a distance of approximately 115 km (72 mi) (Figure 2.5.1-203). At its closest, the Electric fault is approximately 81 km (50 mi) northeast of the site (Figure 2.5.1-203). The Electric fault is a south-side-down normal fault with a maximum observed vertical displacement on the Precambrian surface of approximately 93 m (305 ft) (Reference 2.5.1-325). The Electric fault had recurrent displacement in the Paleozoic; it displaces structure contours on the top of the uppermost Late Silurian Bass Islands Group and the base of the lower Middle Devonian Detroit River Group, but does not offset the base of the overlying Dundee Limestone (Reference 2.5.1-325) (Figure 2.5.1-203). Boyce and Morris (Reference 2.5.1-305) speculate that the Electric and other east-west-trending faults in southwestern Ontario are related to the Mesozoic St. Lawrence Valley system rifting, but this is not supported by the absence of displacements of units younger than the lower Middle Devonian Detroit River Group.

2.5.1.1.4.3.2.6 Fortville Fault

The Fortville fault is a north-northeast-/south-southwest-trending fault in the subsurface of Marion, Hancock, and Madison Counties in Indiana, and is about 66 km (41 mi) long (Reference 2.5.1-338). At its closest, the Fortville fault is approximately 271 km (168 mi) southwest of Fermi 3

(Figure 2.5.1-203). The fault is a steeply southeast-dipping, down-to-the-southeast normal fault on the west flank of the Cincinnati arch. Rupp (Reference 2.5.1-338) indicates that the fault offsets the top of the Precambrian surface and the top of the Middle Silurian Salamonie Dolomite, but not the top of the Middle Devonian Muscatatuck Group. Hasenmueller (Reference 2.5.1-339), however, indicates that the Middle Devonian Muscatatuck Group may be offset.

2.5.1.1.4.3.2.7 Fort Wayne Rift

The Fort Wayne rift is a northwest-southeast-trending crustal structure in the subsurface of western Ohio and eastern Indiana (Figure 2.5.1-203 and Figure 2.5.1-207). At its closest, the Fort Wayne rift is approximately 173 km (107 mi) southwest of the site (Figure 2.5.1-203). On the Precambrian unconformity surface in Ohio, the rift is expressed as a graben bounded by normal faults and a central high bounded on the southwest by the Anna-Champaign fault, and on the northeast by the Logan fault (Reference 2.5.1-237) (Figure 2.5.1-203 and Figure 2.5.1-207). It is coincident with a portion of the east continent gravity high (ECGH) (Reference 2.5.1-227) (Figure 2.5.1-203 and Figure 2.5.1-219). As discussed in Subsection 2.5.1.1.2.2.4, the rift developed along the eastern margin of Laurentia after emplacement of the Eastern Granite-Rhyolite province rocks similar to, and possibly related to, the Keweenawan rifting event that developed the midcontinent rift system (MRS) (Reference 2.5.1-228). The Fort Wayne rift and probably the ECGH are truncated by the Grenville Front tectonic zone. The Fort Wayne rift is the locus of historic seismicity (Figure 2.5.1-207) and is associated with the Anna seismic zone (Subsection 2.5.1.1.4.4.2).

2.5.1.1.4.3.2.8 Grenville Front Tectonic Zone

The GFTZ is a major structural feature in the subsurface of the midcontinent that extends from at least Mississippi northeast and north through Ohio and Ontario, Canada, and northeast into Canada. As discussed in Subsection 2.5.1.1.2.2.5, the GFTZ is essentially the suture zone along which the group of regionally extensive terranes collided with and were accreted (attached) to the southern margin of Laurentia during the Grenville orogeny (Reference 2.5.1-232). The GFTZ truncates the Granite-Rhyolite provinces and all other northern orogens (Figure 2.5.1-203 and Figure 2.5.1-206).

Interpretation of COCORP and GLIMPCE lines help to outline the history of the Grenville orogen and the location and character of the GFTZ. In Canada, the GFTZ is 10 to 100 km (6 to 60 mi) wide and separates moderately to highly metamorphosed rocks with a southeast-dipping structural fabric from cratonic rocks west of the GFTZ (Reference 2.5.1-234). Along GLIMPCE line J in Lake Huron (Figure 2.5.1-213), the GFTZ is delineated by a 32 km (20 mi) wide band of east-dipping reflections that sharply truncates Manitoulin terrane (a Penokean orogen terrane) structures to the west (Reference 2.5.1-216). On COCORP line OH-1 in central Ohio, the GFTZ is delineated by an approximately 50 km (15 mi) wide, 25- to 30-degree-dipping zone of reflections (Figure 2.5.1-213 and Figure 2.5.1-221). COCORP lines OH-1 and OH-2 extending to the east image several Grenville terranes or belts and suture zones, including (from west to east) the CGB, the CMB (ca. 1.3 Ga), and the CGT (Figure 2.5.1-221). In Canada the CMB is subdivided into the western Elzevir and Frontenac – New York lowlands subterranes (Reference 2.5.1-234). The eastern boundary of the CMB is the Coshocton Zone – Carthage-Colton mylonite zone (Reference 2.5.1-234) (Figure 2.5.1-222).

Hauser (Reference 2.5.1-309) interprets the COCORP line OH-1 to suggest a two-phase evolution of the GFTZ. In this model, initial collision resulted in an approximately 14-degree east-dipping foreland thrust ramp and hanging-wall folds within the rocks of the Granite-Rhyolite provinces. These foreland structures are truncated to the east by a wide, approximately 28-degree east-dipping thrust zone. The general lack of a fold-and-thrust belt or foreland basin common to contractional orogens in Canada may be the result of a deeper level of erosion of the Grenville province and its foreland in Canada.

2.5.1.1.4.3.2.9 Howell (or Howell-Northville) Anticline/Fault

The Howell anticline, also known as the Howell-Northville anticline, is a northwest-southeast- (N40° to 60°W) trending anticline in the subsurface that extends approximately 112 km (68 mi) from northwest Wayne County through Livingston County to the western boundary of Shiawassee County, Michigan, as expressed on the residual contour map of the top of the lowest Middle Devonian Dundee Formation (Reference 2.5.1-333) (Figure 2.5.1-203). At its closest, the Howell anticline is approximately 45 km (28 mi) north of Fermi 3 (Figure 2.5.1-203). The structure is probably Precambrian and was a positive

topographic feature during the Cambrian, with recurrent displacement as late as the Mississippian (Reference 2.5.1-330). The southwest flank of the anticline is a steep, asymmetrical, normal fault, down-to-the southwest, with maximum relief of approximately 300 m (1,000 ft) on the top of the Middle Ordovician Trenton Formation (Reference 2.5.1-325). Fisher (Reference 2.5.1-329) suggests that the fault consists of at least three right-stepping en-echelon fault segments. However, Figure 2.5.1-225 is more consistent with three left-stepping en-echelon fault segments (Reference 2.5.1-333). The fault offsets the base, but not the top of the lower Middle Devonian Detroit River Group (Reference 2.5.1-340) (Figure 2.5.1-226), and as shown in this figure the anticline influenced sedimentary deposition through the Early Mississippian Sunbury Shale. There is no evidence of faulting or deformation associated with the Howell anticline after Early Mississippian. The Howell anticline is approximately coincident with the axis of the MRS (MMGA) in southeast Michigan (Figure 2.5.1-203 and Figure 2.5.1-220). The Howell structure may extend southwest to the Detroit River as a series of folds expressed on the structure contour map on the top of the Trenton Formation (Reference 2.5.1-341), one of which may be the Stony Island Anticline (Reference 2.5.1-341). These folds are discussed in more detail in Subsection 2.5.1.2.4.1.

2.5.1.1.4.3.2.10 **Maumee Fault**

The Maumee fault is a northeast-southwest trending normal fault in the subsurface of Henry, Lucas, and Wood Counties in Ohio, and is about 56 km (35 mi) long on the structural contour map on the Precambrian unconformity surface (Figure 2.5.1-203) (Reference 2.5.1-237). At its closest, the Maumee fault is approximately 34 km (21 mi) south of Fermi 3 (Figure 2.5.1-203). The fault is offset about 2 km (1.2 mi) in an apparent left-lateral sense by the Bowling Green fault. The fault trace is coincident with a moderate lineament formed by the Maumee River (Reference 2.5.1-237).

2.5.1.1.4.3.2.11 **Peck Fault**

The Peck Fault, also known as the Sanilac Fault, is a north-south trending fault present in the subsurface of St. Clair and Sanilac Counties (Reference 2.5.1-325; Reference 2.5.1-329; Reference 2.5.1-333). Brigham (Reference 2.5.1-325) characterized the Peck fault as a north-south trending, west-side-down, vertical normal fault based on

structure contour maps on the top of the Trenton Limestone, Clinton group, Guelph formation, Bass Islands group, and Dundee formation. Fisher (Reference 2.5.1-329) described the Peck fault as a N10° to 20°W trending faulted monocline, the fault being an east-dipping thrust. The total length of the Peck Fault is approximately 61 km (38 mi) long (Figure 2.5.1-203). At its closest point, the Peck fault is approximately 133 km (82 mi) north of the site (Figure 2.5.1-203). The Peck fault has a maximum displacement on the Middle Ordovician Trenton group (approximately 91 m [300 ft]) and is present on the structure contour map on the through lowest Middle Devonian Dundee Formation (Reference 2.5.1-325). The Peck fault offsets the contact between early late-Silurian Salina group A-1 Evaporite and overlying A-1 Carbonate units (Reference 2.5.1-329). Noting anomalous patterns on isopach maps of Paleozoic units, Fisher (Reference 2.5.1-329) concludes that movement on the fault occurred through the end of the Paleozoic time. Geologic maps of Michigan (Reference 2.5.1-205 and Reference 2.5.1-442) show early Mississippian Coldwater and Sunbury Shale in the area where the Peck fault has been mapped. The early Mississippian Sunbury Shale is offset by the Peck fault; however, it is unclear whether the overlying early Mississippian Coldwater Shale is offset by the fault. Late Wisconsinan - Holocene glacial and postglacial deposits, including till and lacustrine clay and silt, overlie the Peck fault (Reference 2.5.1-207 and Reference 2.5.1-451). There is no known evidence of Quaternary faulting in Michigan.

2.5.1.1.4.3.2.12 **Royal Center Fault**

The Royal Center fault is a northeast-southwest trending fault in the subsurface of Cass, Fulton, and Kosciusko Counties in Indiana, and is about 77 km (48 mi) long. At its closest, the Royal Center fault is approximately 223 km (138 mi) southwest of Fermi 3 (Figure 2.5.1-203). The fault is a steeply southeast-dipping, down-to-the-southeast normal fault on the north flank of the Kankakee arch. The fault offsets the top of the Precambrian surface and the top of the Middle Silurian Salamonie Dolomite, but not the top of the Middle Devonian Muscatatuck group. (Reference 2.5.1-338)

2.5.1.1.4.3.2.13 **Sharpsville Fault**

The Sharpsville fault is a northeast-southwest-trending, vertical normal fault in the subsurface of Tipton and Howard Counties of central Indiana.

The fault is approximately 21 km (13 mi) long and offsets the top of the Middle Ordovician Trenton Formation down-to-the-southeast on the crest of the Kankakee arch. (Reference 2.5.1-339). The fault juxtaposes the Devonian Muscatatuck Group limestone and dolomite against Silurian Wabash Formation limestone, dolomite, and shale (Reference 2.5.1-339). Based on the above relationship, the youngest deformation on the fault is Devonian. The fault is overlain by glacial till of Wisconsinan to possible Holocene age (Reference 2.5.1-207).

2.5.1.1.4.3.2.14 Transylvania Fault Extension

The Transylvania fault extension is a zone of en-echelon steeply dipping basement faults that extends across northeastern Ohio nearly to the shore of Lake Erie. The zone is defined by six high-angle (>80 degrees), normal, southwest-dipping, down-to-thesouthwest faults: the Pittsburgh-Washington cross-strike structural discontinuity, the Highlandtown fault, the Smith Township fault, the Suffield fault system, the Akron fault, and the Middleburg fault (Reference 2.5.1-237). These faults are mapped on the structure contour map of the Precambrian unconformity surface (Reference 2.5.1-237), and on structure maps on the top of the latest Early Mississippian Berea Sandstone, Devonian Onondaga Limestone, and Silurian Packer Shell horizon (Reference 2.5.1-342). The westernmost of these faults, the Middleburg fault, is approximately 186 km (115 mi) southeast of Fermi 3 at its closest distance (Figure 2.5.1-203). The Transylvania fault extension is an extension of the Transylvania fault zone, a zone of steeply dipping basement faults that extends from the early Mesozoic Gettysburg Basin in Pennsylvania to Ohio. In Pennsylvania, the Transylvania fault zone is mapped as a series of large, subvertical, east-west-trending faults in the Blue Ridge Mountains, the Great Valley region, and the Valley and Ridge province. Westward on the Appalachian Plateau, the fault zone is recognized from subsurface mapping and geophysical studies. The Transylvania fault zone in Pennsylvania originated in the Precambrian and was reactivated during the Middle Ordovician Taconic orogeny, during the terminal Paleozoic Alleghenian orogeny, and during the Early Jurassic faulting of the rift basins along the margin of the continent (Reference 2.5.1-342). Mesozoic faulting has been documented in the early Mesozoic Gettysburg Basin, which lies along the projection of the Transylvania fault extension; however, no Mesozoic rocks are present in the area of the Transylvania fault extension (Reference 2.5.1-442).

Pennsylvanian-Permian age faulting related to Alleghanian deformation is recognized on faults within the Transylvania fault extension (Reference 2.5.1-213; Reference 2.5.1-342; Reference 2.5.1-343).

The geometry of the Akron-Suffield-Smith Township faults suggest that they originated as en-echelon, synthetic faults produced by right-lateral wrenching, with inferred minimum displacement of 21 km (13 mi) and subsequent normal displacements on the faults (Reference 2.5.1-342). Displacement on the Precambrian unconformity surface is 60 – 120 m (200 – 400 ft), while maximum vertical displacement of the Devonian Onondaga Limestone across the Akron-Suffield faults is 60 m (200 ft) and across the Highlandtown fault it is 72 m (240 ft) (Reference 2.5.1-342). Hook and Ferm (Reference 2.5.1-343) postulate that deposition of the Linton channel deposits below the Middle Pennsylvanian (Westphalian D) Upper Freeport coal may have been controlled by movement on the Transylvania fault extension in Cambrian through Lower Carboniferous strata (Pittsburgh-Washington cross-strike structural discontinuity). Post-Lower Pennsylvanian faulting cannot be assessed because of the absence of younger units. The northeast-southwest-trending Akron magnetic boundary crosses between the Middleburg and Akron faults.

The Transylvania fault extension is overlain by alluvium and colluvium of Middle Pleistocene to Holocene age (Reference 2.5.1-207). There is no known evidence of Quaternary tectonic faulting in Ohio.

2.5.1.1.4.3.3 Seismic Zones

Earthquakes in the site region are generally shallow events associated with reactivated Precambrian faults favorably oriented in the modern northeast-southwest compressive stress regime (Reference 2.5.1-344). None of these events has associated surface rupture, and no faults in the site region exhibit evidence of movement since the Paleozoic (Reference 2.5.1-344). Two seismic zones in the study region, the Anna seismic zone and the northeast Ohio seismic (Figure 2.5.1-207) are designated as Class C features in the USGS Quaternary fault and fold database (Reference 2.5.1-316).

2.5.1.1.4.3.3.1 Northeast Ohio Seismic Zone

The Northeast Ohio seismic zone, also called the Ohio-Pennsylvania seismic zone, defines an approximately 50 km (30.5 mi) long, northeast-southwest-trending zone of earthquakes south of Lake Erie on the Ohio-Pennsylvania border (Figure 2.5.1-207) (Reference 2.5.1-328).

The largest historic event in this zone was the January 31, 1986, magnitude (m_b) 5.0 (E[**M**][8] 4.65) event located about 40 km (24.4 mi) east of Cleveland in southern Lake County, Ohio, and about 17 km (10.4 mi) south of the Perry Nuclear Power Plant (Reference 2.5.1-345). The earthquake produced Modified Mercalli intensity (MMI) VI to VII at distances of 15 km (9 mi) from the epicenter and short-duration high accelerations of 0.18 g at the Perry Plant (Reference 2.5.1-345). Thirteen aftershocks were detected by April 15, 1986, with magnitudes ranging from 0.5 to 2.5 and focal depths ranging from 2 to 6 km (1.2 to 3.7 mi) (Reference 2.5.1-345). The aftershocks occurred in a tight cluster about 1 km wide and oriented north-northeast, and focal mechanisms of the aftershocks represent predominantly oblique, right-slip motion on nearly vertical planes oriented N15° to 45°E, with a nearly horizontal *P* (maximum compressive stress) axis (Reference 2.5.1-345), consistent with the modern stress regime.

This earthquake and the aftershocks were within 12 km (7.3 mi) of deep waste disposal injection wells, and the earthquake sequence is possibly due to injection activities at the wells that reactivated favorably oriented, pre-existing fractures (Reference 2.5.1-346; Reference 2.5.1-345). However, the relative distance of the wells from the earthquake cluster (12 km [7.3 mi]), as well as the lack of large numbers of earthquakes that are typical of induced sequences, a history of small to moderate earthquakes in the region prior to well activities, and the attenuation of the pressure field with distance from the wells all argue for a natural origin for the earthquakes (Reference 2.5.1-345).

Nicholson et al. (Reference 2.5.1-345) observe that the 1986 cluster (Figure 2.5.1-207 (Sheet 2 of 3)) is coincident with a N40°E trending gravity and magnetic anomaly, the Akron Magnetic Boundary. Seeber and Armbruster (Reference 2.5.1-346) and Dineva et al. (Reference 2.5.1-328) also associate the Northeast Ohio seismic zone with the Akron Magnetic Boundary, which is also called the Akron magnetic anomaly or lineament. Seeber and Armbruster (Reference 2.5.1-346) speculate that the Akron Magnetic Boundary may be associated with the Niagara-Pickering magnetic lineament/Central Metasedimentary Belt boundary zone as a continental-scale

8.Magnitudes are reported in the magnitude scale designated in the cited reference. E[**M**] is expected moment magnitude and is the uniform magnitude scale used in the project earthquake catalog as described in Subsection 2.5.2.1.

Grenville-age structure. Since the Akron lineament is imaged as ductile shear zones on regional seismic lines and no structures are observed in the overlying Paleozoic sediments, Seeber and Armbruster (Reference 2.5.1-346) acknowledge that the geometry of brittle faulting within or near this ductile deformation may have a complex relationship with the geometry of these shear zones.

In 1987, the first in a series of earthquakes continuing to 2003 occurred within the Northeast Ohio seismic zone near Ashtabula in Ashtabula County, Ohio, northeast of the 1986 earthquakes (Reference 2.5.1-347, Reference 2.5.1-455). The largest events in the sequence include an initial Lg wave magnitude (m_{bLg}) 3.8 (E[**M**] 3.61) earthquake on July 13, 1987; a m_{bLg} 4.3 (E[**M**] 3.86) earthquake on January 26, 2001, which had a MMI of VI; followed by a m_{bLg} 3.0 (E[**M**] 2.92) earthquake on June 3, 2001; and a m_{bLg} 2.3 earthquake on June 5, 2001 (Reference 2.5.1-347). The June 5, 2001, earthquake is not included in the CEUS SSC earthquake catalog of NUREG-2115 due to its small size (E[**M**] less than 2). An event on January 20, 2001, is identified as a blast in the CEUS SSC earthquake catalog. The latest subsequence started in July 2003 with a m_{bLg} 2.5 (E[**M**] 2.29) earthquake (Reference 2.5.1-455).

Seeber et al. (Reference 2.5.1-455) discuss these fore-main-aftershock sequences and interpretations of these events based on information obtained from three short-term deployments of portable seismographs (in 1987, 2001, 2003) and from regional broadband seismograms. The main observations and conclusions from this analysis are as follows:

- A persistent earthquake sequence in northeast Ohio includes multiple distinct fore-main-aftershock sequences that illuminate two faults approximately 4 km (2.5 mi) apart (Figure 2.5.1-267).
- The seismicity is closely associated with injection of waste fluid in the basal Paleozoic formation from 1986 to 1994.
- All the earthquakes originated from a relatively small area (~ 10 km [6 mi] wide) and are assumed to form a single sequence of casually related earthquakes.
- Felt earthquakes started in 1987, a year after the onset of injection. At that time earthquakes were located 0.7 – 2.0 km (0.4 - 1.2 mi) from the injection site. Seismicity continued and in 2001, 5.5 years after the end of injection, hypocenters were then 5 – 9 km (3 - 6 mi) from the injection site. The only known episode of seismicity in Ashtabula is

closely associated with the 1986 – 1994 Class 1 injection, and the pattern of accurate hypocenters is consistent with the one expected for the high pore-pressure anomaly spreading from the injection site.

- This correlation is strong evidence that the seismicity was triggered by the injection.

The July 13, 1987, main shock was close to a deep Class I injection well that was pumping fluids into the Mount Simon Sandstone, the basal Paleozoic unit overlying Precambrian crystalline basement, at a depth of about 1.8 km (1.1 mi), and a number of portable seismographs were deployed to study the aftershocks (Reference 2.5.1-347). The first 13 well-recorded aftershocks defined a nearly vertical fault with a north-northeast orientation (Reference 2.5.1-245). Analysis of a larger set of well-located aftershocks (36) indicates a cluster in a narrow (0.25 km [0.15 mi] wide), east-striking vertical zone about 1.5 km (1 mi) long, extending from a depth of 1.7 km (1 mi) to 3.5 km (2.1 mi) (Reference 2.5.1-346, Figure 2.5.1-266). The first motions are consistent with left-lateral strike-slip movement on an east-west-striking fault, referred to as the Ashtabula fault (Reference 2.5.1-346). The temporal and spatial proximity between injection and earthquake generation suggested that the injection of waste fluids, which commenced in 1986, triggered the seismicity (Reference 2.5.1-345; Reference 2.5.1-346). Seeber and Armbruster concluded that the zone of seismicity represented a pre-existing basement fault brought to failure by the fluid flow and/or increased pore pressure induced by fluid injection. Seeber and Armbruster noted that from 1987 to 1992, the seismicity appeared to migrate westward out to a distance of 5 to 10 km (3 - 6 mi), possibly along the Ashtabula fault. However, in a more recent paper, Seeber et al. (Reference 2.5.1-455) revised their interpretation to conclude that the linear patch of 1987 earthquakes is a portion of the fault activated by high pore pressure rather than a single rupture. Due to poor location constraints on earthquakes from August 1987 to 2001, the location of the M 2.9 (E[**M**] 2.63) earthquake on March, 28, 1992, cannot be definitely associated with the Ashtabula fault (Reference 2.5.1-455).

The Ohio Seismic Network was installed in 1999 and precisely recorded the 2001 earthquakes (Reference 2.5.1-347). A focal mechanism obtained by modeling regional waveforms of the m_{bLg} 4.3 (E[**M**] 3.86) earthquake is consistent with composite focal mechanisms from locally recorded earthquakes. Well-located aftershocks of the June 3, 2001,

m_{bLg} 3.0 (E[**M**] 2.92) and July 17, 2003, m_{bLg} 2.5 (E[**M**] 2.29) earthquakes define a 5 – 7 km (3 - 4 mi) long plane striking 96 degrees and dipping 65 degrees south. (Reference 2.5.1-455, Figure 2.5.1-266) Seeber et al. (Reference 2.5.1-455) interpret this plane as the source fault for the 2001 seismicity, which resembles the postulated 1.5 km (0.9 mi) long, east-west-striking basement fault having left-lateral slip defined by the 1987 seismicity.

The two subparallel faults are 4.5 (2.8 mi) and 0.7 km (0.4 mi) south of the injection well, respectively, and are 4 km (2.5 mi) apart (Figure 2.5.1-266). Seeber et al. (Reference 2.5.1-455) observed quiescence from 1995 to 2000, which they attribute to a lack of favorably oriented structures between these two fault planes. They speculate that seismicity initiates when and where a significant pore-pressure rise intersects pre-existing faults close to failure, turning off when pressure starts dropping back. Seeber et al. (Reference 2.5.1-455) conclude that these faults are pre-existing faults located in the uppermost portion of the Grenville basement and are reactivated by a high pore-pressure anomaly spreading from the injection site.

In the CEUS, the most common types of surficial evidence of large, prehistoric earthquakes are liquefaction features and faults that offset young strata. A paleoseismic liquefaction field study along two of the larger drainages in northeast Ohio, the Grand River and the Cuyahoga River, was conducted by Obermeier (Reference 2.5.1-482) and involved reconnaissance along approximately 25 km (7.6 mi) of stream bank. No evidence of liquefaction was observed along either river. Although the scarcity of suitable exposures precludes definitive statements about prehistoric earthquakes, this led Crone and Wheeler (Reference 2.5.1-316) to classify the Northeast Ohio seismic zone as a Class C feature. Conditions and ages of the sediment encountered along each of these rivers as noted by Obermeier (Reference 2.5.1-482) were summarized in the report, as follows:

- Radiocarbon data from along the Grand River show that many of the exposures searched are at least 2,000 years old. Many others are probably mid-Holocene in age, based on depth and severity of weathering. A few scattered sites are earliest Holocene in age. Liquefaction susceptibility at many of the sites examined is at least moderate.

- Numerous exposures along the Cuyahoga River are at least a few thousand years old, and scattered exposures are up to 8,000 years old, based on radiocarbon data. Conditions are very good for forming liquefaction effects at many places.
- It is unlikely that sediments exposed in a sand pit near the Ashtabula-Trumbull County line experienced strong ground shaking through most or all of Holocene time.

Additional documentation of the 1995 paleoliquefaction field search in northeastern Ohio, which focused on the vicinity of the nuclear power plant near Perry, Ohio, was provided to the U.S. Nuclear Regulatory Commission (NRC) in a letter report submitted by Dr. Obermeier to Dr. Andrew Murphy on May 23, 1996 (Reference 2.5.1-483). From the ages and liquefaction susceptibility of the sediments observed during the reconnaissance, Dr. Obermeier made the following conclusions specific to the Perry nuclear plant:

> "…within 20 km of the plant, the lack of suitable exposures precludes definitive statements concerning whether or not there has been strong seismic shaking for most of Holocene time."
>
> "The lack of exposures with liquefiable sediment more than a few thousand years old, within 20 to 25 km of the plant, precludes any statement concerning whether there could have been strong shaking at the plant locale from even moderate-sized earthquakes (say, M ~ 6) occurring more than a few thousand years ago."
>
> "…one large sand and gravel pit (Pit-CL) of latest Pleistocene sediment, probably with a moderate to high liquefaction susceptibility, is located within 32 km of the plant…The lack of liquefaction features indicates a lack of strong seismic shaking through most or all Holocene time."

The CEUS SSC model presented in NUREG-2115 (Reference 2.5.1-286) utilizes broad regional seismic source zones to represent the occurrence of distributed seismicity in the CEUS. Earthquake recurrence rates are modeled as spacially variable in cells with dimensions of ¼ degree longitude by ¼ degree latitude or ½ degree longitude by ½ degree latitude. As such, the Northeast Ohio seismic zone appears as an area of higher seismicity rate within the larger regional source zones in which it lies (Subsection 2.5.2.2.1).

2.5.1.1.4.3.3.2 Anna Seismic Zone

The Anna seismic zone, also called the Western Ohio seismic zone, coincides with northwest-southeast-trending basement faults associated with the Fort Wayne rift in Shelby, Auglaize, and nearby counties (Figure

2.5.1-207) (Reference 2.5.1-344). Ruff et al. (Reference 2.5.1-348) attribute seismicity to the Anna-Champaign, Logan, and Auglaize faults. This zone has produced at least 40 felt earthquakes since 1875, including events in 1875, 1930, 1931, 1937, 1977, and 1986 that caused minor to moderate damage (Reference 2.5.1-344). The July 12, 1986, event near the town of St. Marys in Auglaize County was the largest earthquake to occur in the zone since 1937 (Reference 2.5.1-344). Schwartz and Christensen (Reference 2.5.1-349) determined a hypocenter of 5 km (3 mi) for the magnitude (m_b) 4.5 (E[**M**] 4.37) earthquake and a focal mechanism (strike = 25°, dip = 90°, rake = 175°) representing mostly strike-slip with a small oblique component approximately parallel to the Anna-Champaign fault and a nearly horizontal *P* axis oriented east-northeast. The earthquake produced an MMI V1 event (Reference 2.5.1-349). Hansen (Reference 2.5.1-344) concluded that the historic record indicates a maximum magnitude of 5, but suggested that this zone was capable of producing a magnitude 6.0 to 7.0 event. Obermeier (Reference 2.5.1-350) investigated stream banks in the vicinity of Anna, Ohio, and portions of the Auglaize, Great Miami, Stillwater, and St. Marys rivers and found no evidence of paleoliquifaction features indicative of a magnitude 7 event in the past several thousand years. Crone and Wheeler (Reference 2.5.1-316) designated the Anna seismic zone as a Class C feature based on the occurrence of significant historical earthquakes and the lack of paleoseismic evidence. The Anna seismic zone is represented in the CEUS SSC model as an area of higher seismicity rate within the larger regional source zones in which it lies (Subsection 2.5.2.2.1).

2.5.1.1.4.4 Significant Seismic Sources at Distance Greater than 320 Km (200 Mi)

More distant sources of large-magnitude earthquakes are the New Madrid seismic zone (NMSZ) and the Wabash Valley seismic zone (WVSZ), which are approximately 800 km (500 mi) and 500 km (300 mi) southwest, respectively, from Fermi 3 (Figure 2.5.1-207). The CEUS SSC study (NUREG-2115) characterizes RLME seismic sources in the NMSZ and the WVSZ. As described in Subsection 2.5.2.4.4, these RLME seismic sources contribute to the seismic hazard at the Fermi 3 site. Recent information used in NUREG-2115 to characterize these sources is described below.

2.5.1.1.4.4.1 New Madrid Seismic Zone

The New Madrid seismic zone (NMSZ) lies within the Reelfoot rift and is defined by post-Eocene to Quaternary faulting, and historical seismicity (Reference 2.5.1-316). The NMSZ, which is approximately 200 km (124 mi) long and 40 km (25 mi) wide, extends from southeastern Missouri to northeastern Arkansas and northwestern Tennessee (Figure 2.5.1-207).

A number of models have been proposed to explain the origin of stresses driving active deformation in the CEUS. Several of the models provide explanations for localization of seismicity and recurrence of large-magnitude events in the NMSZ, as follows:

- The presence of a rift pillow (body of igneous rock in the crust composed of injected high-density mantle material) underlying the Reelfoot rift (Reference 2.5.1-456) causes local stress concentration (Reference 2.5.1-457).
- A weak subhorizontal detachment fault exists in the lower crust above the rift pillow that causes local stress concentration (Reference 2.5.1-458).
- High local heat flow creates high ductile strain rates in the upper mantle and lower crust, causing seismicity in the upper crust (Reference 2.5.1-459; Reference 2.5.1-476).
- Glacial unloading north of the NMSZ at the close of the Wisconsinan increased seismic strain rates in the NMSZ and initiated the Holocene seismicity (Reference 2.5.1-460). Modeling studies (Reference 2.5.1-460) show that the removal of the Laurentide ice sheet approximately 20,000 years ago changed the stress field in the vicinity of New Madrid, causing seismic strain rates to increase by about three orders of magnitude. The modeling predicts that the high rate of seismic energy release observed during late Holocene time is likely to continue for the next few thousand years (Reference 2.5.1-460).
- Some local or regional perturbation of the stress field, pore pressure, or thermal state is responsible for triggering viscous relaxation of a weak lower-crustal zone within an elastic lithosphere. This may cause a sequence of fault ruptures with short recurrence intervals. A strong candidate for this perturbation is recession of the Laurentian ice sheet, approximately 14 ka. (Reference 2.5.1-461).

- Low-permeability seals form around the fault zone as stress accumulates, raising the pore pressure until an earthquake occurs. Temporal clustering may reflect the evolution of pore fluid pressure in a fault zone. (Reference 2.5.1-462)
- Accelerated Late Wisconsin and Holocene denudation above the NMSZ due to the confluence of the Mississippi and Ohio rivers stepping north to Thebes Gap, perhaps in combination with the retreating Laurentide forebulge, may have been sufficient to initiate Holocene seismicity by causing a perturbation in the local stress field (Reference 2.5.1-461; Reference 2.5.1-463).
- Deep-mantle flow combined with the seismic anisotrophy beneath continents invoke mechanical coupling and subsequent shear between the lithosphere and asthenosphere. Two orthogonal sets of shear zones and faults observed on a continental scale mimic orthogonal teleseismic images. Stress caused by the traction leads to repeated reactivation of structures (Reference 2.5.1-477)
- Descent of the ancient Farallon slab into the deep mantle beneath central North America as inferred from high-resolution seismic tomography induces highly localized flow and stresses directly below the NMSZ. This localization arises because of structural variability in the Farallon slab and the low viscosity of the sub-lithospheric upper mantle. It is hypothesized that the mantle-flow-induced surface depression and associated local focusing of bending stresses in the upper crust may operate analogous to previous crustal loading scenarios, with the difference being that the slab related loads reside in the mantle. (Reference 2.5.1-357)
- Fault weakening can lead to repeated earthquakes on intraplate faults (Reference 2.5.1-464). The predicted patterns vary with the weakening history. Stress triggering and migration associated with assumed tectonic loading cause spatiotemporal clustering of earthquakes. Clusters of large intraplate earthquakes can result from cycles of fault weakening and healing, and the clusters can be separated by long periods of quiescence. (Reference 2.5.1-465; Reference 2.5.1-478)
- Strain in the NMSZ over the past several years has accumulated too slowly to account for seismicity over the past approximately 5,000 years, hence excluding steady-state fault behavior. Fault loading, strength, or both may vary with time in the plate interior. Time

variations in stress could be due to local loading and unloading from ice sheets or sediments or after earthquakes on other faults. (Reference 2.5.1-466; Reference 2.5.1-479; Reference 2.5.1-480)

- The NMSZ is associated with a local, NE-SW-trending low-velocity anomaly in the lower crust and upper mantle, instead of high-velocity intrusive bodies proposed in previous studies. The low-velocity anomaly is on the edge of a high-velocity lithospheric block, consistent with the notion of stress concentration near rheological boundaries. This lithospheric weak zone may shift stress to the upper crust when loaded, thus leading to repeated shallow earthquakes. (Reference 2.5.1-467)
- Integrated lithospheric strength, as indicated by S-wave velocity anomalies at depths of 175 km (109 mi) correlates with crustal seismicity. None of the 14 intraplate events with moment magnitudes greater than 7 (including the NMSZ events) occur above mantle lithosphere with δVs greater than 3.5 percent (cratonic lithospheres) (Reference 2.5.1-481).
- Stress changes are caused by the Quaternary denudation/sedimentation history of the Mississippi valley. Flexural stresses are sufficient to trigger earthquakes in a continental crust at failure equilibrium (close to failure). The resulting viscoelastic relaxation leads to failure again on the main fault (lower strength threshold) and on neighboring faults. In the absence of significant far-field loading, this process can only maintain seismic activity for a few thousand years. (Reference 2.5.1-468)

Research conducted since 1986 shows that a distinct fault system is embedded within this source zone. The fault system consists of three distinct segments (Figure 2.5.1-203). These three segments include a southern northeast-trending dextral slip fault referred to as the Cottonwood Grove fault and Blytheville arch, a middle northwest-trending reverse fault referred to as the Reelfoot fault, and a northern northeast-trending dextral strike-slip fault referred to as the New Madrid North fault (Reference 2.5.1-352; Reference 2.5.1-353; Reference 2.5.1-354; Reference 2.5.1-355; Reference 2.5.1-316; Reference 2.5.1-356). In the current east-northeast to west-southwest directed regional stress field, Precambrian and Late Cretaceous–age extensional structures of the Reelfoot rift have been reactivated as right-lateral strike-slip and reverse faults.

Forte et al. (Reference 2.5.1-357) present viscous flow models for North America based on high-resolution seismic tomography that suggest a possible driving mechanism for the intraplate seismicity in the New Madrid region. From analysis of these flow models it is postulated that the descent of the ancient Farallon slab into the deep mantle beneath central North America induces a highly localized flow and stresses directly below the NMSZ. This localization arises because of structural variability in the Farallon slab and the low viscosity of the sublithospheric upper mantle. It is hypothesized that the mantle-flow-induced surface depression and associated local focusing of bending stresses in the upper crust may operate analogously to previous crustal loading scenarios, with the difference being that the slab-related loads reside in the mantle. (Reference 2.5.1-357)

The NMSZ produced three large-magnitude earthquakes (estimates range from magnitude 6.7 to 8.1) between December 1811 and February 1812 (Reference 2.5.1-286). The actual size of these pre-instrumental events is not known with certainty and is based primarily on various estimates of damage intensity and amount and pattern of liquefaction. (Reference 2.5.1-358; Reference 2.5.1-359; Reference 2.5.1-360; Reference 2.5.1-361; Reference 2.5.1-366; Reference 2.5.1-499; Reference 2.5.1-500)

The December 16, 1811, earthquake is inferred to be associated with strike-slip displacement along the southern portion of the NMSZ (Reference 2.5.1-361; Reference 2.5.1-356). Johnston (Reference 2.5.1-361) estimated the December event to have a magnitude of **M** 8.1 ± 0.31. Hough et al. (Reference 2.5.1-360) later re-evaluated the intensity data for the region and concluded that the event had a magnitude of M_w 7.2 to 7.3. Bakun and Hopper (Reference 2.5.1-358) also re-evaluated the intensity data and derived a preferred magnitude of **M** 7.6 for the December 1811 event.More recently, Hough and Page (Reference 2.5.1-500) assessed the magnitude to be M_w 6.7 to 6.9.

The February 7, 1812, New Madrid earthquake is associated with reverse displacement along the middle part of the NMSZ (Figure 2.5.1-207) (Reference 2.5.1-362; Reference 2.5.1-363; Reference 2.5.1-356; Reference 2.5.1-358; Reference 2.5.1-361). This earthquake most likely occurred along the northwest-trending Reelfoot fault that extends approximately 69 km (43 mi) from northwestern

Tennessee to southeastern Missouri (Reference 2.5.1-364; Reference 2.5.1-365). The Reelfoot fault is a northwest-trending southwest-vergent (shortening direction) reverse fault (Reference 2.5.1-363; Reference 2.5.1-366). It forms a topographic scarp developed as a result of fault-propagation folding (Reference 2.5.1-363; Reference 2.5.1-365). Kelson et al. (Reference 2.5.1-363) investigated near-surface deformation along the trace of the scarp and found evidence for three events within the past 2, 400 years. The most recent event was associated with the 1811/1812 earthquake sequence. The penultimate event is estimated to have occurred between A.D. 1260 and 1650. The pre-penultimate event occurred prior to about A.D. 780 to 1000. A range of recurrence intervals for the Reelfoot fault are estimated between 150 to 900 years, with a preferred range of about 400 to 500 years (Reference 2.5.1-363). The geometry and reverse sense of motion of the Reelfoot fault implies that this structure serves as a step-over segment between the southern and northern portions of the fault system (Reference 2.5.1-352; Reference 2.5.1-316). Johnston (Reference 2.5.1-361) estimated a magnitude of **M** 8.0 ±0.33 for the February 1812 event. Hough et al. (Reference 2.5.1-360) later re-evaluated the intensity data for the region and concluded that the February event had a magnitude of M_w 7.4 to 7.5. Bakun and Hopper (Reference 2.5.1-358) also re-evaluated the intensity data from the 1811/1812 sequence and derived a preferred magnitude of **M** 7.8 for the event. Hough and Page (Reference 2.5.1-500) assess the magnitude to be M_w 7.1 to 7.3.

The January 23, 1812, earthquake is inferred to be associated with strike-slip displacement on the New Madrid North fault along the northern portion of the NMSZ (Figure 2.5.1-207) (Reference 2.5.1-356). The interpretation that the January 1812 earthquake occurred along the New Madrid North fault of the NMSZ is based on fault mechanics and limited historical data, and is more poorly constrained than interpretations of the December 16, 1811, and February 7, 1812, earthquakes. Baldwin et al. (Reference 2.5.1-367) conducted paleoseismic investigations along this segment of the fault and although their investigations identified liquefaction evidence for the 1811/1812 earthquake sequence, their data does not support the presence of a major through going fault with repeated late Holocene events.

Johnston (Reference 2.5.1-361) estimated a magnitude of **M** 7.8 ± 0.33 for the January 1812 event. Hough et al. (Reference 2.5.1-360) later re-evaluated the intensity data for the region and concluded that the January event had a magnitude of M_w 7.0. Bakun and Hopper (Reference 2.5.1-358) also re-evaluated the intensity data from 1811/1812 sequence and derived a preferred magnitude of **M** 7.5 for the January 23, 1812, event.Hough and Page (Reference 2.5.1-500) assess the magnitude to be M_w 6.8 to 7.0.

Because there is little surface expression of faults within the NMSZ, earthquake recurrence estimates are based largely on dates of paleoliquefaction and offset geological features. Tuttle et al. (Reference 2.5.1-368; Reference 2.5.1-369) provide recent summaries of paleoseismologic data that suggest that that the average recurrence interval for surface deforming earthquakes in the NMSZ is about 200 to 800 years, with a preferred estimate of 500 years. Paleoliquefaction studies document evidence that prehistoric sand blows, such as those formed during the 1811/1812 earthquakes, probably are compound structures resulting from multiple earthquakes closely clustered in time (earthquake sequences) (Reference 2.5.1-368).

Based on considerations of the above information and review of an updated paleoliquefaction database, the CEUS SSC project developed an RLME source to represent the central faults in the NMSZ. This seismic source is modeled as producing recurring earthquakes in the magnitude range of moment magnitude (**M**) 6.7 to 7.9 with average recurrence intervals of approximately 500 years (Reference 2.5.1-286).

2.5.1.1.4.4.2 Wabash Valley Seismic Zone

The Wabash Valley region in southeastern Illinois and southwestern Indiana has been an area of persistent seismicity and the site of several moderate-magnitude historical earthquakes (**M** 4 to 5.5 (E[**M**] 4.29 to E[**M**] 5.32)) (Reference 2.5.1-374) (Figure 2.5.1-207). Investigations have documented evidence for multiple paleoearthquakes having magnitudes significantly larger than historical events that have occurred in the region. Mapping and dating of liquefaction features throughout most of the southern Illinois basin and in parts of Indiana, Illinois, and Missouri identified energy centers for at least eight Holocene and latest Pleistocene earthquakes having estimated moment magnitudes of **M** 6 to **M** 7.8 (Reference 2.5.1-371; Reference 2.5.1-372). Use of a more

recently developed magnitude-bound curve for the CEUS based on a value of **M** approximately 7.6 to 7.7 for the largest of the 1811-1812 New Madrid earthquakes (reduced from the higher **M** 8 used by Obermeier [Reference 2.5.1-374] in an earlier curve) gives lower estimates of **M** (Reference 2.5.1-503) as shown on Figure 2.5.1-207. The WVSZ is designated a Class A feature in the USGS Quaternary fault and fold database of the United States (Reference 2.5.1-370).

Liquefaction features from the strongest paleoearthquake, an estimated **M** 7.3 to 7.5 event that occurred in about 6100 years BP in the Wabash Valley, cover an area that has a diameter of about 300 km (180 mi) (Reference 2.5.1-373 and Reference 2.5.1-503). Based on the size and distribution of the liquefaction features, the location for this earthquake was in the vicinity of Vincennes, Indiana (Reference 2.5.1-370; Reference 2.5.1-373). The proximity of the energy centers for the two largest earthquakes inferred from the paleoliquefaction data (referred to as the Vincennes and Skelton paleoearthquakes) suggests there is a RLME source in the Wabash Valley (Reference 2.5.1-286). It has been postulated that a broad flexure (bend or stepover) in bedrock structure results in a concentration of stress in this region (Reference 2.5.1-375). This bend or stepover lies near the northern terminus of a 600 km (370 mi) long magnetic and gravity lineament, referred to as the Commerce Geophysical Lineament (CGL), which extends from Vincennes, Indiana, far into Arkansas (Figure 2.5.1-207) (Reference 2.5.1-376; Reference 2.5.1-377). Late Quaternary faulting recently has been identified near this lineament, close to the Missouri-Illinois border (Reference 2.5.1-378). Wheeler and Cramer (Reference 2.5.1-379) discuss the concept of a left-stepover functioning as a restraining bend if the CGL is acting as a right-lateral strike-slip fault in the current tectonic environment. McBride and Kolata (Reference 2.5.1-380) note a possible relationship between the most deformed region of the Precambrian basement (yet to be identified beneath the Illinois basin and the Enterprise subsequence) and some of the largest twentieth-century earthquakes in the central midcontinent. Evaluation of recently acquired industry seismic-reflection profile data from southern Illinois provides additional insights regarding the causative structures for recent earthquakes. McBride et al. (Reference 2.5.1-381; Reference 2.5.1-382; Reference 2.5.1-501) note that earthquakes may be nucleating along compressional structures in crystalline basement (e.g., the 1968 m_b 5.5 (E[**M**] 5.32) earthquake) and thus may occur in parts of the basin where

there are no obvious surface faults or folds. The results of their study suggest that the seismogenic source just north of the New Madrid seismic zone consists, in part, of thrusts in the basement localized along igneous intrusions that are locally coincident with the CGL (Reference 2.5.1-381; Reference 2.5.1-382). McBride et al. (Reference 2.5.1-501) further evaluate major structures within the Illinois basin, including the Wabash Valley fault system and the La Salle anticlinal belt and their possible association with historical earthquakes, including the April 3, 1974, m_b 4.7 (E[**M**] 4.29) earthquake and the June 10, 1987, m_b 5.2 (E[**M**] 4.95) earthquake. Analysis of the June 18, 2002, M_w 4.6 (E[**M**] 4.48) earthquake, which occurred on a steeply dipping fault within the Wabash Valley fault system at a depth of about 18 km (11 mi), may suggest that buried faults associated with a possible Precambrian rift system are being reactivated by the contemporary east/east-northeast-trending regional horizontal compressive stress (Reference 2.5.1-502).

Morphometric analysis of the land surface, detailed geologic mapping, and structural analysis of bedrock indicate westward-dipping surfaces in the Wabash Valley region along the western edge of the CGL in the restraining bend region (Reference 2.5.1-383). The sources for other prehistoric earthquakes suggested by the inferred locations of energy centers elsewhere in southern Illinois, Missouri, and Indiana are less certain. Su and McBride (Reference 2.5.1-384) suggest that all paleoliquefaction features in south-central Illinois and southeastern Missouri may have been induced by the paleoearthquakes that occurred near the potential seismogenic structures identified in south-central Illinois by the re-analysis of industry seismic-reflection data (i.e., the Louden anticline, Centralia fault zone, and Du Quoin monocline). Inferred paleoearthquake centers in southwestern Indiana are close to the Hoosier thrust belt, Mount Carmel fault and Leesville anticline, which are Paleozoic-age faults (Table 2.5.1-201 and Figure 2.5.1-207).

Given the uncertainty in identifying specific sources for prehistoric earthquakes in the southern Illinois and southern Indiana regions, Cramer et al. (Reference 2.5.1-385) presented alternative source geometries to account for the sources of large-magnitude earthquakes in the Southern Illinois basin. Based on consideration of the above information, the CEUS SSC project developed an RLME source to

represent recurrence of large earthquakes in the Wabash Valley seismic zone with moment magnitudes in the range of **M** 6.75 to 7.5.

2.5.1.1.5 Regional Non-seismic Geologic Hazards

The United States Geological Survey has identified several zones of landslides within the (320 km [200 mi] radius) site region (Figure 2.5.1-227; Reference 2.5.1-387). The Kanawha Section of the Appalachian Plateau Physiographic Province is a region of high susceptibility and moderate to high incidence of landslides associated with the weathering of Pennsylvanian- and Permian-age shales and claystones. The Southern New York Section of the Appalachian Plateau Physiographic Province and Central Lowlands Physiographic Province have small regions along major rivers with high incidence of landslides, including the Cuyahoga River near Cleveland and the Maumee River near Toledo. In the vicinity of the Great Lakes moderate susceptibility for landslides exists associated with lacustrine deposits, and moderate incidence for landslides exists associated with wave erosion at the base of cliffs. (Reference 2.5.1-387)

Karst related problems in the (320 km [200 mi] radius) site region are associated with fissures, tubes and caves that are generally less than 300 m (1000 ft) long developed in flat lying carbonate rocks (Figure 2.5.1-228; Reference 2.5.1-388). In northwestern Ohio and adjacent Indiana and southeastern Michigan, karst occurs in Silurian-age limestones and dolomites. In northwestern Ohio areas where the carbonate rocks are covered by less than 6 m (20 ft) of glacial deposits have karst features large enough to cause engineering problems. Some caves with generally less than 1,000 ft of passages are present in northwestern Ohio. Evaporative karst (karst in halite or gypsum deposits) occurs in the central portion of the Michigan basin. (Reference 2.5.1-388)

2.5.1.2 Site Geology

Subsection 2.5.1.2 provides the background information on the physiography, geologic history, stratigraphy, and structural geology in the (40 km [25 m] radius) site vicinity, the (8 km [5 mi] radius) site area, and the (1 km [0.6 mi] radius) site location of Fermi 3 in order to provide a geologic framework for evaluating the local geologic hazards that might affect the Fermi 3 site. In Subsection 2.5.1.2, information presented for the site vicinity applies to the site area and the site location unless

specifically discussed. Where information is presented for the site area, it applies to the site location unless specifically discussed.

2.5.1.2.1 Site Physiography and Geomorphology

Fermi 3 is located in the Eastern Lake section of the Central Lowlands physiographic province, and the (40 km [25 mi] radius) site vicinity includes the St. Lawrence Lowlands physiographic province in Canada (Figure 2.5.1-202). Subsection 2.5.1.1.1.1 and Subsection 2.5.1.1.1.3 cover the overall details of the Central Lowlands and the St. Lawrence Lowlands physiographic provinces, respectively. The St. Clair clay plain is the subdivision of the St. Lawrence Lowlands physiographic province that is in the site vicinity (Figure 2.5.1-250). The St. Clair clay plain is described as a region of low relief with elevations ranging from 175 to 213 m (575 to 700 ft) and is developed on clay tills that are thinly covered with lacustrine deposits. (Reference 2.5.1-222) In adjacent Ohio, the subdivision of the Eastern Lake section is called the Maumee Lake plains (Figure 2.5.1-250) and is described by Brockman (Reference 2.5.1-219) as a “flat-lying Ice-Age lake basin…slightly dissected by modern streams; elevation 174 to 243 m (570 to 800 ft); very low relief (1.5 m[5 ft]).” The surface materials In the Maumee Lake plains include silt, clay and clayey glacial till that overlie Silurian carbonate rocks and shales (Reference 2.5.1-220). The 8 km (5 mi) radius site area is entirely within the Eastern Lake section of the Central Lowlands physiographic province (Reference 2.5.1-218). The 1:24,000 scale U.S. Geological Survey topographic maps for Monroe County show the site area is relatively flat with minor incision (< 15 ft) by east-flowing streams and elevations range from 174 to 185 m (570 ft to 605 ft). Within the 1 km (0.6 mi) radius site location, data from the Fermi 3 subsurface investigation encountered lacustrine deposits over glacial till and the U.S. Geological Survey topographic maps indicate an elevation range from 173 to 180 m (570 to 590 ft) (Figure 2.5.1-229).

In the western Lake Erie basin, which includes much of the eastern site vicinity, geomorphic features have been identified and characterized using both recent bathymetry and previous results of high-resolution seismic survey studies (Reference 2.5.1-472, Reference 2.5.1-487, Reference 2.5.1-494, Reference 2.5.1-495, Reference 2.5.1-496, and Reference 2.5.1-497).

The key geomorphic observations of Holcombe et al. (Reference 2.5.1-472) regarding the lake-floor geomorphology of the western basin of Lake Erie, which are supplemented by additional, more recent interpretation (Reference 2.5.1-495), are as follows:

- The islands and reefs bordering and lying within the western basin have bedrock cores that are erosional remnants of the more resistant Upper Silurian and Lower Devonian dolomites and limestones.
- Overdeepened channels between the islands have been sites of postglacial nondeposition, and probably erosion, due to intense wind-driven water circulation through these restricted passages. The deepest channel depth is the 19 m (62 ft) Starve Island Deep located between the southernmost Bass Island and Marblehead Peninsula.
- The Pelee-Lorain Ridge is interpreted as a late Wisconsinan end moraine upon which sand deposits have been concentrated. This feature is probably associated with a re-advance of the retreating Wisconsin ice sheet, and probably correlates with the proglacial Lake Maumee II.
- The Point Pelee Fan is a fan-shaped delta-like body of sediment that crests at 11 to 12 m (36 to 39 ft) below the present lake level. The fan extends to the east of Point Pelee Ridge, downslope to a depth of at least 18 m (59 ft), and as far south as Pelee-Lorain Ridge. The fan is believed to have been principally formed at the time when the lake level was about 10 to 15 m (33 to 49 ft) lower than at present, prior to deposition of the shallower 3,500 years BP to present sands on the Point Pelee Ridge.
- If the Point Pelee fan is a relict shoreline feature, it may be a former shoreline delta of the Detroit River that formed following the opening of the Port Huron outlet about 4,000 years BP. During this time the newly formed Detroit River was eroding its channel and bringing a heavy load of sediment into Lake Erie. An alternative interpretation for formation of the Point Pelee Fan is that strong westto- east currents have swept around the end of the Point Pelee Ridge and carried sediments eastward.
- Sands being deposited in the main postglacial channel of the Detroit River about the same time as or soon after the Port Huron outlet first opened up filled the channel and spilled over into a large part of the western basin, mostly eliminating topographic expression of the

channel. Location of the main Detroit River Channel may have coincided with a trough in the till surface extending through the western basin as shown by Hobson et al. (Reference 2.5.1-496).

- A fan-shaped sediment accumulation occurs off the Maumee River, which has been a significant deposition site for fluvial sediments brought into Lake Erie following glaciation and at present. The fan probably began forming at its present location only after the most recent rise of Lake Erie into this area. Two sand spits resulting from converging net longshore transport of sand and gravel along the lake shores toward Maumee Bay partially enclose the bay and control the position of the Maumee River Channel.
- Surficial sediments underlying the western basin are described as unconsolidated muds with a high fluid content.
- Channels underlying the main shipping lanes have been excavated by propeller wash where ship traffic increases speed, resulting in resuspension of bottom sediments. Dumpsites for dredge spoils excavated from channels are expressed in the bathymetry by a distinctive hummocky pattern in two areas (one north of the Toledo dredged channel and one west of the dredged west outer channel of the Detroit River).

2.5.1.2.2 Site Geologic History

The (40 km [25 mi] radius) site vicinity for Fermi 3 is located within the North America Craton. The site vicinity is located on the west flank of the Findlay arch at the margin of the Michigan basin (Figure 2.5.1-208 and Figure 2.5.1-218). The regional geologic history of the Precambrian is covered in Subsection 2.5.1.1.2.1 and Subsection 2.5.1.1.2.2. No surface exposures of Precambrian rocks exist in the site vicinity (Figure 2.5.1-230). The site vicinity Phanerozoic geologic history is essentially the same as the (320 km [200 mi] radius) site region presented in Subsection 2.5.1.1.2. All of the major Phanerozoic tectonic events of North America take place outside the (320 km [200 mi] radius) site region (see Subsection 2.5.1.1.3) and are outside the site vicinity, site area, and site location. Some minor reactivation of basement faults has occurred in the site vicinity during the Paleozoic (see Subsection 2.5.1.2.4). Bedrock units exposed in the site vicinity are Silurian and Devonian in age (Figure 2.5.1-230). These bedrock units are overlain by Quaternary sedimentsGeologic Map of the Fermi 3 Site Vicinity.

2.5.1.2.2.1 Paleozoic Depositional History

The Paleozoic depositional history of the (40 km [25 mi] radius) site vicinity extends from the Cambrian into the Devonian. Deposition during the Paleozoic was controlled by repeated transgressions (inundations) and regressions of epeiric seas (Subsection 2.5.1.1.3.2) over the North American Craton. A cratonic sequence is a depositional sequence related to a pair of transgressions and regressions and is bounded by interregional unconformities. Interregional unconformities are time intervals when most of the craton is exposed to erosion. (Reference 2.5.1-275) Of the six cratonic sequences identified for the North American Craton (Reference 2.5.1-275), three sequences exist in the subsurface of the site vicinity: Sauk, Tippecanoe, and Kaskaskia sequences. Because of the relatively uniform geology of the site vicinity featuring nearly horizontal sedimentary rocks (Reference 2.5.1-389), no significant changes in the geologic history are anticipated for the site area and site location. Further details of the cratonic sequences are discussed in Subsection 2.5.1.1.3.2 and Subsection 2.5.1.2.3.

2.5.1.2.2.2 Quaternary History of the Site Area

The Quaternary history of the (320 km [200 mi] radius) site region is covered in Subsection 2.5.1.1.4.1.1. Three ice lobes coalesced on the lower peninsula of Michigan beginning about 24,000 years BP. The area was ice free immediately prior to this (Reference 2.5.1-263). The ice lobes are, from west to east, the Michigan, Saginaw (equivalent to the Huron-Erie lobe on Figure 2.5.1-214), and Erie lobes (Reference 2.5.1-390). The positions of the lobes fluctuated with time and their deposits overlap.

Calkin and Feenstra (Reference 2.5.1-297) and Lewis et al. (Reference 2.5.1-272) provide overviews of the history of development of latest Wisconsinan lakes with respect to ice barriers that affected the 40 km (25 mi) [radius site vicinity and 8 km [5 mi] radius site area. A map showing features of the Erie basin and the relationships and ages of lake phases versus ice margin positions in the study vicinity are shown on Figure 2.5.1-232 and Figure 2.5.1-233, respectively. Maps showing the positions of ice margins and proglacial lake shorelines at different times during the Late Wisconsinan are presented on Figure 2.5.1-234. The sequence of events that affected the site vicinity is summarized below.

At the last glacial maximum (Nissouri Stade) about 18 to 21 ka, the Laurentide ice margin lay south of the Huron and Erie basins (Figure 2.5.1-234a). Ice retreated north of Port Huron, Ontario (out of the site region), during the Erie Interstade and exposed all of Saginaw Bay and southern Lake Huron (Reference 2.5.1-272) (Figure 2.5.1-234b). The shoreline of Glacial Lake Leverett, which was nearly coincident with but slightly lower than modern Lake Erie, would have been in or near the site study vicinity at this time, with water draining into Glacial Lake Leverett from the north through Lake St. Clair.

After the Erie Interstade, all but the Saginaw lobe advanced to nearly the same position as the Nissouri Stade (Reference 2.5.1-263) during what is known as the Port Bruce Stade (Reference 2.5.1-272) (Figure 2.5.1-234c). The Michigan and Erie lobes encroached on the area formerly occupied by the Saginaw (Huron-Erie) lobe with Michigan lobe deposits overlapping Saginaw (Huron-Erie) lobe deposits as far east as St. Joseph County, Indiana, and Erie lobe deposits overlapping Saginaw (Huron-Erie) lobe deposits as far west as Lenawee County, Michigan (Reference 2.5.1-390). The Michigan and Erie lobes continued to discharge water to the southwest across the area vacated by the Saginaw lobe and into Indiana. The Wabash Fort Wayne and Defiance moraines formed at the confluence of the Ontario-Erie and Huron-Erie lobes (Reference 2.5.1-297). The first two of these lie southwest of the site vicinity; the Defiance moraine passes through Ann Arbor, Michigan, and Adrian, Ohio (Figure 2.5.1-232).

The correlation of lake levels and outlets are useful relative stratigraphic tools where they are preserved and not destroyed by later ice advances. The lake plain boundary passes through Ypsilanti and Adrian, Michigan, and trends southwest toward Fort Wayne, Indiana (Reference 2.5.1-297) (Figure 2.5.1-232). Lakes of the Mackinaw Interstade (Glacial Lakes Maumee and Arkona in the site vicinity) (Figure 2.5.1-234d through Figure 2.5.1-234f) and younger lakes have surface expression continuity and preserved landforms that reflect the cumulative response oof the site vicinity to glacial isostatic adjustments (see Subsection 2.5.1.1.4.1.1 and Subsection 2.5.1.2.3.2.1). The Michigan Peninsula has valleys that were lake outlets (Imlay Channel and Grand River Valley in Michigan and the Glacial Grand Valley that allowed the waters of Glacial Lake Arkona, which extended east from the Saginaw lowland into the Lake Erie basin,

to drain west to the Michigan basin) (Reference 2.5.1-263) (Figure 2.5.1-234e and Figure 2.5.1-234f).

Advance of ice during the Port Huron Stade, which did not enter the site vicinity, still affected the site region. It created higher lake levels (Subsection 2.5.1.1.2.3.4.4), and proglacial lakes transgressed the site area. Deposits of Glacial Lakes Whittlesey and Warren, dated as 13,000 and 12,800 years BP, form the bulk of the glacial-age sediments deposited in the site vicinity (Reference 2.5.1-297) (Figure 2.5.1-234h and Figure 2.5.1-234i). Glacial Lake Whittlesey's beaches, with 3 to 5 m (10 to 16 ft) of relief in western Ohio, are nearly continuous and include gravels as well as sand (Reference 2.5.1-297). The younger beaches are sandy, may have multiple ridges, and have been windblown (Reference 2.5.1-297) and are difficult to trace through southeastern Michigan (Reference 2.5.1-391). A lower Lake Warren level, sometimes called Lake Wayne, is named for the broad, flat-topped sandy ridge that may be a modified beach that passes through Wayne, Michigan, 28 km (17.4 mi) west of Detroit (Reference 2.5.1-391).

Holocene lake level history and paleogeography of Lake Erie reinterpreted using the latest bathymetry, water budget data, and published information are described by Holcombe et al. (Reference 2.5.1-487). This publication describes the various factors that influenced Holocene lake history, including blocking and unblocking of outlet sills, erosion of outlet sills, distance from outlet sills, differential isostatic rebound, upper Great Lakes drainage flowing into or bypassing the lake, and climate-driven water budget of the Lake Erie drainage basin. The western basin of Lake Erie as illustrated in a series of postulated paleogeographic maps was not flooded throughout much of the Holocene; flooding of the western basin occurred after about 4,000 years ago during the Nipissing II phase when the final introduction of large volumes of upper Great Lakes water flowed into Lake Erie. Water level in the western basin at that time was several meters lower than at present. The water level of the western basin has risen since this time due to subsidence (glacial isostatic adjustment) and changes in the climate and water budget (Reference 2.5.1-487).

2.5.1.2.3 Site Stratigraphy

The following subsections provide a summary of stratigraphy in the Fermi 3 site vicinity (40 km [25 mi.] radius) and site area (8 km [5 mi.] radius).

The information presented is based on a review of geologic literature, communications with geologists and other researchers who are familiar with previous studies in the site area, and geotechnical and geologic field investigations conducted at and in the vicinity of the Fermi 3 site.

The subsurface investigation conducted for Fermi 3 is discussed in Subsection 2.5.4. Figure 2.5.1-235 and Figure 2.5.1-236 show the locations of borings drilled for the COL application. The boring logs are included in Appendix 2.5DD. To aid in understanding the (1 km [0.6 mi] radius) site location stratigraphy, geologic cross sections through the site are included on Figure 2.5.1-237, Figure 2.5.1-238, Figure 2.5.1-239, and Figure 2.5.1-240. The locations of the geologic cross sections are shown on Figure 2.5.1-235 and Figure 2.5.1-236.

2.5.1.2.3.1 Paleozoic Stratigraphy of the Site Area

The Paleozoic stratigraphy of the 40 km (25 mi) radius site vicinity, the 8 km (5 mi) radius site area and the 1 km (0.6 mi) radius site location is roughly equivalent to the stratigraphy of the 320 km (200 mi) radius site region (Subsection 2.5.1.1.3.2) except for the effects on deposition caused by the proximity of the site to the Findlay arch. For a portion of the Paleozoic, the Findlay arch was a positive topographic feature (higher than the surrounding surfaces). The top of the arch was one of the last areas flooded during a transgression and the first area exposed during a regression. Because the depositional interval on the arch was shorter, the geologic units deposited on the arch were thinner than those in the center of the basin, and the duration of the period of erosion on the arch will be longer (Reference 2.5.1-325; Reference 2.5.1-276). Exposure of soluble units (salt, gypsum, and carbonates) to fresh surface water and groundwater leads to the formation of karst and the removal of these units (Reference 2.5.1-392). This section will concentrate on the stratigraphy of the 8 km (5 mi) radius site area and 1 km (0.6 mi) radius site location as determined from the Fermi 3 subsurface investigation.

Three Paleozoic units are mapped at the surface in the 8 km (5 mi) radius site area including the Silurian Bass Islands Group, the Devonian Garden Islands Formation and Sylvania Sandstone (Figure 2.5.1-241). East of Fermi 3, below the sediments of Lake Erie, the Fermi 2 subsurface investigation encountered the Silurian Salina Group at the top of bedrock (Reference 2.5.1-221). The Devonian-age units are not exposed at the surface in the 1 km (0.6 mi) radius site location (Figure 2.5.1-241). The

oldest geologic unit encountered in the Fermi 3 subsurface investigation was the Silurian Salina Group. This subsection covers in greater detail the geologic units in the site area and site location. Geologic units older than the Silurian Salina Group are briefly discussed in Subsection 2.5.1.1.3.2.

2.5.1.2.3.1.1 Silurian Salina Group

The Silurian Salina Group is within the Tippecanoe II cratonic sequence (Reference 2.5.1-275). The Salina Group overlays the dolomites and reef facies of the Silurian Guelph Dolomite of the Niagara group and is overlain by the Silurian Bass Islands Group (Figure 2.5.1-217). The Salina group in the center of the Michigan basin is subdivided into seven units labeled A through G. Unit A has been subdivided into 4 additional units: A-1 Evaporite, A-1 Carbonate, A-2 Evaporite, and A-2 Carbonate. (Reference 2.5.1-277)

A comparison of the natural gamma logs collected as part of the Fermi 3 subsurface investigation with a natural gamma log located in Monroe County interpreted by the Michigan Geological Survey (Reference 2.5.1-277) determined that four of the seven units of the Salina Group are present in the subsurface at the Fermi 3: Unit B, Unit C, Unit E, and Unit F. Salina Group Unit G may also be present at the site location, but is indistinguishable from Unit F and/or the overlying Bass Islands Group. The classification of the Salina Group units developed by the above comparison of natural gamma logs differs from the classification presented in the Fermi 2 UFSAR. The Fermi 2 classification identifies Salina group units A, C, E, and G. (Reference 2.5.1-221) A comparison of the Fermi 2 classification and the Fermi 3 classification is presented in Table 2.5.1-202.

In the center of the Michigan basin the Salina Group contains economic halite (salt) beds. The site area however, is located in a region with no halite in the Salina and Bass Islands Groups (Reference 2.5.1-393). The Fermi 3 subsurface investigation and the site investigation for Fermi 2 (Reference 2.5.1-221) did not encounter any halite beds.

Unit A-1 Evaporite: Unit A-1 Evaporite is up to 145 m (475 ft) of clean massive halite in the center of the Michigan basin and grades to an anhydrite layer that is 3 to 9.1 m (10 to 30 ft) thick at the margin of the basin (Reference 2.5.1-277; Reference 2.5.1-281). None of the borings

that were part of the Fermi 3 subsurface investigation penetrated to the Unit A-1 Evaporite.

Unit A-1 Carbonate: Unit A-1 Carbonate is light and dark gray limestones and dolomite (micritic) with stromatolites and lenses of poorly developed nodular anhydrite (Reference 2.5.1-281). Unit A-1 Carbonate is 15- to 38 m (50 to 125 ft) thick, and is thinnest in the center of the basin and is thickest along the pinnacle reefs along the margin of the Michigan basin (Reference 2.5.1-277). Unit A-1 is present throughout the Michigan basin. None of the borings that were part of the Fermi 3 subsurface investigation penetrated to the Unit A-1 Carbonate.

Unit A-2 Evaporite: Unit A-2 Evaporite is up to 145 m (475 ft) of clean massive halite in the center of the Michigan basin and grades to an anhydrite layer that is up to 9.1 m (30 ft) thick toward the margin of the basin (Reference 2.5.1-277; Reference 2.5.1-281). This unit pinches out along the Michigan basin margin (Reference 2.5.1-277). None of the borings that were part of the Fermi 3 subsurface investigation penetrated to the Unit A-2 Evaporite.

Unit A-2 Carbonate: Unit A-2 Carbonate is comprised of light and dark gray limestones and dolomite that is less than 46 m (150 ft) thick except near reefs where it can thicken to 84 m (275 ft) (Reference 2.5.1-281). The Unit A-2 Carbonate is present in most of the Michigan basin except in the southwestern portion, where is has been removed by erosion (Reference 2.5.1-277). None of the borings that were part of the Fermi 3 subsurface investigation were penetrated to the Unit A-2 Carbonate.

Unit B Regionally: Unit B is comprised of a halite bed overlain by interbedded halite, shale and dolomite and is over 145 m (475 ft) thick in the center of the Michigan basin. In the southern portion of the basin Unit B is comprised of shale and dolomite. (Reference 2.5.1-277) The halite beds become thinner and grade to anhydrite along the margins of the basin (Reference 2.5.1-281). Salina Group Units A & B represent an overall transgression with minor transgression-regression cycles. The halite beds were deposited during the minor regressions. (Reference 2.5.1-394)

Unit B was the deepest unit encountered as part of the Fermi 3 subsurface investigation. It was encountered at borings RB-C8 and TB-C5 (Figure 2.5.1-236) at an average depth of 129 m (424 ft) below ground surface (Figure 2.5.1-237). The base of Unit B was not

encountered and the thickness of Unit B penetrated during the Fermi 3 subsurface investigation is greater than 15 m (48 ft). The unit is a brown, pale brown, gray, and dark greenish gray dolomite with white anhydrite beds up to 1.1 m (3.6 ft) thick and some shale beds up to 0.3 m (1 ft) thick. The percent recoveries for Unit B recorded during the Fermi 3 subsurface investigation range from 96 to 100 percent. The Rock Quality Designation (RQD) values range from 80 to 100 with an average of 97.1. RQD is defined as the sum of the lengths of pieces of bedrock equal to or greater than 4 inches in length divided by the core run length.

On the natural gamma logs Unit B shows oscillations from low to high values with the thickness of the low values increasing with depth (Figure 2.5.1-242). The low natural gamma values represent layers with more dolomite and anhydrite, with the high values indicating more shale. The gamma logs indicate an increase in dolomite and anhydrite with depth. The boundary between Unit B and Unit C on the natural gamma logs is set at the first decrease in gamma values that is greater than 1.2 m (4 ft) long on the natural gamma log. (Figure 2.5.1-242)

Unit C Regionally: Unit C is composed of greenish-gray shale with some nodular anhydrite and no halite. The unit is widespread in the Michigan basin and averages about 18 m (60 ft) thick, but can be up to 36 m (120 ft) thick. (Reference 2.5.1-277) Unit C marks the beginning of a regression with minor transgressions that ends with Unit G (Reference 2.5.1-394).

Unit C was encountered in the Fermi 3 subsurface investigation at an average depth of 102 m (334 ft) below the ground surface in borings RB-C8 and TB-C5 (Figure 2.5.1-237). The unit is a dark greenish-gray to black claystone and dolomite with interbeds of anhydrite. Toward the base the unit is interbedded with brown to light brownish gray dolomite. The unit is on average 27 m (90 ft) thick. The percent recoveries for Unit C recorded during the Fermi 3 subsurface investigation range from 94 to 100 percent. The RQD values range from 80 to 100 with an average of 97.2.

On natural gamma logs, Unit C has relatively high gamma values with only minor fluctuations (Figure 2.5.1-242). Only one small interval of about 0.3 m (1 ft) shows low values indicating a bed of dolomite or anhydrite. The natural gamma logs indicate that the unit is clayey with interbedded dolomite and anhydrite. The boundary between Unit C and Unit E is established where the natural gamma values become

consistently high with no major fluctuations in natural gamma values. (Figure 2.5.1-242)

Unit D: Unit D is a 12 m (40 ft) thick bed of white halite with a thin dark brown dolomite bed (Reference 2.5.1-277). The unit only occurs in the center of the Michigan basin (Reference 2.5.1-277) and was not encountered in the Fermi 3 subsurface investigation.

Unit E Regionally: Unit E is comprised of gray, greenish-gray and red shale with thin dolomite beds that is from 27 to 36 m (90 to 120 ft) thick (Reference 2.5.1-277). It occurs in all but the southwestern part of the Michigan basin (Reference 2.5.1-277).

Unit E was encountered in 14 borings and was completely penetrated at Borings RB-C8 and TB-C5 (Figure 2.5.1-236) during the Fermi 3 subsurface investigation. Unit E is shown on cross sections on (Figure 2.5.1-237 and Figure 2.5.1-238). The top of Unit E was encountered at an average depth of 73 m (241 ft) below the ground surface with an average thickness of 28 m (93 ft). The unit is comprised of pale brown, grayish-brown, gray, and bluish gray dolomite and argillaceous dolomite with thin shales and claystones, thin gray limestone beds near the top, and up to 2 m (6 ft) zones of interbedded anhydrite and dolomite near the base. The unit is vuggy in places and contains zones with ostracods. In the upper 26 ft of Unit E, occasional beds up to 0.9 m (3 ft) thick exist of poorly-indurated claystone with properties comparable to soil. The percent recoveries for Unit E recorded during the Fermi 3 subsurface investigation range from 30 to 100 percent with an average of 93.6 percent. The RQD values range from 0 to 100 with an average of 71.6.

On the natural gamma logs, Unit E has relatively low gamma values with minor fluctuations indicating dolomites and argillaceous dolomites. The magnitudes of the fluctuations increase with depth indicating an increase in shale approaching the contact with Unit C. At the base of Unit F a gradual increase in gamma values is followed by a rapid decrease. This rapid decrease occurs at about the contact between Unit F and Unit E (Figure 2.5.1-242).

An analysis of boring logs was conducted regarding core loss, and voids, cavities, and tool drops that occurred during the Fermi 3 subsurface investigation. The analysis included comparing available boring logs, photos of the core recovered, caliper and gamma logs, and downhole televiewer logs to determine an explanation of conditions that were

encountered. The analysis indicated that two cavities were encountered in the layers of vuggy dolomite and limestone near the top of the unit. The largest cavity was 0.3 m (1 ft) thick vertically, and shows on the optical televiewer log as a possible opening along bedding that appeared to be clay filled. The other cavity was a 0.06 m (0.2 ft) opening along bedding that showed evidence of water movement. The depths of the vuggy dolomite and limestone varied from 75 to 78 m (245 to 255 ft) below ground surface. Most of the vugs were clay filled. Core loss was determined to be due to either soft weathered rock that washed away during drilling, or when harder layers became stuck in the core barrel and ground the softer or fractured rock.

Unit F: Regionally, Unit F is comprised of halite, anhydrite, shale, shaly dolomite, and dolomites. The shales are gray, greenish-gray, and reddish gray, and the dolomites are gray, buff, and brown. The unit has a maximum thickness of 296 m (970 ft). In southern Michigan the evaporites no longer occur and the unit is composed shale and dolomite. (Reference 2.5.1-277)

Unit F was encountered in 27 borings and completely penetrated in 14 borings during the Fermi 3 subsurface investigation. In the area of the new reactor, the average depth to the top of Unit F is 36 m (119 ft), and the average thickness is 37 m (123 ft). To the south of Fermi 3 at boring P-399 D, the top of Unit F rises to 16 m (51 ft) below the ground surface and to the north at boring P-398 D the top of Unit F rises to 11 m (36 ft) below the ground surface (Figure 2.5.1-237), indicating a broad syncline at the site location. The structure of the syncline is discussed in Subsection 2.5.1.2.4.2. At the location of Fermi 3, cross sections on Figure 2.5.1-239 and Figure 2.5.1-240 also show Unit F.

Unit F contains a wide variety of materials and is the most complex bedrock unit encountered at the site. The unit contains dolomite, limestone, claystone, shale, breccia, sandstone, and poorly indurated clastic sediments. No halite was encountered at Fermi 3. The dolomite layers are very dark gray, dark greenish gray, gray, grayish brown, and light grayish brown; micritic; with some argillaceous (shaly) layers; some vuggy layers; some oolites; and some fossils (ostracodes). The ostracodes and brown colors are near the base of the unit. The limestone layers are dark gray, dark olive gray, dark grayish brown, and brown; crystalline; vuggy; with some argillaceous layers; with anhydrite nodules and bands, calcite nodules, and oolites; and occasional fossils

(brachiopods). The claystone layers are very dark gray, bluish gray, and gray and vary from strong to extremely weak. Some very weak to extremely weak claystones have properties comparable to soil. Some claystones are dolomitic or calcareous, and dolomite and limestone layers occur within some claystones. The shale layers are very dark gray, dark bluish gray, greenish gray, brownish gray, and grayish brown. Some shale layers are dolomitic; with anhydrite and dolomite beds. Weak to extremely weak zones exist within the shales with properities comparable to soil. The breccia layers are gray, brownish gray, and light brownish gray; with clasts of gray to pale yellow, dolomite, limestone, shale, claystone, and siltstone. The matrix of breccia is composed of claystone, clay, and calcite. Soft clay zones exist within the breccias. Subsection 2.5.1.2.3.1.2.1 has a discussion of breccias encountered during the Fermi 3 subsurface investigation. Sandstone was encountered only in boring RB-C6 (Figure 2.5.1-236) and was dark grayish brown and 0.12 m (0.4 ft) thick. The percent recoveries for Unit F recorded during the Fermi 3 subsurface investigation range from 0 to 100 percent with an average of 59.3 percent. The RQD values range from 0 to 100 with an average of 13.4.

The natural gamma log signature for Unit F features moderate to high gamma values with occasional low values that are about 0.6 m (2 ft) thick. Overall the natural gamma log indicates that Unit F is shale and claystone, with beds of carbonate. The contact between Unit F and the overlying Bass Islands Group is a rapid increase from the low gamma values of the Bass Islands to the moderate values of Salina Group Unit F. The gamma values continue to increase below the contact. (Figure 2.5.1-242)

A small low in natural gamma values can be seen about 6.1 m (20 ft) below the top of Unit F (Figure 2.5.1-242). The low corresponds to a 0.76 m (2.5 ft) thick gray micritic argillaceous dolomite. In boring CB-C2, the upper 0.06 m (0.2 ft) of the argillaceous dolomite is weathered to a light brown and has an undulatory surface with an amplitude of 0.03 m (0.1 ft) (Figure 2.5.1-243). The field boring log for CB-C2 describes the layer above the argillaceous dolomite as a 0.37 m (1.2 ft) thick fractured/gravelly limestone, and Figure 2.5.1-243 shows the cemented, rounded and subangular gravel-sized limestone grains. Based on this description, this contact is possibly an unconformity. Briggs and Briggs (Reference 2.5.1-394) note that the recession occurring during the

deposition of Salina Group Units B through G becomes a transgression during the Bass Islands Group deposition. This unconformity may be a possible boundary between a regression and a transgression, and the rocks would have been subaerially exposed, which would result in weathering as encountered in Figure 2.5.1-243.

An analysis of boring logs was conducted regarding core loss, voids, cavities, and tool drops that occurred during drilling of Unit F. The approach used was the same for Unit E. Two cavities were encountered in the layers of vuggy dolomite and limestone near the top of the Salina Group Unit F. The optical televiewer images of one of the voids indicated that the northern wall of the boring was open to a depth of about 0.33 m (13 in) and had a vertical height of about 0.46 m (1.5 ft). The other void was reported as a drilling tool drop of about 0.06 m (2.5 in) and optical televiewer logs were not preformed on this boring. Based upon the core photos, the possible void is a soft zone along bedding. Other core loses were determined to be due to soft weathered rock that washed away during drilling, poorly indurated sediments that washed away, or when harder layers became stuck in the core barrel and ground the softer or fractured rock. The origin of the poorly indurated sediments is unclear, but possible explanations are provided in Subsection 2.5.1.2.3.1.2.1.

Unit G: Unit G is comprised of gray dolomitic shale and shaly dolomite in the center of the Michigan basin; toward the basin margins the unit becomes less argillaceous; and in the southern Michigan the unit is indistinguishable from the overlying Bass Islands Group (Reference 2.5.1-277). This unit is 12 to 24 m (40 to 80 ft) thick (Reference 2.5.1-281). At the site location bedrock layers in both Unit F and the overlying Bass Islands Group fit the description of Unit G. No clear signature exists on the natural gamma logs that can be used to identify Unit G. On cross-section A-K in Lilienthal (Reference 2.5.1-277), the thickness of Unit G is thin (<3 m [10 ft]) in the McClure Oil Co. boring in central Monroe County, Michigan. Because of the thickness of the unit, the lack of distinguishing characteristics, and the lack of a natural gamma log signature, Unit G was not shown on the boring logs and profiles site location of the Fermi 3 subsurface investigation.

2.5.1.2.3.1.2 Silurian Bass Islands Group

The Silurian Bass Islands Group is the uppermost unit in the Tippecanoe II cratonic sequence (Reference 2.5.1-275) and is the uppermost

bedrock unit encountered during the Fermi 3 subsurface investigation. In the site vicinity the Bass Islands Group overlies the Silurian Salina Group and is overlain by the Devonian Bois Blanc Formation and Garden Island Sandstone (Figure 2.5.1-230). In surface exposures the Bass Islands Group is subdivided into two formations, the older Put-in-Bay and younger Raisin River dolomites. In subsurface descriptions in the area, the Bass Islands Group is not subdivided into formations. The upper portion of the Bass Islands Group is a buff dolomite with oolitic dolomite layers, and the lower part is interbedded argillaceous dolomite and buff dolomite (Reference 2.5.1-277). In the center of the Michigan basin, the group contains thin anhydrite and halite beds and the thickness is 91 to 183 m (300 to 600 ft). The unit thins to the southeast margin where it may be only 46 m (150 ft) thick (Reference 2.5.1-281).

The borings for the Fermi 3 subsurface investigation penetrated a maximum of 30 m (99 ft) of the Bass Islands Group. The Bass Islands Group encountered during the Fermi 3 subsurface investigation is dominantly a light gray, light brownish gray, to dark gray micritic dolomite, with the following characteristics:

- The dolomite can be massive, banded, or mottled.
- It contains pitted and vuggy zones with some pits and vugs filled with crystalline anhydrite or calcite.
- Oolites can be found scattered in small zones throughout the Bass Islands Group.
- Stylolites (layers associated with pressure solution) can be found throughout the unit.
- Some zones within the Bass Islands Group have stylolites that completely surround clasts of dolomite giving the zone a brecciated appearance, but these brecciated dolomites are caused by pressure solution and not fracturing.

Minor layers of argillaceous dolomite, dolomitic shale, shale, brecciated dolomite (dolomite layer or layers that have been fractured but the clasts have not significantly moved or rotated), and breccia (rock containing angular gravel and larger size fragments) also occur at Fermi 3. Subsection 2.5.1.2.3.1.2.1 has a discussion of breccias and brecciated dolomites. The shales are dark gray to black and range from partings (< 0.6 cm [<¼ inch]) up to 0.5 m (1.5 ft) thick. Some shale layers are dolomitic. Breccias and brecciated dolomite layers contain clasts of

dolomite from the Bass Islands Group in a finer-grained matrix of clays, dolomite, or calcareous cement. Generally, breccias and brecciated dolomites in the Bass Islands Group encountered during the Fermi 3 subsurface investigation are healed (clasts are cemented with mineral precipitates) or indurated (hardened into rock). The breccias encountered in both the Bass Islands and Salina groups will be discussed in greater detail in Subsection 2.5.1.2.3.1.2.1. The Bass Islands Group contains about fifteen gray clay and weak gray claystone bands that are up to 6-cm (0.2-ft) thick. The top of bedrock at the site is on average 8.5 m (28 ft) below the ground surface and ranges from 3.5 m (11.5 ft) to 9.9 m (32.5 ft) below the ground surface. The percent recoveries for Bass Islands Group recorded during the Fermi 3 subsurface investigation range from 0 to 100 percent with an average of 94.0 percent. The RQD values range from 0 to 100 with an average of 53.7.

Two marker horizons (distinctive rock layers that can be traced throughout the site location) are recognized in the Bass Islands Group. The upper marker horizon is a light brownish gray oolitic dolomite that is up to 2.1-m (6.8-ft) thick. The other marker horizon is a black to very dark gray shale or dolomitic shale that is up to 0.15 m (0.5 ft) thick.

The Bass Islands Group is easily recognized on the natural gamma logs (Figure 2.5.1-242). The natural gamma values are low except in the vicinity of the two marker horizons. Adjacent to the oolitic dolomite marker horizon gray shale beds and argillaceous dolomite exist that appear on the natural gamma logs as zones of higher natural gamma values. The zone of elevated natural gamma readings associated with the oolitic dolomite marker horizon is up to 3 m (10 ft) thick. The black shale marker horizon appears as a spike in natural gamma values that is only about 0.3 m (1 ft) thick on the natural gamma log. (Figure 2.5.1-242)

An analysis of boring logs was conducted regarding core loss, voids, cavities, and tool drops that were encountered during drilling in the Bass Islands Group. The analysis approach was the same as used for Salina Group Units E and F. The analysis indicated that cavities or voids were limited to a depth of 23.8 m (78 ft) below ground surface. The cavities or voids encountered were narrow, generally 3 cm (0.1 ft) along fractures. The open fractures are most likely formed during the unloading of the rock after the glaciers retreated. Some of the voids were filled with clay that appeared to be transported into the fracture. Core losses appear to be caused by fractured rock blocking off the core barrel and grinding

away the rock. Some of the core loss was due to weathered clayey or shaley seams being washed away during drilling.

2.5.1.2.3.1.2.1 Brecciated Dolomite, Breccia, and Poorly Indurated Rock

The Fermi 3 subsurface investigation encountered brecciated dolomite, and breccia within Salina Group Unit F and the Bass Islands Group. Poorly indurated sediments were encountered within Salina Group Unit F and at the top of Salina Group Unit E.

A breccia is a rock comprised of angular gravel and larger clasts (fragments). The clasts can be loose, in a matrix of finer-grained materials, or cemented or partially cemented with calcite, dolomite, quartz or other minerals. A brecciated dolomite is a dolomite that has been fractured, but the asperities (openings normal to the fracture plane) of the fractures are relatively small. The fracture asperities can be unfilled, filled with fine-grained material that washed in or filled with minerals that precipitated from groundwater.

Indurated sediments are those that have hardened into rock. Poorly indurated sediments are weak sediments that have not completely hardened.

Breccias were encountered in the Bass Islands Group and in Salina Group Unit F during the Fermi 3 subsurface investigation. In the Bass Islands Group, the breccias were comprised of clasts of dolomite from the Bass Islands Group with a matrix consisting of indurated fine-grained fragments of Bass Islands Group sediments or cemented with precipitated calcite and anhydrite. The breccias in the Bass Islands Group were healed and younger fractures split clasts and matrix within the breccias.

In Salina Group Unit F the breccias are comprised of clasts of dolomite, limestone, shale, and claystone from the Salina Group in a matrix of claystone or mineral precipitates. The breccias in the Salina Group Unit F range from indurated to poorly indurated. Typically, the matrix of the poorly indurated breccias consists of weak to extremely weak claystone with properties comparable to soil. Percent recoveries from core runs were low in borings in the Salina Group Unit F and the upper portion of Unit E.

Optical televiewer and natural gamma logs indicated that sediments were present in Units E and F. Caliper logs within low recovery zones have

measured increased borehole diameters, indicating that the sides of the borings probably collapsed during and after drilling. The materials visible in the optical televiewer logs within the enlarged portions of Salina Group Units E and F appear to be shales, claystones, and sand layers with thin beds of dolomite. In several borings loose clays and sands were recovered, and these were probably poorly indurated material that was weakened during drilling.

Breccias have been reported in the Salina and Bass Islands groups in southeast Michigan and northwestern Ohio (Reference 2.5.1-395; Reference 2.5.1-396; Reference 2.5.1-392; Reference 2.5.1-397; Reference 2.5.1-398). Several possible origins have been suggested for these breccias including depositional breccias (Reference 2.5.1-395; Reference 2.5.1-392), debris flows (Reference 2.5.1-395), paleokarst (Reference 2.5.1-395; Reference 2.5.1-396; Reference 2.5.1-392; Reference 2.5.1-397; Reference 2.5.1-399), and ancient seismites (Reference 2.5.1-398). Paleokarst is defined as ancient karst commonly buried by younger sediments (Reference 2.5.1-400).

Carlson (Reference 2.5.1-401) provided evidence that the evaporites of the Silurian Salina group in the center of the Michigan basin were deposited on the Findlay arch and other topographic highs. These evaporites were then removed when the rocks on the arch were exposed during the time interval (Silurian to Devonian) that created the unconformity between the Tippecanoe II and Kaskaskia I cratonic sequences (Reference 2.5.1-392; Reference 2.5.1-397). Where the evaporites were removed, caves formed within the remaining bedrock. The resultant caves were filled with quartz sand and shaly material (equivalent to the poorly indurated sediments at Fermi 3), along with breccia. (Reference 2.5.1-399) Carlson (Reference 2.5.1-397) reported finding Devonian Sylvania Sandstone within Salina Group Unit G. In Delphi, Indiana near the edge of the 320 km (200 mi) radius site region, Devonian-age fossils (conodonts) were found in calcareous shaly material that fills caves in the Salina Group (Reference 2.5.1-402). The presence of Devonian age sediments and fossils indicates that any filling that may have occurred in caves and voids ancient rather than recent.

Seismites are sediments that were seismically disturbed while they were still soft. Onash and Kahle (Reference 2.5.1-398) suggest that breccias in the Bass Islands Group found in quarries in Monroe County, Michigan

and northwestern Ohio are ancient seismites indicating earthquakes during the Silurian.

2.5.1.2.3.1.3 Devonian Garden Island Formation

The Devonian Garden Island Formation is exposed in the (8 km [5 mi] radius) site area (Figure 2.5.1-241) but not in the (1 km [0.6 m] radius) site location nor in the Fermi 3 subsurface investigation (Figure 2.5.1-241). The Garden Island Formation, the oldest Devonian unit, is known from islands in northern Lake Michigan where it is comprised of dolomitic sandstone, dolomite and cherty dolomite that is up to 6.1 m (20 ft) thick. It occurs in isolated locations in the subsurface in northern Michigan and overlies the Bass Islands Group. (Reference 2.5.1-403)

2.5.1.2.3.1.4 Devonian Bois Blanc Formation

The Devonian Bois Blanc Formation overlies the Garden Island Formation where both units are present; elsewhere, it overlies the Bass Islands Group. The unit is comprised of up to 110 m (360 ft) of gray limestones, dolomitic limestones, and dolomites that contain chert beds and fossils (brachiopods) (Reference 2.5.1-403). The Bois Blanc Formation thins to the southeast and disappears in Monroe County (Reference 2.5.1-277). The unit is not exposed at the surface in the (40 km [25 mi] radius) site vicinity (Figure 2.5.1-230), but is identified in the subsurface in central Monroe County (Reference 2.5.1-277). The Bois Blanc and Garden Island formations are the basal units of the Kaskaskia I cratonic sequence and mark the beginning of a transgression (Reference 2.5.1-276).

2.5.1.2.3.1.5 Devonian Sylvania Sandstone

The Devonian Detroit River Group includes the Sylvania Sandstone (oldest), Amherstburg Formation and Lucas Formation (youngest). The Sylvania Sandstone overlies the Bois Blanc and Garden Island formations, if present; elsewhere, it rests directly on the Bass Islands Group. (Reference 2.5.1-403) The unit is comprised of up to 6.1 m (20 ft) of fine- to medium-grained, well rounded, quartz sandstone cemented with dolomite (Reference 2.5.1-277). The Sylvania Sandstone is exposed in the (8 km [5 mi] radius) site area (Figure 2.5.1-241) and the site vicinity (Figure 2.5.1-230).

2.5.1.2.3.1.6 Devonian Amherstburg Formation

The Devonian Amherstburg Formation overlies the Sylvania Sandstone and is comprised of 99 m (325 ft) of brown and drab, fossiliferous, porous, dolomite, limestone, and sandstone (Reference 2.5.1-403; Reference 2.5.1-281). The Amherstburg Formation is not exposed in the (8 km [5 mi] radius) site area, but is exposed in the (40 km [25 mi] radius) site vicinity (Figure 2.5.1-230).

2.5.1.2.3.1.7 Devonian Lucas Formation

The Devonian Lucas Formation overlies the Amherstburg Formation and is comprised of up to 305 m (1,000 ft) of micritic dolomites and anhydrite at the base, massive anhydrite in the middle, and halite beds at the top (Reference 2.5.1-403; Reference 2.5.1-281). Other units exposed in the (40 km [25 mi] radius) site vicinity include the Devonian Dundee Limestone, the Traverse Group, and Antrim Shale. These units are not discussed because they are in the western portion of the site vicinity and are generally covered in Subsection 2.5.1.1.3.2.3 Kaskaskia cratonic sequence.

2.5.1.2.3.2 Quaternary Stratigraphy and Geomorphology

Quaternary surficial geologic units exposed in the site vicinity (40 km [25 mi] radius) consist primarily of till of Wisconsinan age overlain by a thin mantle of lacustrine and eolian sands or locally thicker beach-dune ridge deposits formed along late-glacial lake shorelines. Alluvium is present along the larger drainages that are incised into the lacustrine/till plain that is present throughout the site vicinity.

The distribution of surficial deposits and landforms within the site vicinity (40 km [25 mi] radius) is shown on Figure 2.5.1-231. The site area (8 km [5 mi] radius) is located in a glaciolacustrine section on the western edge of Lake Erie (Figure 2.5.1-244). The following subsections discuss the glacial and postglacial lake strandlines and related geomorphic features (Subsection 2.5.1.2.3.2.1), Quaternary deposits and soils in the site vicinity and site area (Subsection 2.5.1.2.3.2.2), and Quaternary stratigraphy of the site location (Subsection 2.5.1.2.3.2.3).

2.5.1.2.3.2.1 Glacial Lake Strandlines and Related Geomorphic Features

The Quaternary surficial map shown on Figure 2.5.1-231 shows a number of previously mapped latest Pleistocene and Holocene

shorelines within the site vicinity. The paleo-shorelines (also referred to as relict shorelines) are defined based on various geomorphic features, including wave-cut cliffs and terraces, beach ridges, and delta deposits (Reference 2.5.1-488, Reference 2.5.1-490). The term strandline (the line of intersection of the slope of a terrace and that of a cliff) can also describe the location of the shoreline associated with these geomorphic features (Reference 2.5.1-489).

Early mapping of beaches and correlative moraines in the Huron and Erie basins was summarized by Leverett and Taylor (Reference 2.5.1-490), who recognized “hinge lines” between untilted areas (to the south) and tilted or warped areas (to the north) (see discussion of shoreline deformation patterns in Subsection 2.5.1.1.4.1.1). The site vicinity lies southwest of the mapped hinge lines for the late glacial shorelines in the “zone of horizontality” where previous mapping would suggest there has not been differential vertical deformation of the paleoshorelines (Figure 2.5.1-251 and Figure 2.5.1-252). Leverett (Reference 2.5.1-488) discusses the strandline features associated with Lakes Maumee, Arkona, Whittlesey, and Wayne in the southeastern part of Michigan.

For northeastern Ohio, Totten (Reference 2.5.1-489) identifies three prominent wave-cut cliffs (or sets of cliffs) and terraces south of Lake Erie; on each terrace there are two to six beach ridges (Figure 2.5.1-255). The most prominent beach ridges recognized south of Lake Erie, from highest to lowest, are Maumee I, II, III; Whittlesey; Arkona I, II, III; Warren I, II, III; Wayne; Grassmere; and Lundy. Totten (Reference 2.5.1-489) notes that the wave-cut strandlines do not occur at exactly the same elevations as the beach ridges. However, the Maumee, Whittlesey, and Warren beach ridges in northeast Ohio occur at the top of prominent cliffs; consequently the cliff and overlying ridge share a common frontal slope and are considered a single feature. Although the cliff and terrace features have been identified with the associated beaches, these erosional forms are earlier than the beaches that are in front or upon them. Totten (Reference 2.5.1-489) therefore gives the cliffs and terraces separate designations of Upper, Middle, and Lower, with the former names of Maumee, Whittlesey, and Warren, respectively, in parentheses.

Totten (Reference 2.5.1-489) concludes that in earlier episodes prior to the most recent late Wisconsinan (Woodfordian) ice advance, the major activity was wave erosion, forming cliffs and terraces as the modern lake

is doing. At the various lake levels following the Woodfordian glaciation, the major activity was the deposition of beach and dune ridges, rather than cliff and terrace cutting. Calkin and Feenstra (Reference 2.5.1-297) agree with Totten (Reference 2.5.1-489) that some segments of the deglacial Great Lakes shore features may be associated with relict or re-excavated wave-cut terraces and bluffs, but suggest that for at least the Whittlesey shoreline, the entire set of features (wave-cut terraces in bedrock and drift, 5 – 8 m [16 – 26 ft] below Whittlesey storm beach crests) is related to a single lake phase. Calkin and Feenstra (Reference 2.5.1-297) acknowledge, however, that current erosion rates observed along the Lake Erie coast would be too slow to explain the very wide, buried terraces described by Totten (Reference 2.5.1-489).

Based on geomorphic position and elevation, the mapped paleo-shorelines in the site vicinity are correlated to glacial and postglacial lake levels that postdate the most recent major glacial advance approximately 14,800 years BP (Reference 2.5.1-294) as described by Eschman and Karrow (Reference 2.5.1-391) and Calkin and Feenstra (Reference 2.5.1-297) (Figure 2.5.1-256). A topographic profile illustrating the morphology of the paleo-shoreline features near the Fermi 3 site vicinity is shown on Figure 2.5.1-257. In the following descriptions of the lake levels, the elevations represent averages of the shorelines, which have been differentially upwarped north of Cleveland, Ohio, and Detroit, Michigan, by glacial isostatic adjustment along an apparent maximum uplift trend of 020 to 030 degrees (Reference 2.5.1-297). The following descriptions are based on Calkin and Feenstra (Reference 2.5.1-297) unless noted otherwise.

2.5.1.2.3.2.1.1 Lake Maumee

Three distinct lake levels, stabilized at average elevations of 244 m (800 ft), 238 m (780 ft), and 232 m (760 ft), are referred to as Maumee I, Maumee III, and Maumee II, respectively. Leverett and Taylor (Reference 2.5.1-490) suggested that the lowest phase preceded and was submerged by the Middle Maumee phase. More recent mapping suggests that the Lowest Maumee level was either reoccupied after the Middle phase or may actually have been third rather than second in the sequence (Reference 2.5.1-297 and Reference 2.5.1-489).

2.5.1.2.3.2.1.2 Lake Arkona

Beaches of glacial Lake Arkona in the Lake Erie basin occur at 216 m (710 ft) or as much as 9 m below those of the younger Lake Whittlesey. Drainage of Lake Arkona is postulated to have been marked by distinct intervals of outlet erosion, or isostatic and climatic events combined during more uniform downcutting of the outlet to produce three lake levels. Three beaches at 216 m (710 ft), 213 m (700 ft), and 212 m (695 ft) are referred to as Highest (Arkona I), Middle (Arkona II), and Lowest (Arkona III), respectively. Strands south of the Port Huron area in Michigan showed evidence of erosion and modification by Whittlesey waters. The highest of the Arkona strands in this area was noted to be gravelly and barely recognizable. Deltaic sediments associated with the Arkona extend out from the general line of the shoreline (Reference 2.5.1-490). Arkona shore features in Ontario and in northern Ohio are locally gravelly, discontinuous, poorly developed, and lack good beach ridge form. An age of 13,600 ± 500 BP for a lagoon deposit near Cleveland, Ohio, at 210 m (690 ft) may date Lowest Lake Arkona. The lagoon deposits are overlain by probably deeper water sediments assigned to Lake Whittlesey.

2.5.1.2.3.2.1.3 Lake Whittlesey

The Lake Whittlesey strands are among the strongest and best developed in the Great Lakes region. A number of radiocarbon ages closely bracket the inception of Lake Whittlesey at about 13,000 years BP during the Port Huron readvance, following the post-Arkona low lake phase (Lake Ypsilanti) at the end of the Mackinaw Interstade. In the Lake Erie basin, waters that rose to form Lake Whittlesey at about 226 m (740 ft) submerged the Lake Arkona strands. Leverett (Reference 2.5.1-488) states that the Whittlesey beach is between elevations 224 and 227 m (735 and 745 ft) in the untilted part in northern Ohio and southeastern Michigan. In the Michigan portion of the Lake Erie basin the strand is nearly continuous. The Whittlesey strand occurs nearly everywhere as a strong single ridge or bluff.

2.5.1.2.3.2.1.4 Lakes Warren and Wayne

Glacial Lake Warren developed in the Lake Erie and Lake Huron basins as the ice margin retreated from the outermost Port Huron Moraine to allow Lake Whittlesey to drain along the ice margin into the Saginaw Bay area of the Lake Huron basin (Figure 2.5.1-232). Highest Lake Warren

(Warren I) is at about 209 – 210 m (686 – 689 ft) in elevation. Lowest Warren (Warren III) existed at about 203 – 204 m (666 – 669 ft). A commonly weaker intermediate level (Middle Warren or Warren II) at about 206 m (675 ft) is represented locally. (Reference 2.5.1-297 and Reference 2.5.1-391) Totten (Reference 2.5.1-489) reports an age of 13, 050 ± 100 BP (ISGS-437) for wood collected from an organic horizon beneath basal Warren I (Middle Warren) beach gravel in northeastern Ohio. Several published dates between 12,100 and 12,000 BP from post-Warren sediments yield minimum ages for this lake.

The Lake Warren beaches contrast with those of Lake Whittlesey in that they are sandier and less gravelly. The beaches occur as multiple ridges. Less commonly, Warren strands are represented by wave-cut landforms. As a group, the Warren strands are strongly developed and easily traced throughout the basin. Leverett (Reference 2.5.1-488) notes that the Upper Warren beach is associated with a large sandy delta of the Raisin River in eastern Lenawee County, Michigan, and that it varies greatly in geomorphic expression, being weak where there were wide shallows in front of it.

Ice-margin retreat during the Warren phase is postulated to have allowed for eastward drainage from Lake Wayne. Leverett (Reference 2.5.1-488) cites evidence for submergence and modification of the Wayne shoreline by later stages of Lake Warren. Referring to mapping of shoreline features in northeastern Ohio, Totten (Reference 2.5.1-489) does not preclude the possibility of fluctuating lake levels, but concludes that the ridges on the south shore of Lake Erie in that area are progressively younger at lower elevations. Leverett (Reference 2.5.1-488) describes multiple ridges of similar height that stand 1 – 1.5 m (3 – 5 ft) above the intervening areas at the general elevation of Lake Wayne. It is further noted by Leverett that the sandy belt in which the Wayne beach developed is up to 5 – 8 km (3 – 5 mi.) wide or more in places, with the beach near its outer border. The Wayne phase may have been followed by a brief period of even lower lake level when waters in the Lake Erie basin were lowered to levels below the Niagara Escarpment (Reference 2.5.1-297).

2.5.1.2.3.2.1.5 Lake Grassmere and Lake Lundy Glacial Lake Phases

The drop in the lake level from Lowest Warren to nonglacial early Lake Erie was marked by brief pauses that are in turn now represented by

generally weak and very discontinuous shore features. These features have been assigned, on the basis of their relative positions below Lake Warren strands, to the following lake phases of successively younger age: Lake Grassmere at 195 m (640 ft) and Lake Lundy at 189 – 192m (620 – 630 ft). The dashed line for Lake Grassmere shown on Figure 2.5.1-257 represents the published lake elevation, while the band width associated with Lake Grassmere indicates the range of closely related flat surfaces identified from the DEM data. Beaches that are projected to the Lake Grassmere and Lake Lundy levels generally are sandy, have a relief of less than 1 – 2 m (3 - 7 ft), and are discontinuous. Thus these strandlines have been mapped only locally. Some of the identified beach ridges are probably offshore bars formed in earlier lakes and some may be wind-blown sand.

2.5.1.2.3.2.1.6 Post-Lake Lundy Lake Levels

Subsiding waters in the northeastern Lake Erie basin lowered lake levels below the Niagara Escarpment about 12,400 years BP. This marked the formation of nonglacial early Lake Erie at 40 m (131 ft) below present level (Reference 2.5.1-297). Glacioisostatic uplift, with the modulating effect of changes of inflow discharge from the upper Great Lakes, raised lake levels from an initial two- or three-basin early Lake Erie phase to an integrated lake within 4 m (13 ft) of the present level by 3,400 years BP (Reference 2.5.1-487).

2.5.1.2.3.2.2 Quaternary Deposits and Soils in the Site Vicinity

The thickness of unconsolidated sediment overlying bedrock in Monroe County varies from a few centimeters to more than 46 m (150 ft). In general, the sediments are less than 15 m (50 ft) over most of the area. The thickest deposits are associated with well-defined valleys carved into the rock surface, particularly in the southeastem, westem, and northwestem townships in the county. (Reference 2.5.1-389).

2.5.1.2.3.2.2.1 Glacial Deposits

The oldest Quatemary material identified in the site vicinity is till that directly overlies Paleozoic bedrock and is overlain by a thin mantle of lacustrine and shoreline deposits. Compilation and review of over 2,500 soil test borings, water well logs, and oil and gas records show that the bedrock surface in Monroe County appears to be nearly everywhere overlain by till described as an unstratified stiff, blue-gray clay admixed

with varying proportions of silt, sand, pebbles, and cobbles (Reference 2.5.1-389).

Only limited exposures of the till units were observed during the field reconnaissance. The best exposures of till were observed in Quatemary excavations completed at the Denniston Quarry approximately 16 km (10 mi) southwest of the Fermi 3 site (Reference 2.5.1-498) (Figure 2.5.1-258). Two till units, an upper brown till and a lower gray till, were well exposed in these excavations (Figure 2.5.1-260, Figure 2.5.1-261, and Figure 2.5.1-262). Both till units, which are very compact and hard , are silt and clay rich. The tills are sparsely pebbly, and cobbles and boulders are rare, except for basal clast pavements. The brown till is sandier, especially in the upper parts of the unit, and locally exhibits a fissile or subhorizontal blocky structural fabric. The underlying gray till generally has fewer gravel clasts, with the exception of some cobbles and boulders that are present in the basal part of the unit. In the Denniston Quarry exposures, the lower till unit locally includes larger boulders and blocks of the underlying Bass Islands Group bedrock. The more abundant, larger blocks appear to be localized in the vicinity of the nearby paleokarst features and are likely due to the plucking of more easily eroded bedrock in these zones by the overriding glacier. Larger blocks of bedrock would tend to be deposited close to their source.

In the Denniston Quarry excavations, the two till units are separated by a clast pavement and locally by possible glaciofluvial sediments in poorly defined channels at the base of the brown till (Figure 2.5.1-260). Clast pavements are common at the base of fine-grained glacial till associated with the late Pleistocene Laurentide ice sheet (Reference 2.5.1-491; Reference 2.5.1-492). The clast pavement observed at the Denniston Quarry is typical of clast pavements described in the literature in that it consists of a layer of rounded-to-subrounded cobbles and small boulders, generally one clast thick, with individual clasts separated from each other by enclosing sediment. Settling of clasts through low-strength, fine-grained deforming subglacial sediment, followed by clast abrasion by overriding deforming sediment analogous to a debris flow, is suggested by Clark (Reference 2.5.1-491) as a formative mechanism for explaining the observed characteristics of such clast pavements. Hicock (Reference 2.5.1-492) notes that subglacial processes, including lodgment, deformation, meltout, and erosion, are probably all end-members in a continuum of pavement-forming processes.

The exact ages of the till units in the site vicinity are unknown. As discussed in Subsection 2.5.1.2.3.2.3, an upper brown and lower gray till also were identified from boring samples at the Fermi 3 site. Both till units are assumed to be Woodfordian in age (MIS 2), based on the location and geomorphic position of the till units relative to late Wisconsinan end and ground moraines (Figure 2.5.1-205), the presence of calcareous material in the less-weathered or oxidized parent material of both units, and the lack of buried soils between the two units to indicate significant periods of subaerial exposure. It is not certain whether the two units are significantly different in age or whether the brown color of the upper till unit is primarily due to oxidation of the upper part of a till related to a single glacial advance, as has been noted in Ohio till units (Reference 2.5.1-220).

The available data do not permit a conclusive correlation of the till units to substages within the Woodfordian. The uniform, clayey texture of the lower gray till unit suggests that it may have formed as the glacier advanced across lacustrine sediments (possibly sediments deposited in Lake Everett formed during the Erie Interstadial between about 16 and 15.5 ka (Figure 2.5.1-234). The clay-rich character of the till, however, is similar to that of the Hiram Till mapped throughout northeastem Ohio, which was deposited prior to 14,050 years ago, probably 17,000 years ago (Reference 2.5.1-220). Slightly older tills deposited by different lobes of ice recognized locally in northeastem Ohio, such as the Lavery Till, which is assumed to be about 19,000 years old, also have a similar color and texture. The differing texture and color of the two till units exposed in the Denniston quarry excavations, as well as the clast pavement between the two till units, suggest a change in the provenance of the overriding ice sheet lobe or a change in the subglacial dynamics, but do not provide proof of an interval of deglaciation.

2.5.1.2.3.2.2.2 Lacustrine and Beach Ridge Deposits

Lacustrine and shoreline deposits overlying the till units observed in the site vicinity vary in thickness from less than a meter to several meters in the high beach-dune ridge complexes. The deposits include laminated silt and clay and finely bedded, fine- to moderate-grained sand that appears to have been deposited in lacustrine or beach environments (Figure 2.5.1-259), and more massive, thicker sands and gravels deposited as beach ridges or in deltas formed at the mouths of larger drainages.

2.5.1.2.3.2.2.3 Fluvial Deposits

Recent alluvium occurs along the major stream valleys. Streams have not deeply incised into the till and underlying bedrock throughout most of the lacustrine/till plain. For example, the Raisin River, one of the larger streams near the site is only incised about 1.5 to 3.2 m (4.9 to 10.5 ft) below the lacustrine/till plain surface along portions of the drainage upstream of Monroe, Michigan. Deeper incision into bedrock only occurs in the lower reaches. The greatest incision occurs in the southem part of the site vicinity where the thickness of sediments in valleys appears to be as much as 25 m (80 ft). (Reference 2.5.1-389)

2.5.1.2.3.2.2.4 Soil Maps

The general soil map for Monroe County shows that majority of the lacustrine/till plain that is present in the site vicinity (40 km [25 mi] radius) is underlain by soils of the Pewamo-Selfridge-Blount and HoytvilleNappanee associations (Reference 2.5.1-405). These nearly level, very poorly drained to somewhat poorly drained, silty, loamy, and sandy soils formed on till plains, ground moraines, and lake plains. Thicker sandy soils (the Oakville-Ted row-Granby association) are formed in the glacial outwash plains and delta complexes in the westem part of the site vicinity. The floodplains of rivers and streams incised into the lacustrine-till plain are mapped as the Sloan or Ceresco soil series. The Sloan series consists of very poorly drained , moderately or moderately slowly permeable soils formed in waterworked loamy material. The Ceresco series consists of somewhat poorly drained, moderately or moderately rapidly permeable soils on incised floodplains of rivers and large streams. These soils have a coarse-textured B horizon; the underlying parent material is described as fine sandy loam, sandy loam, or silt loam.

2.5.1.2.3.2.3 Quaternary Stratigraphy of the Site Location

This section concentrates on the Quaternary units encountered as part of the Fermi 3 subsurface investigation including, listed from oldest to youngest, glacial till, lacustrine deposits, and fill.

2.5.1.2.3.2.3.1 Glacial Till

Glacial till predominantly overlies the top of bedrock (Bass Islands Group) over the entire 1 km (0.6 mi) radius site location. At the top of bedrock, there is often sand or gravel that may represent weathered

bedrock. To the west and northwest of the Fermi 3 site near borings MW-381 and MW-393 (Figure 2.5.1-235), the glacial till is immediately below the top soil. Throughout the remainder of the site location the glacial till is overlain by lacustrine deposits. The glacial till ranges from 1.8 to 5.8 m (6 to 19 ft) thick. The glacial till is subdivided into an upper and lower unit based on color. The composition of the glacial till is comprised of predominantly of fines with variable amounts of sand, and gravel, with cobbles.

The lower glacial till is a gray to dark gray, lean clay with sand or gravel (CL), silt with sand or gravel (ML), or clayey graded gravel (GC). The individual boring logs from the Fermi 3 subsurface investigation show that the glacial till is homogeneous; however, variations in glacial till composition between borings in the Fermi 3 subsurface investigation indicates some heterogeneity in the lower glacial till across the site.

The upper glacial till is brown to grayish brown, lean clay with sand or a trace of gravel (CL). The Fermi 3 subsurface investigation did not attempt to determine the age or correlation of these glacial tills to the Quaternary stratigraphy presented in Subsection 2.5.1.1.2.3.4.

2.5.1.2.3.2.3.2 Lacustrine Deposits

Quaternary lacustrine (lake) deposits overlie the glacial till except near borings MW-381 and MW-393 (Figure 2.5.1-235). The thickness of the lacustrine deposits ranges from 0 to 2.7 m (0 to 8.7 ft). The lacustrine deposits are laminated gray, dark gray, and reddish brown lean clay (CL) and fat clay (CH). In some areas the lacustrine deposits are overlain by a thin layer of peat or organic soil. At Fermi 2 and Fermi 3 the top of the lacustrine deposits may have been removed and replaced with fill described in Subsection 2.5.1.2.3.2.3.3. The lacustrine deposits are the sediments from lakes that covered the site area after the glaciers receded (Subsection 2.5.1.1.2.3.4.4).

2.5.1.2.3.2.3.3 Fill

During the construction of existing Fermi 1 and Fermi 2, a lagoon at the site was filled with a variety of materials including gravel/cobble fill, some of the fill material came from an onsite quarry in the Bass Islands Group (Reference 2.5.1-221). In the immediate location of Fermi 3, this fill is classified as cobbles, well graded gravel (GW), poorly graded gravel (GP), well graded gravel with silt (GW-GM), and boulders.

To the east and west of the gravel/cobble fill, some finer-grained fills were encountered during the Fermi 3 subsurface investigation in the following areas:

- At boring MW-386, lean clays with sand and gravel (CL) were encountered. This is near Fermi 1. (Figure 2.5.1-235)
- At borings MW-383 and MW-384, predominantly lean clay fill with sand (CL) and gravel was encountered. Borings MW-383 and MW-384 are located south and southwest of Fermi 3 (Figure 2.5.1-235).

2.5.1.2.3.2.3.4 Soils of Site Location

Soils in the site location (1 km [0.6 mi] radius from the site) include the Lenawee ponded and Lenawee–Del Rey associations. The Lenawee ponded association consists of nearly level, very poorly drained silty soils on lake plains near Lake Erie and adjacent to large rivers. In some places it is formed on sand deposits in beach areas. The Lenawee-Del Rey association consists of nearly level, somewhat poorly drained silty soils formed on lake plains. (Reference 2.5.1-404)

Detailed soil units within the Lenawee ponded and Lenawee–Del Rey associations are shown on Figure 2.5.1-245 (Reference 2.5.1-405) and include Lenawee silty clay loam, ponded; Blount loam; Del Rey silt loam; Fulton silty clay loam; Milton clay loam; beaches; Toledo silty clay loam; aquents and pits; and urban land (Reference 2.5.1-404). The Lenawee silty clay loam, ponded, is dark grayish brown and is formed on lake plains; approximately 5 percent of mapped areas include beach sand. It is a nearly level, poorly drained soil in flat areas and drainageways. The Del Rey silt loam is formed in loamy and clayey lacustrine deposits on lake plains and is nearly level and somewhat poorly drained. Its substratum extends to 150 cm (60 in) and is mottled silty clay loam with thin, very fine-grained sand layers. The Toledo silty clay loam is a nearly level, very poorly drained soil in low areas and natural drainageways that is formed in clayey, calcareous lacustrine sediments in lake plains. The Blount loam, on 0 to 3 percent slopes is a nearly flat, somewhat poorly drained soil on upland flats, formed on water-reworked glacial till plains. The Fulton silty clay loam on 0 to 3 percent slopes is a nearly level, somewhat poorly drained soil on slight rises and knolls that is formed in clayey and calcareous lacustrine deposits. The Milton clay loam on 2 to 6 percent slopes is a moderately deep, gently sloping, well-drained soil on

knolls. It is formed in loamy, calcareous glacial till underlain by limestone. Some well-drained sandy soils over clayey soils are included in this unit. (Reference 2.5.1-405)

In addition to soil units, the following deposits are shown on Figure 2.5.1-245. Beach sands thicker than 1.5 m (5 ft) from Lake Erie are shown as beaches. Aquents are nearly level and consist of poorly drained soils that have had 20 to 60 cm (8 to 24 in) of soil material removed. Aquents also include low, wet areas that have been filled with nonsoil material and then covered with soil material. The Pits-Aquents complex consists of open excavations and pits, the bottoms of which are nearly level aquent soils. Urban land includes level areas covered by streets, parking lots, buildings, and other structures that obscure or alter the soils to the point that identification is not feasible. (Reference 2.5.1-405)

2.5.1.2.4 Structural Geology of Site Vicinity (40 km[25 mi] Radius)

As discussed in Subsection 2.5.1.1.4 the site lies within a tectonically stable continental region of the North American Craton. Precambrian and Paleozoic structures are present in the site vicinity, but as noted below there is no evidence that these structures are capable tectonic sources.

The following discussion of structures within the site vicinity was based on a review of published literature, discussions with geologists from the Ohio Geological Survey and Michigan Geological Survey, interpretation of high-altitude imagery and aerial photographs, and field and helicopter reconnaissance conducted during August 2007 and December 2009. Identification and characterization of structures at the site is based on subsurface information developed as part of previous studies conducted for Fermi 2 and results of more recent drilling completed as part of the Fermi 3 subsurface investigations.

2.5.1.2.4.1 Structures Within the Site Vicinity

Major Precambrian structures in the site vicinity include the GFTZ and the MRS, which intersect in the site vicinity (Figure 2.5.1-203). These structures, which are buried beneath a thick (approximately 1100 m [3600 ft] section of Paleozoic sediments, are interpreted from potential field and seismic data as discussed in detail in Subsection 2.5.1.1.2.2.4.

The structure of Paleozoic rocks in the subsurface in the site vicinity has been interpreted from boring and geophysical data obtained primarily

from oil and gas exploration (Reference 2.5.1-406; Reference 2.5.1-407; Reference 2.5.1-408; Reference 2.5.1-333) and limited quarry exposures.

The surface of the Precambrian basement unconformity is regular with a gentle gradient ranging from about 0.3 degree (5.9 m/km [31 ft/mi]) to locally about 1 degree [Chatham Sag] (16 m/km [85 ft/mi]) on the northwest flank of the Findlay arch northwest into the Michigan basin and about 1 degree (6 m/km [32 ft/mi]) southeast into the Appalachian basin (Reference 2.5.1-325). Dips on Paleozoic units through the lower Middle Devonian Detroit River Group are similar (Reference 2.5.1-325) and define the pattern of Paleozoic rocks in the site vicinity (Reference 2.5.1-325) (Figure 2.5.1-241). The youngest Paleozoic rocks at Fermi 3 are the Upper Silurian Bass Islands Group. Younger Paleozoic rocks were either deposited and eroded or not deposited on the crest of the positive Findlay arch.

No Quaternary faults are known within the site vicinity. The Bowling Green fault and the Maumee fault are bedrock faults mapped within 40 km (25 mi) of the site (Figure 2.5.1-246). The Howell anticline and associated fault, which is mapped to within 45 km (28 mi) of the site, are discussed in Subsection 2.5.1.1.4.3.2. A series of folds are recognized in subsurface bedrock units along the southeastern projected trend of the Howell anticline/fault structure (Reference 2.5.1-341). Two possible fault trends associated with the small New Boston and Sumpter oil and gas pools in Huron Township and Sumpter Township, Wayne County, Michigan, respectively, are mapped along the southwestern flank of this series of folds (Reference 2.5.1-406). Additional shorter faults are mapped in southwestern Ontario, including two subparallel unnamed faults, one of which is associated with the Colchester oil and gas field (Reference 2.5.1-409). Structures within the site vicinity (40 km [25 mi] radius) are described in more detail below.

The central and northern segments of the Bowling Green fault are located approximately 40 km (25 mi) from the site (Geologic Map of the Fermi 3 Site VicinityFigure 2.5.1-230; Subsection 2.5.1.1.4.3.2). The Bowling Green fault displaces the Precambrian unconformity surface down to the west (Reference 2.5.1-237) and has approximately 122 m (400 ft), down to the west displacement on the top of the Middle Silurian Lockport Dolomite (Reference 2.5.1-332). The Bowling Green fault has had at least six episodes of displacement through the Middle Silurian

(Reference 2.5.1-332; Figure 2.5.1-223). Onasch and Kahle (Reference 2.5.1-332) speculate that fault-parallel, east-dipping thrust faults with maximum displacements of less than 5 m (16 ft), generally on the east side of the fault, may represent younger deformation (post-Middle Silurian to Cenozoic). The youngest unit displaced by the Bowling Green fault is the latest Silurian Bass Islands Group; no younger units except for unfaulted Pleistocene glacial deposits occur along the fault (Reference 2.5.1-332).

The northeast-southwest-trending Maumee fault is coincident with the Maumee River in northwest Ohio, and extends to the shore of Lake Erie (Figure 2.5.1-230; Subsection 2.5.1.1.4.3.2). The Maumee fault is a normal fault that trends northeast-southwest and is expressed on the Precambrian unconformity surface (Reference 2.5.1-237). The Maumee fault is offset in an apparent left-lateral sense about 2 km (1.2 mi) by the Bowling Green fault. No geomorphic expression of the Maumee fault was identified in aerial photographs or during the helicopter reconnaissance (August 2007) along the mapped trace of the fault where it is overlain by late Pleistocene glacial lacustrine deposits.

Offshore of where the Maumee River enters Lake Erie, a linear northeast-trending channel (Figure 2.5.1-230 and Figure 2.5.1-231) has been excavated and dredged for shipping traffic entering Toledo Harbor (Reference 2.5.1-472; Reference 2.5.1-473; Reference 2.5.1-474; Reference 2.5.1-475). The dredged channel includes 11 km (7 mi) of channel on the Maumee River and 29 km (18 mi) on the bay (Reference 2.5.1-475).

The southeast end of the Howell anticline/fault extends into the northwest corner of Wayne County, 45 km (28 mi) north of the site (Figure 2.5.1-230). As discussed in Subsection 2.5.1.1.4.3.2 the Howell anticline is interpreted as a steep, asymmetrical, northwest-southeast trending, northwest-plunging, faulted anticline, having maximum relief of approximately 300 m (1000 ft) on the top of the Middle Ordovician Trenton Formation (Reference 2.5.1-325). The Howell fault offsets the base but not the top of the lower Middle Devonian Detroit River Group (Reference 2.5.1-340). In detail, this second order structure, which is superimposed on the flanks of the first order Findley arch, is probably more complex, consisting of several en-echelon folds and associated faults, as expressed in the structure contour maps on the top of lower Middle Devonian Dundee Formation, Middle Devonian Traverse

Formation, and Early Mississippian Sunbury Shale (Figure 2.5.1-225). Overall, the Howell fault trends northwest-southeast and is normal, steeply dipping to vertical, and down-to-the-southwest.

To gain an understanding of the bedrock structure in the site vicinity, available structure contour maps were reviewed. No available structure contour map covered the entire site vicinity sufficiently to provide a complete interpretation; therefore, structure contour maps for the following have been combined on Figure 2.5.1-247:

- Structure contours of the top of the Devonian Dundee Limestone (Reference 2.5.1-333),
- Structure contours of the top of the Devonian Sylvania Sandstone (Reference 2.5.1-341), and
- Structure contours of the top of the Ordovician Trenton Formation (Reference 2.5.1-341).

The structure contours on the top of the Trenton Formation in Figure 2.5.1-247 define a number of folds in the site vicinity. A subsequent map of structure contours on the top of the Trenton Formation covering the site vicinity (Reference 2.5.1-352) (Figure 2.5.1-248a) does not show these folds. The discussion presented below uses a conservative approach that assumes the folds defined by the structure contours from Reference 2.5.1-341 presented in Figure 2.5.1-247 exist.

A series of north to northwest-southeast trending, southeast plunging synclines and intervening anticlines are expressed in structure contour maps on the top of the Ordovician Trenton Formation along the southeastern projected trend of the Howell anticline in Wayne and northeast Monroe Counties (Reference 2.5.1-341) (Figure 2.5.1-247). Newcombe (Reference 2.5.1-341) also discusses a structure exposed in the Livingston Channel of the Detroit River, the Stony Island anticline. Based on a contour map of the top of the Lower Devonian Sylvania Sandstone, the anticline trends approximately N30ºW and lies slightly to the southwest of the anticlinal axis as expressed in the older (lower) Trenton Limestone (Figure 2.5.1-247). This structure is also defined by rock exposures in the Anderdon quarry in Ontario, the Patrick quarry near the south end of Grosse Isle, Michigan, and the Sibley quarry near Sibley Michigan. Newcombe (Reference 2.5.1-341) observes that the Stony Island anticline is almost directly in line with the Howell anticline/fault structure to the northwest.

In a publication that focuses on the Albion-Scipio oil field in southern Michigan, Ells (Reference 2.5.1-406) shows in the site vicinity two possible northwest-southeast-trending faults associated with the small New Boston and Sumpter oil pools. These pools were previously identified by Cohee (Reference 2.5.1-410). Uncertain locations of the possible faults are illustrated on Figure 2.5.1-230. The southwestern possible fault associated with the Sumpter oil pool possibly extends into the site area (8 km [5 mi] radius). The Ells (Reference 2.5.1-406) figure showing these possible faults is scaled at approximately one inch equals 96 km (60 mi), and a note on the map states “Fault Trends Not To Scale”, therefore, the exact location of these faults is uncertain. In fact, Ells (Reference 2.5.1-406) mislabeled the oil pools from Cohee (Reference 2.5.1-410), associating the southwestern possible fault with the New Boston oil pool and the northeastern possible fault with the Sumpter oil pool. The Ells (Reference 2.5.1-406) report is based on well data, maps, and unpublished studies by the Michigan Department of Natural Resources. However, these possible faults are not discussed by Ells (Reference 2.5.1-406) in the report, nor were they identified by Cohee or other reports reviewed for this study.

Based on the analysis of 20 oil wells, elevation constraints were obtained for the top of the Devonian Dundee Formation, Devonian Sylvania Formation, Silurian Bass Islands Group, and the Ordovician Trenton Formation that provide approximate apparent dips for the region across the Sumpter Pool and New Boston Pool possible faults (Figure 2.5.1-265; Figure 2.5.1-267). The top of the Devonian Dundee Formation, which underlies the Pleistocene glacial deposits, shows no abrupt changes in elevation and appears to be a broad, flat-lying surface at a regional scale. Elevation data were obtained for the Sylvania Formation from well numbers (Figure 2.5.1-265): 11746, 19214, 19484, 28435, 27980, 3701, 32883, 19549, 10877, 5830, 9873, 10211. Elevation data were obtained for the Bass Islands Group from well numbers: 13867, 11746, 19260, 19214, 3265, 19484, 28435, 27980, 3701, 32883, 19789, 19549, and 9546. The elevations associated with these two formations collectively record shallow apparent dips to the north-northeast of 0.2 and 0.13 degrees, respectively, across the Sumpter Pool and New Boston Pool possible faults. These approximate apparent dips are based on elevation changes of approximately 90 m (298.5 ft) across 25 km (15.5 mi) in the Sylvania Formation and approximately 55 m (184 ft) across 25 km (15.5

mi) in the Bass Islands Group. The well data suggest that there may be significant local relief on the tops of the Silurian units.

The variability in the elevation of the top of Sylvania and Bass Islands Group surfaces is likely a result of dissolution associated with paleokarst development. On a more regional scale, the structure contour map on the top of the Bass Islands Group shown in Figure 2.5.1-248 also shows closed depressions and variable relief that is consistent with karst development during the late Silurian – Devonian period of subaerial exposure and erosion (see Subsection 2.5.1.2.3.1.2.1). Similar relief is not observed in the picks for the top of the underlying Ordovician Trenton Formation.

The well data suggest that the elevation of the top of the Trenton Formation in the vicinity of the Sumpter Pool possible fault may be slightly higher (on the order of 10 m (33 ft) to 20 m (66 ft) than the picks for the top of the Trenton Formation in the vicinity of the New Boston Pool possible fault. The apparent dip based on these elevation is approximately 0.07 to 0.14 degrees to the northeast. These apparent dips were extracted from well numbers: 2637, 19484, 19214, 5830, 10656, 10877, 10430, 9546, 10099, 10211, 19260, 3265, 11746, and 9873. There is no consistent vertical displacement across the possible structures, however, that demonstrates the presence of discrete faults. The inferred locations of the possible faults lie along the southwestern flank of an anticline expressed in the top of Ordovician Trenton Formation as mapped by Cohee (Figure 2.5.1-247). There is nothing in the character of the contours on the southwest flank of the anticline (e.g., offset contours or very steep contours) that provides evidence for the possible faults. No evidence for the possible faults is present on the structure contour map on the top of the Trenton Formation as illustrated in Reference 2.5.1-325 (Figure 2.5.1-248a). In summary, there is little evidence for these two possible faults and, if present, their exact locations, extent, and association with any oil pools are unclear.

The Ordovician Trenton Formation is the source zone for the New Boston and Sumpter oil pools (Figure 2.5.1-247). Two wells were drilled in 1942 in the New Boston field in Sec. 18, Huron Township, Wayne County, Michigan, with the producing zone at a depth of 36.6 m (120 ft) below the top of the Trenton Formation (Reference 2.5.1-410). One well was drilled in 1941 in Sec. 22, Sumpter Township, Wayne County, Michigan, with production zones at depths of 3-5.2 m (10-17 ft) and 13 -22.6 m (43-74 ft)

below the top of the Trenton Formation. As discussed above, there is no discussion in any of the reports reviewed for this study about the nature of structures associated with the New Boston and Sumpter fields. In southeastern Michigan, oil in the Trenton Formation is generally found along folds in zones of dolomitization associated with fracture zones that are sometimes related to pre-existing faults (Reference 2.5.1-411); so the New Boston and Sumpter fields may be associated with pre-existing faults. However, the fields, which occur along the northwestern ends of the postulated faults, are small, and any associated folds/faults, if present, are likely minor structures. There is no evidence of any dolomitization, deformation, or displacement in rocks younger than about Upper Silurian. The lack of dolomitization and deformation indicates that if these possible faults do exist, they became inactive at the end of the Silurian.

Two faults were identified within the Silurian Bass Islands Group Dolomite along a south-southwest-facing wall on the north side of the Denniston Quarry in Monroe County, Michigan. The two faults offset two approximately 1 m (3 ft)-thick light gray dolomite beds in a reverse sense. The faults dip to the west-southwest and are spaced approximately 10 m (33 ft) apart. The average orientation of the western fault is N15°W 58°SW and of the eastern fault is N2°W 60°SW. The relative offsets across the west and east fault are 1.4 m (4.6 ft) and 1.3 m (4.4 ft), respectively. The two faults cross-cut subhorizontal bedding that dips slightly to the east up to 5 degrees. The western fault terminates approximately 2 m (6.6 ft) from the top of the outcrop and is therefore an intraformational structure, whereas the eastern fault is traceable to the top of bedrock. An investigation of the latest Pleistocene till and lacustrine deposits along the projection of the two faults provided evidence for no faulting in the overlying Quaternary deposits that are about 12,000 ka. (Reference 2.5.1-498)

Minor broad, shallow, north and northwest-southeast- trending folds superimposed on the Findley arch are also expressed in the structural contours on the top of the Upper Silurian Bass Islands Group in southern Ontario (Reference 2.5.1-325) (Figure 2.5.1-248b). Minor fold structures identified at Fermi 3 have a similar northwest-southeast trend as discussed below in Subsection 2.5.1.2.4.2. These minor folds may be third order structures that are structurally related to the distal end of the Howell anticline/fault structure as it dies out to the southeast. By

association with the Howell anticline/fault structure, these minor folds and postulated faults are assumed to be comparable in age to the Howell anticline/fault structure that is older than late Mississippian.

Ells (Reference 2.5.1-406) also shows in the site vicinity a probable north-northwest/south-southeast-trending fault associated with the Colchester oil pool in Essex County, southeastern Ontario, Canada. Burges and Hadley (Reference 2.5.1-413) show the Colchester oil field coincident with a northwest-southeast trending syncline with about 12.2 m (40 ft) of relief. The oil pool is interpreted to be associated with a zone of dolomitization along a fracture zone in the Middle Ordovician Trenton Formation. The syncline in the uppermost Ordovician and middle and lower Silurian rock overlying the Trenton Formation resulted from shrinkage accompanying dolomitization of the Trenton Formation. Bailey Geological Services and R.G. Cochrane subsequently interpreted the Colchester oil pool as two subparallel north-northwest/south-southeast trending normal, down-to-the-east faults (Reference 2.5.1-412). These structures are shown on Figure 2.5.1-230.

2.5.1.2.4.2 Structures Within the Site Location

Previous investigations, including borings and mapping of excavations for Fermi 2, and recent borings for Fermi 3 provide site-specific data to evaluate deformation at Fermi 3.

Previous and recent borings at the site indicate that the Silurian Salina Group and Bass Islands Group rocks underlying the site are folded into a broad, shallow syncline (Figure 2.5.1-237). Structural contours on the oolitic dolomite within the Bass Islands Group (Figure 2.5.1-249) are slightly irregular in shape. This is possibly indicating that these surfaces had some relief prior to folding. The axis of the syncline trends approximately N50°W. The flanks of the syncline dip less than 4º. The plunge of the syncline could not be determined because the surface of the marker horizons is irregular.

2.5.1.2.4.3 Discontinuities

Two joint sets have been mapped at the site in a quarry less than 1.6 km (1 mi) from the site and in excavations for Fermi 2 site structures (Reference 2.5.1-221). These joint sets trend N21° to 60°W and N54° to 72°E. Several trends of joint sets have been observed at quarries and outcrops in Michigan, Ohio, and Ontario, Canada. The most prominent trends are N40° to 60°W and N45° to 60°E. A primary joint set trending

approximately N24°E is present in the Ottawa Lake quarry in Monroe County, Michigan (Reference 2.5.1-414) (Figure 2.5.1-230). Four primary joint sets are present in the Waterville quarry in northwest Ohio, trending approximately N45°W, N45° to 50°E, N5°E, and N80° to 90°W (Reference 2.5.1-414). Observed joint orientations along the northeast-southwest-trending Middle Devonian Columbus Limestone cuesta in northwest Ohio range from N50° to 70°E to N35°W near the summit of the cuesta (Reference 2.5.1-414). Three primary joint sets are present in the Flat Rock quarry in northwest Ohio, trending approximately N45° to 65°E, N15°W to N15°E, and N40° to 50°W (Reference 2.5.1-414). Two primary joint sets in the Upper Devonian Ohio Shale in northwest Ohio, trending approximately N60°E and orthogonal, are present at Frink Run and Slate Run (Reference 2.5.1-414). Joints in the Middle Devonian Delaware Limestone observed in outcrops in northwest Ohio trend N55° to 60°E and N55° to 60°W (Reference 2.5.1-414). The primary east-northeast-striking joint set in the region is interpreted to be related to contemporary stresses (Reference 2.5.1-415). Joint patterns in southwest Ontario, Canada, indicate strong east-west and north-northwest/south-southeast trends, and a weaker north-south trend (Reference 2.5.1-416).

Based upon discontinuity data collected from 40 test borings for detailed foundation studies at the Fermi 2 site, the Bass Islands dolomite is highly jointed with a variable frequency of jointing. Joints are relatively tight and discontinuous and usually display only very minor solution activity. The dominant trends of joints are N45º to 60ºW and N40º to 50ºE and are nearly vertical in dip. Where the rock is densely fractured, intervals have closely spaced joints that form fragmented zones. Fractures are oriented from 0º (horizontal) to 90º (vertical), and the thickness and depths of these zones are variable throughout the Fermi 2 site. The fragmented zones range in thickness from a few inches to as much as 1.3 m (4.5 ft), and average approximately 0.6 m (1 ft). (Reference 2.5.1-221)

At the quarry 1.6 km (1 mi) southwest of Fermi 3 and in excavations for Fermi 2, vertical joints ranged from open to closed, with some filled with gypsum, antydrite, or selenite. Two joint sets were mapped. These joint sets trend N21° to 60°W and N54° to 72°E. The quantity and degree of openness of jointing tends to decrease with depth in all excavations at the Fermi 2 site. (Reference 2.5.1-221)

The majority of the fractures in the foundation rock for Fermi 2 are tight, with some filled with soft gray clay. There are displacements, tectonic breccias, or slickensided surfaces, other than slickensides associated with stylolites. The fractures are grouped into three orthogonal sets. The dominant or major joint set trends from N21º to 38º W and dips from 60º to 80º to the southwest. Generally, these joints vary in length from 5 to 30 feet, but some are as much as 20 m (65 ft) long. Spacing between joints is from 1.2 to 6 m (2 to 10 ft). A minor set of joints trend from N54º to 72º E and dips from 30º to 60º to the northwest. Generally, these joints vary in length from 0.6 to 3.0 m (1 to 5 ft) but some are as much as 9.1 m (30 ft) long. Joints of the minor set are more irregular than the major set. Some minor joints terminate against major joints. Bedding plane joints, which undulate but are essentially horizontal, are spaced from 15 cm (6 in) to 1.2 m (2 ft) apart. These joints are generally tight but occasionally have minor openings which are often clay filled. (Reference 2.5.1-417)

During the Fermi 3 subsurface investigation jointing was observed throughout the Bass Islands Group and Salina Group Unit F. The joints encountered are opening-mode fractures. The joint density in the Bass Islands Group and Salina Group Unit F varies from isolated joints to groups of closely spaced joints referred to on the logs as highly fractured zones. The existence of joints and fracture zones is confirmed on the optical televiewer logs; however, the field boring logs have more joints and fracture zones possibly indicating mechanical breaking of the core during the drilling process. The orientations vary from horizontal to vertical with near horizontal and near vertical fractures dominating. The joint apertures were from tight or hairline up to several inches. Some joints were filled with anhydrite, calcite, or clay while others had no filling. A small percentage of joints have weathering along the joint walls or display minor dissolution (solutioning). Below Salina Group Unit F, the joint density decreases, and joints are rare in Salina Group Units C and B, but mineral (anhydrite) filled joints are present even in the deepest formations.

Joint orientations vary from horizontal to vertical, with near horizontal and near vertical joints dominating. Optical televiewer logging completed for the Fermi 3 project determined the presence of low angle (< 45º) bedding planes, low angle fractures (< 45º), and high angle fractures (> 45º). The dominant strike orientations of the bedding planes are north-northeast

and west-northwest. The dominant strike orientations of all fracture planes are north-northwest and west-northwest. (Reference 2.5.1-418)

2.5.1.2.5 Site Geologic Hazard Evaluation

This section covers the non-seismic geologic hazards in the 40 km (25 mi) radius site vicinity including landslides and karst. The Landslide Overview Map of the conterminous United States (Figure 2.5.1-227) indicates the site vicinity, site area, and site location are in a region of moderate landslide susceptibility. The susceptibility is based on the presence of lacustrine deposits (lake beds). The (8 km [5 mi] radius) site area has a maximum relief of 10.7 m (35 ft) (Subsection 2.5.1.2.1) and is best described as relatively flat with no steep slopes. The lacustrine deposits in the (1 km [0.6 mi] radius) site location are up to 3 m (9 ft) thick. The natural slopes are probably not landslide prone; however, the stability of the lacustrine deposits should be considered in excavation design (Reference 2.5.1-387). The stability considerations for excavations are addressed in Subsection 2.5.4.2.1.1.2, Subsection 2.5.4.5.2, and Subsection 2.5.4.5.3.1.

The National Atlas Map showing the Engineering Aspects of Karst indicates the site vicinity, site area, and site location are in an area that can have fissures, tubes, and caves up to 300 m (1,000 ft) long below at least 3 m (10 ft) of noncarbonate overburden (Figure 2.5.1-228) (Reference 2.5.1-388). Davies et al. (Reference 2.5.1-388) emphasize that active karst in adjacent areas of northwestern Ohio occurs in areas where the noncarbonate overburden is less than 6 m (20 ft) thick. In the 1 km (0.6 mi) radius site location, the combined thickness of the till and lacustrine deposits is over 6 m (20 ft), indicating that the probability for karst is low.

Several sinkholes have been mapped in southwestern and southern Monroe County (Bedford, Whiteford, and Ida Townships). At least seven sinkholes are located in Devonian-age Detroit River group, which is outside the 8 km (5 mi) radius site area. Two sinkholes are in the Bass Islands Group. No sinkholes are in the (8 km [5 mi] radius) site area. (Reference 2.5.1-419; Reference 2.5.1-389; Reference 2.5.1-420)

In the Denniston Quarry located near Monroe, Michigan, disrupted zones interpreted as filled caves or paleokarst features related to Silurian/Devonian karst development were observed. The disrupted zones have the following features:

- Breccias composed of gravel- to boulder-sized dolomite fragments in either a fine-grained sediment matrix or carbonate cement.
- The host Bass Islands dolomite bedrock bedding is deflected downward adjacent to the disrupted zone. At some locations, tilted blocks of Bass Islands dolomite adjacent to the disrupted zone extend into the disrupted zone from their original layer.
- Discordant layers that appear to drape over the host rock along the margins of the disrupted zone.
- Horizontal bedded sediments within the disrupted zone that do not match the materials in the surrounding host rock.
- Near the top of the disrupted zones some porosity exists between the larger fragments.

No open caves or modern karst features were identified in Denniston Quarry. An investigation of the latest Pleistocene till and lacustrine deposits in the vicinity of two paleokarst features revealed that the overlying Quaternary deposits, which are about 12,000 ka, were undeformed indicating no recent karst activity. (Reference 2.5.1-498)

Subsection 2.5.1.2.3.1.2.1 discussed breccias and soft zones and potential explanations for their presence at the site. The formation of paleokarst was indicated as a possible reason for breccias and soft zones, with paleokarst episodes related to the dissolution of evaporite minerals, primarily halite and gypsum (Reference 2.5.1-392; Reference 2.5.1-397). Since no halite exists at the site (Subsection 2.5.1.2.3.1.1) and only minor amounts (nodule fillings and beds less than 3 cm [0.1 ft]) of gypsum and anhydrite exist in the Bass Islands Group and in Salina Group Unit F, the potential for modern evaporite karst is small.

The presence of voids was evaluated and discussed in Subsection 2.5.1.2.3 for applicable stratigraphic units.

2.5.1.2.6 Site Engineering Geology

This section covers the engineering issues related to the (40 km [25 mi] radius) site area, (8 km [5 mi] radius) site-vicinity, and the (1 km [0.6 mi] radius) site location.

2.5.1.2.6.1 Engineering Behavior of Soil and Rock

Subsection 2.5.4.2 covers the engineering behavior of the soils and rock at the site location.

2.5.1.2.6.2 Zones of Alteration, Weathering, and Structural Weakness

Jointing of the bedrock is discussed in Subsection 2.5.1.2.4.3. Stylolites were observed in the Bass Islands Group. The interlocking nature of the stylolite surfaces makes them stronger than joints.

Pits and vugs were encountered in both the Bass Islands and Salina groups during the Fermi 3 subsurface investigation. The vugs range up to 5 cm (2 in) in diameter. The percentage of vugs in some intervals of the core can be as high as 40 percent. Fracture connectivity and vugs can provide networks of pores that provide the hydraulic conductivity in the rock mass.

2.5.1.2.6.3 Unrelieved Residual Stresses in Bedrock

High horizontal compressive stresses in bedrock can result in pop-ups and valley bulging of bedrock features that develop for high horizontal compressive stresses. Pop-ups are surficial folds in competent rock layers caused by high horizontal stress and a lack of a vertical confining stress. Pop-ups usually occur in areas where continental glaciers have removed the overburden or in man-made excavations in bedrock, such as quarries. Pop-ups have been recognized in western New York State, Ontario, the northeastern United States (Reference 2.5.1-421), and southwestern and central Ohio (Reference 2.5.1-422). Pop-ups have also been recognized in the beds of western Lake Ontario, eastern Lake Erie, and in western Lake Huron (Reference 2.5.1-423, Reference 2.5.1-424).

Valley bulging is surficial folding that occurs in stream valleys incised into horizontally bedded sedimentary rocks. The vertical stress difference between the valley and the surrounding hills causes softer rock layers (shales and claystones) to be forced from below the hills into the valleys creating high horizontal stresses that can form surficial folds.

No pop-ups have been reported in southeastern Michigan or adjacent areas in Ohio and Indiana, but surficial folding of Devonian shales has been observed in northwestern Ohio (Reference 2.5.1-421). Since the 8

km (5 mi) site area is relatively flat, the conditions conducive to valley bulging are not present.

2.5.1.2.6.4 Weak or Unstable Subsurface Conditions

Weak poorly indurated sediments in Salina Group Unit F and the upper part of Unit E were encountered during the Fermi 3 subsurface investigation. This poorly indurated material had a tendency to wash away during drilling, resulting in low sample recovery values. Occasionally, samples were recovered from these poorly indurated sediments and the materials consisted of claystones, sands, and clays with interbedded thin dolomite layers. Optical televiewer logs collected during the Fermi 3 subsurface investigation show that sediments were present in the zones of poor recovery. Seismic velocities and other material properties for these poorly indurated sediments are reported in Subsection 2.5.4.2.

2.5.1.2.6.5 Deformational Zones

Jointing at the site was addressed in Subsection 2.5.1.2.4.3. One slickenside was observed during the Fermi 3 subsurface investigation. It appeared to have minor displacement and was probably associated with soft sediment deformation (syndepositional) or collapse during a paleokarst event (Subsection 2.5.1.2.3.1.2.1).

2.5.1.2.6.6 Prior Earthquake Effects

No reports or studies exist on liquefaction and paleoliquefaction in the (40 km [25 mi] radius) site vicinity. Refer to Subsection 2.5.2.1 for a discussion of seismicity.

2.5.1.2.6.7 Effects of Human Activity

This section covers the effects and potential effects of human activity on the site vicinity of Fermi 3 including oil and gas production, subsurface gas storage, dissolution mining of salt, and other potential mining activity.

2.5.1.2.6.7.1 Petroleum Production

The Black River and Trenton carbonates are potential areas for hydrocarbon production in southeastern Michigan (Reference 2.5.1-425). Ells (Reference 2.5.1-425) stated southeastern Michigan has been completely explored and that no additional fields will be found. Wylie et al. (Reference 2.5.1-426) evaluated drilling data and well cuttings for borings that penetrated the Black River and Trenton carbonates and

identified several potential areas for future oil and gas exploration in Michigan. The Deerfield-Summerville reservoir is one of the most productive in Michigan and is located west and just outside of the (40 km [25 mi] radius) site vicinity. Although many of the criteria used to predict future development exist in Monroe County, none of the potential areas for exploration are in the site vicinity. (Reference 2.5.1-426)

A search of the Michigan and Ohio petroleum databases reveals that no active production is occurring within the (40 km [25 mi] radius) site vicinity. At one time oil production was occurring in southern Wayne County about 24 km (14.9 mi) from the Fermi 3 site, but these wells have been plugged. Several producing oil wells within the site vicinity in Ohio have been plugged. No producing oil wells exist in or have existed in the (8 km [5 mi] radius) site area.

2.5.1.2.6.7.2 Subsurface Gas Storage Potential

Several areas of subsurface gas storage exist in the state of Michigan and are mostly associated with abandoned natural gas fields. One example of a converted gas field is the Northville field in northwestern Wayne County. The Northville gas storage area is outside the (40 km [25 mi] radius) site vicinity. It is preferable to convert former natural gas fields to gas storage areas. Since no former natural gas fields are within the site vicinity, the potential for subsurface gas storage is low. The Michigan Oil and Gas well database indicates two liquid petroleum gas storage facilities located about 24 km (14.9 mi) from the Fermi 3 site. No subsurface gas storage facilities are located within the (8 km [5 mi] radius) site area.

2.5.1.2.6.7.3 Dissolution Mining of Salt

The thickness of the salt in the Salina Group decreases from the center of the Michigan basin to the southeast. The outer margin (zero contour) of the salt is in Wayne County. The nearest occurrence of salt to the Fermi 3 site is about 16 to 24 km (10 to 15 mi). (Reference 2.5.1-393) Salt has been mined in Wayne County about 27.4 km (17 mi) from the Fermi 3 site (Reference 2.5.1-427). Since no salt deposits exist in the (8 km [5 mi] radius) site area, salt mining is unlikely.

2.5.1.2.6.7.4 Mining of Metallic Minerals

A region of non-economic deposits of Mississippi Valley-Type mineralization including galena (lead), sphalerite (zinc), fluorite, celestite,

and barite has been identified in northwestern Ohio and adjacent states including Monroe County, Michigan (Reference 2.5.1-428). Since these deposits are non-economic, no mining is anticipated.

2.5.1.2.6.7.5 Groundwater Withdrawal

Groundwater issues related to Fermi 3 are covered in Subsection 2.4.12.

2.5.1.2.6.8 Construction Groundwater Control

Groundwater control during construction of the Fermi 3 site is covered in Subsection 2.5.4.5.

2.5.1.2.6.9 Unforeseen Site Geologic Conditions

The excavations for safety-related structures will be geologically mapped. Unforeseen geologic conditions encountered in the excavation will be evaluated. The NRC will be notified when any excavations for safety related structures are open for their inspection and evaluation.

2.5.1.2.7 Site Groundwater Conditions

The surface deposits at the Fermi 3 site consist of a permeable artificial fill that overlies less permeable lacustrine deposits and glacial till. These lower permeability materials form a confining layer over the Silurian Bass Islands and Salina groups which are bedrock aquifers at the site location. Fracture networks and vugs in the Bass Islands Group may provide pathways for fluid migration. Detailed information on the groundwater conditions is in Subsection 2.4.12.

2.5.1.2.8 Tsunami and Seiche Hazards

Fermi 3 is located on the western shore of Lake Erie. Tsunami and seiche hazards are covered in Subsection 2.4.5 and Subsection 2.4.6.

2.5.1.3 References

2.5.1-201 Environmental Systems Research Institute (ESRI), ESRI ArcGIS 9.1, Data & Maps, Media Kit, Redlands, California, 2006.

2.5.1-202 National Aeronautics and Space Administration (NASA)/U.S. Geological Survey (USGS), “SRTM, Shuttle Radar Topography Mission, SRTM 30 data,” http://www2.jpl.nasa.gov/srtm/, 2005.

2.5.1-203 Fenneman, N.M., and D.W. Johnson, “Physical Divisions of the United States [Physiography],” http://water.usgs.gov/GIS/dsdl/physio.e00.gz, U.S. Department of the Interior, Geological Survey, scale 1:7,000, 000, 1946.

2.5.1-204 Bostock, H.S., Physiographic Region of Canada, Geological Survey of Canada, “A” Series Map, 1254A, MIRAGE (Map Image Rendering Database for Geoscience) Project, 1970.

2.5.1-205 Schruben, P.G., R.E. Arndt, and W.J. Bawiec, “Geology of the Conterminous United States at 1:250,000 Scale — A Digital Representation of the 1974 P.B. King and H.M. Beikman Map, ” U.S. Geological Survey, Digital Data Series 11, Release 2, 2006.

2.5.1-206 Wheeler, J.O., P.F. Hoffman, K.D. Card, A. Davidson, B.V. Sanford, A.V. Okulitch, and W.R. Roest (comps.), “Geological Map of Canada,” Geological Survey of Canada, Map D1860A, 1997.

2.5.1-207 Fullerton, D.S., C.A. Bush, and J.N. Pennell, “Map of Surficial Deposits and Materials in the Eastern and Central United States (East of 102° West Longitude),” U.S. Geological Survey Geologic Investigations Series I-2789, online edition, Version 1.0, http://pubs.usgs.gov/imap/i-2789/, accessed 5 September 2007.

2.5.1-208 Ontario Geological Survey, “Quaternary Geology, Seamless Coverage of the Province of Ontario,” Data Set 14, 1997.

2.5.1-209 Lloyd, O.B., Jr., and W.L. Lyke, “Ground Water Atlas of the Uniated States: Illinois, Indiana, Kentucky, Ohio, Tennessee,” Hydrologic Investigations Atlas HA 730-K, U.S. Geological Survey, 1995, http://pubs.usgs.gov/ha/ha730/index.html, accessed 31 January 2008.

2.5.1-210 Van Schmus, W.R., “Tectonic Setting of the Midcontinent Rift System,” *Tectonophysics*, Vol. 213, pp. 1 – 15, 1992.

2.5.1-211 Van Schmus, W.R., M.E. Bickford, and A. Turek, “Proterozoic Geology of the East-Central Midcontinent Basement,” in van de Pluijm, B.A., and P.A. Catacosinos, eds., “Basement and Basins of Eastern North America,” Geological Society of America, Special Paper 308, pp. 7 – 32, 1996.

2.5.1-212 King, P.B., “The Tectonics of Middle North America: Middle North America East of the Cordilleran System,” Princeton University Press, Princeton, NJ, 1951.

2.5.1-213 Root, S., and Onasch, C.M.,”Structure and Tectonic Evolution of the Transitional Region between the Central Appalachian Foreland and Interior Cratonic Basins,” *Tectonophysics,* Vol. 305, pp. 205 – 223, 1999.

2.5.1-214 Cannon, W.F., M.W. Lee, W.J. Hinze, K.J. Schulz, and A.G. Green, “Deep Crustal Structure of the Precambrian Basement beneath Northern Lake Michigan, Midcontinent North America,” *Geology*, Vol. 19, pp. 207 – 210, March 1991.

2.5.1-215 Hinze, W.J., “The Crust of the Northern U.S. Craton: A Search for Beginnings,” in van der Pluijm, B.A., and P.A. Catacosinos, eds., “Basement and Basins of Eastern North America,” Geological Society of America, Special Paper 308, pp. 187 – 201, 1996.

2.5.1-216 Green, A.G., B. Milkereit, and eight others, “Crustal Structure of the Grenville Front and Adjacent Terranes,” *Geology*, Vol. 16, pp. 788 – 792, September 1988.

2.5.1-217 Hoffman, P.F., “United Plates of America, the Birth of a Craton: Early Proterozoic Assembly and Growth of Laurentia,” *Annual Review of Earth and Planetary Sciences*, Vol. 16, pp. 543 – 603, 1988.

2.5.1-218 Thornbury, W.D., “Regional Geomorphology of the United States,” John Wiley & Sons, New York, 1965.

2.5.1-219 Brockman, C.S., “Physiographic Regions of Ohio,” Ohio Geological Survey, 1998.

2.5.1-220 White, G.W., “Glacial Geology of Northeastern Ohio,” Ohio Geological Survey, Bulletin 68, 1982.

2.5.1-221 Fermi 2 Updated Final Safety Analysis Report, Section 2.5.1, Revision 14, November 2006

2.5.1-222 Chapman, L.J. and Putman, D.F., “The Physiography of Southern Ontario,” Ontario Research Foundation; University of Toronto Press, p. 386, 1966.

2.5.1-223 Thruston, P.C., Williams, H.R., Sutcliffe, R.H., and Stott, G.M., "Geology of Ontario," Ontario Geological Survey Special Volume 4, p. 1525, 1991.

2.5.1-224 Stanford, B.V., "Chapter 10 St. Lawrence Platform – Introduction," in Stott, D.F. and Aitken, J.D. (Eds), Sedimentary Cover of the Craton in Canada, Geological Society of America, Geology of North America, vol. D-1, pp. 709-722, 1993.

2.5.1-225 Thurston, P.C., "Geology of Ontario: Introduction," in Thruston, P.C., Williams, H.R., Sutcliffe, R.H., and Stott, G.M., Geology of Ontario, Ontario Geological Survey Special Volume 4, pp. 3-26, 1991.

2.5.1-226 Keller, G.R., E.G. Lidiak, W.J. Hinze, and L.W. Braile, "The Role of Rifting in the Tectonic Development of the Midcontinent, U.S.A.," *Tectonophysics*, Vol. 94, p. 391 – 412, 1983.

2.5.1-227 Drahovzal, J.A., D.C. Harris, L.H. Wickstrom, D. Walker, M.T. Baranoski, B. Keith, and Lloyd C. Furer, "The East Continent Rift Basin: A New Discovery," Ohio Geological Survey, Information Circular 57, Columbus, Ohio, 1992.

2.5.1-228 Atekwana, E.A., "Precambrian Basement beneath the Central Midcontinent United States as Interpreted from Potential Field Imagery," in van der Pluijm, B.A., and P.A. Catacosinos, eds., "Basement and Basins of Eastern North America," Geological Society of America, Special Paper 308, pp. 33 – 44, 1996.

2.5.1-229 Stark, T.J., "The East Continent Rift Complex: Evidence and Conclusions," in Ojakangas, R.W., A.B. Dickas, and J.C. Green, *Middle Proterozoic to Cambrian Rifting, Central North America*, Geological Society of America, Special Paper 312, pp. 253 – 266, 1997.

2.5.1-230 Daniels, P.A., Jr., and R.D. Elmore, "Upper Keweenawan Rift-Fill Sequence, Mid-Continent Rift System, Michigan," Michigan Basin Geological Society Field Trip Guidebook, September 1988.

2.5.1-231 Gordon, M.B., and M.R. Hempton, "Collision-Induced Rifting: The Grenville Orogeny and the Keweenawan Rift of North America," *Tectonophysics*, Vol. 127, pp. 1 – 25, 1986.

2.5.1-232 Hauser, E.C., “Midcontinent Rifting in a Grenville Embrace,” In van der Pluijm, B.A., and P.A. Catacosinos, eds., “Basement and Basins of Eastern North America,” Geological Society of America, Special Paper 308, pp. 67 – 75, 1996.

2.5.1-233 Cannon, W.F., “Closing of the Midcontinent Rift — A Far-Field Effect of Grenvillian Compression,” *Geology*, Vol. 22, pp. 155 – 158, February 1994.

2.5.1-234 Culotta, R.C., T. Pratt, and J. Oliver, “A Tale of Two Sutures: COCORP’s Deep Seismic Surveys of the Grenville Province in the Eastern U.S. Midcontinent,” *Geology*, Vol. 18, pp. 646 – 649, July 1990.

2.5.1-235 Brown, L., L. Jensen, J. Oliver, S. Kaufman, and D. Steiner, “Rift Structure beneath the Michigan Basin from COCORP Profiling,” *Geology*, Vol. 10, pp. 645 – 649, December 1982.

2.5.1-236 Cannon, W.F., A.G. Green, D.R. Hutchinson, and nine others, “The North American Midcontinent Rift beneath Lake Superior from GLIMPCE Seismic Reflection Profiling,” *Tectonics*, Vol. 8, No. 2, pp. 305 – 332, April 1989.

2.5.1-237 Baranoski, M.T., “Structure Contour Map on the Precambrian Unconformity Surface in Ohio and Related Basement Features,” Ohio Geological Survey Map PG-23, Columbus, Ohio, scale 1:500,000, with 18-page description, available on CD-ROM, 2002.

2.5.1-238 Pratt, T., R. Culotta, E. Hauser, D. Nelson, L. Brown, S. Kaufman, J. Oliver, and W. Hinze, “Major Proterozoic Basement Features of the Eastern Midcontinent of North America Revealed by Recent COCORP Profiling,” *Geology*, Vol. 17, pp. 505 – 509, June 1989.

2.5.1-239 Howell, P.D., and B.A. van der Pluijm, “Early History of the Michigan Basin: Subsidence and Appalachian Tectonics,” *Geology*, Vol. 18, pp. 1195 – 1198, December 1990.

2.5.1-240 Howell, P.D., and B.A. van der Pluijm, “Structural Sequences and Styles of Subsidence in the Michigan Basin,” *GSA Bulletin*, Vol. 111, No. 7, No. 7, pp. 974 – 991, July 1999.

2.5.1-241 Catacosinos, P.A., W.B. Harrison III, R.F. Reynolds, D.B. Westjohn, and M.S. Wollensak, “Stratigraphic Nomenclature for Michigan,” Michigan Basin Geological Society chart, 2000.

2.5.1-242 Flint, R.F., “Glacial and Pleistocene Geology,” John Wiley and Sons, New York, p. 553, 1957.

2.5.1-243 Jennings, C.E., J.S. Aber, G. Balco, R. Barendregt, P.R. Bierman, J. Mason, C.W. Rovey II, M. Roy, and L.H. Thorleifson, “Middle Pleistocene Glaciations in North America, ” in Gibbard, P., and J. Ehlers, eds., *Encyclopedia of Quaternary Science, History of Quaternary Glaciations*, Elsevier, 2006.

2.5.1-244 Imbrie, J., J.D. Hays, D.G. Martinson, A. MacIntyre, A.C. Mix, J.J. Morley, N.G. Pisias, W. Prell, and N.J. Shackleton, “The Orbital Theory of Pleistocene Climate: Support for a Revised Chronology of Marine $\delta^{18}O$ Record,” in Berger, A.L., J. Hays, G. Kukla, and B. Salzman, eds., “Milankovitch and Climate, Part 1,” Reidel Publishing Co., Norwell, Massachusetts, pp. 269 – 305, 1984.

2.5.1-245 Ruddiman, W.F., M.E. Raymo, D.G. Martinson, B.M. Clement, and J. Backman, “Pleistocene Evolution: Northern Hemisphere Ice Sheets and North Atlantic Ocean,” *Paleoceanography*, Vol. 4, pp. 353 – 412, 1989.

2.5.1-246 Fullerton, D.S., “Stratigraphy and Correlation of Glacial Deposits from Indiana to New York and New Jersey,” *Quaternary Science Reviews*, Vol. 5, pp. 23 – 37, 1986.

2.5.1-247 Mickelson, D.M., L. Clayton, D.S. Fullerton, and H.W. Borns, Jr., “The Late Wisconsin Glacial Record of the Laurentide Ice Sheet in the United States,” in Porter, S.C., ed., “Late Quaternary Environments in the United States, Volume 1, The Late Pleistocene,” University of Minnesota Press, Minneapolis, pp. 3 – 37, 1983.

2.5.1-248 Hofer, J.W., and J.P. Szabo, “Port Bruce Ice-Flow Directions based on Heavy-Mineral Assemblages in Tills from the South Shore of Lake Erie in Ohio,” *Canadian Journal of Earth Sciences/Revue Canadienne des Sciences de la Terre*, Vol. 30, No. 6, 1993, pp. 1236 – 1241, http://www.csa.com/, accessed 25 August 2007.

2.5.1-249 Mickelson, D.M., and P. Colgan, “The Southern Laurentide Ice Sheet,” in Gillespie, A.R., S.C. Porter, and B.F. Atwater, eds., The Quaternary Period, Vol. 1 of the Developments in

Quaternary Science series"The Quaternary Period," *Developments in Quaternary Science*, Vol. 1, Elsevier, Amsterdam, pp. 1 – 16, 2004.

2.5.1-250 Ekberg, M.P., T.V. Lowell, and R. Stuckenrath, "Late Wisconsin Glacial Advance and Retreat Patterns in Southwestern Ohio, USA," *Boreas*, Vol. 22, No. 3, pp. 189 – 204, 1993.

2.5.1-251 Lowell, T.V., "The Application of Radiocarbon Age Estimates to the Dating of Glacial Sequences: An Example from the Miami Sublobe, Ohio, USA," *Quaternary Science Reviews*, Vol. 94, pp. 113 – 118, 1995.

2.5.1-252 Reimer P.J., M.G.L. Baillie, E. Bard, and 26 others, "IntCal04 Terrestrial Radiocarbon Age Calibration, 0-26 Cal Kyr BP," *Radiocarbon*, Vol. 46, No. 3, v-1334, pp. 1029 – 1058, 2004.

2.5.1-253 Hughen, K., and the IntCal Working Group, "IntCal04 Update-A Preliminary Extension of the ^{14}C-calendar Age Curve Back to 50 ka," *Geophysical Research Abstracts*, Vol. 9, pp. 10215, 2007.

2.5.1-254 Jennings, C.E., "Terrestrial Ice Streams — A View from the Lobe," *Geomorphology*, Vol. 75, No. 1-2, pp. 100 – 124, 2006.

2.5.1-255 Roy, M., P.U. Clark, R.W. Barendregt, J.R. Glasmann, and R.J. Enkin, "Glacial Stratigraphy and Paleomagnetism of Late Cenozoic Deposits of the North-Central United States," *Geological Society of America Bulletin*, Vol. 226, No. 1-2, pp. 30 – 41, 2004.

2.5.1-256 Eschman, D.F., "Summary of the Quaternary History of Michigan, Ohio and Indiana," *Journal of Geological Education*, Vol. 33,, No. 3, pp. 161 – 167, May 1985.

2.5.1-257 Shackleton, N.J., A. Berger, and W. Peltier, "An Alternative Astronomical Calibration of the Lower Pleistocene Timescale Based on ODP Site 677," *Transactions of the Royal Society of Edinburgh: Earth Sciences*, Vol. 81, pp. 251 – 261, 1990.

2.5.1-258 Spell, T., and I. McDougall, "Revisions to the Age of the Brunhes-Matuyama Boundary and the Pleistocene Geomagnetic Polarity Time Scale," *Geophysical Research Letters*, Vol. 19, pp. 1181 – 1184, 1992.

2.5.1-259 Renne, P., A. Deino, R. Walter, B. Turrin., I Swisher, C.C.T. Becker, G. Curtis, W. Sharp, and A.R. Jaouni, “Intercalibration of Astronomical and Radioisotopic Time,” *Geology*, Vol. 22, pp. 783 – 786, 1994.

2.5.1-260 Eyles, N., and J.A. Westgate, “Restricted Regional Extent of the Laurentide Ice Sheet in the Great Lakes Basins during Early Wisconsin Glaciation,” *Geology*, Vol. 15, pp. 537 – 540, 1987.

2.5.1-261 Curry, B.B., and M.J. Pavich, “Absence of Glaciation in Illinois during Marine Isotope Stages 3 through 5,” *Quaternary Research*, Vol. 46, pp. 19 – 26, 1996.

2.5.1-262 Miller, B.B., W.D. McCoy, W.J. Wayne, and C.S. Brockman, “Ages of Whitewater and Fairhaven Tills in Southwestern Ohio and Southeastern Indiana,” in Clark, P.U., and P.D. Lea, eds., “The Last Interglacial-Glacial Transition in North America,” Geological Society of America, Special Paper 270, pp. 89 – 98, 1992.

2.5.1-263 Eschman, D.F., and D.M. Mickelson, “Correlation of Glacial Deposits of the Huron, Lake Michigan and Green Bay Lobes in Michigan and Wisconsin,” *Quaternary Science Reviews*, Vol. 5, pp. 53 – 57, 1986.

2.5.1-264 Szabo, J.P., “Reevaluation of Early Wisconsinan Stratigraphy of Northern Ohio,” in Clark, P.U. and P.D. Lea, eds., “The Last Interglacial-Glacial Transition in North America,” Geological Society of America, Special Paper 270, pp. 99 – 107, 1992.

2.5.1-265 Dreimanis, A., “Early Wisconsinan in the North-Central Part of the Lake Erie Basin: A New Interpretation,” in Clark, P.U., and P.D. Lea, eds., *“The Last Interglacial-Glacial Transition in North America*,” Geological Society of America, Special Paper 270, pp. 109 – 118, 1992.

2.5.1-266 Hicock, S.R., and A. Dreimanis, “Sunnybrook Drift in the Toronto Area, Canada: Reinvestigation and Reinterpretation,” in Clark, P.U., and P.D. Lea, eds., “The Last Interglacial-Glacial Transition in North America,” Geological Society of America, Special Paper 270, pp. 139 – 161, 1992.

2.5.1-267 Pavich, M.J., and O.A. Chadwick, “Soils and the Quaternary Climate System,” in Gillespie, A.R., S.C. Porter, and B.F. Atwater, eds., “The Quaternary Period,” Vol. 1 of the Developments in Quaternary Science series, Elsevier, Amsterdam, pp. 311 – 330, 2004.

2.5.1-268 Dyke, A.S., J.T. Andrews, P.U. Clark, J.H. England, G.H. Miller, J. Shaw, and J.J. Veilette, “The Laurentide and Innuitian Ice Sheets during the Last Glacial Maximum,” *Quaternary Science Reviews*, Vol. 21, pp. 9 – 31, 2002.

2.5.1-269 White, G.W., “Pleistocene Deposits of the Northwestern Allegheny Plateau, U.S.A.,” *Quarterly Journal of the Geological Society of London*, Vol. 124, pp. 131 – 151, 1968.

2.5.1-270 Frolking, T.A., and J.P. Szabo, “Quaternary Geology along the Eastern Margin of the Scioto Lobe in Central Ohio,” Ohio Geological Survey, Guidebook No. 16, Columbus, Ohio, 1998.

2.5.1-271 White, G.W., “Classification of Glacial Deposits of Northeastern Ohio,” U.S. Geological Survey, Bulletin 1121-A, pp. 12, 1960.

2.5.1-272 Lewis, C.F., T.C. Moore, D.K. Rea, D.L. Dettman, A.M. Smith, and L.A. Mayer, “Lakes of the Huron Basin: Their Record of Runoff from the Laurentide Ice Sheet,” *Quaternary Science Reviews*, Vol. 13, pp. 891 – 992, 1994.

2.5.1-273 Evenson, E.B., W.R. Farrand, D.F. Eschman, D.M. Mickelson, and L.J. Maher, “Greatlakean Substage: A Replacement for Valderan Substage in the Lake Michigan Basin,” *Quaternary Research*, Vol. 6, No. 3, pp. 411 – 424, 1976.

2.5.1-274 Larsen, C.E., “Lake Level, Uplift, and Outlet Incision, the Nipissing and Algoma Great Lakes,” in Karrow, P.F., and P.E. Calkin, eds., *Quaternary Evolution of the Great Lakes*, Geological Association of Canada, Special Paper 30, pp. 63 – 76, 1985.

2.5.1-275 Sloss, L.L., “Tectonic evolution of the craton in Phanerozoic time,” in Sloss, L.L., ed., “Sedimentary Cover-North American Craton,” Geological Society of America, “The Geology of North America,” Vol. D-2, pp. 25-51, 1988.

2.5.1-276 Fisher, J.H., M.W. Barratt, J.B. Droste, R.H. Shaver, "Michigan Basin," in Sloss, L.L., ed., "Sedimentary Cover-North American Craton," Geological Society of America, "The Geology of North America," Vol. D-2, pp. 361-382, 1988.

2.5.1-277 Lilienthan, R.T., 1978. “Stratigraphic Cross-sections of the Michigan Basin,” Michigan Geological Survey, Report of Investigation 19, 39 pp. 89 plates, 1978.

2.5.1-278 Milici, R.C. and W. de Witt, “The Appalachian Basin,” in Sloss, L.L., ed., “Sedimentary Cover-North American Craton,” Geological Society of America, “The Geology of North America,” Vol. D-2, pp. 427-469, 1988.

2.5.1-279 Sloss, L.L., “Introduction,” in Sloss, L.L., ed., “Sedimentary Cover-North American Craton,” Geological Society of America, “The Geology of North America,” Vol. D-2, pp. 1-3, 1988.

2.5.1-280 Heckel, P.H., “Origin of Phosphatic Black Shale Facies in Pennsylvanian Cyclothems of Midcontinent North America,” *American Association of Petroleum Geologists Bulletin*, Vol. 61, pp. 1045-1068, 1977.

2.5.1-281 Catacosinos, P.A., D.B. Westjohn, W.B. Harrison, III, M.S. Wollensak, and R. F. Reynolds, "Stratigraphic Lexicon for Michigan," Michigan Geological Survey Bulletin 8, pp. 56, 2001.

2.5.1-282 Wylie, A.S., J.R. Wood, and W.B. Harrison, III, "Michigan Trenton-Black River Opportunities Identified with Sample Attribute Mapping," Oil & Gas Journal, Vol. 102, pp. 29-35, 2004.

2.5.1-283 Mesolella, K.J., J.D. Robinson, L.M. McCormick, and A. R. Ormiston, "Cyclic Deposition of Silurian Carbonates and Evaporites in Michigan Basin," American Association of Petroleum Geologists Bulletin, Vol. 58, pp. 34-62, 1974.

2.5.1-284 Sparling, D.R., “The Bass Islands Formation in its Type Region,” *The Ohio Journal of Science*, Vol. 70, pp. 1-33, 1970.

2.5.1-285 Eyles, N., and N.E. Williams, “The Sedimentary and Biological Record of the Last Interglacial-Glacial Transition at Toronto, Canada,” in Clark, P.U., and P.D. Lea, eds., “The Last Interglacial-Glacial Transition in North America,” Geological Society of America, Special Paper 270, pp. 119 – 137, 1992.

2.5.1-286 Electric Power Research Institute, U.S. Department of Energy, and U.S. Nuclear Regulatory Commission, “Technical Report: Central and Eastern United States Seismic Source Characterization for Nuclear Facilities,” NUREG-2115, U.S. Nuclear Regulatory Commission, Washington, D.C., 2012.

2.5.1-287 Zoback, M.L., and M.D. Zoback, “Tectonic Stress Field of the Continental United States,” in L.C. Pakiser and W.D. Mooney, eds., “Geophysical Framework of the Continental United States,” Geological Society of America, Memoir 172, pp. 523 – 541, 1989.

2.5.1-288 Richardson, R.M., and L.M. Reding, “North American Plate Dynamics,” *Journal of Geophysical Research*, Vol. 96, pp. 12, 201 – 12, 223, 1991.

2.5.1-289 Zoback, M.L., “Stress Field Constraints on Intraplate Seismicity in Eastern North America,” *Journal of Geophysical Research*, Vol. 97, No. B8, pp. 11, 761 – 11, 782, 1992.

2.5.1-290 Heidbach, O., M. Tingay, A. Barth, J. Reinecker, D. Kurfess, and B. Müller, “The World Stress Map Database Release 2008,“ doi:10.1594/GFZ.WSM.Rel2008, 2008, http://www.world-stress-map.org, accessed 20 November 2009.

2.5.1-291 Sella, G.F., S. Stein, T.H. Dixon, M. Craymer, R.S. James, S. Mazzotti, and R.K. Dokka, “Observation of Glacial Isostatic Adjustment in ‘Stable’ North America with GPS,” *Geophysical Research Letters*, Vol. 34, L02306, doi:10.1029/2006GL027081.

2.5.1-292 Wu, P., and P. Johnston, “Can Deglaciation Trigger Earthquakes in N. America?” *Geophysical Research Letters*, Vol. 27, No. 9, pp. 1323 – 1326, May 1, 2000.

2.5.1-293 Mazzotti, S., and J. Adams, “Rates and Uncertainties on Seismic Moment and Deformation in Eastern Canada,” *Journal of Geophysical Research*, Vol. 110, B09301, doi: 10.1029/2004JB003510, 2005

2.5.1-294 Lewis, C.F.M., and T.W. Anderson, “Postglacial Lake Levels in the Huron Basin: Comparative Uplift Histories of Basins and Sills in a Rebounding Glacial Marginal Depression,” in Karrow, P.F., and P.E. Calkin, *Quaternary Evolution of the Great Lakes*, Geological Association of Canada, Special Paper 30, 1985.

2.5.1-295 Farrand, W.R., “Postglacial Uplift in North America,” *American Journal of Science*, Vol. 260, No. 3, March 1962, pp. 181 – 199, http://www.csa.com/, accessed 25 August 2007.

2.5.1-296 Coakley, J.P., and C.F.M. Lewis, “Postglacial Lake Levels in the Erie Basin,” in Karrow, P.F., and P.E. Calkin, eds., *Quaternary Evolution of the Great Lakes*, Geological Association of Canada, Special Paper 30, pp. 195 – 212, 1985.

2.5.1-297 Calkin, P.E., and B.H. Feenstra, “Evolution of the Erie-Basin Great Lakes,” in Karrow, P.F., and P.E. Calkin, eds., *Quaternary Evolution of the Great Lakes*, Geological Association of Canada, Special Paper 30, 1985. pp. 149 – 170, http://www.csa.com/, accessed 25 August 2007.

2.5.1-298 Mainville, A., and M.R. Craymer, “Present-Day Tilting of the Great Lakes Region Based on Water Level Gauges,” *GSA Bulletin*, Vol. 117, No. 7/8, pp. 1070 – 1080, July/August 2005.

2.5.1-299 Dater, D., D. Metzger, and A. Hittelman (comps.), “Land and Marine Gravity CD-ROMS,” U.S. Department of Commerce, National Oceanic and Atmospheric Administration, Nation Geophysical Data Center, Boulder, Colorado, 1999.

2.5.1-300 North American Magnetic Anomaly Group (NAMAG; Bankey, V., A. Cuevas, D. Daniels, and 15 others), “Digital Data Grids for the Magnetic Anomaly Map of North America,” U.S. Geological Survey, Open-File Report 02-414, jointly sponsored by the Geological Survey of Canada, U.S. Geological Survey, and Consejo de Recursos Minerales de Mexico, 2002.

2.5.1-301 Hinze, W.J., R.L. Kellogg, and N.W. O’Hara, “Geophysical Studies of Basement Geology of Southern Peninsula of Michigan,” *American Association of Petroleum Geologists Bulletin*, Vol. 59, No. 9, pp. 1562 – 1584, September 1975.

2.5.1-302 Lucius, J.E., and R.R.B. von Frese, “Aeromagnetic and Gravity Anomaly Constraints on the Crustal Geology of Ohio,” *Geological Society of America Bulletin*, Vol. 100, pp. 104 – 116, January 1988.

2.5.1-303 Harbi, H.M., “2-D Modeling of Southern Ohio Based on Magnetic Field Intensity, Gravity-Filled Intensity and Well Log Data,” Master of Science Thesis, The University of Akron, December 2005.

2.5.1-304 Carter, T.R., R.A. Trevail, and R.M. Easton, “Basement Controls on Some Hydrocarbon Traps in Southern Ontairo, Canada,” in van de Pluijm, B.A., and P.A. Catacosinos, eds., “Basement and Basins of Eastern North America,” Geological Society of America, Special Paper 308, pp. 95 – 107, 1996.

2.5.1-305 Boyce, J.I., and W.A. Morris, “Basement-Controlled Faulting of Paleozoic Strata in Southern Ontario, Canada: New Evidence from Geophysical Lineament Mapping,” *Tectonophysics*, Vol 353, pp. 151 – 171, 2002.

2.5.1-306 Easton, R.M., and T.R. Carter, “Geology of the Precambrian Basement beneath the Paleozoic of Southwestern Ontario,” in R.W. Ojakangas et al., eds., *Basement Tectonics*, Vol. 10, pp. 221 – 264, 1995.

2.5.1-307 Zhu, T., and L.D. Brown, “Consortium for Continental Reflection Profiling Michigan Surveys: Reprocessing and Results,” *Journal of Geophysical Research*, Vol. 91, No. B11, pp. 11,477 – 11,495, October 10, 1986.

2.5.1-308 Behrendt, J.C., A.G. Green, W.F. Cannon, D.R. Hutchinson, M.W. Lee, B. Milkereit, W.F. Agena, and C. Spencer, “Crustal Structure of the Midcontinent Rift System: Results from GLIMPCE Deep Seismic Reflection Profiles,” *Geology*, Vol. 16, pp. 81 – 85, January 1988.

2.5.1-309 Hauser, E.C., “Grenville Foreland Thrust Belt Hidden beneath the Eastern U.S. Midcontinent,” *Geology*, Vol. 21, pp. 61 – 64, January 1993.

2.5.1-310 Mereu, R.F., D.P. Epili, and A.G. Green, “Pg shings: preliminary results from the onshore GLIMPCE refraction experiment” *Tectonophysics*, Vol. 173, pp. 617 – 626, 1990.

2.5.1-311 Johnston, A.C., “The Seismicity of ‘Stable Continental Interiors,’” in Gergersen, S., and P. Basham, eds., *Earthquakes at the North American Passive Margin: Neotectonics and Postglacial Rebound*, NATO ASI Series C: Mathematical and Physical Sciences, Kluwer Academic Publishers, Dordrecht, Netherlands, Vol. 266, pp. 299 – 327, 1989.

2.5.1-312 Johnston, A.C., and L.R. Kanter, “Earthquakes in Stable Continental Crust,” *Scientific American*, March 1990.

2.5.1-313 Johnston, A.C., K.J. Coppersmith, L.R. Kanter, and C.A. Cornell, “The Earthquakes of Stable Continental Regions,” Final Report submitted to Electric Power Research Institute, TR-102261, Vols. 1 and 3, 1994.

2.5.1-314 Crone, A.J., M.N. Machette, and J.R. Bowman, “Episodic Nature of Earthquake Activity in Stable Continental Regions Revealed by Paleoseismicity Studies of Australian and North American Quaternary Faults,” *Australian Journal of Earth Sciences*, Vol. 44, pp. 203 – 214, 1997.

2.5.1-315 Electric Power Research Institute, “Volumes 5 – 10, Seismic Hazard Methodology for the Central and Eastern United States, Tectonic Interpretations,” July 1986.

2.5.1-316 Crone, A.J., and R.L. Wheeler, “Data for Quaternary Faults, Liquefaction Features, and Possible Tectonic Features in the Central and Eastern United States, East of the Rocky Mountain Front,” U.S. Geological Survey, Open-File Report 00-0260, 2000.

2.5.1-317 Wheeler, R., “Known or Suggested Quaternary Tectonic Faulting, Central and Eastern United States—New and Updated Assessments for 2005,” U.S. Geological Survey, Open-File Report 2005-1336, 2005.

2.5.1-318 Ells, G.D., “Architecture of the Michigan Basin,” in Stonehouse, H.B., ed., “Studies of the Precambrian of the Michigan Basin,” Michigan Basin Geological Society, Field Trip Guidebook, pp. 60 – 88, 1969.

2.5.1-319 Catacosinos, P.A., P.A. Daniels, Jr., and W.B. Harrison III, “Structure, Stratigraphy, and Petroleum Geology of the Michigan Basin,” American Association of Petroleum Geologists, Memoir 51, Chapter 30, pp. 561 – 601, 1991.

2.5.1-320 Fisher, J.H., “Tectonic Evolution of the Michigan Basin,” abs., Geological Society of America, Abstracts with Programs, North-Central Section, pp. 573, 1983.

2.5.1-321 Prouty, C.E., “Tectonic Development of Michigan Basin,” abs., *American Association of Petroleum Geologists Bulletin*, Vol. 70, pp. 1069, 1986.

2.5.1-322 Prouty, C.E., “Trenton Exploration and Wrenching Tectonics—Michigan Basin and Environs,” in B.D. Keith (ed.), “The Trenton Group (Upper Ordovician Series) of Eastern North America—Deposition, Diagenesis, and Petroleum,” American Association of Petroleum Geologists, *Studies in Geology*, 29, pp. 207-236, 1988.

2.5.1-323 Haimson, B.C., “Additional Stress Measurements in the Michigan Basin,” abstract from meeting, in EOS, *Transactions of the American Geophysical Union*, pp. 1209, 1978.

2.5.1-324 Fisher, J.H., and M.W. Barratt, “Exploration in Ordovician of Central Michigan Basin,” *American Association of Petroleum Geologists Bulletin*, Vol. 69, pp. 2065 – 2076, 1985.

2.5.1-325 Brigham, R.J., “Structural Geology of Southwestern Ontario and Southeastern Michigan,” Ontario Department of Mines and Northern Affairs, Petroleum Resource Section, Paper 71-2, pp. 110, 1971.

2.5.1-326 Wallach, J.L., A.A. Mohajer, and R.L. Thomas, “Linear Zones, Seismicity, and the Possibility of a Major Earthquake in the Intraplate Western Lake Ontario Area of Eastern North America,” *Canadian Journal of Earth Sciences*, Vol. 35, pp. 762 – 786, 1998.

2.5.1-327 Muskett, R.R., “Crustal Seismo-Magnetic and Lake Loading Piezomagnetic Responses near Lake Erie, Painesville, Ohio,” *Proceedings of the American Geophysical Union Fall Meeting*, 1999.

2.5.1-328 Dineva, S., D. Eaton, and R. Mereu, “Seismicity of the Southern Great Lakes: Revised Earthquake Hypocenters and Possible Tectonic Controls,” *Bulletin of the Seismological Society of America*, Vol. 94, No. 5, pp. 1902 – 1918, October 2004.

2.5.1-329 Fisher, J.A., "Fault Patterns in Southeastern Michigan," Master of Science Thesis, Department of Geology, Michigan State University, 1981.

2.5.1-330 Fisher, J.F., "Early Paleozoic History of the Michigan Basin," in Michigan Basin Geological Society, *Studies of the Michigan Basin*, pp. 89 – 93, 1969.

2.5.1-331 Buehner, J.H., and S.H. Davis, Jr., "Albion-Pulaski-Scipio-Trend Field," in Wollensak, M.S., ed., "Oil and Gas Fields of the Michigan Basin," Volume 1, Michigan Basin Geological Society, pp. 37 – 48, 1969.

2.5.1-332 Onasch, C.M., and C.F. Kahle, "Recurrent Tectonics in a Cratonic Setting: An Example from Northwestern Ohio," *Geological Society of America Bulletin*, Vol. 103, pp. 1259 – 1269, 1991.

2.5.1-333 Aangstrom Precision Corporation, Structure Contour Maps, Mt. Pleasant, Michigan, 1989:
(a) Dundee Residual Structure Contour Map, scale 1:600,000.
(b) Dundee Structure Contour Map, scale 1:600,000.
(c) Sunbury Shale Residual Structure Contour Map, scale 1:600,000.
(d) Sunbury Shale Structure Contour Map, scale 1:600,000.
(e) Traverse Limestone Residual Structure Contour Map, scale 1:600,000.
(f) Traverse Limestone Structure Contour Map, scale 1:600, 000.

2.5.1-334 Faust, T.H., K. Fujita, K.G. Mackey, L.J. Ruff, and R.C. Ensign, "The September 2, 1994 Central Michigan Earthquake," *Seismological Research Letters*, Vol. 68, No. 3, pp. 460 – 464, 1997.

2.5.1-335 Arndt, B.P., "Deerfield Field," in Wollensak, M.S., ed., "Oil and Gas Fields of the Michigan Basin," Volume 2, Michigan Basin Geological Society, pp. 295 – 301, 1991.

2.5.1-336 Root, S., "Recurrent Basement Faulting and Basin Evolution, West Virginia and Ohio: The Burning Springs — Cambridge Fault Zone," in van de Pluijm, B.A., and P.A. Catacosinos, eds., "Basement and Basins of Eastern North America," Geological Society of America, Special Paper 308, pp. 127 – 137, 1996.

2.5.1-337 Schumaker, R.C., "The Effect of Basement Structure on Sedimentation and Detached Structural Trends within the Appalachian Basin," in McDowell, R.C., ed., "The Lowry Volume: Studies in Appalachian Geology," *Virginia Tech Geological Sciences*, Memoir 3, pp. 67 – 81, 1986.

2.5.1-338 Rupp, J.A., "Structure and Isopach Maps of the Paleozoic Rocks of Indiana," Indiana Geological Survey, Special Report 48, 1991.

2.5.1-339 Hasenmueller, W.A., "Bedrock Geologic Map of the Western Quarter of the Muncie and Eastern Quarter of the Lafayette 1:100,00-scale Quadrangles, Central Indiana," Open-File Study 00-17, 2000

2.5.1-340 Checkley, W.G., "Northville Field," in Wollensak, M.S., ed., "Oil and Gas Fields of the Michigan Basin," Volume 1, Michigan Basin Geological Society, pp. 115 – 122, 1969.

2.5.1-341 Newcombe, R.B., "Oil and Gas Fields of Michigan: A Discussion of Depositional and Structural Features of the Michigan Basin," Michigan Geological Survey, Publication 38, 1933.

2.5.1-342 Root, S.I., and R.H. MacWilliams, "The Suffield Fault, Stark County, Ohio," *Ohio Journal of Science*, Vol. 86, No. 4, pp. 161 – 163, 1986.

2.5.1-343 Hook, R.W., and J.C. Ferm, "Paleoenvironmental Controls on Vertebrate-Bearing Abandoned Channels in the Upper Carboniferous," *Palaeogeography, Pelaeoclimatology, Palaeoecology*, Vol. 63, pp. 159 – 181, 1988.

2.5.1-344 Hansen, M.C., "Earthquakes and Seismic Risk in Ohio," *Ohio Geology*, Summer 1993.

2.5.1-345 Nicholson, C., E. Roeloffs, and R.L. Wesson, "The Northeastern Ohio Earthquake of 31 January 1986: Was It Induced?" *Bulletin of the Seismological Society of America*, Vol. 78, No. 1, pp. 188 – 217, February 1988.

2.5.1-346 Seeber, L., and J.G. Armbruster, "Natural and Induced Seismicity in the Lake Erie – Lake Ontario Region: Reactivation of Ancient Faults with Little Neotectonic Displacement," *Géographie Physique et Quaternaire*, Vol. 47, No. 3, pp. 363 – 378, 1993.

2.5.1-347 Hansen, M.C., G.E. Larsen, E.M. Swinford, and L.J. Ruff, "Seismic Spotlight Shines on Ashtabula," *Ohio Geology*, No. 3, 2001.

2.5.1-348 Ruff, L., R. LaForge, R. Thorson, T. Wagner, and F. Goudaen, "Geophysical Investigations of the Western Ohio – Indiana Region," Final Report 1986 – September 1992, NUREG/CR-3145, prepared for the Division of Engineering, Office of Nuclear Regulatory Research, U.S. Nuclear Regulatory Commission, January 1994.

2.5.1-349 Schwartz, S.Y., and D.H. Christensen, "The 12 July 1986 St. Marys, Ohio Earthquake and Recent Seismicity in the Anna, Ohio Seismogenic Zone," *Seismological Research Letters*, Vol. 59, No. 2, pp. 57 – 62, April – June 1988.

2.5.1-350 Obermeier, S.F., "Paleoseismic Liquefaction Studies — Central U.S. and Pacific Northwestern U.S.," in Jacobsen, M.L., comp., "National Earthquake Hazards Reduction Program Annual Project Summaries: XXXVI, Volume II," U.S. Geological Survey, Open-File Report 95-210, pp. 606 – 609, 1995.

2.5.1-351 Electric Power Research Institute (EPRI), "Probabilistic Seismic Hazard Evaluations at Nuclear Power Plant Sites in the Central and Eastern United States," Technical Report NP-6395-D, 1989.

2.5.1-352 Van Arsdale, R.B., "Seismic Hazards of the Upper Mississippi Embayment," U.S. Army Corps of Engineers Waterways Experiment Station, Contract Report GL-98-1, 1998.

2.5.1-353 Crone, A., "Defining the Southwestern End of the Blytheville Arch, Northeastern Arkansas: Delineating a Seismic Source Zone in the New Madrid Region," *Seismological Research Letters*, Vol. 69, No. 4, 1998.

2.5.1-354 Russ, D.P., "Style and Significance of Surface Deformation in the Vicinity of New Madrid, Missouri," in McKeown, F.A., and L.C. Pakiser, eds., "Investigations of the New Madrid Missouri, Earthquake Region," U.S. Geological Survey, Professional Paper 1236, pp. 95 – 114, 1982.

2.5.1-355 Schweig, E.S., and M.A. Ellis, "Reconciling Short Recurrence Intervals with Minor Deformation in the New Madrid Seismic Zone," *Science*, Vol. 264, pp. 1308 – 1311, 1994.

2.5.1-356 Johnston, A.C., and E.S. Schweig, “The Enigma of the New Madrid Earthquakes of 1811-1812,” *Annual Review of Earth and Planetary Sciences,* Vol. 24, pp. 339 – 384, 1996.

2.5.1-357 Forte, A.M., J.S. Mitrovica, R. Moucha, N.A. Simmons, and S.P. Grand, “Descent of the Ancient Farallon Slab Drives Localized Mantle Flow below the New Madrid Seismic Zone,” *Geophysical Research Letters*, Vol. 34, L04308, doi:10.1029/2006GL027895, pp. 5, 2007.

2.5.1-358 Bakun, W.H., and M.G. Hopper, “Magnitudes and Locations of the 1811 – 1812 New Madrid, Missouri, and the 1886 Charleston, South Carolina, Earthquakes,” *Bulletin of the Seismological Society of America*, Vol. 94, No. 1, pp. 64 – 75, 2004.

2.5.1-359 Atkinson, G., B. Bakun, P. Bodin, D. Boore, C. Cramer, A. Frankel, P. Gasperini, J. Gomberg, T. Hanks, B. Herrmann, S. Hough, A. Johnston, S. Kenner, C. Langston, M. Linker, P. Mayne, M. Petersen, C. Powell, W. Prescott, E. Schweig, P. Segall, S. Stein, B. Stuart, M. Tuttle, and R. Van Arsdale and 22 others, “Reassessing the New Madrid Seismic Zone,” EOS, *Transactions of the American Geophysical Union*, Vol. 81, No. 35, pp. 397 and 402 – 403, 2000.

2.5.1-360 Hough, S.E., J.G. Armbruster, L. Seeber, and J.F. Hough, “On the Modified Mercalli Intensities and Magnitudes of the 1811 – 12 New Madrid Earthquakes,” *Journal of Geophysical Research*, Vol. 105, pp. 23,839 – 23,864, 2000.

2.5.1-361 Johnston, A.C., “Seismic Moment Assessment of Earthquakes in Stable Continental Regions — III. New Madrid 1811 – 1812, Charleston 1886, and Lisbon 1755,” *Geophysical Journal International*, Vol. 126, No. 3, pp. 314 – 344, 1996.

2.5.1-362 Kelson, K.I., R.B. Van Arsdale, G.D. Simpson, and W.R. Lettis, “Assessment of the Style and Timing of Surficial Deformation along the Central Reelfoot Scarp, Lake County, Tennessee,” *Seismological Research Letters*, Vol. 63, No. 3, pp. 349 – 356, 1992.

2.5.1-363 Kelson, K.I., G.D. Simpson, R.B. Van Arsdale, C.C. Haraden, and W.R. Lettis, "Multiple Late Holocene Earthquakes along the Reelfoot Fault, Central New Madrid Seismic Zone," *Journal of Geophysical Research*, Vol. 101, No. B3, pp. 6151 – 6170, 1996.

2.5.1-364 Van Arsdale, R.B., R.T. Cox, A.C. Johnston, W.J. Stephenson, and J.K. Odum, "Southeastern Extension of the Reelfoot Fault," *Seismological Research Letters*, Vol. 70, No. 3, 1999.

2.5.1-365 Van Arsdale, R.B., "Displacement History and Slip Rate on the Reelfoot Fault of the New Madrid Seismic Zone," *Engineering Geology*, Vol. 55, pp. 219 – 226, 2000.

2.5.1-366 Mueller, K., and J. Pujol, "Three-Dimensional Geometry of the Reelfoot Blind Thrust: Implication for Moment Release and Earthquake Magnitude in the New Madrid Seismic Zone," *Bulletin of the Seismological Society of America*, Vol. 91, pp. 1563 – 1573, 2001.

2.5.1-367 Baldwin, J.N., A.D. Barron, and K.I. Kelson, J.B. Harris, and S.M. Cashman, 2002, "Preliminary Paleoseismic and Geophysical Investigation of the North Farrenburg Lineament, Farrenburg, Missouri: Deformation Associated with the New Madrid North Fault?" Eastern Section-*Seismological Research Letters*, Vol. 73, No. 3, pp. 395 – 413, May/June 2002.

2.5.1-368 Tuttle, M.P., E.S. Schweig, J.D. Sims, R.H. Lafferty, L.W. Wolf, and M.L. Haynes, "The Earthquake Potential of the New Madrid Seismic Zone," *Bulletin of the Seismological Society of America*, Vol. 92, No. 6, pp. 2080 – 2089, 2002.

2.5.1-369 Tuttle, M.P., E.S. Schweig, E.S. Campbell, P.M. Thomas, J.D. Sims, and R.H. Lafferty, "Evidence for New Madrid Earthquakes in A.D. 300 and 2350 B.C.," *Seismological Research Letters*, Vol. 76, No. 4, pp. 489 – 501, 2005.

2.5.1-370 Obermeier, S.F., and Crone, A.J., comps., "Fault Number 1024, Wabash Valley Liquefaction Features," in Quaternary Fault and Fold Database of the United States, 1994, U.S. Geological Survey Website, http://earthquakes.usgs.gov/regional/qfaults, accessed 22 December 2007.

2.5.1-371 Munson, P.J., S.F. Obermeier, C.A. Munson, and E.R. Hajic, "Liquefaction Evidence for Holocene and Latest Pleistocene in the Southern Halves of Indiana and Illinois — A Preliminary Overview," *Seismological Research Letters*, Vol. 68, No. 4, pp. 523 – 536, 1997.

2.5.1-372 McNulty, W.E., and S.F. Obermeier, "Liquefaction Evidence for at Least Two Strong Holocene Paleoearthquakes in Central and Southwestern Illinois, USA," *Environmental and Engineering Geoscience*, Vol. 5, No. 2, pp. 133 – 146, 1999.

2.5.1-373 Green, R.A., S.F. Obermeier, and S.M. Olson, "Engineering Geologic and Geotechnical Analysis of Paleoseismic Shaking Using Liquefaction Effect: Field Examples," *Engineering Geology*, Vol. 76, pp. 263 – 293, 2005.

2.5.1-374 Obermeier, S.F., "Liquefaction Evidence for Strong Earthquakes of Holocene and Latest Pleistocene Ages in the States of Indiana and Illinois, USA," *Engineering Geology*, Vol. 50, pp. 227 – 254, 1998.

2.5.1-375 Hildenbrand, T.G., and D. Ravat, "Geophysical Setting of the Wabash Valley Fault System," *Seismological Research Letters*, Vol. 68, No. 4, pp. 567 – 585, 1997.

2.5.1-376 Harrison, R.W., and A. Schultz, "Tectonic Framework of the Southwestern Margin of the Illinois Basin and Its Influence on Neotectonism and Seismicity," *Seismological Research Letters*, Vol. 73, No. 5, pp. 698 – 731, September/October 2002.

2.5.1-377 Earthquakes in the Central Illinois Basin," *Seismological Research Letters*, Vol. 73, No. 5, pp. 640 – 659, September/October 2002.

2.5.1-378 Langenheim, V.E., and T.G. Hildenbrand, "Commerce Geophysical Lineament — Its Source, Geometry, and Relation to the Reelfoot Rift and New Madrid Seismic Zone," *GSA Bulletin*, Vol. 109, No. 5, pp. 580 – 595, May 1997.

2.5.1-379 Wheeler, R.L., and C.H. Cramer, "Updated Seismic Hazard in the Southern Illinois Basin — Geological and Geophysical Foundations for Use in the 2002 USGS National Seismic-Hazard Maps," *Seismological Research Letters*, Vol. 73, No. 5, pp. 776 – 791, 2002.

2.5.1-380 McBride, J.H., and D.R. Kolata, “Upper Crust beneath the Central Illinois Basin, United States,” *Geological Society of America Bulletin*, Vol. 111, pp. 372 – 394, 1999.

2.5.1-381 McBride, J.H, M.L. Sargent, and C.J. Potter, “Investigating Possible Earthquake-Related Structure beneath the Southern Illinois Basin from Seismic Reflection,” *Seismological Research Letters*, Vol. 68, No. 4, pp. 641 – 649, 1997.

2.5.1-382 McBride, J.H., T.G. Hildenbrand, W.J. Stephenson, and C.J. Potter,” Interpreting the Earthquake Source of the Wabash Valley Seismic Zone (Illinois, Indiana, and Kentucky) From Seismic Reflection, Gravity, and Magnetic Intensity.” ,” *Seismological Research Letters*, Vol. 73, No. 5, pp. 660 – 686, 2002.

2.5.1-383 Fraser, G.S., T.A. Thompson, G.A. Olyphant, L. Furer, and S.W. Bennett, “Geomorphic Response to Tectonically Induced Ground Deformation in the Wabash Valley,” *Seismological Research Letters*, Vol. 68, No. 4, pp. 662 – 674, 1997.

2.5.1-384 Su, W.J., and J.H. McBride, “Final Technical Report — Study of a Potential Seismic Source Zone in South-Central Illinois (abs.),” Technical Report Submitted to the U.S. Geological Survey under USGS External Grant Number 99HQGR0075, 1999.

2.5.1-385 Cramer, C.H., R.L. Wheeler, and C.S. Mueller, “Uncertainty Analysis for Seismic Hazard in the Southern Illinois Basin,” *Seismological Research Letters*, Vol. 73, No. 5, pp. 792 – 805, 2002.

2.5.1-386 Petersen, M.D., A.D. Frankel, S.C. Harmsen, C.S. Mueller, K.M. Haller, R.L. Wheeler, R.L. Wesson, and seven others, "Documentation for the 2008 Update of the United States National Seismic Hazard Maps," U.S. Geological Survey Open-File Report 2008-1128, 2008.

2.5.1-387 Radbruch-Hall, D.H., R.B. Colton, W.E. Davies, I. Lucchitta, B.A. Skipp, and D.J. Varnes, "Landslide overview map of the conterminous United States," U.S. Geological Survey, Professional Paper 1183, pp. 25, 1982.

2.5.1-388 Davies, W.E., J.H. Simpson, G.C. Ohlmacher, W.S. Kirk, and E.G. Newton, "Engineering Aspects of Karst," U.S. Geological Survey, National Atlas of North America, 1 map with text, 1984.

2.5.1-389 Mozola, A.J., “Geology for Environmental Planning in Monroe County, Michigan,” Michigan Geological Survey, Report of Investigation 13, pp. 26, 6 plates, 1970.

2.5.1-390 Zumberge, J.H., “Correlation of Wisconsin Drifts in Illinois, Indiana, Michigan, and Ohio,” *Geological Society of America Bulletin*, Vol. 71, No. 8, pp. 1177 – 1188, 1960.

2.5.1-391 Eschman, D.F., and P.F. Karrow, “Huron Basin Glacial Lakes: A Review,” in Karrow, P.F., and P.E. Calkin, eds., *Quaternary Evolution of the Great Lakes*, Geological Association of Canada, Special Paper 30, pp. 79 – 93, 1985.

2.5.1-392 Johnson, R.L., “Evaporite Dissolution Features of the Upper Silurian Bass Islands Dolomite, Southeastern Michigan,” Abstracts with Programs, Geological Society of America, Vol. 10, pp. 257, 1978.

2.5.1-393 Landes, K.K., “The Salina and Bass Islands Rocks in the Michigan Basin,” U.S.Geological Survey, Oil and Gas Investigation Map 40, 1 map, 1945.

2.5.1-394 Briggs, L.I. and D. Briggs, "Niagara-Salina Relationships in the Michigan Basin," in Kesling, R.V. (ed.), "Silurian Reef-Evaporite Relationships," Michigan Basin Geological Society, Field Conference, pp. 1-23, 1974.

2.5.1-395 Sparling, D.R., “The Bass Islands Formation in Its Type Region,” *Ohio Journal of Science*, Vol. 70, pp. 1-33, 1970.

2.5.1-396 Treesh, M.I., and C. F. Kahle, "Cayugan Peritidal Dolomites on Catawba and South Bass Islands, Ohio: An Interpretation of Sedimentary Structures and Brecciation," Abstracts with Programs, Geological Society of America, Vol. 4, pp. 50, 1972.

2.5.1-397 Carlson, E.H., “Evaporite-solution Breccias and Caves of the Bass Islands Region, Western Lake Erie,” Abstracts with Programs, Geological Society of America, Vol. 23, pp. 6, 1991.

2.5.1-398 Onash, C M, and C.F. Kahle, "Seismically Induced Soft-sediment Deformation in Some Silurian Carbonates, Eastern U.S. Midcontinent," in Ettenson, F.R., N. Rast, and C.E. Brett, Ancient Seismites, Geological Society of America, Special Paper 359, pp. 165-176, 2002.

2.5.1-399 Casey, G.D., “Hydrogeologic Framework of the Midwestern Basins and Arches Region in Parts of Indiana, Ohio, Michigan, and Illinois,” U.S. Geological Survey, Professional Paper 1423-B, pp. 46, 1996.

2.5.1-400 Choquette, P.W., and N.P. James, "Introduction," in James, N.P., and P.W. Choquette, Paleokarst. Springer-Verlag, New York, pp. 1-21, 1988.

2.5.1-401 Carlson, E.H., “Stoichiometry and Degree of Ordering in Dolomite and Indicators of Missing Evaporites,” Abstracts with Programs, Geological Society of America, Vol. 27, pp. 173, 1995.

2.5.1-402 Shaver, R.H., “A Field Trip on the Great Carbonate-Rock Facies in the Silurian System of Western Ohio and Northern Indiana,” Indiana Geological Survey and Indiana University, Field Trip Guide and Supplements, pp. 35, 1989.

2.5.1-403 Gardner, W.C., “Middle Devonian Stratigraphy and Depositional Environments in the Michigan Basin,” Michigan Basin Geological Society, Special Paper 1, pp. 132, 1974.

2.5.1-404 U.S. Department of Agriculture, Soil Conservation Service, “Soil Survey of Monroe County, Michigan,” written in cooperation with the Michigan Agricultural Experiment Station, November 1981.

2.5.1-405 U.S. Department of Agriculture, “Soil Survey Geographic (SSURGO) Database for Monroe County, Michigan,” 2005.

2.5.1-406 Ells, G.D., “Structures Associated with the Albion-Scipio Oil Field Trend,” Michigan Geological Survey, Open-File Report 62-1, 1962

2.5.1-407 Wollensak, M.S., ed., “Oil and Gas Fields of the Michigan Basin,” Volume 1, Michigan Basin Geological Society, 1969.

2.5.1-408 Wollensak, M.S., ed., “Oil and Gas Fields of the Michigan Basin,” Volume 2, Michigan Basin Geological Society, 1991.

2.5.1-409 Tanglis, C. (comp.), “Surface Faults in the Southwestern District, Southern Ontario,” Ontario Geological Survey, 1995.

2.5.1-410 Cohee, G.V., “Cambrian and Ordovician Rocks in Michigan Basin and Adjoining Areas,” *American Association of Petrolem Geologists Bulletin*, Vol. 32 No. 8, pp. 1417-1448, 1948.

2.5.1-411 Landes K.K., “Porosity through Dolomitization,” *American Association of Petroleum Geologists Bulletin*, Vol 30, No. 3, pp. 305-318, 1946.

2.5.1-412 Bailey Geological Services Ltd., and R.G. Cochrane, “Evaluation of the Conventional and Potential Oil and Gas Reserves of the Silurian Sandstone Reservoirs of Ontario 1985,” Ontario Geological Survey, Open File Report 5578, 1986.

2.5.1-413 Burgess, R.J. and C.J. Hadley, “Geology of the Colchester oil pool, Southwestern Ontario,” *Oil in Canada*, Vol. 13, No. 2, pp. 28-33, 1960.

2.5.1-414 Dean, S.L., B.R. Kulander, J.L. Forsyth, and R.M. Tipton, “Field Guide to Joint Patterns and Geomorphological Features of Northern Ohio, *The Ohio Journal of Science*, Vol. 91, No. 1, pp. 2 – 15, March 1991.

2.5.1-415 Engelder, T., “Is There a Genetic Relationship between Selected Regional Joints and Contemporary Stress within the Lithosphere of North America?” *Tectonics*, Vol. 1, No. 2, pp. 161 – 177, April 1982.

2.5.1-416 Brigham, R.J., and C.G. Winder, “Structural Geology of Paleozoic Sediments in Southwestern Ontario,” *Proceedings of the Fifth Annual Conference of the Ontario Petroleum Insitute, Inc., London, Ontario*, November 1966.

2.5.1-417 Dames & Moore, “Rock Foundation Treatment, Residual Heat Removal Complex, Fermi II Nuclear Power Plant”, Final Report for the Detroit Edison Company, pp.11 – 12, 1974.

2.5.1-418 ARM Geophysics, “Geophysical Well Logging, DTE Fermi 3 COL, Monroe, Michigan,” 2008.

2.5.1-419 Sherzer, W.H., “Geological Report on Monroe County, Michigan,” Michigan Geological Survey, Vol. VII, pp. 240, 1900.

2.5.1-420 Black, T.J., “Evaporite Karst in Michigan,” in Johnson, K.S. and J.T. Neal, eds., “Evaporite Karst and Engineering/Environmental Problems in the United States,” Oklahoma Geological Survey, Circular 109, pp. 315-320, 2003.

2.5.1-421 Sbar, M.L. and L.R. Sykes, “Contemporary Compressive Stress and Seismicity in Eastern North America: An example of Intra-plate Tectonics,” *Geological Society of America Bulletin*, Vol. 84, pp. 1861-1882, 1973.

2.5.1-422 Steck, C.D., “Surficial Neotectonics Faults and Folds in Southwestern and Central Ohio,” Unpublished Master’s Thesis, Ohio State University, pp. 173, 1999.

2.5.1-423 Wallach, J.L., A.A. Mohajer, G.H. McFall, J.R. Bowlby, M. Pearce, and D.A. McKay, "Pop-ups as Geological Indicators of Earthquake-prone Areas in Intraplate Eastern North America," Quaternary Proceedings, Vol. 3, pp. 67-83, 1993.

2.5.1-424 Blasco, S.M., C.F.M. Lewis, R.D. Jacobi, R.D. Covill, D. Keyes, D. Armstrong, and R.A. Harmes, "Bedrock Pop-ups Western Lake Ontario, Eastern Lake Erie, and Eastern Lake Huron; Evidence of Neotectonics Activity on the Lake Bed of the Southern Great Lakes," Abstracts with Programs, Geological Society of America, Vol. 35, pp. 76-77, 2003.

2.5.1-425 Ells, G.D., “Future oil and gas possibilities in Michigan Basin,” American Association of Professional Geologists, Memoir 15, Vol. 2, 1971

2.5.1-426 Wylie, A.S., J.R. Wood, and W.B. Harrison, III, “Michigan Trenton-Black River Opportunities Identified With Sample Attribute Mapping,” *Oil and Gas Journal*, Vol. 102, pp. 29-35, 2004.

2.5.1-427 Cook, C.W., “The Brine and Salt Deposits of Michigan,” Michigan Geological Survey, Publication 15, pp. 188, 1914.

2.5.1-428 Carlson, E.H., "The Occurrence of Mississippi Valley-Type Mineralization in Northwestern Ohio," in Kisvarsanyi, G., S.K. Grant, W.P. Pratt, and J.W. Koenig, Eds., International Conference on Mississippi Valley Type Lead-Zinc Deposits, University of Missouri-Rolla, pp. 424-435, 1983.

2.5.1-429 Kamin, T.C., and W.M. Campbell, “Akron Field, T14N-R8E, Akron Township, Tuscola County,” in Wollensak, M.S., ed., “Oil and Gas Fields of the Michigan Basin,” Volume 2, Michigan Basin Geological Society, pp. 321 – 341, 1991.

2.5.1-430 Fowler, J.H., and S.F. Schaefer, “Burdell Field, T20N-R10W, Burdell Township, Osceola County,” in Wollensak, M.S., eded., “Oil and Gas Fields of the Michigan Basin,” Volume 2, Michigan Basin Geological Society, pp. 343 – 352, 1991.

2.5.1-431 Griffin, W.D., “South Buckeye Field, T18N-R1W, Buckeye Township, Gladwin County,” in Wollensak, M.S., ed., “Oil and Gas Fields of the Michigan Basin,” Volume 2, Michigan Basin Geological Society, pp. 441 – 451, 1991.

2.5.1-432 Barratt, M.W., “Falmouth Field, T122N-R7W, Reeder Township, Missaukee County,” in Wollensak, M.S., ed., “Oil and Gas Fields of the Michigan Basin,” Volume 2, Michigan Basin Geological Society, pp. 371 – 380, 1991.

2.5.1-433 Schneider, J.J., C.N. Tinker, and P.D. Ching, “Kawkawlin Field, T14N-R4E, Monitor Township, Bay County,” in Wollensak, M.S., ed., “Oil and Gas Fields of the Michigan Basin,” Volume 2, Michigan Basin Geological Society, pp. 405 – 414, 1991.

2.5.1-434 Duszynski, J., “New Lothrop Field, T8N-R4E, Hazelton Township, Shiawassee County,” in Wollensak, M.S., ed., “Oil and Gas Fields of the Michigan Basin,” Volume 2, Michigan Basin Geological Society, pp. 7 – 14, 1991.

2.5.1-435 Schneider, J.J., C.N. Tinker, and P.D. Ching, “Rose City Field, T24N-R2E, Foster Township, Ogemaw County,” in Wollensak, M.S., ed., “Oil and Gas Fields of the Michigan Basin,” Volume 2, Michigan Basin Geological Society, pp. 431 – 440, 1991.

2.5.1-436 Lundy, C.L., “Shaver Field, T10N-R4W, Sumner Township, Gratiot County,” in Wollensak, M.S., ed., “Oil and Gas Fields of the Michigan Basin,” Volume 2, Michigan Basin Geological Society, pp. 493 – 499, 1991.

2.5.1-437 Cheek, W.M., “West Branch Field, T22N-R2E, West Branch Township, Ogemaw County,” in Wollensak, M.S., ed., “Oil and Gas Fields of the Michigan Basin,” Volume 2, Michigan Basin Geological Society, pp. 453 – 458, 1991.

2.5.1-438 Balthazor, D.A., “Williams Field, T14N-R3E, Williams Township, Bay County,” in Wollensak, M.S., ed., “Oil and Gas Fields of the Michigan Basin,” Volume 2, Michigan Basin Geological Society, pp. 15 – 28, 1991.

2.5.1-439 Billingham, A., “Winterfield Field, T20N-R6E, Winterfield Township, Clare County,” in Wollensak, M.S., ed., “Oil and Gas Fields of the Michigan Basin,” Volume 2, Michigan Basin Geological Society, pp. 95 – 102, 1991.

2.5.1-440 U.S. Geological Survey EROS Data Center, “National Elevation Dataset,” http://gisdata.usgs.net/ned//, 1999.

2.5.1-441 National Geophysical Data Center, National Oceanic and Atmospheric Administration (NOAA), “Great Lakes Bathymetry,” Bathymetric Data, http://www.ngdc.noaa.gov/mgg/greatlakes/greatlakes.html, accessed 17 August 2007.

2.5.1-442 Michigan Department of Environmental Quality, “Bedrock Geology Map of Michigan,” Geologic Survey Division, 1987.

2.5.1-443 Gray, H.H., C.H. Ault, S.J. Keller, and D. Harper, “Bedrock Geologic Map of Indiana,” Indiana Geological Survey, Miscellaneous Map 48, scale 1:500,000, 2002.

2.5.1-444 National Geophysical Data Center, National Oceanic and Atmospheric Administration (NOAA), “2-Minute Gridded Global Relief Data (ETOPO2v2) June, 2006,” Bathymetric Data, http://www.ngdc.noaa.gov/mgg/fliers/01mgg04.html, accessed 1 January 2007.

2.5.1-445 (Not Used)

2.5.1-446 Indiana Geological Survey, “Structural Features of Indiana (Indiana Geological Survey, Line Shapefile,” 2002. http://129.79.145.7/arcims/statewide_mxd/dload_page/geology.html, accessed 2 June 2008.

2.5.1-447 Taylor, K.B., R.B. Herrmann, M.W. Hamburger, G.L. Pavlis, A. Johnston, C. Langer, and C. Lam, “The Southeastern Illinois Earthquake of 10 June 1987,” *Seismological Research Letters*, Volume 60, No. 3, pp. 101-110, July – September 1989.

2.5.1-448 Slucher, E.R., E.M. Swinford, G.E. Larson, and D.M. Powers, “Bedrock Geologic Map of Ohio,” Ohio Geological Survey, Map BG-1, version 6.0, scale 1:500,000, 2006.

2.5.1-449 Armstrong, D.K., and J.E.P. Dodge, “Paleozoic Geology of Southern Ontario,” Ontario Geological Survey, Miscellaneous Release — Data 219, 2007.

2.5.1-450 Pavey, R.R., R.P. Goldthwait, C.S. Brockman, D.N. Hull, E.M. Swinford, and R.G. Van Horn, “Quaternary Geology of Ohio,” Ohio Geological Survey, Map M-2, 1:500,000-scale map and 1:250,000-scale GIS files, 1999.

2.5.1-451 Michigan Department of Natural Resources, “Quaternary Geology of Michigan,” Edition 2.0, digital map, 1998.

2.5.1-452 Ontario Geological Survey, “Quaternary Geology, Seamless Coverage of the Province of Ontario,” Data Set 14, 1997.

2.5.1-453 Wickstrom, L.H., “A New Look at Trenton (Ordovician) Structure in Northwestern Ohio,” *Northeastern Geology*, Vol. 12, No. 3, pp. 103-113, 1990.

2.5.1-454 Wickstrom, L.H., J.D. Gray, and R.D. Stieglitz, “Stratigraphy, Structure, and Production History of the Trenton Limestone (Ordovician) and Adjacent Strata in Northwestern Ohio,” Ohio Department of Natural Resources, Division of Geological Survey, Report of Investigations No. 143, 78 pp., 1992.

2.5.1-455 Seeber, L., Armbruster, J.G., and Kim, W.-Y., “A Fluid-Injection-Triggered Earthquake Sequence in Ashtabula, Ohio: Implications for Seismogenesis in Stable Continental Regions,” Bulletin of the Seismological Society of America, Vol. 94, No. 1, pp. 76-87, 2004.

2.5.1-456 Mooney, W.O., Andrews, M.C., Ginzburg, A., Peters, D.A., and Hamilton, RM., "Crustal Structure of the Northern Mississippi Embayment and a Comparison with Other Continental Rift Zones," *Tectonophysics*, Vol. 94, pp. 327 - 348, 1983.

2.5.1-457 Grana, J.P., and Richardson, RM., "Tectonic Stress within the New Madrid Seismic Zone," *Journal of Geophysical Research*, Vol. 101, pp. 5445 - 5458, 1996.

2.5.1-458 Stuart, W.O., Hildenbrand, T.G., and Simpson, RW., "Stressing of the New Madrid Seismic Zone by a Lower Crust Detachment Fault," *Journal of Geophysical Research*, Vol. 102, No. 27, pp. 623 - 627,633, 1997.

2.5.1-459 Liu, L., and Zoback, M.D., "Lithospheric Strength and Intraplate Seismicity in the New Madrid Seismic Zone," *Tectonics*, Vol. 16, pp. 585 - 595,1997.

2.5.1-460 Grollimund, B., and Zoback, M.D., "Did Deglaciation Trigger Intraplate Seismicity in the New Madrid Seismic Zone?" *Geology*, Vol. 29, No.2, pp. 175 - 178, 2001.

2.5.1-461 Kenner, S.J., and Segall, P., "A Mechanical Model for Intraplate Earthquakes: Application to the New Madrid Seismic Zone," *Science*, Vol. 289, pp. 2329-2332, doi:1 0.1126/science.289.5488.2329, 2000.

2.5.1-462 Crone, A.J., De Martini, P.M., Machette, M.N., Okumura, K., and Prescott J.R, "Paleoseismicity of Two Historically Quiescent Faults in Australia: Implications for Fault Behavior in Stable Continental Regions," *Bulletin of the Seismolological Society of America*, Vol. 93, pp. 1913 - 1934, 2003.

2.5.1-463 Van Arsdale, R, Bresnahan, R, McCallister, N., and Waldron, B., “Upland Complex of the Central Mississippi River Valley: Its Origin, Denudation, and Possible Role in Reactivation of the New Madrid Seismic Zone," in Stein, S., and Mazzotti, S. (editors), *Continental Intraplate Earthquakes: Science, Hazard, and Policy Issues*, Geological Society of America Special Paper 425, pp.177 -192, doi:10.1130/2007.2425(13), 2007.

2.5.1-464 Lyakhovsky, V., Ben-Zion, Y., and Agnon, A, "Earthquake Cycle, Fault Zones, and Seismicity Patterns in a Rheologically Layered Lithosphere," *Journal of Geophysical Research*, Vol. 106, pp. 4103 - 4120,2001.

2.5.1-465 Li, Q., Liu, M., and Stein, S., "Spatiotemporal Complexity of continental intraplate seismicity: Insights from Geodynamic Modeling and Implications for Seismic Hazard Estimation," *Bulletin of the Seismological Society of America*, Vol. 99, No.1, pp. 52 - 60,2009.

2.5.1-466 Calais, E., and Stein, S., "Time-Variable Deformation in the New Madrid Seismic Zone," *Science*, Vol. 323, pp. 1442, doi:0.1126/science.1168122, 2009.

2.5.1-467 Zhang, Q., Sandvol, E., and Liu, M., "Lithospheric Velocity Structure of the New Madrid Seismic Zone: A Joint Teleseismic and Local P Tomographic Study," *Geophysical Research Letters*, Vol 36, doi:10.1029/2009Gl037687, 2009.

2.5.1-468 Calais, E., Freed, A, Van Arsdale, R., and Stein, S., "TimeVariable Deformation in the New Madrid Seismic Zone," abstract, U.S. Geological Survey Sponsored Meeting of Central and Eastern US (CEUS) Earthquake Hazards Program, October 28-29,2009, Memphis, TN., 15 pp., 2009.

2.5.1-469 Hildenbrand, T.G., and Hendricks, J.D., "Geophysical Setting of the Reelfoot Rift and Relations Between Rift Structures and the New Madrid Seismic Zone," in Shedlock, K.M., and Johnston, AC., eds., "Investigations of the New Madrid Seismic Zone," U.S. Geological Survey Professional Paper 1538-E, pp. E1- E30, 1995.

2.5.1-470 St. louis University Earthquake Center, North American Focal Mechanisms, Web page, http:/lwww.eas.slu.edu/ Earthquake Center/MECH.NA/20080418093700/index.html, accessed 15 December 2009.

2.5.1-471 Counts, R.C., Durbin, J.M., and Obermeier, SF, "Seismic Ground Failure Features in the Vicinity of the lower Wabash and Ohio River Valleys," in Maria, AN., and Counts, R.C., eds., *From the Cincinnati Arch to the Illinois Basin: Geological Field Excursions along the Ohio River Valley*, Geological Society of America Field Guide 12, pp. 57 - 79, doi:10.1130/2008.fld012(05), 2008.

2.5.1-472 Holcombe, T.L., Warren, J.S., Taylor, L.A., Reid, D.F., and Herdendorf, C.E., "Lakefloor Geomorphology of Western Lake Erie," *Journal of Great Lakes Research*, Vol. 23, No.2, pp. 190-201, 1987.

2.5.1-473 Great Lakes Dredging Team, "Toledo Harbor Revisited: Changing Open Water Placement Policy for Western Lake Erie," Case Study Series, http://www.glc.org/dredging/case /documents/Toledo_final.pdf, 2005, accessed 18 November 2009.

2.5.1-474 Francy, D.S., Struffolino, P., Brady, A.M.G., and Dwyer, D.F., "A Spatial Multivariable Approach for Identifying Proximate Sources of Escherichia coli to Maumee Bay, Lake Erie, Ontario," U.S. Geological Survey, OpenFile Report 2005-1386, 2005.

2.5.1-475 U.S. Army Corps of Engineers, "Toledo Harbor Ohio Fact Sheet," http://www.lre.usace.army.mil/ETSpubs/HFS /Toledo%20Harbor.pdf, accessed 18 November 2009.

2.5.1-476 Liang, C., and Langston, C.A, "Three-Dimensional Crustal Structure of Eastern North America Extracted from Ambient Noise," *Journal of Geophysical Researc*h, Vol. 114, p. B03310, 2009.

2.5.1-477 Sims, P.K., Saltus, R.W., and Anderson, E.D., "Preliminary Precambrian Basement Structure Map of the Continental United States - An Interpretation of Geologic and Aeromagnetic Data," U.S. Geological Survey Open-File Report 2005-1029,2005.

2.5.1-478 McKenna, J., Stein, S., and Stein, C.A., "Is the New Madrid Seismic Zone Hotter and Weaker than Its Surroundings?" in Stein, S., and Mazzotti, S., eds., "Continental Intraplate Earthquakes: Science, Hazard, and Policy Issues," Geological Society of America Special Paper 425, pp. 167 - 175, doi:10.1130/2007.2425(12),2007.

2.5.1-479 Newman, A., Stein, S., Weber, J., Engeln, J., Mao, A., and Dixon, T., "Slow Deformation and Lower Seismic Hazard at the New Madrid Seismic Zone," Science, Vol. 284, No. 5414, pp. 619-62,1999.

2.5.1-480 Calais, E., Han, J.Y., DeMets, C., and Nocquet, J.M., "Deformation of the North American Plate Interior from a Decade of Continuous GPS Measurements," *Journal of Geophysical Research*, Vol. 111,B06402, doi:1 0.1 029/2005JB004253, 2006.

2.5.1-481 Mooney, W.D., and Ritsema, J., "Mmax and Lithospheric Structure in Central and Eastern North America," abstract, Meeting of Central and Eastern U.S. (CEUS) Earthquake Hazards Program, October 28-29,2009, Memphis, TN, Office, p. 25, 2009.

2.5.1-482 Obermier, S., “Paleoseismic Liquefaction Studies - Central and Eastern US,” USGS Annual Report, Volume 37, 1995, accessed in 1998 at http://erp-web.er.usgs.gov/reports/VOL37/CU/obermeir.htm, paper copy provided by Russ Wheeler on November 17, 2009.

2.5.1-483 Obermier, S., “Summary of 1995 Paleoliquefaction Field Search in the Vicinity of Perry, Ohio,” Letter submitted to Dr. Andrew Murphy, U.S. Nuclear Regulatory Commission, 10 pp., May 23, 1996.

2.5.1-484 Stein, S., Sleep, N., Geller, R., Wang, S., and Kroeger, G., 1979, “Earthquakes Along the Passive Margin of Eastern Canada,” Geophysical Research Letters, Vol. 6, pp. 537-540, 1979.

2.5.1-485 James, T.S., and Bent, A.L., “A Comparison of Eastern North American Seismic Strain Rates to Glacial Rebound Strain Rates,” Geophysical Research Letters, Vol. 21, pp. 2127-2130, 1994.

2.5.1-486 Clark, J.A., Hendricks, M., Timmermans, T.J., Struck, C., and Hilverda, K.J., “Glacial Isostatic Deformation of the Great Lakes Region,” Geological Society of America Bulletin, Vol. 106, pp. 19-31, 1994.

2.5.1-487 Holcombe, T.L., Taylor, L.A., Reid, D.F., Warren, J.S., Vincent, P.A., and Herdendorf, C.E., “Revised Lake Erie Postglacial Lake Level History Based on New Detailed Bathymetry,” Journal of Great Lakes Research, Vol. 29, No. 4, pp. 681-704, 2003.

2.5.1-488 Leverett, F.B., “Correlation of Beaches with Moraines in the Huron and Erie Basins,” *American Journal of Science*, Vol. 237, pp. 456-475, 1939.

2.5.1-489 Totten, S.M., “Pleistocene Beaches and Strandlines Bordering Lake Erie,” in White, G.W., “Glacial Geology of Northeastern Ohio,” State of Ohio Department of Natural Resources Division of Geological Survey, Bulletin 68, pp. 52-60, 1982.

2.5.1-490 Leverett, F., and Taylor, F.B., “The Pleistocene of Indiana and Michigan and the History of the Great Lakes,” U.S. Geological Survey Monograph 53, 529 pp., 1915.

2.5.1-491 Clark, P.U., “Striated Clast Pavements: Products of Deforming Subglacial Sediment?,” *Geology*, Vol. 19, pp. 530-533, 1991.

2.5.1-492 Hicock, S.R., “On Subglacial Stone Pavements in Till,” *The Journal of Geology*, Vol. 99, No. 4, pp. 607-619, 1991.

2.5.1-493 (Not Used)

2.5.1-494 Holcombe, T.L., Taylor, L.A., Warren, J.S., Vincent, P.A., Reid, D.F., and Herdendorf, C.E., “Lake-floor Geomorphology of Lake Erie,” National Environmental Satellite, Data, and Information Service, NATIONAL GEOPHYSICAL DATA CENTER, World Data Center A for Marine Geology and Geophysics Research Publication RP-3, 26 pp plus 8 plates and 9 figures, 2005.

2.5.1-495 National Geophysical Data Center, Great Lakes Data Rescue Project – Lake Erie and Lake Saint Clair Bathymetry, “Lake Erie and Lake Saint Clair Geomorphology,” http://www.ngdc.noaa.gov/mgg/greatlakes/lakeerie_cdrom/html/e_gmorph.htm.

2.5.1-496 Hobson, G. D., Herdendorf, C.E., and Lewis, F.M., “High Resolution Reflection Seismic Survey in Western Lake Erie,” Proceedings of the 12th Conference on Great Lakes Research,” pp. 210-224, 1969.

2.5.1-497 Carter, C. H., Williams, S., Fuller, J.A., and Meisburger, E.P., "Regional Geology of the Southern Lake Erie (Ohio) Bottom: A Seismic Reflection and Vibracore Study," U.S. Corps of Engineers Coastal Research Center, Miscellaneous Report No. 82-15, 1982.

2.5.1-498 Black & Veatch letter to Detroit Edison Company, "Denniston Quarry Investigation Technical Memorandum," Letter No. BVDE2- 2010-0038, February 4, 2010.

2.5.1-499 Mueller, K., Hough, S.E., and Bilham, R. "Analyzing the 1811-1812 New Madrid earthquakes with recent instrumentally recorded aftershocks," *Nature*, Vol. 429, pp. 284-288, 2004.

2.5.1-500 Hough,S.E., and Page, M., "Toward a consistent model for strain accrual and release for the New Madrid seismic zone, central United States," *Journal of Geophysical Research*, Vol. 116, B03311, 2011.

2.5.1-501 McBride, J.H., Leetaru, H.E., Bauer, R.A., Tingey, B.E., and Schmidt, S.E.A., "Deep faulting and structural reactivation beneath the southern Illinois basin," *Precambrian Research*, Vol. 157, pp. 289-313, 2007.

2.5.1-502 Kim, W.-Y, "The 18 June 2002 Caborn, Indiana, earthquake: Reactivation of ancient rift in the Wabash Valley seismic zone?" *Bulletin of the Seismological Society of America,* Vol. 93, No. 5, pp. 2201-2211, 2003.

2.5.1-503 Olson, S.M., Green, R.A., and Obermeier, S.F., "Revised magnitude bound relation for the Wabash Valley seismic zone of the central United States," *Seismological Research Letters*, Vol. 76, No. 6, pp. 756-771, 2005.

2.5.1-504 Nelson, W.J., "Structural Features in Illinois," Illinois State Geological Survey, Bulletin 100, 1995

Table 2.5.1-201 Regional Tectonic Structures Within 320 km (200 mi) (Sheet 1 of 8) [EF3 COL 2.0-26-A]

Name	Location	Closest Distance to Site	Structure Trend, Plunge and Any Associated Fault	Trend, Type of Fault, Dip, Sense of Displacement	Unit/Age/Amount of Maximum Deformation/Offset	Unit/Age/Amount of Youngest Deformation/Offset	Age of Oldest Unfaulted Unit	Associated Oil and Gas Field	Means of Identification[(a)]	Source
MAJOR STRUCTURES										
Akron Magnetic Boundary (AMB)	NE Ohio	170 km (106 mi)	NE-SW trending magnetic anomaly (low) associated with possible pre-existing basement structure			Possible lake-loading-induced seismicity	n/a		G	Reference 2.5.1-237; Reference 2.5.1-327 Reference 2.5.1-207
Albion-Scipio Fault (ASF)	Hillsdale and Calhoun counties, Michigan	108 km (67 mi)	NW-SE trending anticline associated with en-echelon wrench faults			Offsets the Middle Ordovician Trenton Formation and the Mississippian Coldwater Shale	Late Wisconsinan to Holocene till and glaciofluvial deposits	Albion-Pulaski-Scipio-Trend oil and gas field	B, G	Reference 2.5.1-331 Reference 2.5.1-207
Northern Segment Bowling Green Fault (BGF), also known as the Lucas-Monroe Monocline (LMM) in Michigan	Lenawee/ Monroe counties northwest to Livingston County, Michigan	48 km (28 mi)	NW-SE trending asymmetrical anticline(s) with steeply dipping SW flank (faulted); merges with Howell anticline at north end	Several NW-SE trending, normal, steeply dipping to vertical, right- and left- stepping, southwest-side-down faults; includes Deerfield anticline, a N-S trending, north-plunging anticline with normal, steeply dipping to vertical, down-to-the-west fault on west	Top of Middle Ordovician Trenton Formation is offset 61 m (200 ft) down-to-the-west	Offsets top of Early Mississippian Sunbury Shale on structure contour map	Late Wisconsinan to Holocene till and glaciofluvial deposits	Deerfield oil field	B, G	Reference 2.5.1-333; Reference 2.5.1-335 Reference 2.5.1-207
Central Segment Bowling Green Fault, also known as the Lucas-Monroe Monocline	Hancock County, Ohio north to Lenawee/ Monroe counties, Michigan	40 km (24 mi)		N10 – 20°W trending, normal, vertical fault, down-to-the-west with recurrent, variable displacements (see Figure 2.5.1-223). Waterville Quarry exposures suggest thrusts are interformational ramp faults (see Episode VI on Figure 2.5.1-223)	Offsets top of Middle Silurian Lockport Dolomite approximately 122 m (400 ft)	Slickensides and offset bedding in uppermost Late Silurian Bass Islands Group; <5 m (16 ft) thrusting in Cenozoic is highly speculative	Late Silurian to Early Devonian. Late Wisconsinan to Holocene till and lacustrine deposits		S, B, G	Reference 2.5.1-332; Reference 2.5.1-237; Reference 2.5.1-207
Southern Segment Bowling Green Fault (BGF)	Wood County sorth to Marion County, Ohio	101 km (62 mi)		SE trending, normal, steeply dipping to vertical, down-to-the-northeast splays (Outlet and Marion faults) and down-to-the-west fault splays (see Figure 2.5.1-203)	Offsets Precambrian unconformity surface		Late Silurian to Early Devonian. Late Wisconsinan to Holocene till and lacustrine deposits		B, G	Reference 2.5.1-237 Reference 2.5.1-207

Table 2.5.1-201 Regional Tectonic Structures Within 320 km (200 mi) (Sheet 2 of 8) [EF3 COL 2.0-26-A]

Name	Location	Closest Distance to Site	Structure Trend, Plunge and Any Associated Fault	Trend, Type of Fault, Dip, Sense of Displacement	Unit/Age/Amount of Maximum Deformation/Offset	Unit/Age/Amount of Youngest Deformation/Offset	Age of Oldest Unfaulted Unit	Associated Oil and Gas Field	Means of Identification[(a)]	Source
Burning Springs Anticline (BSA) (50 – 150 km long)	West Virginia	327 km (203 mi)	N-S trending anticline faulted in core; splays into several right-stepping traces at Ohio River; may extend south to include Mann Mountain anticline	N-S trending, normal, steeply east-dipping fault, down-to-the-east with recurrent displacements, including: a. Offsets Precambrian unconformity surface south of the Ohio River b. Reactivation during Silurian restricting salt deposition to a basin east of the fault c. Recurrent movement during deposition of Devonian through Permian strata d. NW directed Alleghanian age thrusting on decollements in Late Silurian Salina Group salts at the salt edge and development of imbricate ramp thrusts coring anticline in Salina Group and younger strata	300 m (980 ft) down-to-the-east on base of Cambrian	Only folding in Late Silurian Salina Group through Pennsylvanian-Permian units	Middle Pleistocene to Holocene colluvium, and Late Wisconsinan to Holocene alluviym		B, G	Reference 2.5.1-237; Reference 2.5.1-336; Reference 2.5.1-337 Reference 2.5.1-207
Cambridge Arch (CA) (100 km long)	Eastern Ohio	118 km (73 mi)	N20°W trending fault-bounded arch (horst) with half graben (Parkersburg-Lorain syncline) on west; splays into three arches at Ohio River	N20°W trending normal faults, dipping >80°, bounding 1.5 km (0.9 mi) wide uplifted block (horst) with some right-lateral slip at north end	≈80 m (262 ft) structural relief on Devonian Onondaga Limestone	Late Permian	Late Wisconsinan to Holocene till and glaciofluvial deposits		S (north end), B, G	Reference 2.5.1-237; Reference 2.5.1-336 Reference 2.5.1-207
Chatham Sag and Electric Fault	SW Ontario, Canada	81 km (50 mi)	E-W trending sag defined by mutual plunges of Findlay and Algonquin arches and bound on the north by EW trending Electric fault	E-W trending, normal, vertical, south-side-down	Precambrian surface displaced about 93 m (305 ft) vertically	Present on the structure contour map on the uppermost Late Silurian Bass Islands Group but probably does not displace the base of the Middle Devonian Dundee Formation	Middle Devonian Dundee Formation. Pleistocene glaciolacustrine deposits		B, G	Reference 2.5.1-325 Reference 2.5.1-207

Table 2.5.1-201 Regional Tectonic Structures Within 320 km (200 mi) (Sheet 3 of 8) [EF3 COL 2.0-26-A]

Name	Location	Closest Distance to Site	Structure Trend, Plunge and Any Associated Fault	Trend, Type of Fault, Dip, Sense of Displacement	Unit/Age/Amount of Maximum Deformation/Offset	Unit/Age/Amount of Youngest Deformation/Offset	Age of Oldest Unfaulted Unit	Associated Oil and Gas Field	Means of Identification[(a)]	Source
Cholchester Fault	Essex County, southeast Ontario	52 km (32 mi)	North-northwest-trending faults or syncline	Two subparallel, northwest-trending down-to-the-east faults. Zone of dolomitization along a fracture zone in the Middle Ordovician Trenton Formation	Interpreted 12.2 m (40 ft) of relief on syncline in Middle Ordovician and Lower to Middle Silurian rocks	Middle Ordovician through Middle Silurian	Pleistocene glaciolacustrine deposits	Colchester Oil Pool	B, G	Reference 2.5.1-406 Reference 2.5.1-409 Reference 2.5.1-412 Reference 2.5.1-413 Reference 2.5.1-207
Fort Wayne Rift	Western Ohio and eastern Indiana	173 km (107 mi)	NW-SE trending fault-bounded graben with central high	NW-SE trending, normal, vertical, northeast-side-down Anna-Champaign fault and southwest-side-down Logan fault forming central high; unnamed northeast and southwest side-down fault bounding graben		Truncated by GFTZ (1.25 Ga to 980 Ma); seismically active	Paleozoic sediments		B, G	Reference 2.5.1-237 Reference 2.5.1-207
Fortville Fault (FF)	Marion, Hancock, and Madison counties, Indiana	271 km (168 mi)	N-NE to S-SW trending, normal fault, steeply southeast dipping, down-to-the-southeast; on west flank of Cincinnati arch	Offsets top of Precambrian surface	Offsets top of Middle Silurian Salamonie Dolomite but not top of Middle Devonian Muscatatuck Group	Lower Mississippian	Late Wisconsinan to Holocene till and glacial outwash deposits		B, G	Reference 2.5.1-338 Reference 2.5.1-207
Grenville Front Tectonic Zone (GFTZ)	Mississippi north and north through Ohio and NE Canada	0 km (0 mi)	NE to N to NE trending zone of faults 10 – 100 km (6 – 60 mi) wide	NE to N-NE trending thrust faults, dipping east. Suture zone associated with Grenville orogeny	Probably tens of km of E-W crustal shortening during Grenville orogeny (1.25 Ga to 980 Ma)	Movement along the Bowling Green fault is attributed to reactivation of GFTZ. Uppermost Late Silurian Bass Islands Group offset by central segment of Bowling Green fault	Movement along the Bowling Green fault is attributed to reactivation of GFTZ. Uppermost Late Silurian Bass Islands Group offset by central segment of Bowling Green fault		B, G	Reference 2.5.1-237; Reference 2.5.1-234

Table 2.5.1-201 Regional Tectonic Structures Within 320 km (200 mi) (Sheet 4 of 8) [EF3 COL 2.0-26-A]

Name	Location	Closest Distance to Site	Structure Trend, Plunge and Any Associated Fault	Trend, Type of Fault, Dip, Sense of Displacement	Unit/Age/Amount of Maximum Deformation/Offset	Unit/Age/Amount of Youngest Deformation/Offset	Age of Oldest Unfaulted Unit	Associated Oil and Gas Field	Means of Identification[(a)]	Source
Hoosier Thrust Belt - Louisville Uplift	SW Indiana	393 km (244 mi)		Series of N-NW trending thrust faults, west-dipping (Hoosier thrust fault) bound on east by N-NW trending, foreland-style thrust fault (Louisville uplift)	Hoosier thrust belt is developed within the Precambrian (Mesoproterozoic) Centralia Group and truncated by overlying unconformity; Louisville uplift has ≈8 km (5 mi) of vertical uplift dated at 600 Ma, reactivated in Paleozoic. (see discussion of Wabash Valley Seismic Zone)	Precambrian	Paleozoic units		B, G	Reference 2.5.1-338; Reference 2.5.1-229
Howell Anticline/Fault (HA) (100 km long; 145 km if folds near Detroit River included)	Wayne northwest to Shiawassee counties, Michigan. May extend southeast to Detroit River to Stony Island Anticline and associated folds (see Minor Structures)	45 km (27 mi) / 5-15 km (3.1-9.3 mi) if folds near Detroit River included	NW-SE trending, NW plunging anticline, faulted on NW flank	Fault is NW-SE trending, normal, near-vertical, NE dipping, down-to-the-southwest	Anticline is expressed in the Precambrian unconformity surface; offsets top of Middle Ordovician Trenton Formation >300 m (1000 ft)	Influences deposition of Early Mississippian Sunbury Shale	Lower Middle Devonian Detroit River Group. Late Wisconsinan and Holocene till, glaciofluvial and lacustrine deposits	Northville oil and gas field (southeast) and Fowlerville gas field (northwest). New Boston and Sumpter oil and gas fields associated with folds near Detroit River	B, G	Reference 2.5.1-340; Reference 2.5.1-237
Maumee Fault (MF)	Henry, Lucas, and Wood counties, Ohio	34 km (21 mi)	NE-SW trending fault	NE-SW trending, normal, vertical	Offset by central segment of Bowling Green fault; coincident with Maumee River lineament	Unknown	Unknown		G	Reference 2.5.1-237
Mount Carmel Fault / Leesville Anticline	Monroe, Lawrence, and Washington counties, Indiana	397 km (246 mi)	N-NW trending anticlines over graben along southwest side of antithetic normal fault associated with east-dipping thrust fault along NE margin of Illinois basin	N-SW trending, normal, southwest-dipping, down-to-the-southwest	Associated with paleoliquefaction centers (see discussion of Wabash Valley Seismic Zone)	Middle Mississippian	Pleistocene and Holocene alluvium and colluvium		B, G	Reference 2.5.1-338; Reference 2.5.1-229

Table 2.5.1-201 Regional Tectonic Structures Within 320 km (200 mi) (Sheet 5 of 8) [EF3 COL 2.0-26-A]

Name	Location	Closest Distance to Site	Structure Trend, Plunge and Any Associated Fault	Trend, Type of Fault, Dip, Sense of Displacement	Unit/Age/Amount of Maximum Deformation/Offset	Unit/Age/Amount of Youngest Deformation/Offset	Age of Oldest Unfaulted Unit	Associated Oil and Gas Field	Means of Identification[(a)]	Source
Peck Fault (PF) (also known as Sanilac Fault)	St. Clair and Sanilac counties, Michigan	133 km (82 mi.)	N-S trending fault (Figure 2.5.1-203). N10° – 20°W trending faulted monocline (Reference 2.5.1-329)	N-S trending, normal, vertical, west-side-down (Reference 2.5.1-325). N10° – 20°W trending, east dipping thrust fault (Reference 2.5.1-329)	91 m (300 ft.) on Middle Ordovician Trenton Group (Reference 2.5.1-325). Sanilac fault repeats early Late Silurian Salina Group A-1 Evaporite unit with approximately 29 m (95 ft.) of net slip (Reference 2.5.1-329)	Present on structure contour map on top of lowest Middle Devonian Dundee Formation (Reference 2.5.1-325). Fault offsets contact between early Late Silurian Salina Group A-1 Evaporite and A-1 Carbonate units (Reference 2.5.1-329). Early Mississippian Sunbury Shale	Late Wisconsinan and Holocene till and glacial and postglacial lacustrine deposits		B, G	Reference 2.5.1-325; Reference 2.5.1-329; Reference 2.5.1-333 Reference 2.5.1-207
Royal Center Fault (RCF)	Cass, Fulton, and Kosciusko counties, Indiana	223 km (138 mi.)	NE-SW trending, normal, steeply southeast dipping, down-to-the-southeast	NE-SW trending, normal, steeply southeast dipping, down-to-the-southeast	Approximately 100 on the top of the Cambrian Mount Simon sandstone	Offsets top of Middle Silurian Salamonie Dolomite and the Mississippian Black Shale	Late Wisconsinan and Holocene till, glacial outwash and ice contact deposits		B, G	Reference 2.5.1-338 Reference 2.5.1-207
Sharpsville Fault (SF)	Tipton and Howard counties, Indiana	286 km (177 mi.)	NE-SW trending fault	NE-SW trending, normal, vertical, down-to-the-southeast		Offsets top of Middle Ordovician Trenton Formation and Devonian rocks	Late Wisconsinan and Holocene till		B	Reference 2.5.1-339 Reference 2.5.1-207
Transylvania Fault Extension (TFE)	NE Ohio	186 km (115 mi.)	Zone of NW to S-SE trending faults including the Pittsburg-Washington cross-strike structural discontinuity, Highland Town, Smith Township, Suffield, Akron, and Middleburg faults	NW-SE trending, early right-lateral-wrench faults with minimum of 21 km (13 mi.) of lateral displacement, reactivated normal, steeply (80°) southwest-dipping, down-to-the-southwest faults	60 – 120 m (200 – 400 ft.), vertical, down-to-the-southwest, on Precambrian unconformity surface	72 m (240 ft.) vertical, down-to-the-southwest on Devonian Onondaga Limestone; controls deposition of strata as young as Pennsylvanian[6]	Mid-Pleistocene to Holocene alluvium and colluvium		B, G	Reference 2.5.1-237; Reference 2.5.1-342 Reference 2.5.1-207
MINOR STRUCTURES										
(Note: Minor structures are identified from oil and gas explorations reports that focus on the producing horizons; only limited information cited below is available to evaluate the age of youngest deformation or the oldest unfaulted unit.)										
Akron Anticline	Tuscola County, Michigan	180 km (110 mi.)	E-W trending anticline			Lower Middle Ordovician St. Peter Sandstone	Late Wisconsinan and Holocene glacial and postglacial lacustrine deposits	Akron deep oil and gas field	B, G	Reference 2.5.1-429 Reference 2.5.1-207

Table 2.5.1-201 Regional Tectonic Structures Within 320 km (200 mi) (Sheet 6 of 8) [EF3 COL 2.0-26-A]

Name	Location	Closest Distance to Site	Structure Trend, Plunge and Any Associated Fault	Trend, Type of Fault, Dip, Sense of Displacement	Unit/Age/Amount of Maximum Deformation/Offset	Unit/Age/Amount of Youngest Deformation/Offset	Age of Oldest Unfaulted Unit	Associated Oil and Gas Field	Means of Identification[(a)]	Source
Burdell Anticline	Osceola County, Michigan	130 km (90 mi)	Faulted dome	Two intersecting N-NW and N-NE trending faults, normal, vertical	Faults top of Early to Middle Ordovician Foster Formation with vertical closure of about 46 m (150 ft)	Overlying St. Peter Sandstone not faulted but domed; deformation extends up into the Late Silurian Salina Group A-2 Carbonate	Late Wisconsinan and Holocene till	Burdell oil and gas field	B, G	Reference 2.5.1-430 Reference 2.5.1-207
Clayton Anticline	Arenac and Ogemaw counties, Michigan	250 km (155 mi)	NW-SE trending anticline faulted on NE flank	NW-SE trending fault, down-to-the-northeast	Top of Middle Ordovician Glenwood Formation faulted	Deformation extends up into the latest Late Devonian Berea Sandstone	Late Wisconsinan and Holocene glacial and postglacial lacustrine deposits	Cayton gas field	B, G	Reference 2.5.1-431 Reference 2.5.1-207
Clearville Fault	SW Ontario, Canada	138 km (85 mi)	N-NW trending fault	N-NW trending, normal, vertical west-side-down	Present on the Precambrian surface; 52 m (170 ft) on top of Middle Silurian Clinton Group	Probably present on structure contour map on top of Lower Devonian Detroit Group	Pleistocene till and glaciolacustrine deposits	Clearville oil field	B, G	Reference 2.5.1-325 Reference 2.5.1-207
Dawn Fault	SW Ontario, Canada	99 km (61 mi)	E-W trending fault	E-W trending, normal, vertical, south-side-down	Probably 47 m (155 ft) on top of Middle Silurian Clinton Group; 60 m (≈200 ft) trough on uppermost Silurian Bass Islands Group	Displaces base but not top of lower Devonian Detroit River Group	Pleistocene till and glaciolacustrine deposits	Dawn gas field	B, G	Reference 2.5.1-325 Reference 2.5.1-207
Dover Syncline/Fault	SE Ontario, Canada	85 km (52 mi)	E-W fault	E-W, normal, vertical, down-to-the-south	Present on the structure contour map on the top of the Middle Ordovician Trenton Group with ≈45 m (≈150 ft) of relief		Pleistocene glaciolacustrine deposits	Dover oil and gas field	B, G	Reference 2.5.1-325 Reference 2.5.1-207
Falmouth Anticline	Missaukee County, Michigan	300 km (186 mi)	NW-SE trending anticline (dome) with Paleozoic units draped over recurrently active basement faults			Earliest Middle Devonian Dundee Limestone faulted	Late Wisconsinan and Holocene glaciofluvial and ice contact deposits	Falmouth gas field	B, G	Reference 2.5.1-432 Reference 2.5.1-207
Kawkawlin Anticline	Bay County, Michigan	190 km (120 mi)	NW-SE trending asymmetrical anticline with steeply dipping SW flank			Earliest Middle Devonian Dundee Limestone deformed	Late Wisconsinan and Holocene glacial and postglacial lacustrine deposits and till	Kawkawlin gas field	B, G	Reference 2.5.1-433 Reference 2.5.1-207
Kimball-Colinville Monocline/Fault	crosses St. Clair River, Michigan/Ontario	123 km (76 mi)	NW-SE trending fault	NW-SE trending, steeply SW dipping faulted monocline	64 m (210 ft) on uppermost Silurian Bass Islands Group; possibly more on lower Middle Devonian Detroit River Group	Probably present on structure contour map on top of Middle Devonian Dundee Formation	Pleistocene till and glaciolacustrine deposits	Kimball-Colinville oil and gas field	B, G	Reference 2.5.1-325 Reference 2.5.1-207

Table 2.5.1-201 Regional Tectonic Structures Within 320 km (200 mi) (Sheet 7 of 8) [EF3 COL 2.0-26-A]

Name	Location	Closest Distance to Site	Structure Trend, Plunge and Any Associated Fault	Trend, Type of Fault, Dip, Sense of Displacement	Unit/Age/Amount of Maximum Deformation/Offset	Unit/Age/Amount of Youngest Deformation/Offset	Age of Oldest Unfaulted Unit	Associated Oil and Gas Field	Means of Identification[a]	Source
New Lothrop Anticline	Shiawassee County, Michigan	140 km (87 mi)	N-NW to S-SE trending, NW plunging anticline		18.3 m (60 ft) relief on top of lowermost Middle Devonian Dundee Limestone	Uppermost Late Devonian Berea Sandstone (production formation)	Late Wisconsinan and Holocene glacial and postglacial lacustrine deposits	New Lothrop oil field	B	Reference 2.5.1-434 Reference 2.5.1-207
Rose City Anticline	Ogemaw County, Michigan	280 km (170 mi)	NW-SE trending asymmetrical anticline with steeply dipping northeast flank			Earliest Middle Devonian Dundee Limestone deformed	Late Wisconsinan and Holocene glacial and postglacial outwash and till	Rose City gas field	B, G	Reference 2.5.1-435 Reference 2.5.1-207
Shaver Anticline	Gratiot and Montcalm counties, Michigan	190 km (118 mi)	NW-SE trending anticline			Deforms Early Mississippian Brown Limestone unit of Michigan Formation	Late Mississippian Triple Gypsum	Shaver gas field	B, G	Reference 2.5.1-436 Reference 2.5.1-207
South Buckeye Anticline	Gladwin County, Michigan	234 km (145 mi)	NW-SE trending asymmetrical anticline with steeply dipping southwest flank			Earliest Middle Devonian Dundee Limestone deformed	Late Wisconsinan and Holocene glacial and postglacial lacustrine deposits	South Buckeye oil and gas field	B, G	Reference 2.5.1-431 Reference 2.5.1-207
Stony Island Anticline (SIA)	Wayne County, Michigan	18 km (11 mi)	N30°W trending anticline with steeply dipping (50°SW) southwest flank; may be southeast extension of Howell anticline (see Major Structures)			Lower Middle Devonian Sylvania Sandstone deformed	Late Wisconsinan and Holocene glacial and postglacial lacustrine deposits		S, B	Reference 2.5.1-341 Reference 2.5.1-207
West Branch Anticline	Ogemaw County, Michigan	270 km (168 mi)	NW-SE trending faulted anticline	NW-SE trending, normal, steeply dipping, down-to-the southwest (1 SW dipping, southeast of axis), down-to the northeast (1 NE dipping, northeast of axis and 1 main, NE dipping, on NE flank); 2-3 N-NE trending, normal, steeply east-dipping, down-to-the-east on SE nose		Earliest Middle Devonian Dundee Limestone deformed/faulted; about 53.3 m (175 ft) of closure on top of Early Ordovician Prairie du Chien Group	Late Wisconsinan and holocene till, glaciofluvial and ice contact deposits	West Branch gas field	B, G	Reference 2.5.1-437 Reference 2.5.1-207

Table 2.5.1-201 Regional Tectonic Structures Within 320 km (200 mi) (Sheet 8 of 8) [EF3 COL 2.0-26-A]

Name	Location	Closest Distance to Site	Structure Trend, Plunge and Any Associated Fault	Trend, Type of Fault, Dip, Sense of Displacement	Unit/Age/Amount of Maximum Deformation/Offset	Unit/Age/Amount of Youngest Deformation/Offset	Age of Oldest Unfaulted Unit	Associated Oil and Gas Field	Means of Identification[a]	Source
Williams-Larkin Anticline	Bay County, Michigan	200 km (120 mi)	NW-SE trending, NW plunging anticline (Larkin may be a dome)			Latest Late Devonian Berea Sandstone (production formation)	Late Wisconsinan and Holocene glacial and postglacial lacustrine deposits	Larkin-Williams oil and gas field	B	Reference 2.5.1-438 Reference 2.5.1-207
Winterfield Anticline	Clare County, Michigan	280 km (174 mi)	NW-SE trending anticline (dome)			Deforms top of lower Middle Devonian Detroit River Group massive anhydrite unit with vertical relief of about 21 m (70 ft)	Late Wisconsinan and Holocene till, glaciofluvial outwash	Winterfield oil and gas field	B, G	Reference 2.5.1-439 Reference 2.5.1-207

a) B = Borings; G = Geophysical; S = Surface

Table 2.5.1-202 Site Stratigraphy for Fermi 2 and Fermi 3 [EF3 COL 2.0-26-A]

Soil or Rock Unit		
Fill		
Lacustrine Deposits		
Glacial Till	Upper (brown)	
	Lower (gray)	
Bass Islands Group		
	Fermi 2	Fermi 3
Salina Group	Unit G	Unit F
	Unit E	
	Unit C	Unit E
		Unit C
		Unit B
	Unit A	

Figure 2.5.1-201 Fermi 3 Site Region and Site Vicinity Planametric Maps [EF3 COL 2.0-26-A]

Figure 2.5.1-202 Fermi 3 Site Regional Physiographic Map [EF3 COL 2.0-26-A]

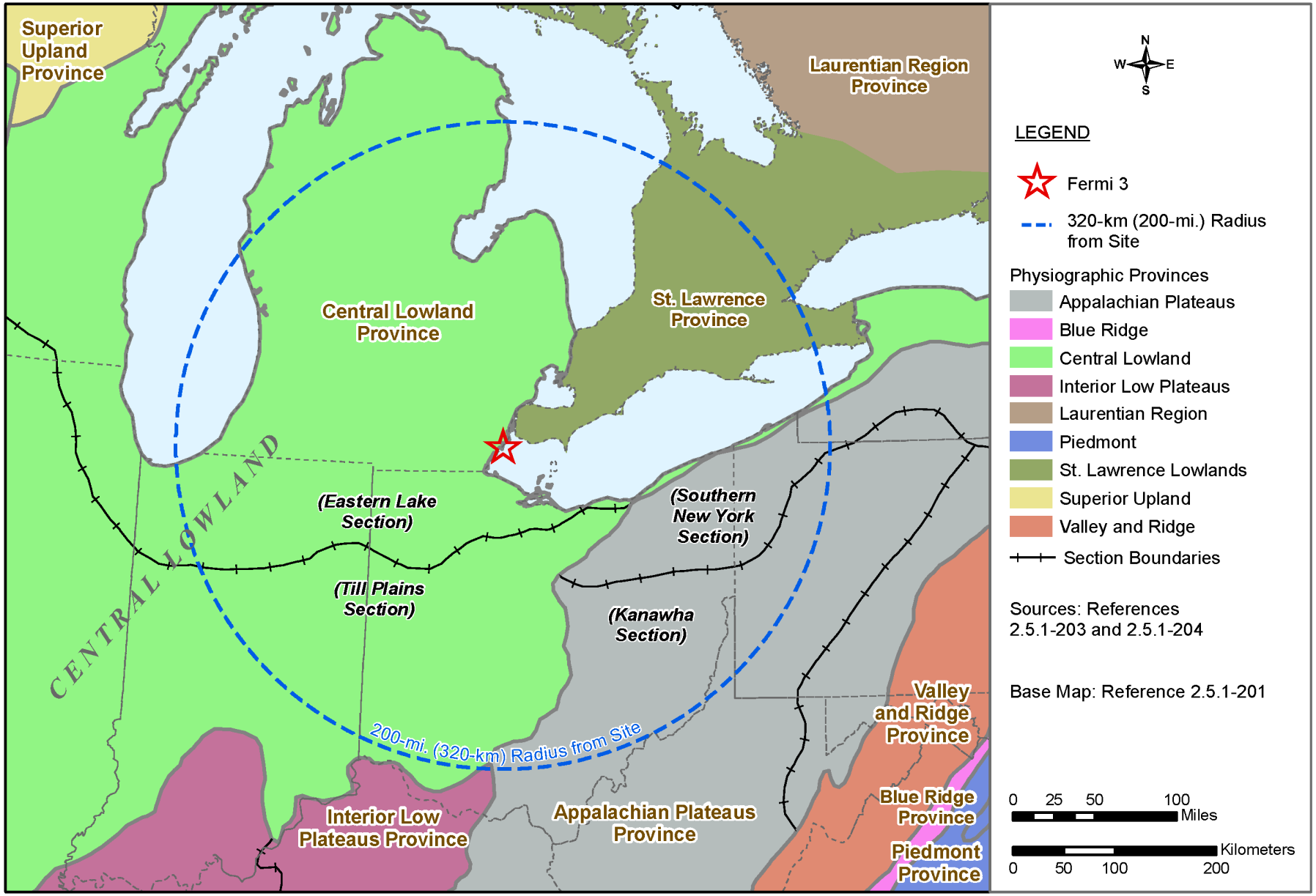

Figure 2.5.1-203 Fermi 3 Site Region Map of Tectonic Structures [EF3 COL 2.0-26-A]

Figure 2.5.1-204 Geologic Map of the Fermi 3 Site Region [EF3 COL 2.0-26-A]

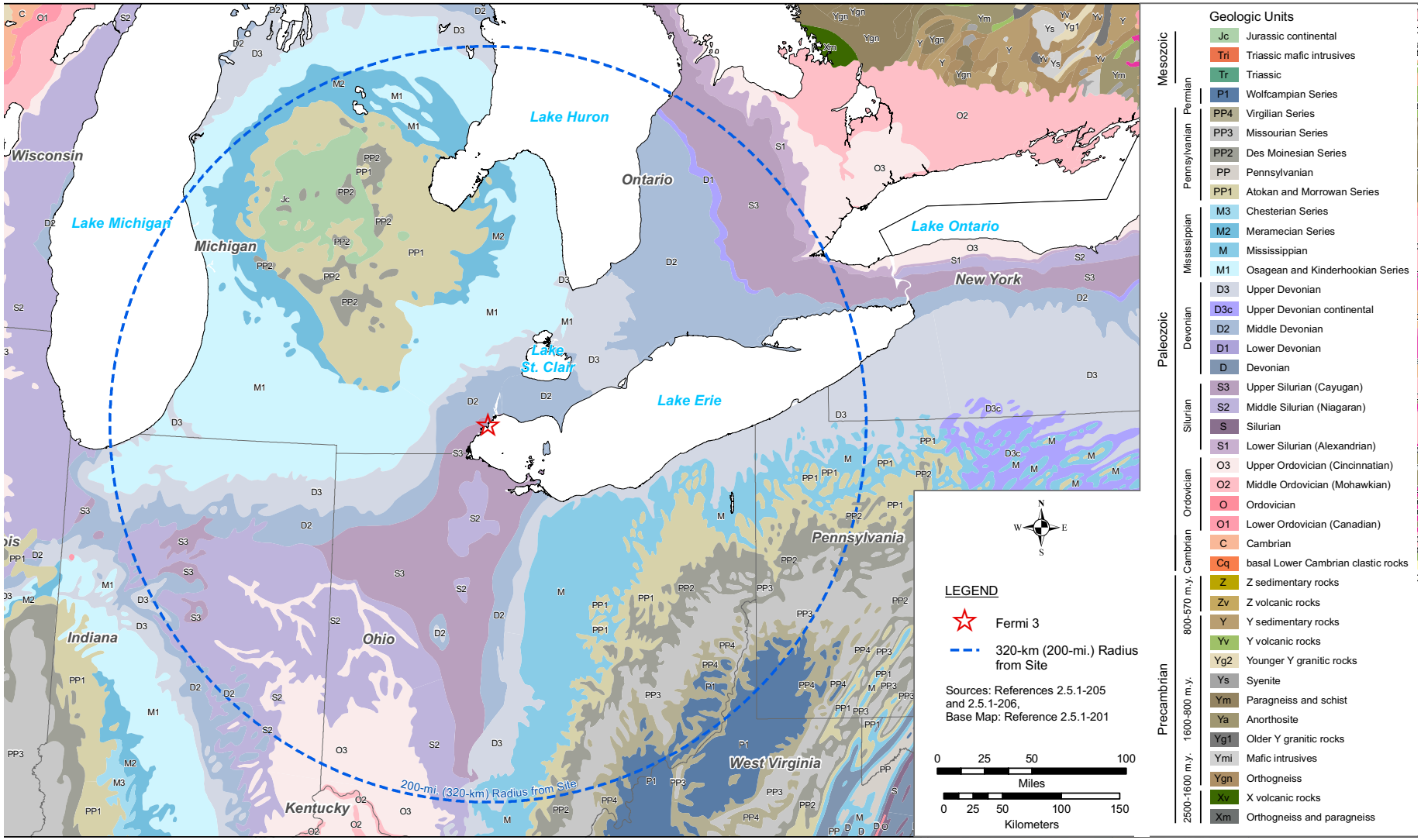

Figure 2.5.1-205 Quaternary Geology Map of the Fermi 3 Site Region [EF3 COL 2.0-26-A]

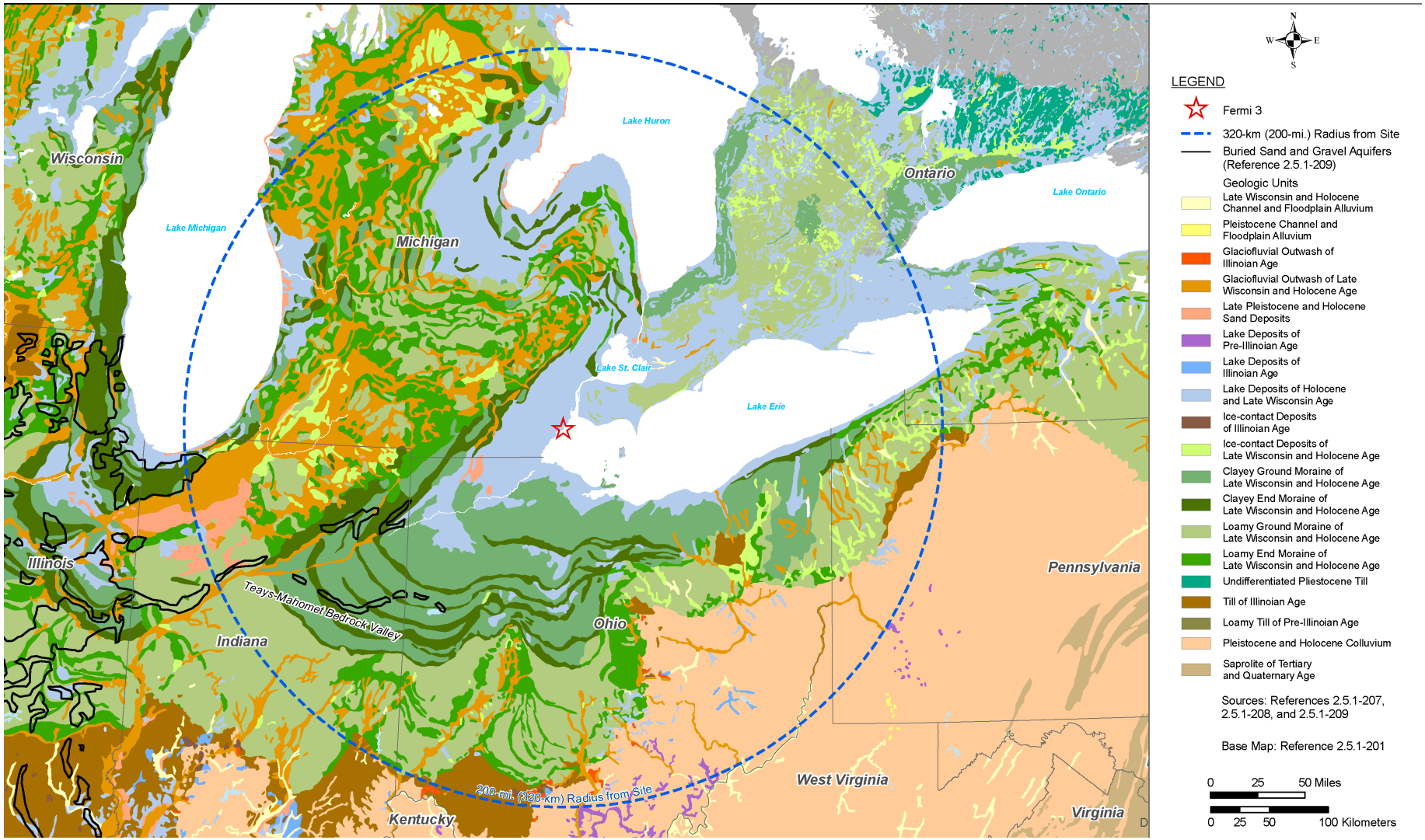

Figure 2.5.1-206 Basement Crustal Provinces in the Fermi 3 Site Region [EF3 COL 2.0-26-A]

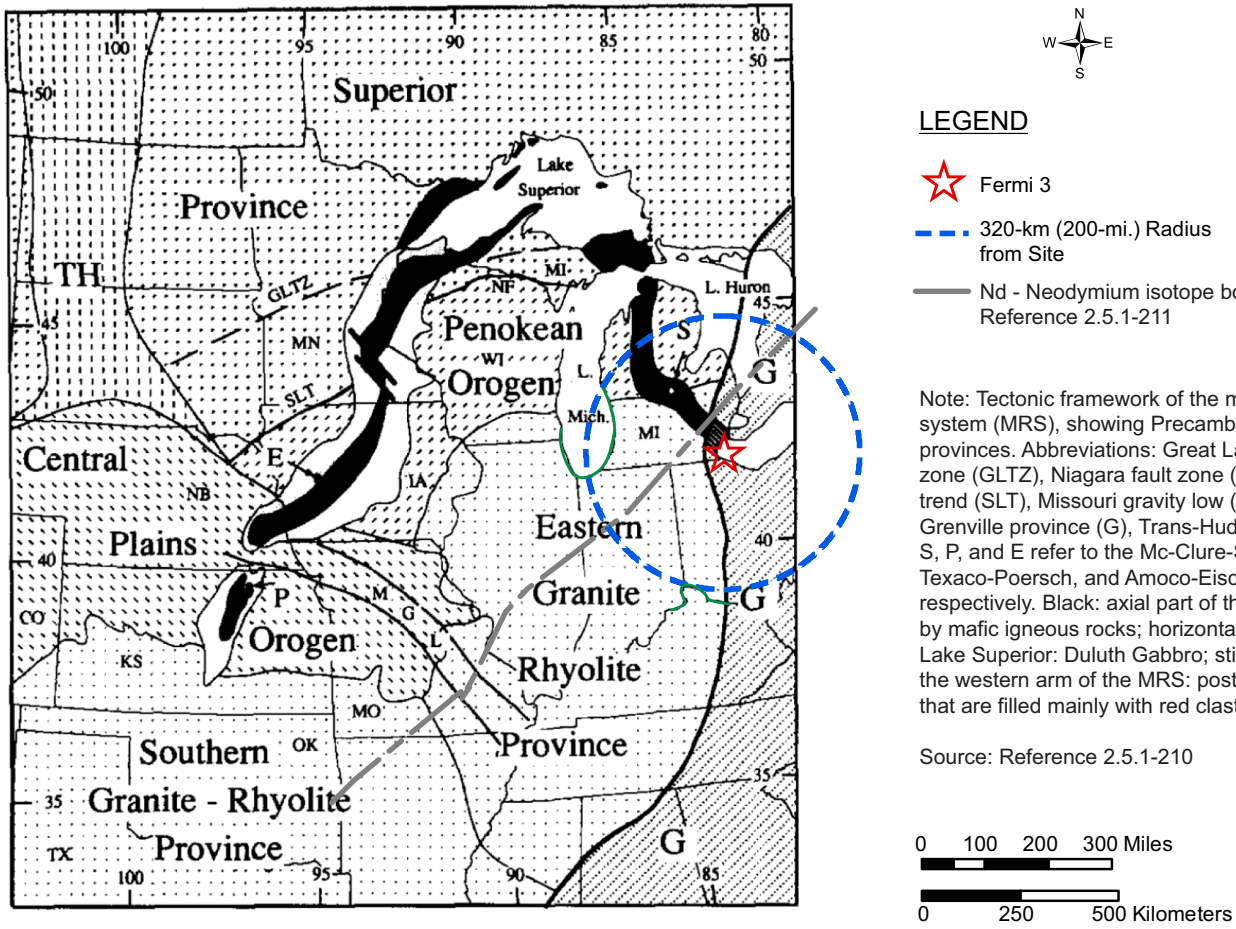

Source: Reference 2.5.1-210

Figure 2.5.1-207 Regional Seismicity and tectonic Features in the Fermi 3 Site Region (Sheet 1 of 3)[EF3 COL 2.0-26-A]

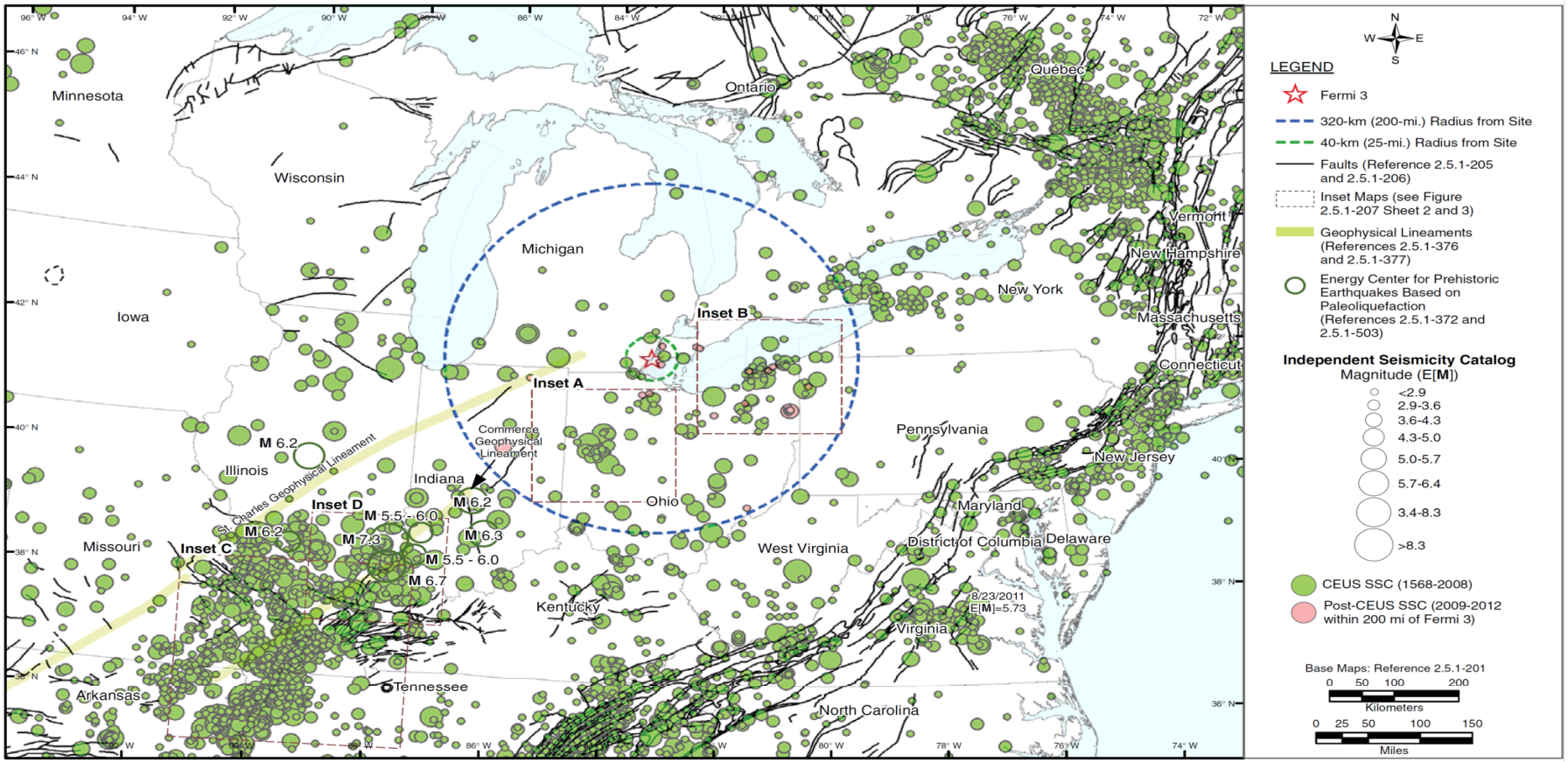

Figure 2.5.1-207 Regional Seismicity and tectonic Features in the Fermi 3 Site Region (Sheet 2 of 3)[EF3 COL 2.0-26-A]

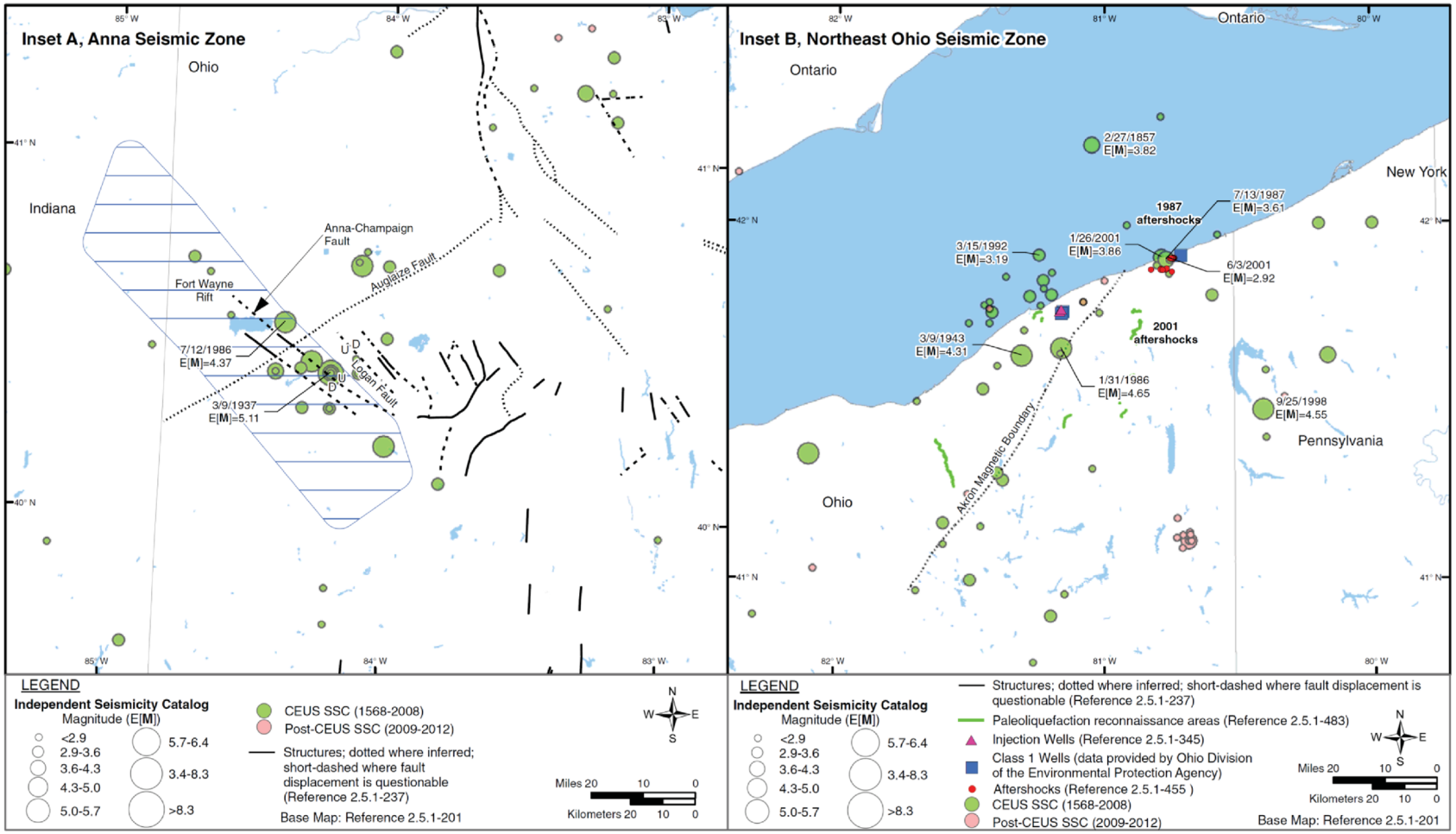

Figure 2.5.1-207 Regional Seismicity and tectonic Features in the Fermi 3 Site Region (Sheet 3 of 3)[EF3 COL 2.0-26-A]

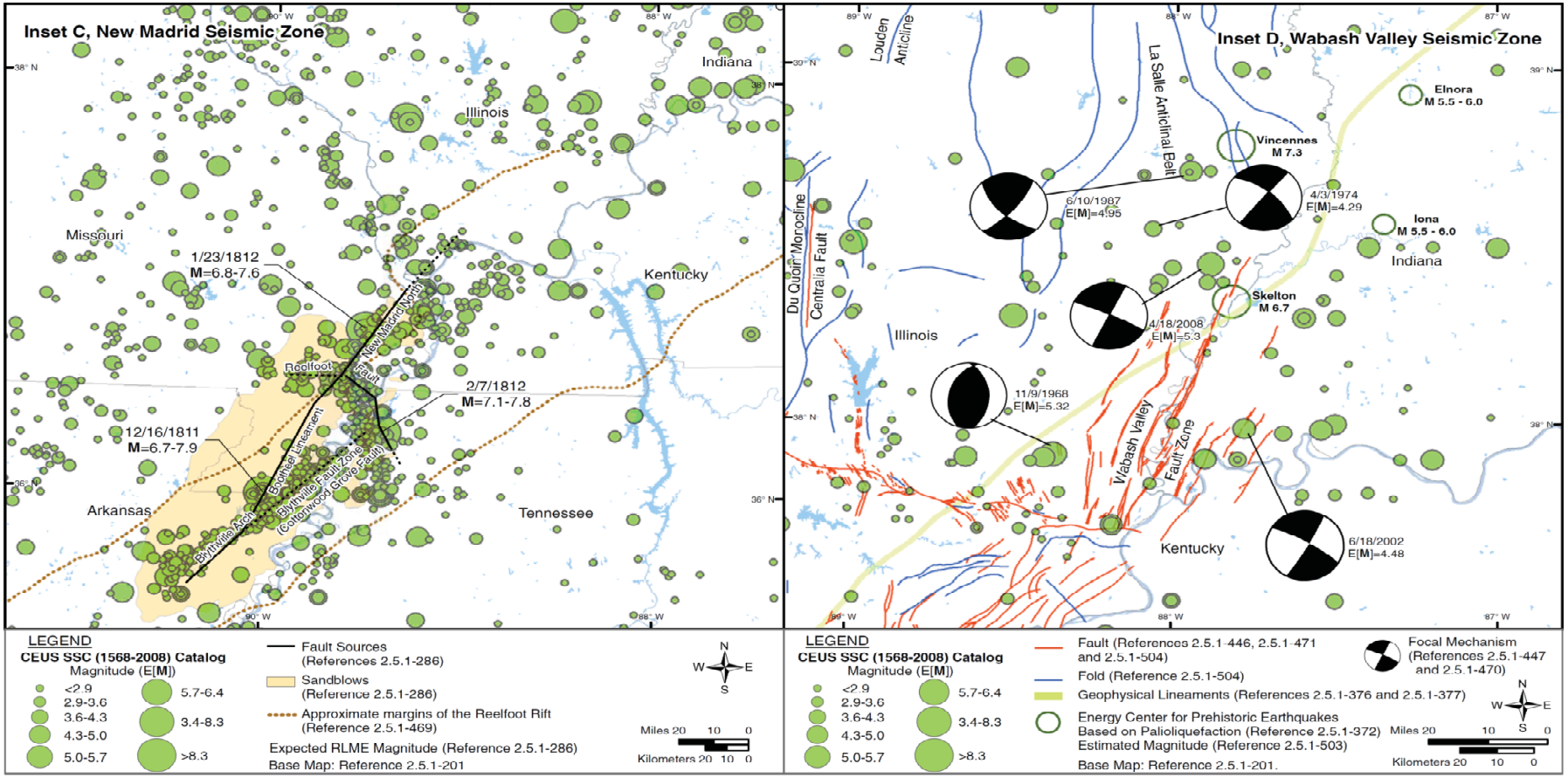

Figure 2.5.1-208 Paleozoic Basins and Arches in the Fermi 3 Site Region
[EF3 COL 2.0-26-A]

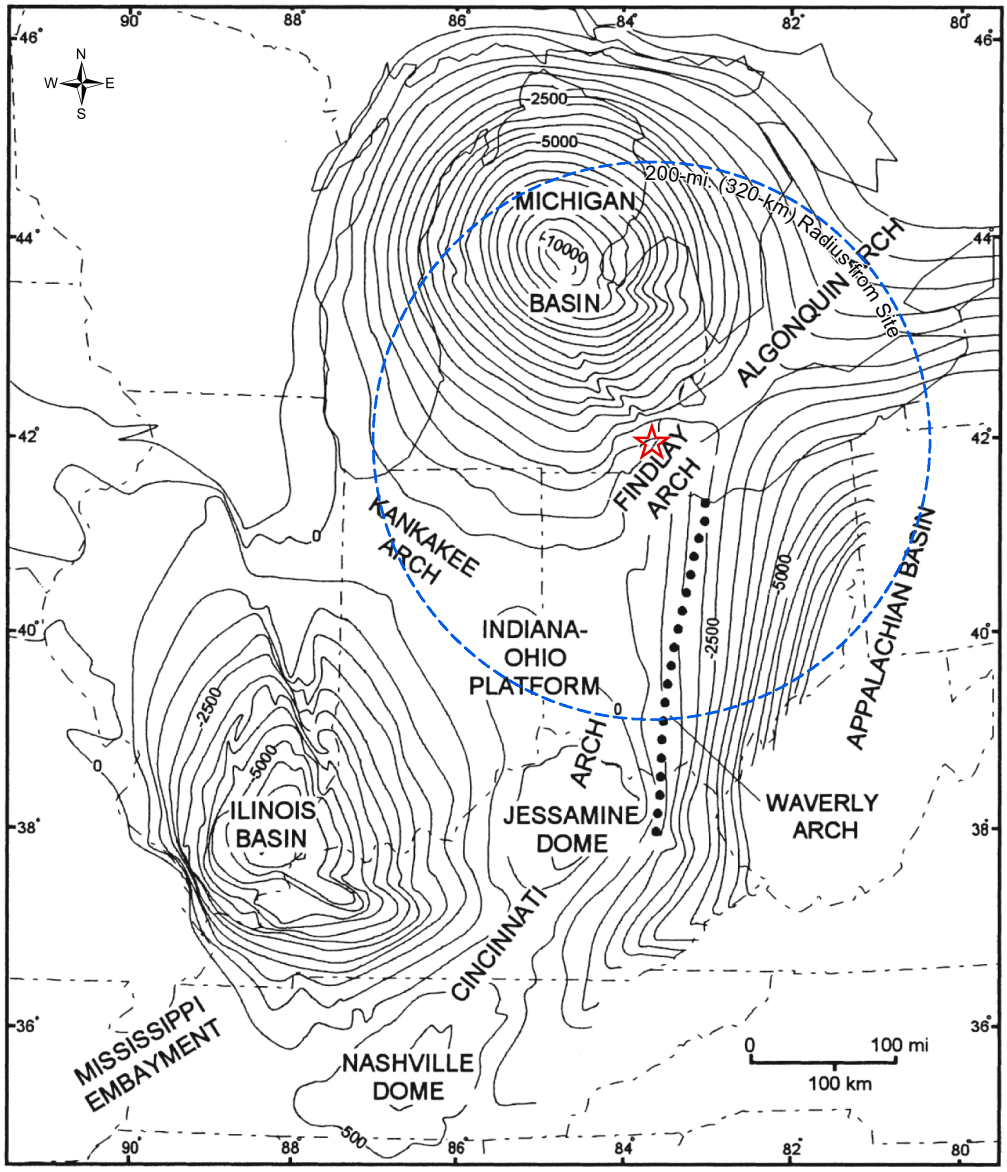

LEGEND

☆ Fermi 3

320-km (200-mi.) Radius from Site

Source: Reference 2.5.1-213

Figure 2.5.1-209 Geologic Timescale [EF3 COL 2.0-26-A]

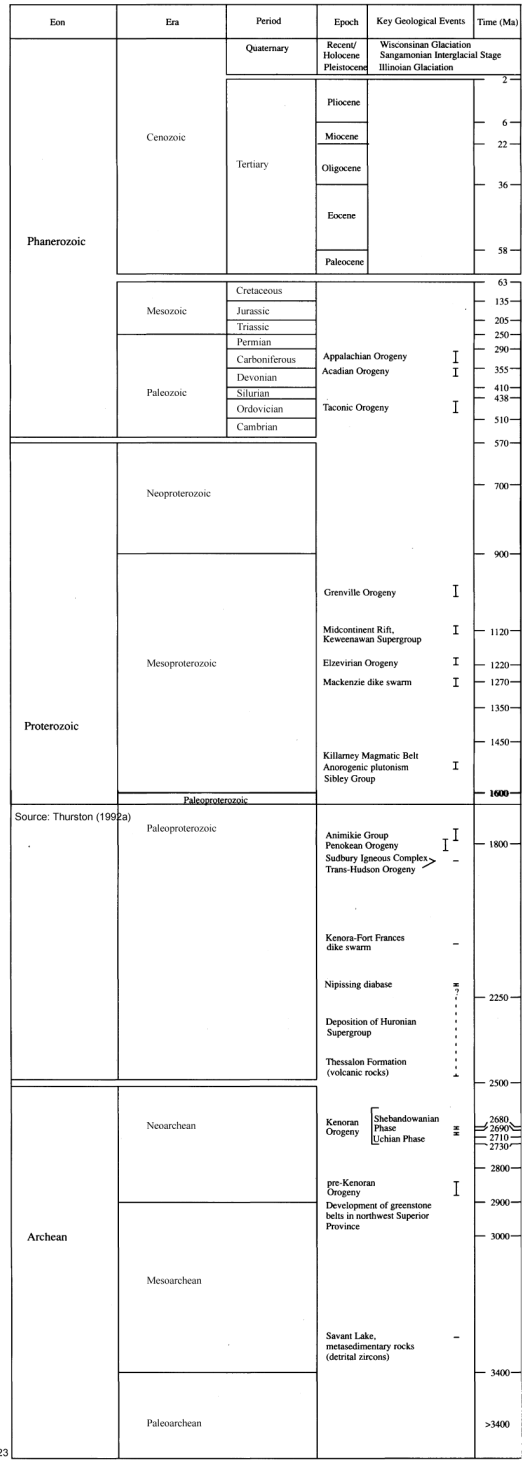

Source: Reference 2.5.1-223

Figure 2.5.1-210 Map and Schematic History of Penokean Orogeny [EF3 COL 2.0-26-A]

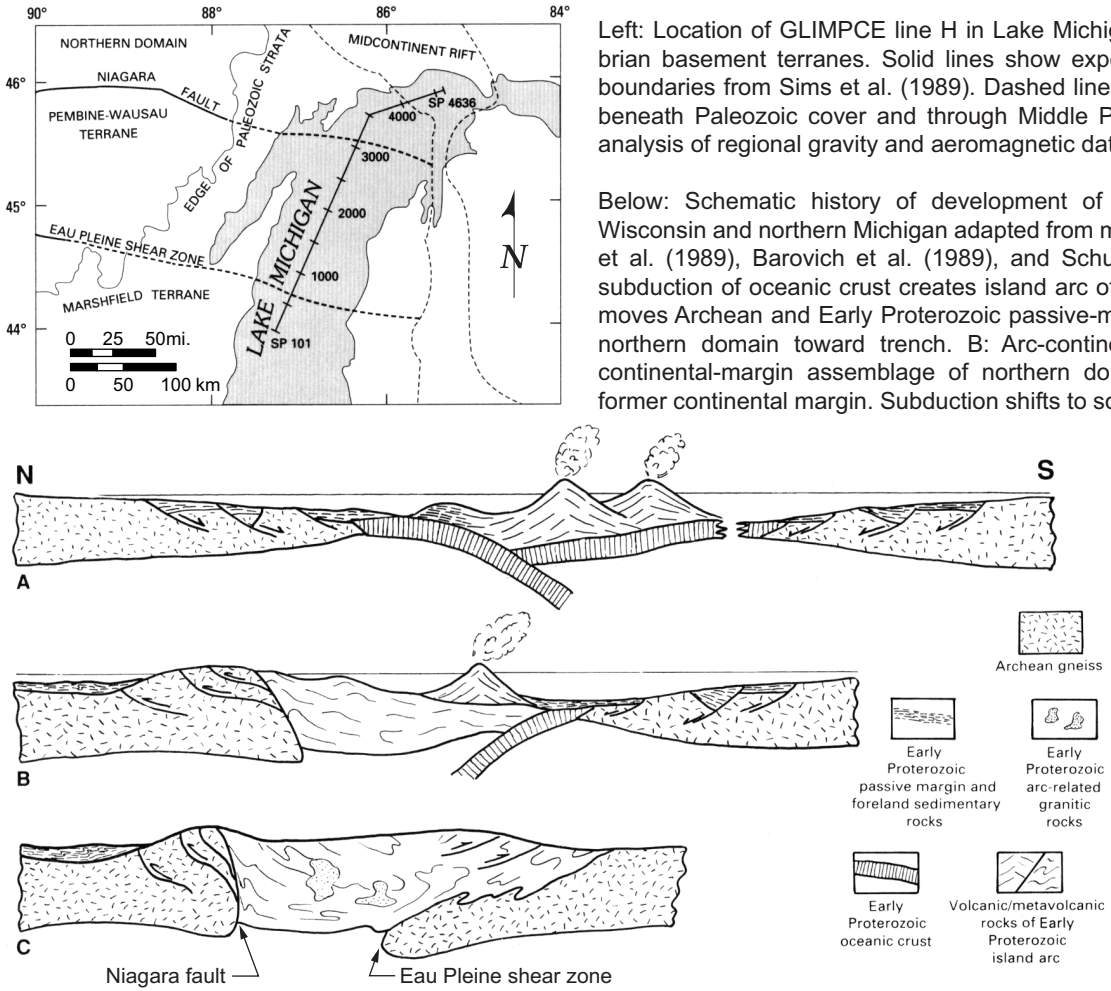

Left: Location of GLIMPCE line H in Lake Michigan and disposition of Precambrian basement terranes. Solid lines show exposed Early Proterozoic terrane boundaries from Sims et al. (1989). Dashed lines indicate boundaries projected beneath Paleozoic cover and through Middle Proterozoic plutonic rocks, from analysis of regional gravity and aeromagnetic data.

Below: Schematic history of development of Early Proterozoic terranes in Wisconsin and northern Michigan adapted from models by Hoffman (1987), Sims et al. (1989), Barovich et al. (1989), and Schulz et al. (1991). A: Southward subduction of oceanic crust creates island arc of Pembine-Wausau terrane and moves Archean and Early Proterozoic passive-margin and foredeep deposits of northern domain toward trench. B: Arc-continent collision deforms arc and continental-margin assemblage of northern domain. Compression rethickens former continental margin. Subduction shifts to south of original arc and reverses polarity, moving Archean and Early Proterozoic rocks of Marshfield terrane toward younger arc complex and trench. C: Collision of Marshfield terrane with arc causes further compression of arc and northern domain and subducts leading edge of continental margin of Marshfield terrane beneath arc.

Source: Reference 2.5.1-214

Source: Reference 2.5.1-214

Figure 2.5.1-211 Hypothetical Model for the Nature and Continuity of Structures of the Midcontinent Rift System
[EF3 COL 2.0-26-A]

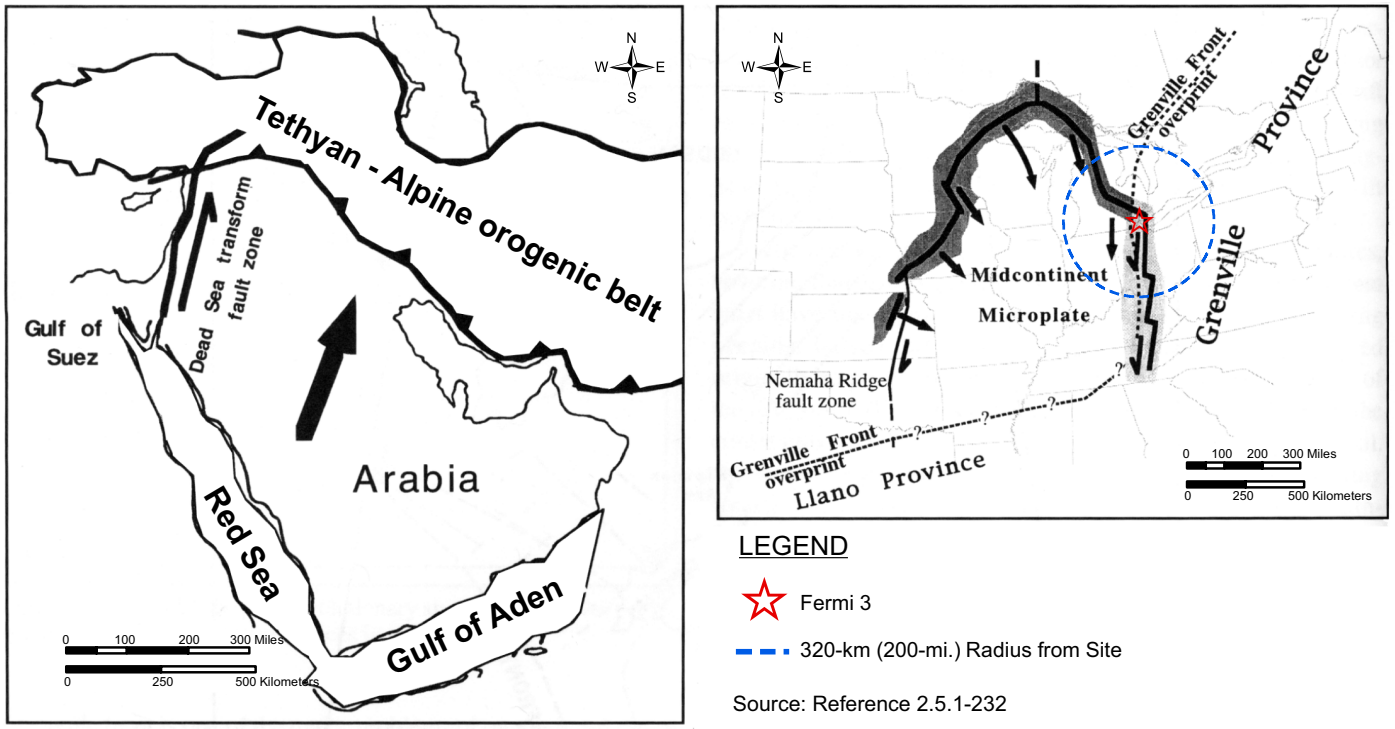

Source: Reference 2.5.1-232

Figure 2.5.1-212 Schematic History of the Grenville Orogeny [EF3 COL 2.0-26-A]

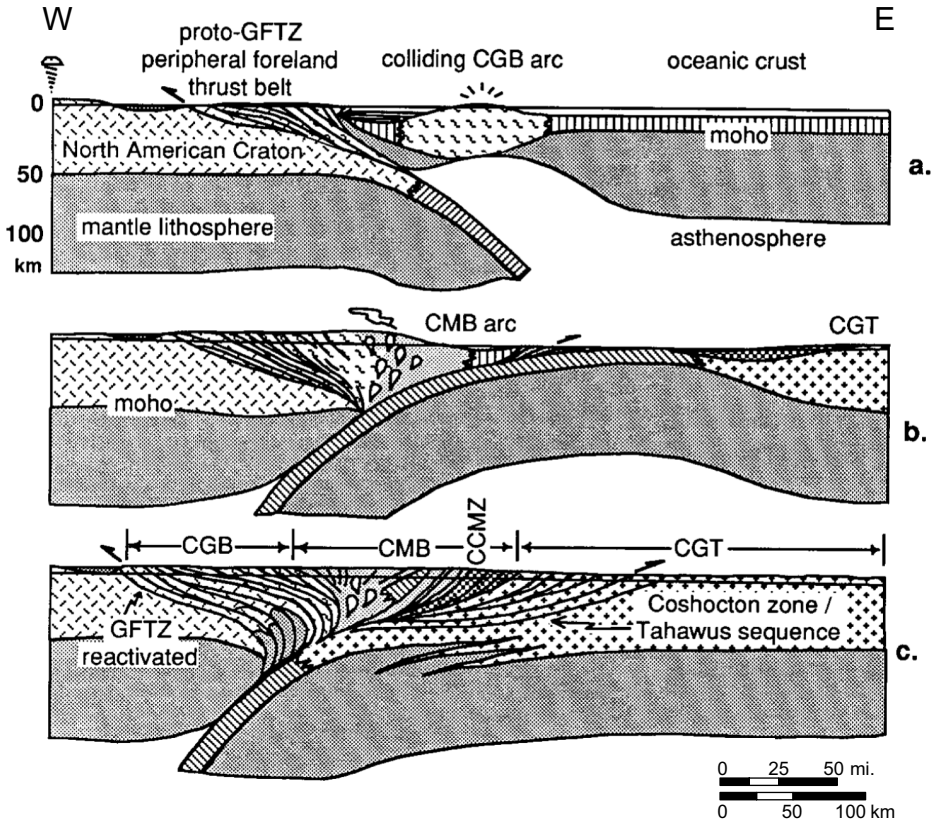

a: Collision of central gneiss belt (CGB) island arc with North American craton along east-dipping proto-Grenville Front tectonic zone (GFTZ).

b: Reversal of subduction polarity and construction of Andean arc in central metasedimentary belt (CMB).

c: 1.3-1.0 Ga collision of eastern CMB and central granulite terrane (CGT) along west-dipping Coshocton zone and Carthage-Colton mylonite zone (CCMZ). Back-arc basin may have opened and closed between phases b and c.

Source: Reference 2.5.1-234

Source: Reference 2.5.1-234

Figure 2.5.1-213 Map Showing Locations of Seismic Lines [EF3 COL 2.0-26-A]

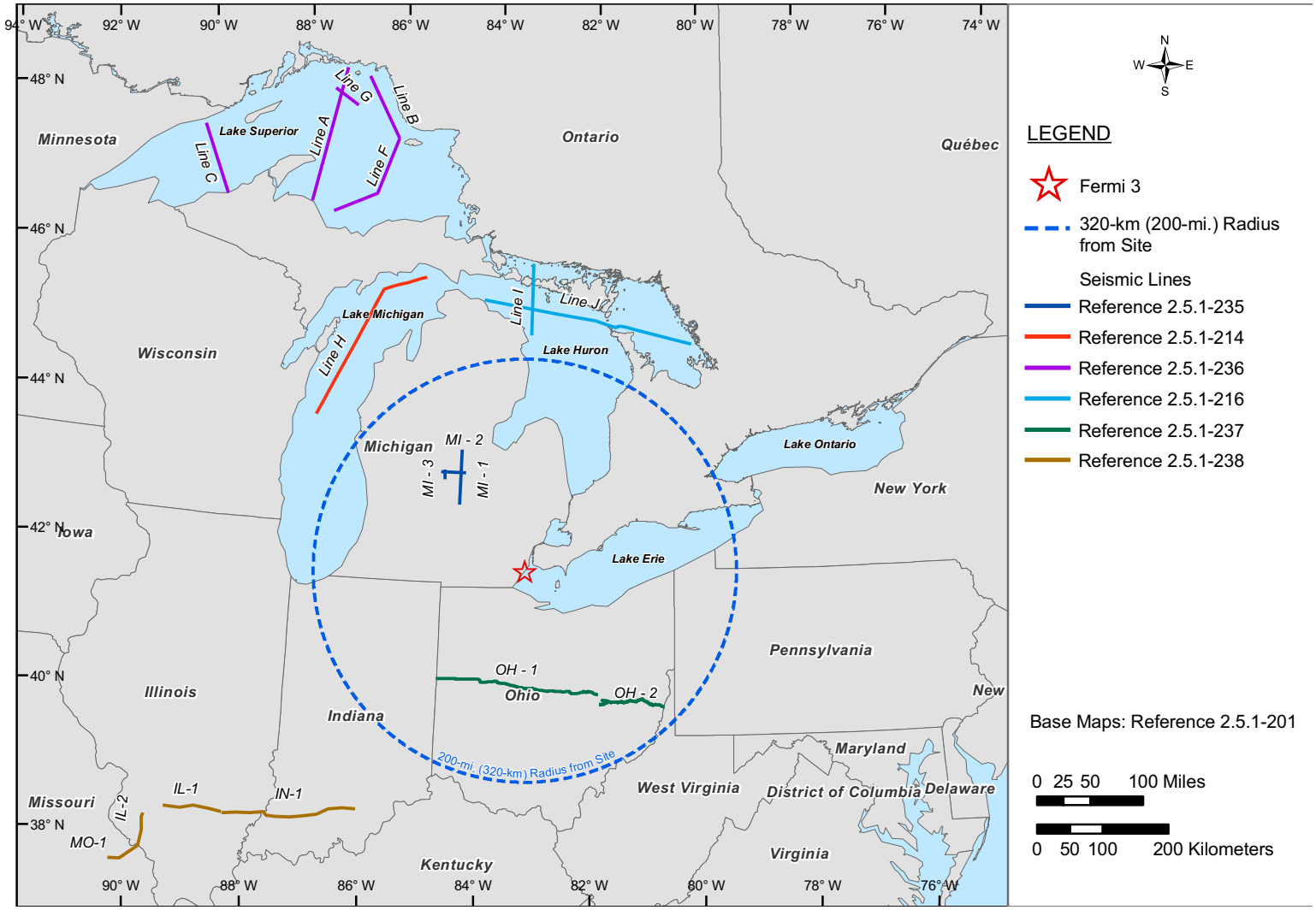

Figure 2.5.1-214 Late Wisconsin Glacial Lobes, Sublobes, and Inferred Ice Flow Pathways [EF3 COL 2.0-26-A]

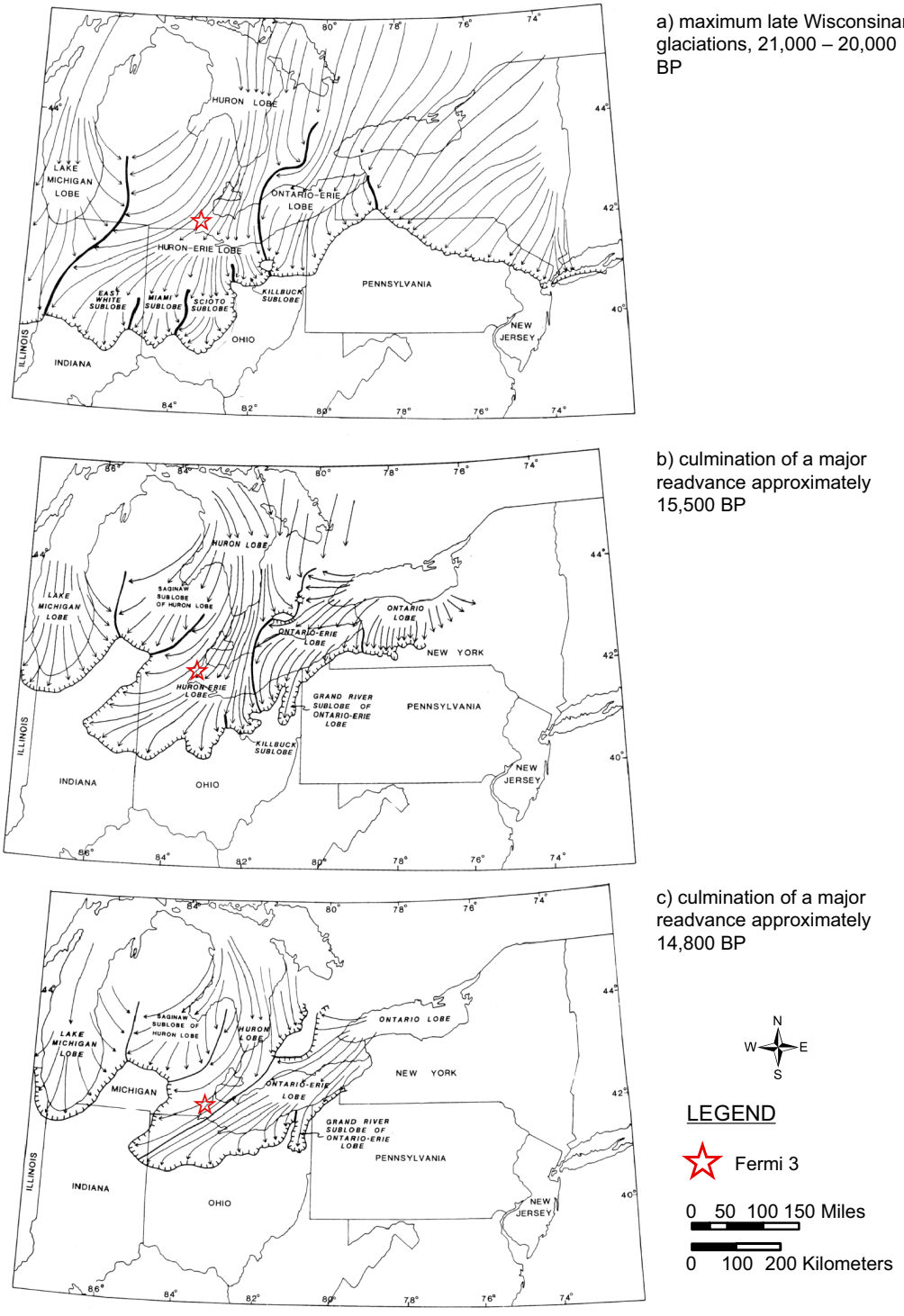

a) maximum late Wisconsinan glaciations, 21,000 – 20,000 BP

b) culmination of a major readvance approximately 15,500 BP

c) culmination of a major readvance approximately 14,800 BP

Source: Reference 2.5.1-246

Figure 2.5.1-215 Wisconsinan Stadial Interstadial Terminology [EF3 COL 2.0-26-A]

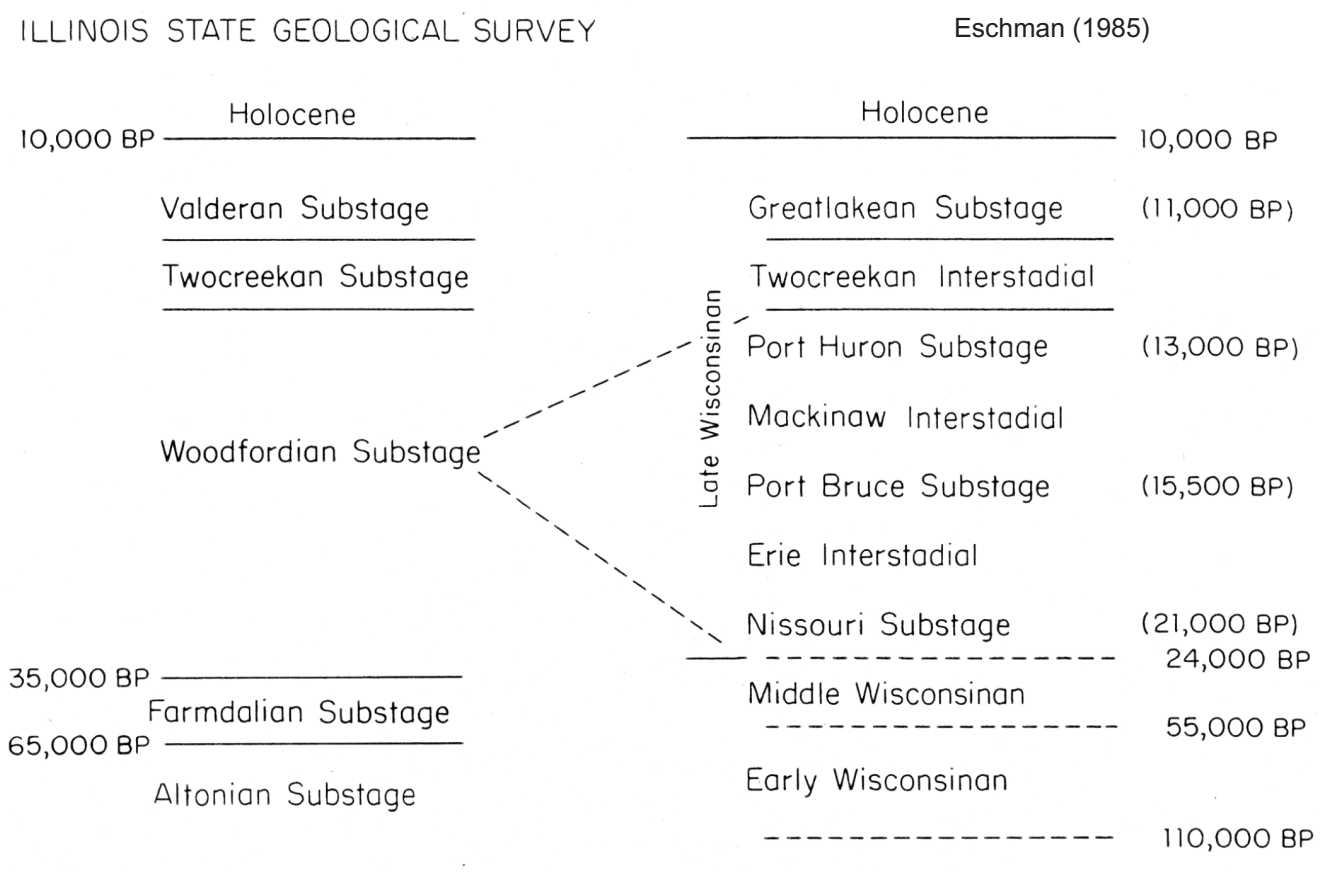

Source:modified from Reference 2.5.1-256

Figure 2.5.1-216 Summary Diagram of Lake Levels, Outlets, Inflows, Phases, and "Age" vs. Radiocarbon Age for the Northern Huron Basin
[EF3 COL 2.0-26-A]

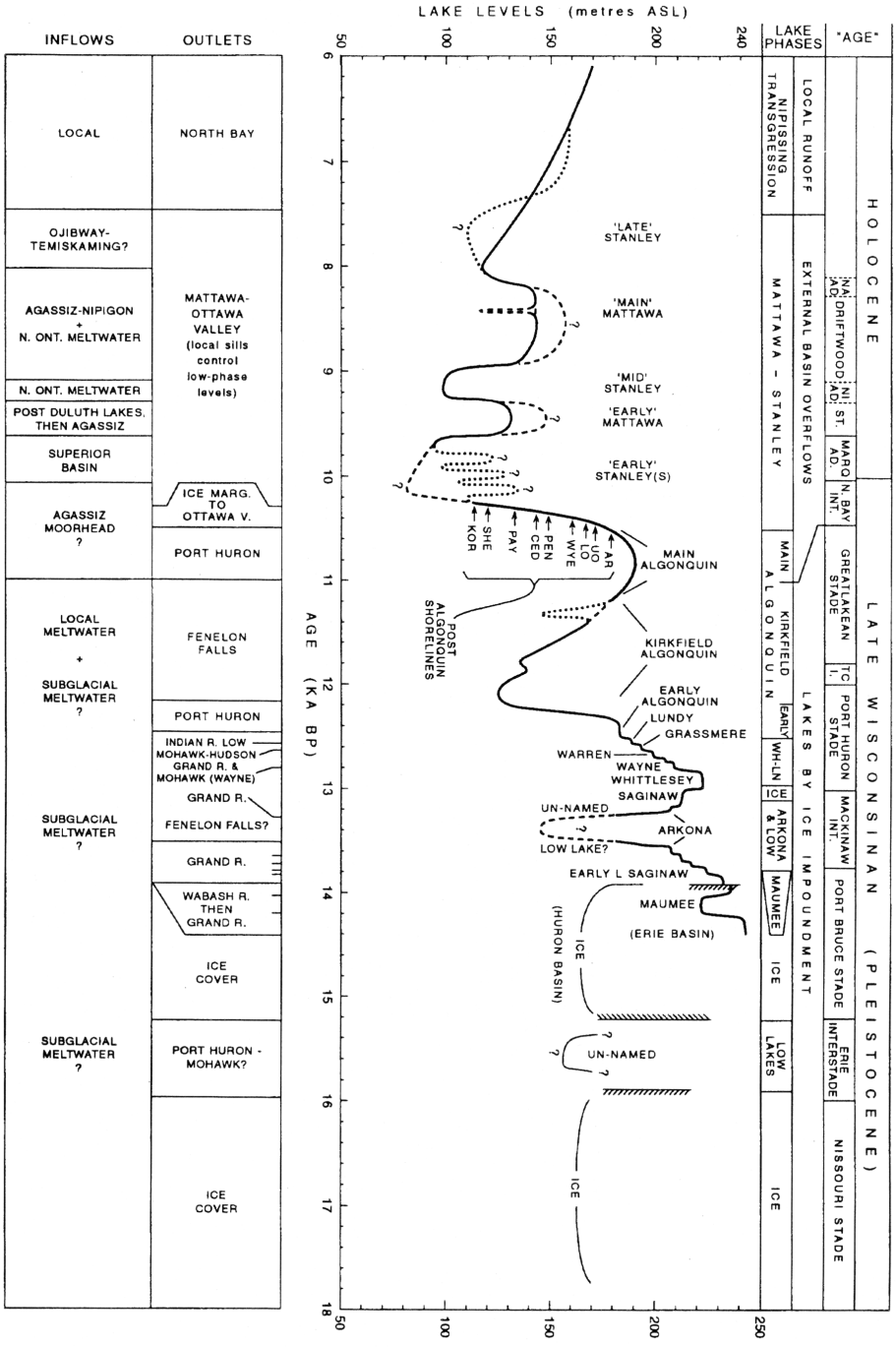

Note: Abbreviations under 'age' and lake phases are I or INT = Interstade; ST = Stade; AD = advance; NA = Nakina; NI = Nipigong; WH-LN = Whittlesey-Lundy. Abbreviations under outlets and inflows are MARG = margin; V = valley; R = river; N. ONT = northern Ontario.

Source: Reference 2.5.1-272

Figure 2.5.1-217 Stratigraphic Column for Michigan [EF3 COL 2.0-26-A]

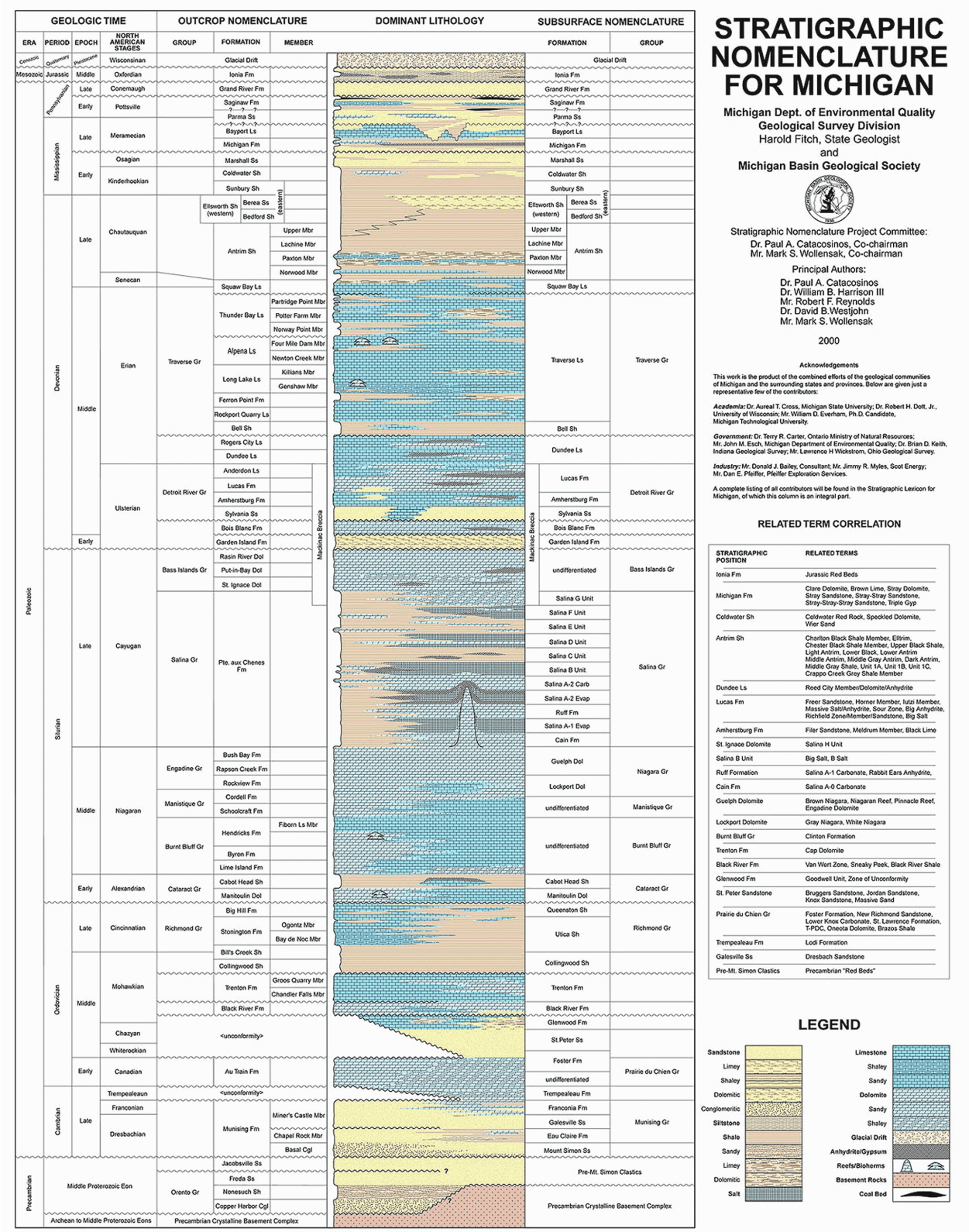

Figure 2.5.1-218 Geologogmic Cross-Section of the (320 km [200 mi] Radius) Site Region [EF3 COL 2.0-26-A]

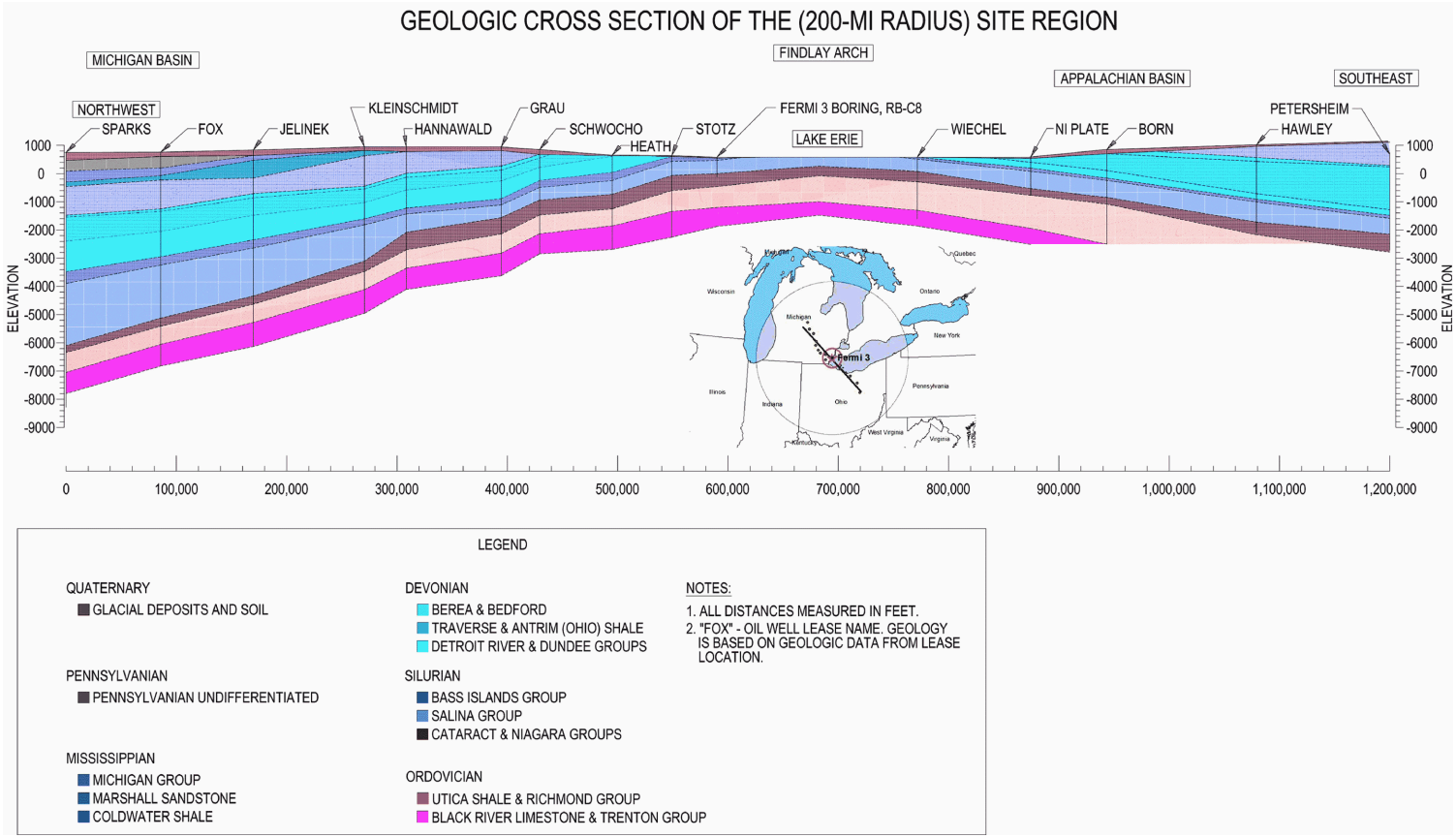

Figure 2.5.1-219 World Stress Map Showing Maximum Horizontal Stress Trajectory in the Fermi 3 Site Region

[EF3 COL 2.0-26-A]

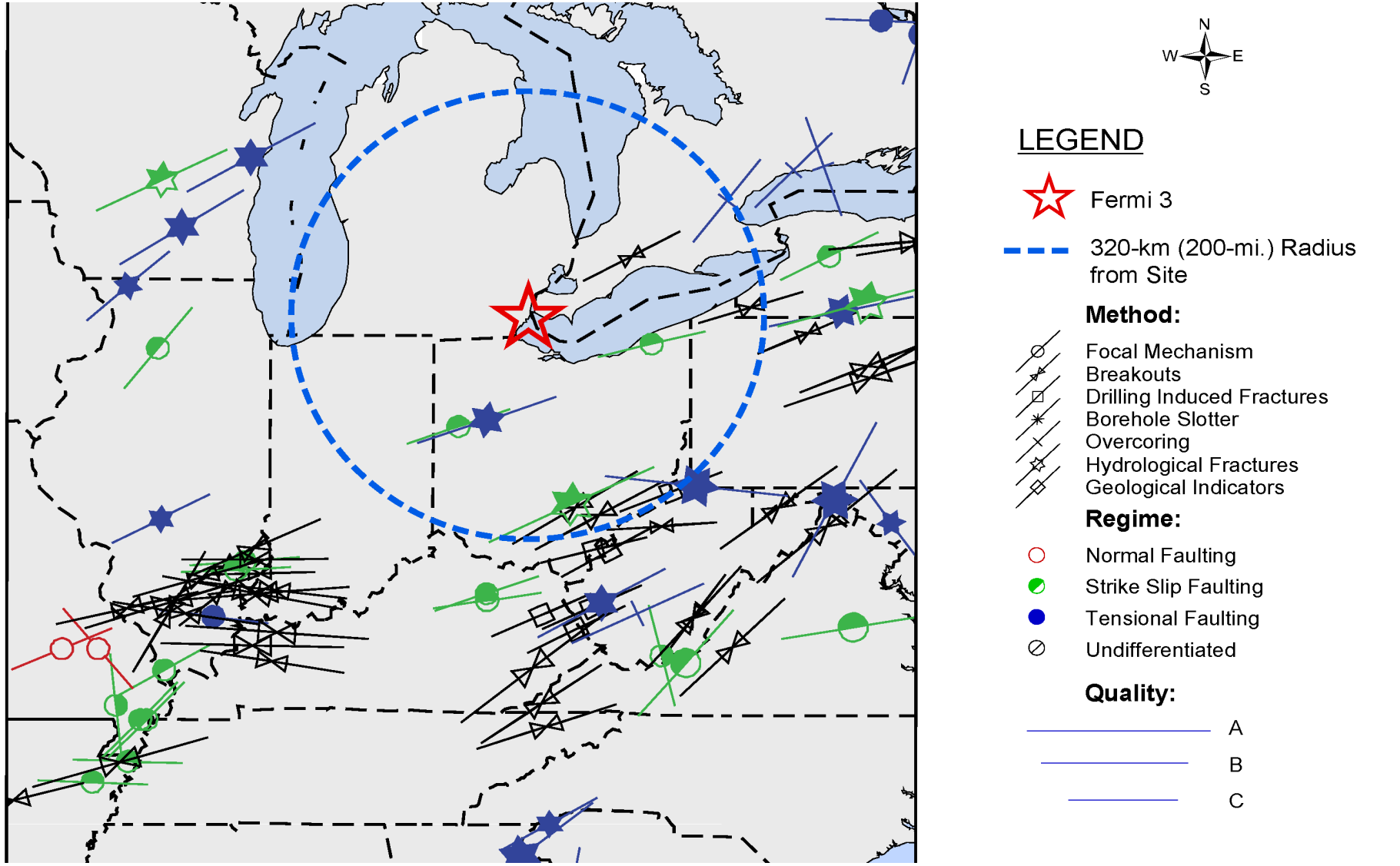

Source: Reference 2.5.1-290

Figure 2.5.1-220 Bouguer Gravity Map of the Fermi 3 Site Region [EF3 COL 2.0-26-A]

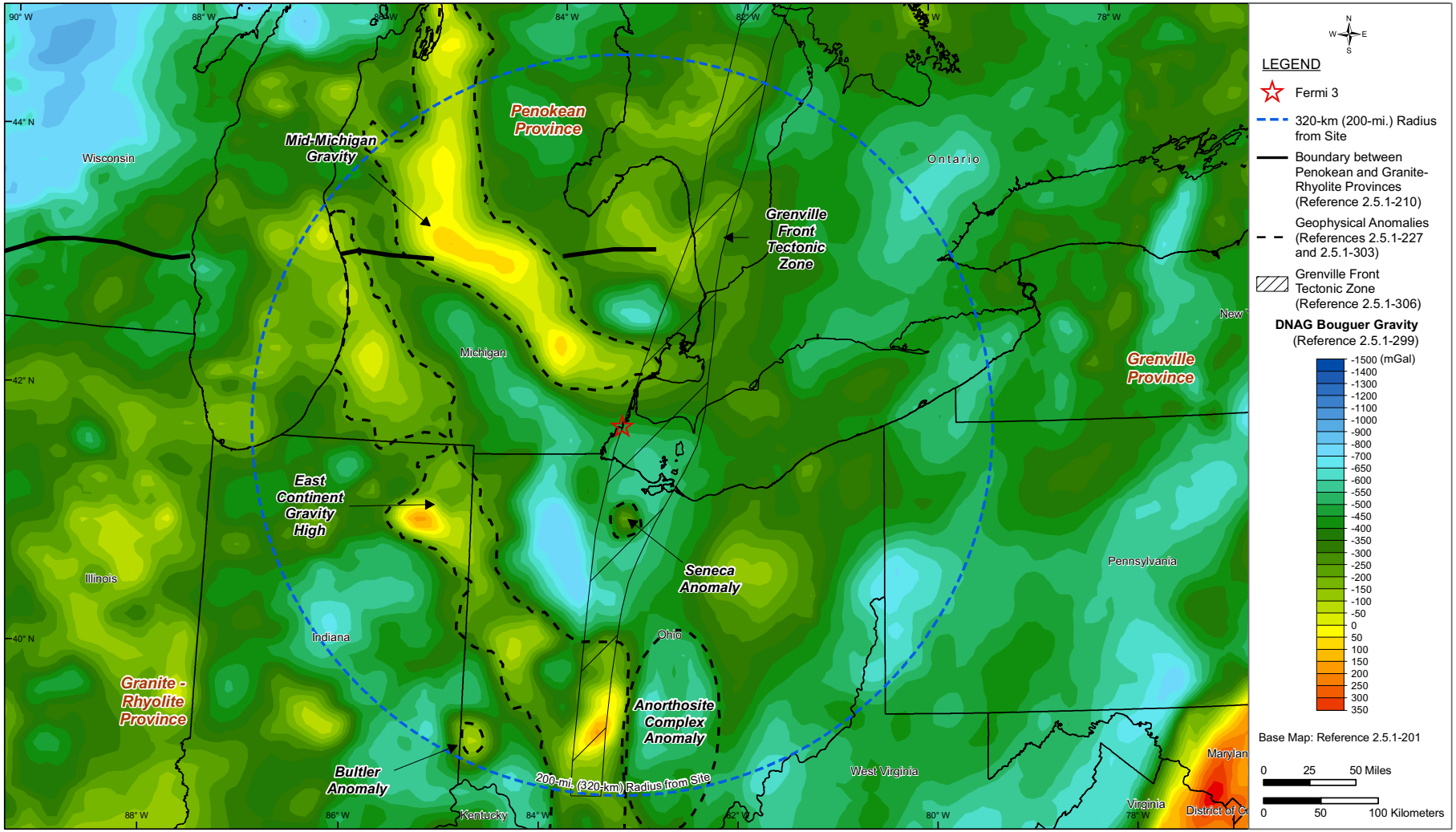

Figure 2.5.1-221 Magnetic Anomaly Map of the Fermi 3 Site Region [EF3 COL 2.0-26-A]

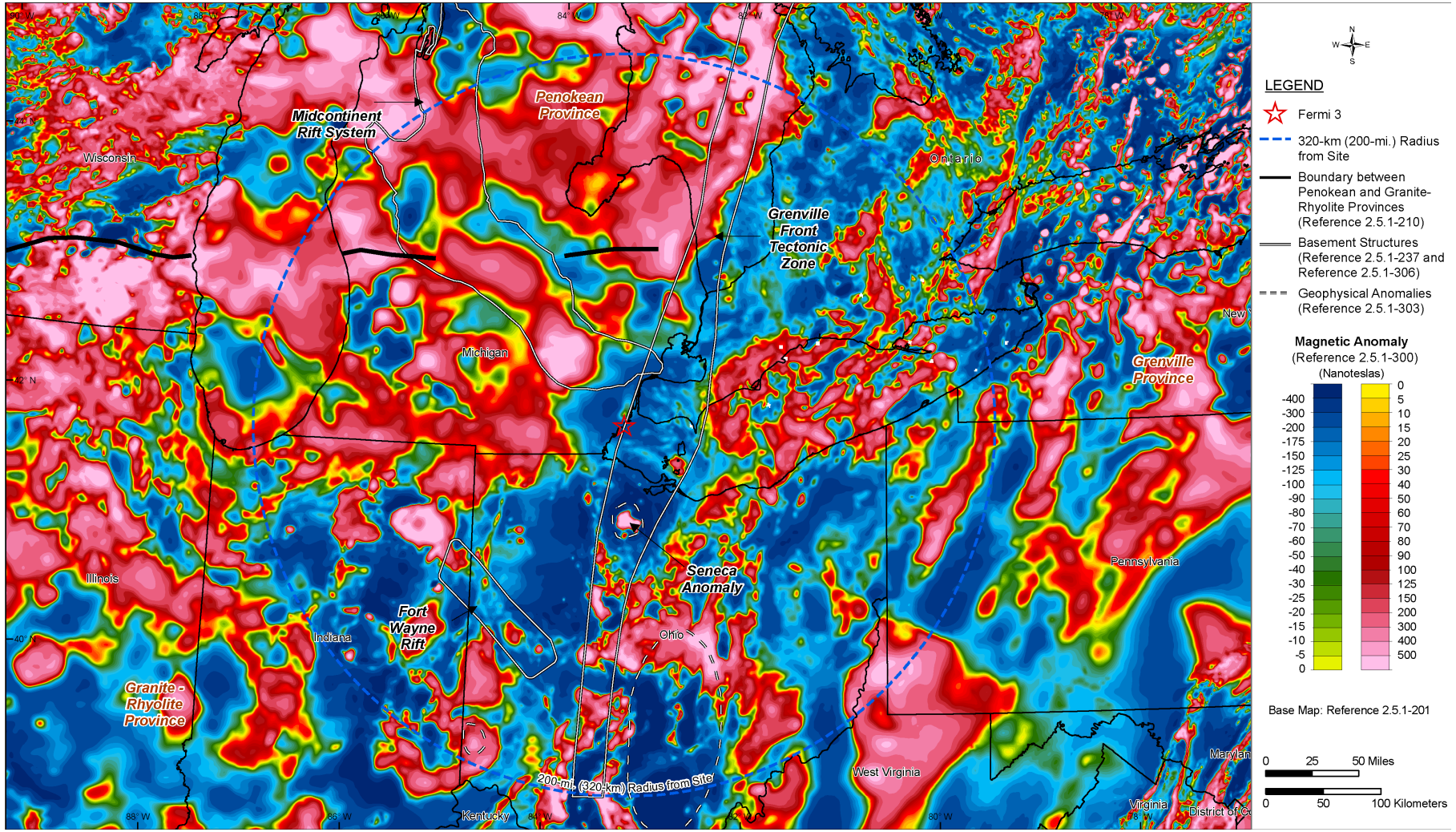

Figure 2.5.1-222 Interpretation of COCORP Lines OH-1 and OH-2 [EF3 COL 2.0-26-A]

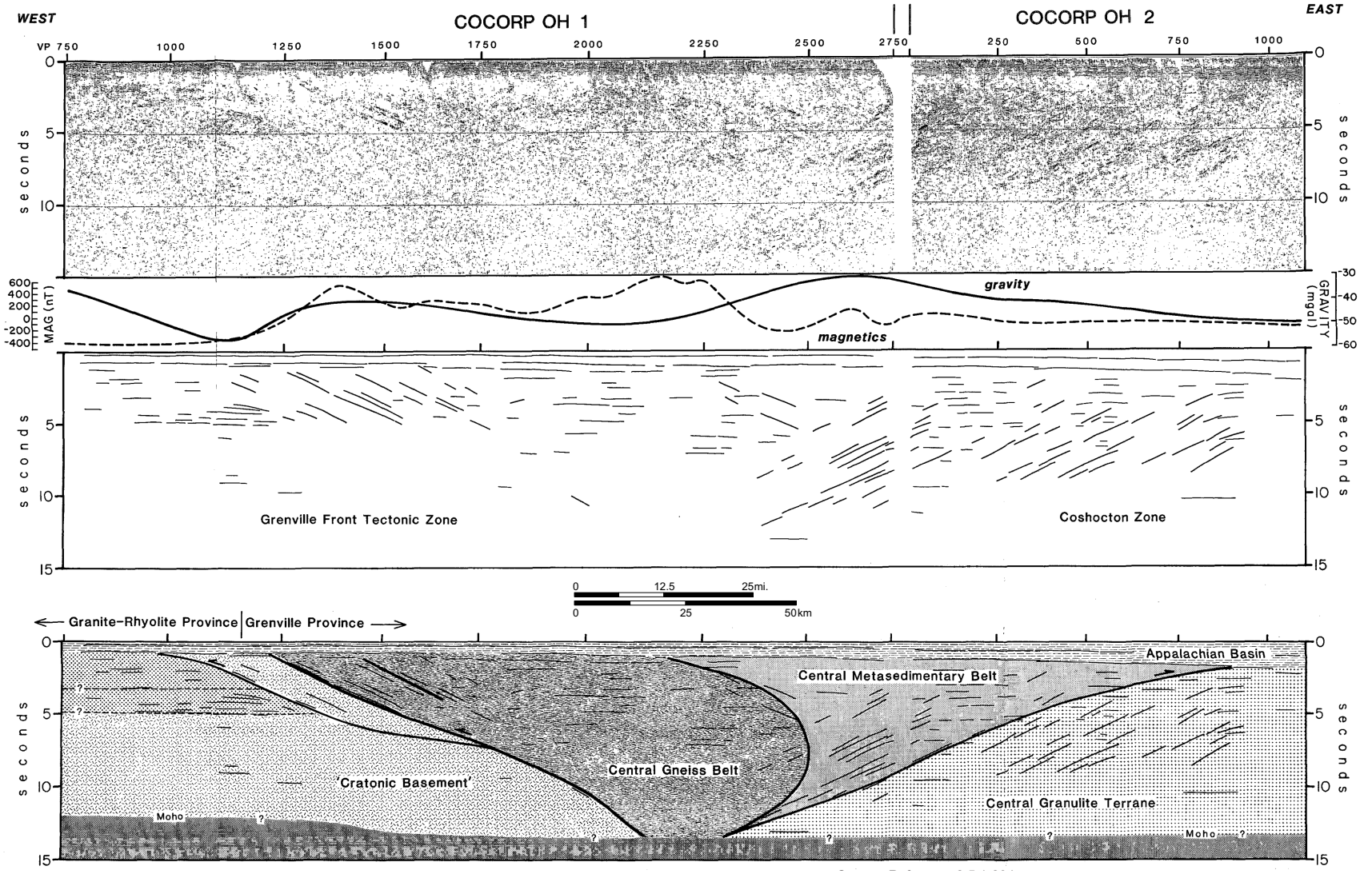

Source: Reference 2.5.1-234

Figure 2.5.1-223 Summary of Displacement History of Bowling Green Fault [EF3 COL 2.0-26-A]

SUMMARY OF DISPLACEMENT HISTORY OF BOWLING GREEN FAULT

Episode	Sense	Displacement	Evidence	Age
I	East-down	32 m	Greater thickness of strata between top of Trenton Ls. and top of Lockport Dol. on east side of fault	Late Ordovician-Early Silurian
II	West-down	50 m	Greater thickness of strata between top of Lockport Dol. and top of Tymochtee Dol. on west side of fault	Early-Middle Silurian
III	Left (?) lateral	?	Slickenlines in Tymochtee Dol. and Bass Islands Gp. in fault zone	Post-Middle Silurian
IV	West-down	>70 m	Slickenlines in Tymochtee Dol. and Bass Islands Gp. in fault zone; offset of Tymochtee-Bass Islands contact	Post-Middle Silurian
V	East-down	Depends on IV	Slickenlines, drag folds, minor fault sense in Tymochtee Dol. and Bass Islands Gp. in fault zone	Post-Middle Silurian
VI	Thrust	<5 m	Slickenlines, offset of bedding in Tymochtee Dol. and Bass Island Gp. in fault zone	Post-Middle Silurian-Cenozoic

Source: Reference 2.5.1-332

Abbreviations:
Dol. = Dolomite
Gp. = Group
Ls. = Limestone
? = uncertain

Source: Reference 2.5.1-332

Figure 2.5.1-224 Photograph and Cross-Section of an Exposure of the Bowling Green Fault in Waterville Quarry

[EF3 COL 2.0-26-A]

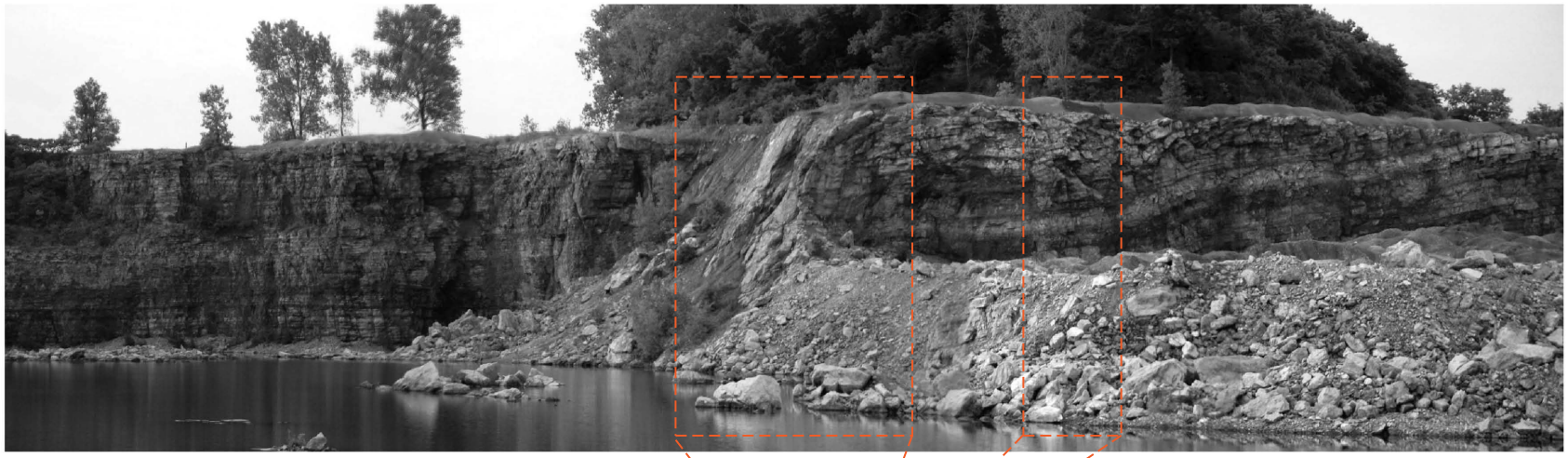

A. Photograph of a portion of SE wall, Waterville Quarry, taken in August, 2007.

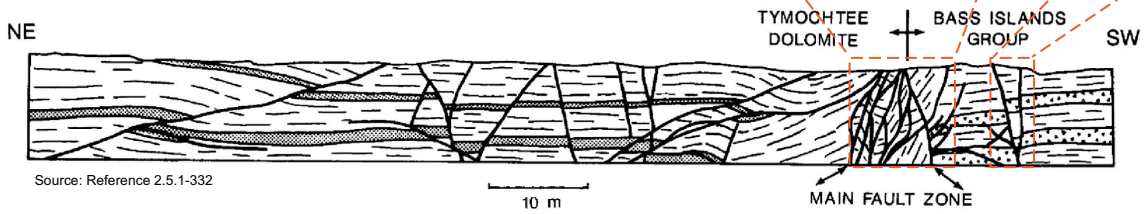

B. Interpretation of SE wall of Waterville Quarry

Source: Reference 2.5.1-332

Figure 2.5.1-225 Structure Contour Maps Showing the Howell Anticline and the Lucas-Monroe Monocline

[EF3 COL 2.0-26-A]

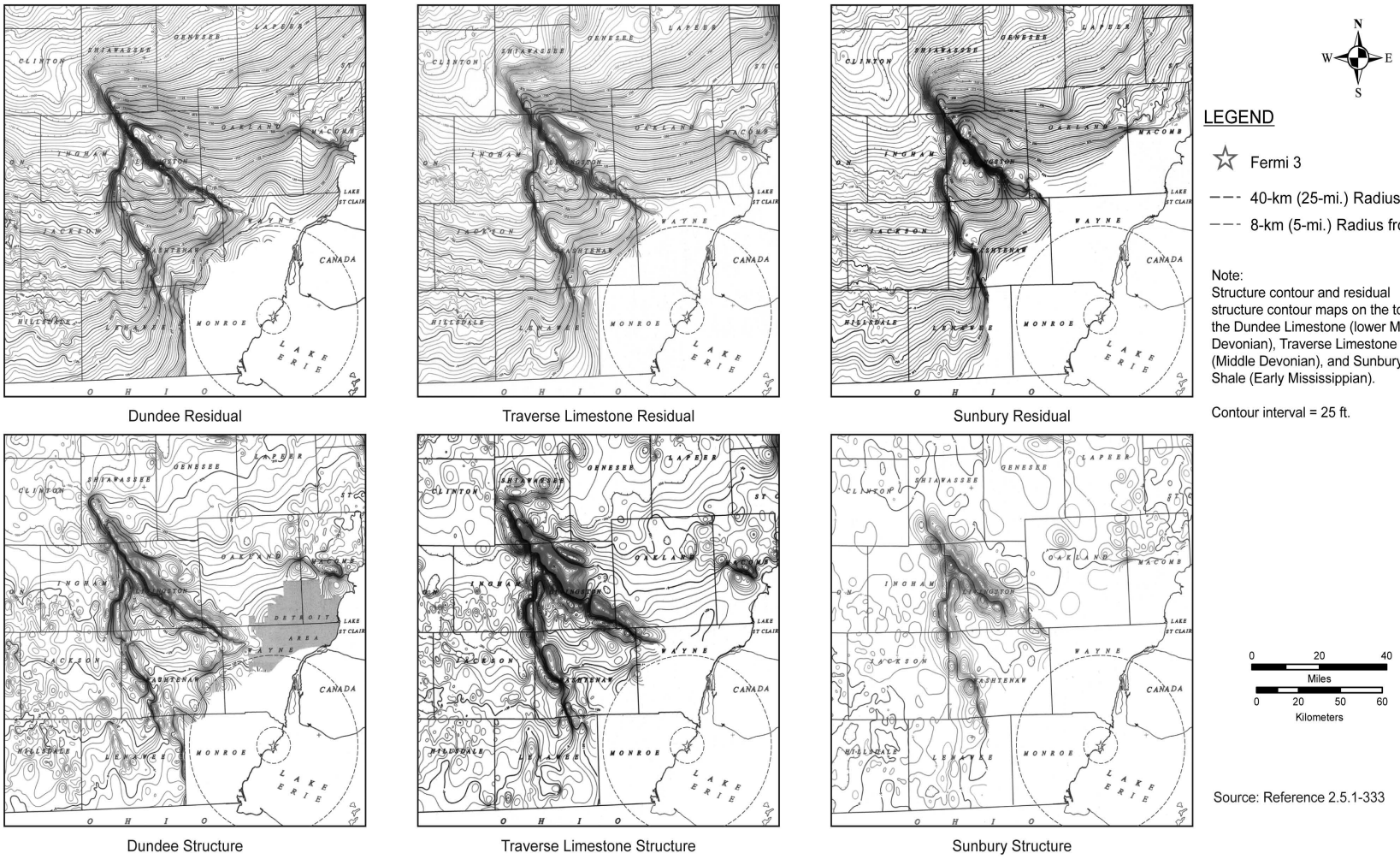

Source: Reference 2.5.1-332

Figure 2.5.1-226 Geologic Cross-Section of Howell Anticline [EF3 COL 2.0-26-A]

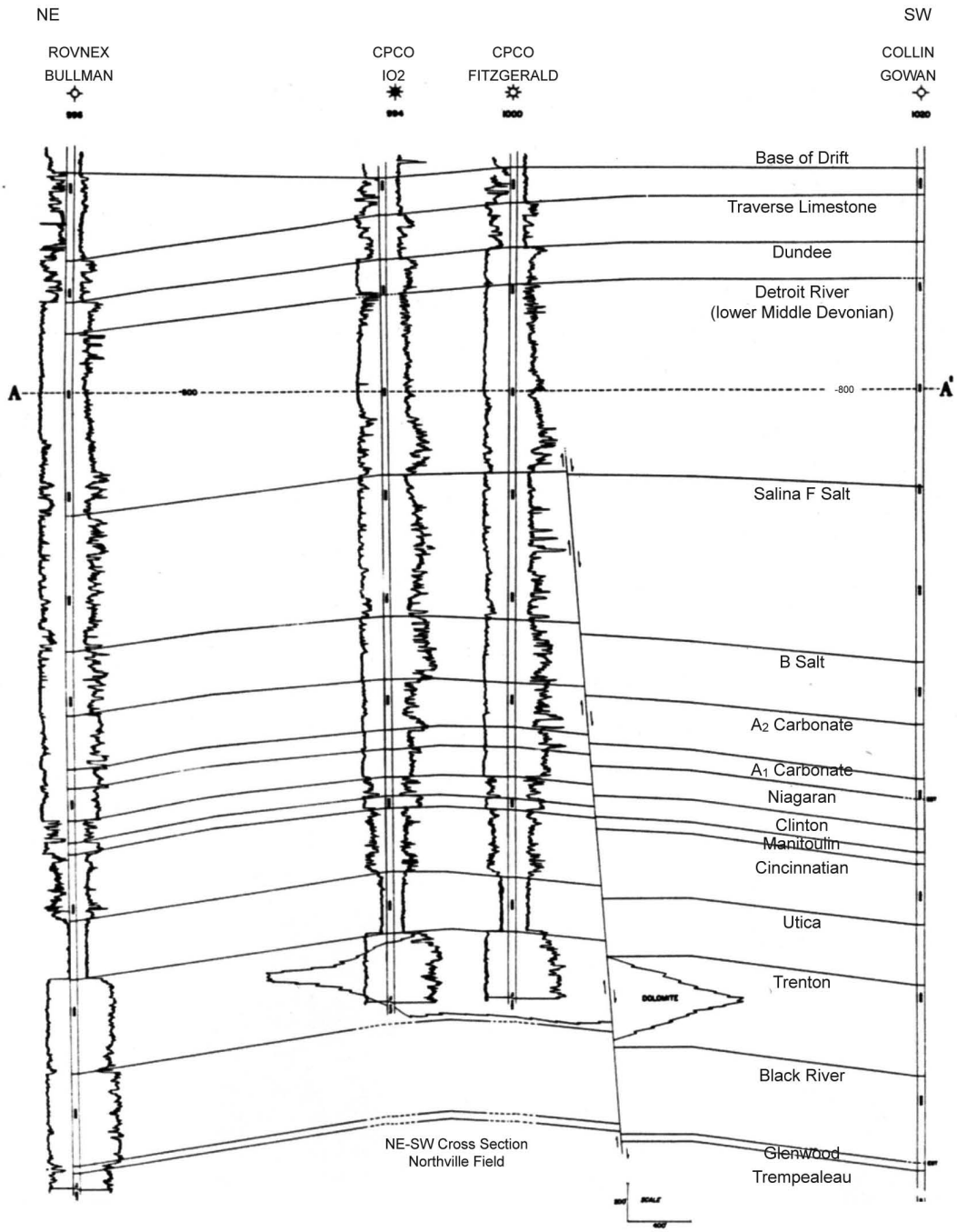

Source: Reference 2.5.1-340

Figure 2.5.1-227 Landslide Hazard Map for the Fermi 3 Site Region

[EF3 COL 2.0-26-A]